AD-A020 437

VIBRATORY RESPONSE AND ACOUSTICAL RADIATION OF A
WATER-LOADED, TURBULENCE-EXCITED PLATE-CAVITY
SYSTEM--OPTION 6

Ralph C. Leibowitz

David W. Taylor Naval Ship Research and Development
Center
Bethesda, Maryland

July 1975

048128

DAVID W. TAYLOR
NAVAL SHIP RESEARCH AND DEVELOPMENT CENTER

Bethesda, Md. 20084

Report 2976F

ADA020437

VIBRATORY RESPONSE AND ACOUSTICAL RADIATION OF A WATER-LOADED, TURBULENCE-EXCITED PLATE-CAVITY SYSTEM — OPTION 6

by

Ralph C. Leibowitz

APPROVED FOR PUBLIC RELEASE: DISTRIBUTION UNLIMITED

D D C

FEB 12 1976

C

SHIP ACOUSTICS DEPARTMENT
RESEARCH AND DEVELOPMENT REPORT

July 1975

Report 2976F

223

MAJOR DTNSRDC ORGANIZATIONAL COMPONENTS
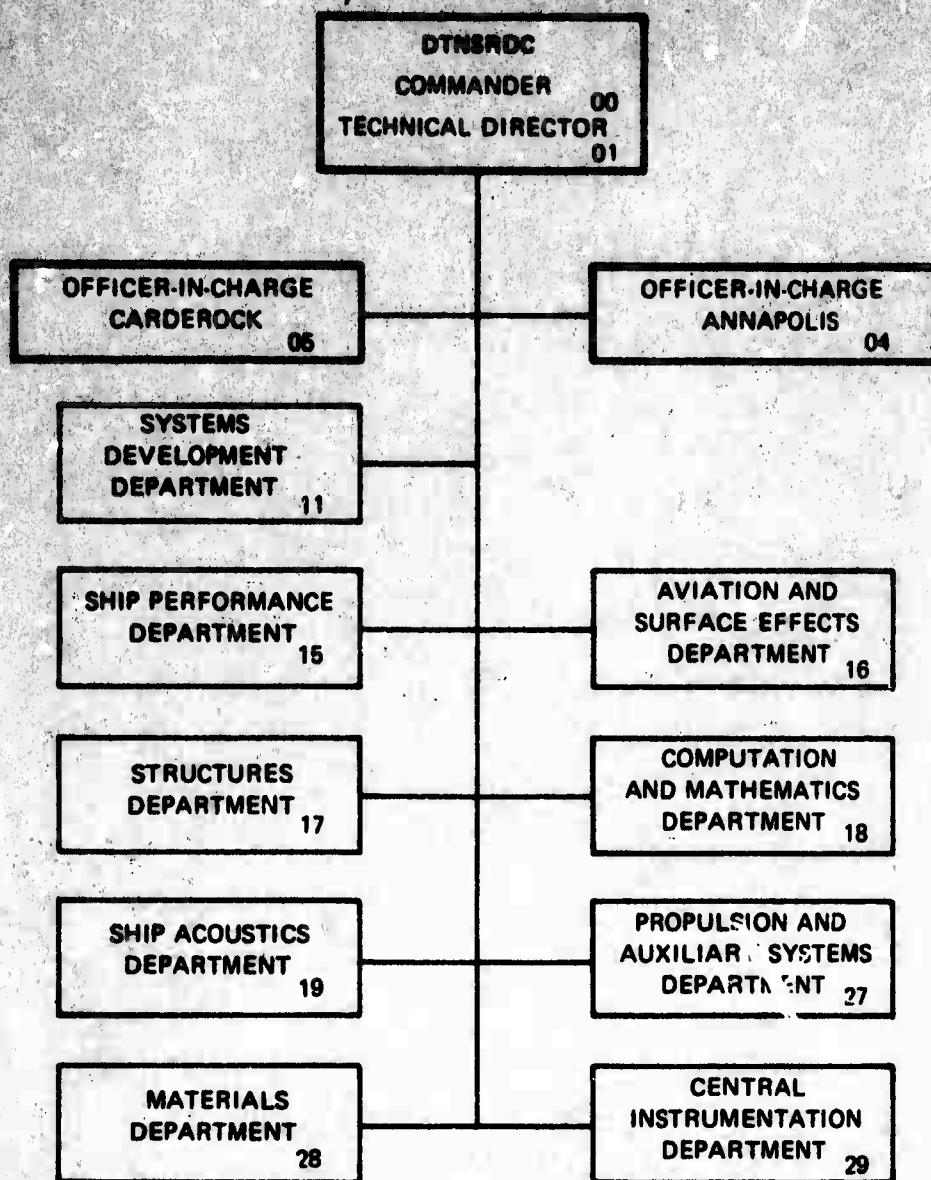
```
                    ┌─────────────────────────┐
                    │        DTNSRDC          │
                    │      COMMANDER      00  │
                    │  TECHNICAL DIRECTOR     │
                    │                     01  │
                    └─────────────────────────┘
                                 │
        ┌────────────────────────┴────────────────────────┐
┌──────────────────────┐                    ┌──────────────────────┐
│  OFFICER-IN-CHARGE    │                    │  OFFICER-IN-CHARGE    │
│  CARDEROCK        06  │                    │     ANNAPOLIS     04  │
└──────────────────────┘                    └──────────────────────┘

┌──────────────────────┐
│      SYSTEMS          │
│   DEVELOPMENT         │
│   DEPARTMENT      11  │
└──────────────────────┘

┌──────────────────────┐            ┌──────────────────────┐
│  SHIP PERFORMANCE     │            │    AVIATION AND       │
│  DEPARTMENT       15  │            │  SURFACE EFFECTS      │
│                       │            │  DEPARTMENT       16  │
└──────────────────────┘            └──────────────────────┘

┌──────────────────────┐            ┌──────────────────────┐
│    STRUCTURES         │            │    COMPUTATION        │
│  DEPARTMENT       17  │            │  AND MATHEMATICS      │
│                       │            │  DEPARTMENT       18  │
└──────────────────────┘            └──────────────────────┘

┌──────────────────────┐            ┌──────────────────────┐
│  SHIP ACOUSTICS       │            │  PROPULSION AND       │
│  DEPARTMENT       19  │            │  AUXILIARY SYSTEMS    │
│                       │            │  DEPARTMENT       27  │
└──────────────────────┘            └──────────────────────┘

┌──────────────────────┐            ┌──────────────────────┐
│    MATERIALS          │            │     CENTRAL           │
│  DEPARTMENT           │            │  INSTRUMENTATION      │
│               28      │            │  DEPARTMENT       29  │
└──────────────────────┘            └──────────────────────┘
```

ii

REPORT DOCUMENTATION PAGE	READ INSTRUCTIONS BEFORE COMPLETING FORM	
1. REPORT NUMBER 2976F	2. GOVT ACCESSION NO.	3. RECIPIENT'S CATALOG NUMBER
4. TITLE (and Subtitle) VIBRATORY RESPONSE AND ACOUSTICAL RADIATION OF A WATER-LOADED, TURBULENCE-EXCITED PLATE-CAVITY SYSTEM—OPTION 6	5. TYPE OF REPORT & PERIOD COVERED	
	6. PERFORMING ORG. REPORT NUMBER	
7. AUTHOR(s) Ralph C. Leibowitz	8. CONTRACT OR GRANT NUMBER(s)	
9. PERFORMING ORGANIZATION NAME AND ADDRESS David W. Taylor Naval Ship Research & Development Center — Bethesda, Md. 20084	10. PROGRAM ELEMENT, PROJECT, TASK AREA & WORK UNIT NUMBERS SF 43.452.702, Task 18185 Work Unit 1-1960-010	
11. CONTROLLING OFFICE NAME AND ADDRESS Naval Sea Systems Command (SEA 037) Washington, D.C.	12. REPORT DATE July 1975	
	13. NUMBER OF PAGES 229	
14. MONITORING AGENCY NAME & ADDRESS(if different from Controlling Office)	15. SECURITY CLASS. (of this report) UNCLASSIFIED	
	15a. DECLASSIFICATION/DOWNGRADING SCHEDULE	

16. DISTRIBUTION STATEMENT (of this Report)

APPROVED FOR PUBLIC RELEASE: DISTRIBUTION UNLIMITED

17. DISTRIBUTION STATEMENT (of the abstract entered in Block 20, if different from Report)

18. SUPPLEMENTARY NOTES

19. KEY WORDS (Continue on reverse side if necessary and identify by block number)

Vibration and Acoustic Pressure Radiation Plate-Cavity (Parallelepiped) System
1. Intermodal Coupling
2. Simply-Suported and Clamped Boundaries
3. Water and Air Fluid Media

(See reverse side)

20. ABSTRACT (Continue on reverse side if necessary and identify by block number)

This report presents a method and computer program for calculating certain spectral quantities for the vibration as well as the external (half-space) and internal (cavity) acoustic radiation of a plate-cavity system represented as a rectangular parallelepiped. The upper surface of the plate, lying outside of the cavity, is excited by boundary layer turbulence. The lower surface of the plate covers the cavity. The walls of the cavity are either all rigid or uniformly nearly absorbtive, i.e., nearly all rigid. The plate is thin, flat, flexible, isotropic,

(See reverse side)

DD FORM 1473 EDITION OF 1 NOV 65 IS OBSOLETE
1 JAN 73
S/N 0102-014-6601

Block 20 Continued

rectangular, and finite and is either simply supported or clamped-clamped at its boundaries which are contiguous with an infinite, rigid, planar, baffle. The fluid at the boundaries of both sides of the plate, external and internal to the plate cavity system, may consist of any combination of heavy (or dense) and light fluid media. Thus, the plate is acoustically coupled to the external flow field and to the field within the cavity.

The method treats intermodal auto- and cross-resistive and reactive coupling, associated with structural-acoustic interaction, induced by the fluid in the half-space above the plate and by the fluid in the cavity beneath the plate. Excluding cavity effects, the half-space coefficients are analytically evaluated for acoustically fast (surface) modes, acoustically slow (edge and corner) modes, and all possible combinations of these modes. The results therefore represent a more complete calculation of the intermodal coefficients than those obtained by Davies. The results are also shown to be of greater generality than those of Davies because in almost all cases, they reduce to his first order results as a special case.

The vibroacoustic spectral quantities for the plate-cavity system which are mathematically formulated and programmed (for computations in narrow bands) include.

1. The cross-spectral density and power spectral density of plate displacement.
2. The cross-spectral density and power spectral density of cavity acoustic pressure for hard or almost hard walls.
3. The complex spectral density of power generated in the half-space above the plate.
4. The cross-spectral density and power spectral density of acoustic pressure in the distant far field of the half-space.

Additional results of the analysis (but presently excluding computer programs) are:

5. A general formulation, requiring analytical evaluation, for the cross-spectral density and (by implication) power spectral density of the acoustic pressure anywhere in the half-space, thereby including the near-field acoustic pressure above the plate.
6. The spectral density of complex power generated in the cavity.

The sample computer results presented are based on the response and radiation of resonant acoustically slow modes which pertain to frequencies below the critical frequency.

Block 19 Continued

4. Radiation into Semiinfinite Half-Space
5. Radiation into Cavity

Mathematical Analysis
Turbulence-Induced Vibration and Radiation of Plate-Cavity System
Digital Computer Program and Computations
Continuum Approach

TABLE OF CONTENTS

Page

LIST OF FIGURES

LIST OF TABLES

NOTATION

A_i, K_i	Turbulent boundary layer constants $A_1=1.6$, $A_2=7.2$, $A_3=12.0$, $K_1=0.47$, $K_2=3.0$, $K_3=14.0$
A_p	Plate area
$\overline{A}_{tr}$	Cofactor of element $\overline{a}_{tr}$ in the determinant det (a_{tr}); see Equation (35)
a, b	Plate lengths in x- and y-directions, respectively
a', b'	Equivalent plate lengths in x- and y-directions, respectively, used in computations for clamped-clamped plates; see Appendix E
$\overline{a}_{rr}$, $\overline{a}_{rs}$	Intermodal coupling coefficients, $\overline{a}_{rr}$ being the auto terms and $\overline{a}_{rs}$ the cross terms
C_f	Local coefficient of skin friction equal to $\dfrac{\tau_w}{\frac{1}{2}\rho\, U_\infty^2}$
c	Cavity depth
c_o	Speed of sound in half-space
e	Base for natural or Naperian system of logarithms; equal to 2.718
F	Equal to $\dfrac{\delta^*}{U_\infty}$
f	Frequency variable
f_{mn}, $\overline{f}_{mn}$	Plate *in vacuo* and fluid-loaded resonance frequencies, respectively
$G(\overline{x}/\overline{x}'; \omega)$	Plate Green function
$G_p(\overline{x}, z/\overline{x}', z'; \omega) \equiv$ $G_p(\overline{\xi}/\overline{\xi}'; \omega)$	Cavity Green function
$G_p(\overline{x}/\overline{x}'; \omega)$	Cavity Green function for source and field points at (lower) surface of plate; Figure 1
$G_p^0(\overline{x}, z/\overline{x}', z'; \omega) \equiv$ $G_p^0(\overline{\xi}/\overline{\xi}'; \omega)$	Half-space Green function
$G_p^0(\overline{x}/\overline{x}'; \omega)$	Half-space Green function for source and field points at (upper) surface of plate; Figure 1
$G_p^0(\kappa_x, k_y)$	Fourier transform of $G_p^0(\overline{x}/\overline{x}')$

$H_0^{(1)}, H_0^{(2)}$	Hankel functions of zero order, first and second kinds respectively
$I_1(\beta)$	Defined by Equations (56b) or (57)
$I_{nr}(\beta)$	Equal to $\left.\dfrac{1-(-1)^n \cos b\beta}{(\beta^2-k_n^2)(\beta^2-k_r^2)}\right\|_{n \neq r}$
$\bar{I}^{rr}(\omega), \bar{I}^{rs}(\omega)$	Cavity coupling coefficients, $\bar{I}^{rr}$ being the joint coupling coefficient and $\bar{I}^{rs}$ the cross-coupling coefficient of the cavity
i	Equal to $\sqrt{-1}$, an imaginary number
$\hat{i}$	Unit vector along x-axis
j_0	Bessel function of the first kind and order zero
$\bar{J}^{rr}(\omega), \bar{J}^{rs}(\omega)$	Half-space coupling coefficient, $\bar{J}^{rr}$ being the joint coupling coefficient and $\bar{J}^{rs}$ the cross-coupling coefficient of the half-space
$j_{nn}^2(\omega), j_{tn}^2(\omega)$	Joint and cross-acceptance functions, respectively
K_1	Equal to $k_m k_n k_q k_r$
k, k_0	Acoustic wavenumber in half-space to $\dfrac{\omega}{C_0}$; k is also used as an index
$\bar{k}$	Vector wavenumber
k_c	Acoustic wavenumber in cavity
k_m, k_n	Plate mode wavenumbers along the x- and y-directions, respectively; respectively equal to $\dfrac{m\pi}{a}$ and $\dfrac{n\pi}{b}$ (for simply supported thin plates)
k_{mn}	Surface wavenumber of plate equal to $\sqrt{k_m^2 + k_n^2}$
k_x, k_y, k_z	Wavenumber variables along the x-, y- and z-directions, respectively
L, L'	Operators, equal to $k + iM\dfrac{\partial}{\partial x}$ and $k + iM\dfrac{\partial}{\partial x'}$ respectively
$Lw, \hat{LW}$	Equal to $(k + iM\dfrac{\partial}{\partial x})w$ and its Fourier transform, respectively
M	Mach number for fluid in half-space
M_s	Modal mass of plate (mode s)
m	Plate mass per unit area
m, n	Mode numbers

m_c	Cavity added mass per unit area equal to $\dfrac{\rho_c \coth k_{mn} c}{k_{mn}}$
$m_{\text{total added mass}}$	Cavity plus half-space added mass per unit area Equal to $\dfrac{\rho_c \coth k_{mn} c}{k_{mn}} + \dfrac{\rho}{k_{mn}}$; see Appendix G
n	Equal to α, β, γ for a cavity mode; see Appendix B
$P, P_{k_m}, P_{k_m k_q}$	Principal value of the integral, principal value of the integral with respect to $x = k_m$, and principal value of the integral with respect to both $x = k_m$ and $x = k_q$, respectively
$p_2(\bar{x}, z)$	Acoustic pressure in the half-space
$P_{2_T}(\bar{x}; \omega)$	Fourier transform of truncated random acoustic pressure in the half-space
$p_{b\ell}(\bar{x})$	Blocked (turbulent) pressure at the surface of the plate
$P_{b\ell}(\bar{x}, \omega)$	Fourier transform of truncated random exciting blocked pressure at the plate surface
$\langle p_{b\ell}^2 \rangle_t$	Mean square blocked (turbulent) pressure
$p^i(\bar{x}, z)$	Acoustic pressure in cavity
$P_{i_T}(\bar{x}, \omega)$	Fourier transform of truncated random acoustic pressure in the cavity
P_{mn}^i	Acoustic pressure in cavity for a mode mn; see Appendix G
$p^0(\bar{x})$	External pressure field acting on plate Equal to $p_2(\bar{x}) + p_{b\ell}(\bar{x})$
R_{mnqr}	Coupling coefficient connecting the m, n mode to the q, r mode, per unit area
$R(\eta, \mu, \tau)$	Cross-correlation function for turbulence pressures
$\bar{r}, \bar{r}'$	Radius vector from origin measured by an observer at rest and by an observer moving with the system, respectively
r_n	Specific wall resistance
S, S'	Fixed and moving frames of reference, respectively
S_{mnqr}	Modal radiation coupling term, per unit area
$S_{p_2}(\bar{\xi}|\bar{\xi}'; \omega)$	Cross-spectral density of half-space acoustic pressure

$S_{p_2 v}(\bar{x}/\bar{x}'; \omega)$	Cross-spectral density of pressure p_{2_T} at position $\bar{x}$ with velocity v_T at position $\bar{x}'$
$S_{p_{b\ell}}(\omega)$	Fixed microphone (or power) spectrum of fluctuating boundary layer pressure
$S_{p_{b\ell}}(\bar{x}/\bar{x}'; \omega)$	Cross-spectral density of blocked (turbulent) pressure
$S_{p_i}(\bar{\xi}/\bar{\xi}'; \omega)$	Cross-spectral density of cavity acoustic pressure
$S_{p_i v}(\bar{x}/\bar{x}'; \omega)$	Cross-spectral density of pressure p_i at position $\bar{x}$ with velocity v_T at position $\bar{x}'$
$S_w(\bar{x}/\bar{x}'; \omega)$	Cross-spectral density of plate displacement
$S_s(k_x, k_y)$	Shape function representing Fourier transform of mode shape of plate, given by Equation (50) (for mode s)
$\mathcal{S}_{qr}$	Shape function representing the Fourier transform of L^2 and the plate mode (for mode qr); see Appendix E
T_{mnqr}	Modal mass coupling term, per unit area
t, t'	Time variable
U_∞	Free-stream velocity
U_c	Turbulence convection velocity = $0.8\ U_\infty$
$\bar{u}$	Acoustic velocity
u_i	Components of acoustic velocity; i=x,y,z
V	Cavity volume equal to $a \cdot b \cdot c$
$\bar{V}$	Fluid velocity vector
V_i	Components of fluid steady velocity; i=x, y, z
$V_T(\bar{x}; \omega)$	Fourier transform of truncated random plate velocity
$v_T(\bar{x}, t)$	Truncated velocity of plate displacement
$W_T(\bar{x}, \omega)$	Fourier transform of truncated random displacement
$\bar{w}(\bar{x}), w(\bar{x})$	Vector and scalar displacements, respectively
$w_p(x, y, t)$	Velocity of plate (at z=0)

$(\dot{w}_p)_{mn}$	Plate modal velocity for mode mn
$W_{rad}^{ext}(\omega)$	Spectral density of (complex) power radiated to half-space
$W_{rad}^{int}(\omega)$	Spectral density of (complex) power radiated into the cavity
$\bar{x}, \bar{x}'$	(x, y) and (x', y'), respectively
$x, y, z; x', y', z'$	Cartesian coordinates
x_i, x_i'	Components x, y, z and x', y', z', respectively, of Cartesian coordinates
x_n	Specific wall reactance
$\bar{Y}_s$	Plate mode s *in vacuo* receptance
$Z_{mn}(x, y, z)$	Modal impedance for mode mn
z_n	Specific wall impedance
a	Wall absorbtion coefficient
a, β	Equal to k_x and k_y, respectively
a, β, γ	Cavity mode indices
a_1, a_1'	Equal to $\sqrt{k^2-\beta^2}$ and $\sqrt{\beta^2-k^2} \equiv i\sqrt{k^2-\beta^2}$, respectively
a_n	Cavity wall absorption coefficient
$\bar{a}_{rt}$	Intermodal receptance; see Equation (35)
β_n	Specific cavity wall admittance
$\Gamma_{p_2}^2(\omega)$	Modal acoustic pressure (mode r) acting on top (i.e., half-space side) of plate; defined by Equation (25)
$\Gamma_{p_{b\ell}}^r(\omega)$	Modal blocked (turbulent) pressure (mode r) acting on top (i.e., half-space side) of plate; defined by Equation (24)
$\Gamma_{p_{b\ell_T}}^r(\omega)$	Modal blocked pressure for truncated random (turbulence) excitation (mode r) acting on top (i.e., half-space side) of plate; defined by Equation (24) with $p_{b\ell} \rightarrow p_{b\ell_T}$
$\Gamma_{p_i}^r(\omega)$	Modal acoustic pressure (mode r) acting on bottom (i.e., cavity side) of plate; defined by Equation (26)

∇ Vector differential operator equal to $\hat{i}\frac{\partial}{\partial x} + \hat{j}\frac{\partial}{\partial y} + \hat{k}\frac{\partial}{\partial z}$ where i, j, k are unit vectors along x, y, z, respectively

∇^2 La Placian, operator equal to $\frac{\partial^2}{\partial x^2} + \frac{\partial^2}{\partial y^2} + \frac{\partial^2}{\partial z^2}$

δ Change in density of fluid produced by acoustic rarefactions and condensations

$\delta(\beta - k_n)$ Delta function; $\int \delta(\beta - k_n)\, d\beta = \begin{cases} 1, & \beta = k_n \\ 0, & \beta \neq k_n \end{cases}$

δ_{nr} Kronecker delta function; $\delta_{nr} = \begin{cases} 1, & n = r \\ 0, & n \neq r \end{cases}$

δ^* Boundary layer displacement thickness

ϵ A small quantity

$\epsilon_a, \epsilon_\beta, \epsilon_\gamma$ Equal to $\begin{cases} 1 \text{ for } a, \beta, \gamma = 0 \\ 2 \text{ for } a, \beta, \gamma > 0 \end{cases}$

ζ Defined by Equation (7)

ζ_s Decay or damping ratio defined as ratio of damping to critical damping for mode s; see Reference 5, page 141

η, μ Equal to x-x' and y-y', respectively (except where otherwise stated in text)

η_s Structural damping loss factor (mode s) equal to $2\zeta_s \dfrac{\omega}{\omega_s}$

θ Eddy lifetime for steady convection or eddy decay period; see Reference 1, Page 35

Λ_n Imaginary part of $\bar{\lambda}_n$ given by Equation (103)

λ_n Real part of λ_n given by Equation (102)

$\bar{\lambda}_n$ Complex value of cavity mode eigenvalue; see Equation (101)

μ_{mn} Eigenvalue for fluid-loaded plate equal to $(k_{mn}^2 - k^2)^{1/2}$

$\nu, \partial\nu$ Normal to plate (drawn into the cavity) and partial differential of the normal at the plate surface, respectively

$\bar{\xi}, \bar{\xi}'$ Coordinates x, y, z and x', y', z' respectively representing points in half-space or in the interior of the cavity

ξ_n Specific cavity wall conductance

$\bar{\xi}_r$ Plate mode r normal coordinate

$\Pi_{rad}^{ext}\|_{\Delta\omega}$, $\Pi_{rad}^{int}\|_{\Delta\omega}$	Total power in band $\Delta\omega$ generated in half-space and in the interior of the cavity, respectively
ρ, ρ_c	Fluid mass density in half-space and in cavity, respectively
ρ_s	Structural mass density of plate
σ_n	Specific cavity wall susceptance
τ	Time delay variable equal to t-t'
τ_w	Local wall shear stress
$\Phi_{p_{b\ell}}(k_x, k_y, \omega)$	Wavenumber-frequency spectrum of the blocked pressure
$\phi(x, y, z, t)$	Velocity potential in the cavity space
$\phi_n(\bar{\xi})$	Cavity mode eigenfunction
$\Psi(k_x, k_y, z)$	Fourier transform of acoustic velocity potential in half-space
$\psi(x, y, z)$	Acoustic velocity potential in half-space; phase angle
$\psi^s(\bar{x})$	Plate mode s eigenfunction
$\Omega(k_x, k_y)$	Equal to $\Psi\|_{z=0} \equiv \Psi(k_x, k_y, 0)$
ω	Circular frequency variable
ω_s	Plate mode s resonance frequency
$*$	Complex conjugate
$\|\ \|$	Magnitude
$Re(I), I_m(I)$	Real and imaginary parts of I, respectively
$\langle \ldots \rangle_t$	Time average
$x \rightarrow y$	Indicates that x "becomes" or "approaches" or "implies" y
$x \leftrightarrow y$	Interchange of the symbols x and y
$\mathcal{F}$	Fourier transform
T	Truncation of random variable
Σ_i	Summation over all values for i

ABSTRACT

This report presents a method and computer program for calculating certain spectral quantities for the vibration as well as the external (half-space) and internal (cavity) acoustic radiation of a plate-cavity system represented as a rectangular parallelepiped. The upper surface of the plate, lying outside of the cavity, is excited by boundary layer turbulence. The lower surface of the plate covers the cavity. The walls of the cavity are either all rigid or uniformly nearly absorbtive, i.e., nearly all rigid. The plate is thin, flat, flexible, isotropic, rectangular, and finite and is either simply supported or clamped-clamped at its boundaries which are contiguous with an infinite, rigid, planar, baffle. The fluid at the boundaries of both sides of the plate, external and internal to the plate cavity system, may consist of any combination of heavy (or dense) and light fluid media. Thus, the plate is acoustically coupled to the external flow field and to the field within the cavity.

The method treats intermodal auto- and cross-resistive and reactive coupling, associated with structural-acoustic interaction, induced by the fluid in the half-space above the plate and by the fluid in the cavity beneath the plate. Excluding cavity effects, the half-space coefficients are analytically evaluated for acoustically fast (surface) modes, acoustically slow (edge and corner) modes, and all possible combinations of these modes. The results therefore represent a more complete calculation of the intermodal coefficients than those obtained by Davies. The results are also shown to be of greater generality than those of Davies because in almost all cases, they reduce to his first order results as a special case.

The vibroacoustic spectral quantities for the plate-cavity system which are mathematically formulated and programmed (for computations in narrow bands) include:

1.   The cross-spectral density and power spectral density of plate displacement.

2.   The cross-spectral density and power spectral density of cavity acoustic pressure for hard or almost hard walls.

3.   The complex spectral density of power generated in the half-space above the plate.

4.   The cross-spectral density and power spectral density of acoustic pressure in the distant far field of the half-space.

Additional results of the analysis (but presently excluding computer programs) are:

5.   A general formulation, requiring analytical evaluation, for the cross-spectral

1

density and (by implication) power spectral density of the acoustic pressure anywhere in the half-space, thereby including the near-field acoustic pressure above the plate.

6. The spectral density of complex power generated in the cavity.

The sample computer results presented are based on the response and radiation of resonant acoustically slow modes which pertain to frequencies below the critical frequency.

ADMINISTRATIVE INFORMATION

BACKGROUND

Ship designers are interested in the sound radiated from vibrating complex structures excited by turbulent wall pressure fluctuations. They wish to minimize significant radiation directed both outward to the medium external to the hull (making the structure detectable) and inward to the structure interior, e.g., internal to a sonar or to a trough (hindering the capabilities of detection and other gear within the structure as well as adding an unacceptable amount of self-noise to the human environment). Hence, a method for computing the vibro-acoustic response of structures immersed in a turbulent fluid is of value to the designer by permitting him to select appropriate structural parameters, geometry, damping coatings, and treatments to suppress structural vibration and the associated radiation of sound.

Four computer programs are available[1] for determining the vibratory response of a finite rectangular plate to fully developed turbulence and the associated acoustic radiation. Several computational frameworks are provided which can be modified and extended through additional research to furnish more accurate and realistic programs to meet naval needs. The chief objective of the original study was to furnish a base for future development.

Extension of these computations are also available[2-6]. Option 1 includes a correction in the computer programs to account for the effects of the boundary layer thickness and pressure pickup dimensions on the mathematical model representing the observed pressure statistics and on the corresponding vibroacoustic response.[2] Option 2 includes the vibration modes and natural frequencies of thin, finite, rectangular plates with clamped and rotational supports and cylindrical curvature in the programs.[3] Option 3 includes fluid loading (i.e.,

---

[1]References are listed on page 204.

2

added mass) of these plates in the programs.[4] Option 4 includes radiation damping (i.e., added damping) of these plates in the programs.[5] Option 5 derives simple expressions for computing the far-field mean-square acoustic pressures of arbitrarily excited plates; it expands the applicability of the program by treating turbulence excitation in particular.[6] The chief results of the research performed in References 1 through 5 are presented in Reference 39. To summarize, the overall program now includes the vibratory and far-field response of turbulence-excited, simple and clamped plates in water and in air.

INTRODUCTION

The studies cited above treat the computation of the turbulence-induced vibratory response of a hull plate and the associated outgoing far-field acoustic radiation. To meet another significant naval need, we now proceed to complement the foregoing computation by considering a more complex model, the plate-cavity system.[7,8] This model treats the turbulence-induced vibratory response of the (hull) plate and the radiation from the plate both outward to the medium and inward to the cavity. For example, the model could idealize (1) a trough with the plate representing a structure covering the cavity and interfacing with the exterior fluid or (2) a sonar dome with the plate representing a sonar window to the exterior fluid. For simplicity, the model in the present investigation is chosen to represent a trough. The trough is simulated as a rectangular parallelepiped cavity covered by a thin rectangular plate imbedded in an infinite, solid, planar baffle. The upper surface (z<o) of the trough is excited by a turbulent boundary layer being convected along the x-axis; see Figure 1.

The chief objectives of the present study are to investigate the basic physical mechanisms associated with (1) plate-acoustic field interaction for the fluid-loaded plate-cavity system and (2) the contribution of turbulence excitation to the acoustic pressure fields, i.e., to flow-induced noise internal and external to a fluid-loaded plate-cavity system. This includes the development of an experimental computer program to determine the feasibility of actually making computations by using the methods developed here. Running time for a particular computation is also evaluated.

The most significant results of the present investigation are (1) the computation of the intermodal coupling coefficients for a fluid-loaded rectangular plate and (2) the development of a method and computer program for calculating certain spectral quantities for the vibration as well as for the external (half-space) and internal (cavity) acoustic radiation of a turbulence-excited plate-cavity system represented as a rectangular parallelepiped. For the present analysis, five sides of the cavity are considered as rigid or almost rigid and the flexible plate that represents the sixth side as flush-mounted in an infinite rigid planar baffle. The densities of the fluids in the half-space and in the cavity are arbitrary, allowing for any

3
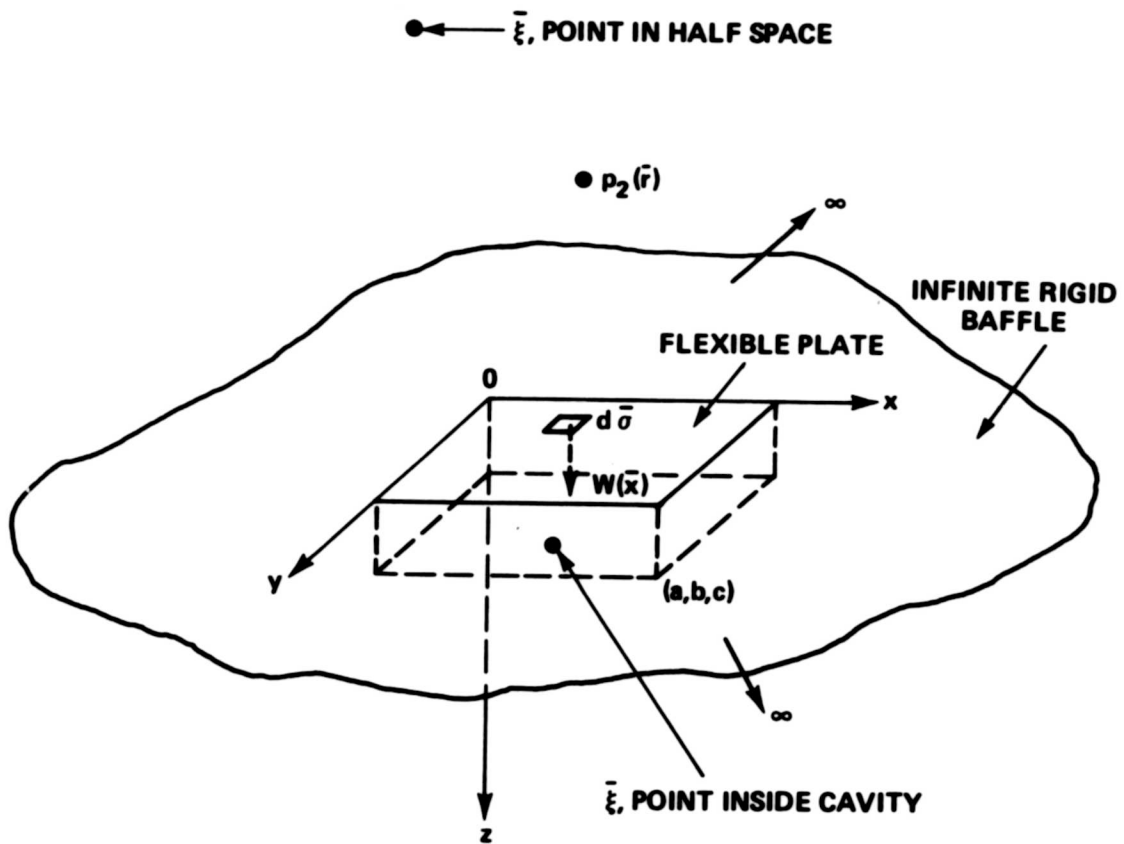
Figure 1 — Plate with Coordinate System-Fluid Occupies Half-Space $z < 0$

combination of heavy and light fluid loading on the upper and lower sides of the plate. Thus, in general, the plate covering the cavity is acoustically coupled to both the external flow field and the field within the cavity.

Davies[9,10] has derived expressions for the half-space intermodal coupling coefficients for a thin, flat, flexible, isotropic, simply supported finite rectangular plate with a dense fluid on one side. The coefficients occur in analysis when the normal vibration response of the plate is expanded in a series of *in vacuo* modes.[7,8] The effect of plate-fluid interaction leads to a coupling of *in vacuo* modes represented by an infinite set of simultaneous linear equations to be solved for the infinite number of unknown modal response amplitudes. The coefficients in these equations, defined by integrals which couple an (mn) *in vacuo* plate mode to a (qr) *in vacuo* plate mode,* have been evaluated approximately by Davies for various wavenumber and frequency regimes. The results lead to a fundamental understanding of the mechanisms associated with vibroacoustic response of plate-fluid systems. Leibowitz[4,5] has compared and summarized the earlier work of various researchers in this area. He has also used some of the results to compute the turbulence-induced vibrations and radiations of thin, simply supported and clamped finite rectangular plates in an infinite rigid baffle subject to water loading.

The report develops and extends earlier presentations in detail.[8-11] Note that Reference 11 restricts itself to offering a more complete and exact calculation of the half-space intermodal coefficients than given by Davies through a term-by-term evaluation of lower and higher order terms comprising the coefficients; Davies presented only first-order approximate evaluations for the coupling coefficients. In general, the results represent more exact approximations for the coefficients which, as shown by a comparison of results, reduce identically to Davies first-order asymptotic results for nearly all cases.

In computer calculations, the intermodal coupling coefficients evaluated here are more generally and easily used than the more limited evaluations by Davies; see Davies[9] and Leibowitz [4-6] for further discussion and application of the coefficients.

In computing spectral quantities for the response and radiation of a fluid-loaded plate-cavity system excited by boundary layer turbulence, the turbulence excitation function is assumed to be described by a semiempirical model devised by Maestrello.[1,12] The development of an experimental computer program designed to enable the calculation of the spectral quantities is documented. The computer program permits the calculation of the narrow-band cross-spectral density and spectral density of (1) the plate displacement, (2) the cavity acoustic pressure for hard or almost hard walls, and (3) the acoustic pressure in the distant

---

*That is, the coefficients express the plate-fluid interaction by means of the coupling.

5

far field in the half-space. Computer calculation of the complex spectral density of power generated in the half-space above the plate is also allowable. The sample computer results presented are for resonant acoustically slow modes which correspond to frequencies below the critical frequency.

DISCUSSION

SUMMARY OF RESULTS

Table 1 summarizes the key features of several earlier investigations (referenced in the table[7, 13-23]) of the vibroacoustic response and noise reduction of a finite, closed panel-cavity system subject to various types of panel excitation; complementary material is cited in the bibliography. The present study extends this work by allowing for the effects of plate-dense fluid interaction (including coupling of the plate to both the fluid in the half-space and in the cavity) on the plate vibration and acoustic fields generated in the half-space and in the cavity. We treat a boundary-layer, turbulence-excited plate-cavity system. The identification and location of the chief results of the study are given in Table 2 together with a commentary on their agreement with those of Davies. Note that J_R^{mnqr} and J_x^{mnqr} respectively represent the radiation (real) and reactive components of the half-space intermodal coupling coefficient J^{mnqr}, which were obtained by evaluation of Equation (53) for the various modal designations given in the table. Also the results for I^{mnqr} were found for almost hard walls or hard walls only and for a simply supported plate enclosing these walls of the cavity. Lastly, we observe that the programmed analytical (working) expressions for the vibroacoustic spectral quantities include only the contributions of the joint acceptances; the contributions of the cross acceptances have been shown to be negligible.

Additional results are discussed below.

METHOD OF ATTACK AND THEORETICAL RESULTS

A brief survey of the material to be found in Appendix A through G is given below. The survey will help the reader to rapidly target a particular topic as well as appreciate the general approach to the problem.

Appendix A – Presents the derivation of the wave equation for a convected fluid, thereby including the Mach number (M) in the basic equation. With a flexible plate treated as one surface of a plate-cavity system (hitherto described), solutions in the form of integral equations are derived by means of a Green function-Fourier transform-normal mode approach. The solutions as a function of M are:

**TABLE 1 — VIBROACOUSTIC RESPONSE AND NOISE REDUCTION OF A
FINITE CLOSED PANEL-CAVITY SYSTEM SUBJECT TO
VARIOUS TYPES OF PANEL EXCITATION**

TABLE 1 – VIBRO-ACOUSTIC RESPONSE AND NOISE REDUCTION OF A FINITE CLOSED PANEL-CAVITY SYSTEM SUBJECT TO VARIOUS TYPES OF PANEL EXCITATION

REFERENCE	AUTHORS NOTATION		THEORETICAL APPROACH	MAJOR ASSUMPTIONS AND LIMITATIONS
7	A_p	panel area, equal to $b \times c$	Two different approaches are presented, namely	**For SEA Approach**
	a, b, c	dimensions of cavity, lying along the x, y, and z axes respectively	(1) Statistical energy analysis (SEA)	1. Assumptions inherent to the statistical energy method.
	C_{Nr}, D_{Mq}	coefficients representing modal amplitudes for the Nr and Mq modes respectively	(2) Integral equation approach using Green's function	2. Internal power loss is negligible for small enclosures.
	c	speed of sound in air		**For Integral Equation Approach**
	f, f_c, f_s	frequency, critical frequency, and frequency of the structure for mode s respectively		1. Acoustically induced coupling of the structural modes.
	$G_p^o(x/\xi; \omega)$	Green's function for space outside the cavity		2. Any damping if present is considered in the analysis to be due to panel flexure; thus, internal acoustic damping effects for small enclosures are ignored.
	g	gravitational constant		
	h	panel thickness		3. In vacuo modes and natural frequencies of the structure are available; the mode functions are orthogonal.
	$j_M^2(\omega), j_N^2(\omega)$	joint acceptance functions for panel mode numbers M and N respectively		
	k	acoustic wavenumber, equal to ω/c		4. $\lim_{r \to o} r^2 \frac{\partial S}{\partial r} = 4\pi$, $\lim_{r \to o} r^2 S = o$, Sommerfeld radiation condition, and $\frac{\partial G_p^o}{\partial \nu} = o$.
	L_3	equal to $4(a+b+c)$		
	M, N	panel mode numbers		
	N	total number of modes		5. Completeness of the set of functions $\Psi_s(\bar{x})$ representing the in vacuo modes of the structures, i.e., the structural displacement can be constructed from a linear combination of the functions.
	M_p	panel mass		
	M_s	modal mass approximately equal to $\frac{M_p}{4}$		
	NR	noise reduction		
	n	a point on the structure		6. Rectangular parallelopiped enclosure (i.e., x) is rigidly baffled exposing only the simply supported flexible panel to external excitation which is estimated to be the blocked pressure, i.e., the radiation pressure associated with the external acoustic field is ignored.
	n_1	modal density of a room of volume V_1, equal to $\frac{4nV_1 f^2}{c^3}$ (asymptotic expression)		
	n_3	modal density of a room of volume $V_3 (= abc)$, equal to $\frac{4\pi V_3 f^2}{c^3} + \frac{\pi S_3 f}{2c^2} + \frac{L_3}{8c}$		
	P_1, P_3	exterior and interior pressures respectively		
	$\langle P_r^2 \rangle, \langle P_3^2 \rangle$	space average mean square exterior and interior pressures, respectively, considering the internal field reverberant		
	P_r	panel perimeter		
	p, q, r	cavity wavenumber		
	Q	quality factor, equal in a modal average sense to $\frac{1}{\eta_p}$		
	Q^s	quality factor (or dynamic magnification factor) equal to $\frac{\Delta f_s}{f_s} = \frac{\pi}{\delta_s}$; at resonance $Q^s = \frac{1}{\eta_s} = \frac{1}{2\zeta_s}$		
	R_s^{mech}	by definition, equal to $4R_{mech}^s$. Hence, equal to $4\eta_s\omega_s M_s = \eta_s\omega_s M_p$		
	R_{mech}^s	modal mechanical resistance equal to $\int_a [\Psi^s(\bar{x})]^2 d\sigma = \eta_s\omega_s M_s$ for the uncoupled modal equation with damping present where $\int_s [\Psi^s(\bar{x})]^2 d\sigma \approx \frac{S}{4}$ assuming all higher modes have approximately the same modal mass, i.e., uniform areal mass		
	R_{mech}^{avg}	modal average mechanical resistance over a band of frequencies containing N modes, equal to $\frac{1}{N}\sum_{N, \Delta\omega} R_s^{mech} = \frac{1}{N}\sum_{N, \Delta\omega} \eta_s\omega_s M_p = M_p(\frac{1}{N}\sum_{N, \Delta\omega} \eta_s\omega_s) = \eta_p\omega M_p$. where ω is the band center frequency		
	R_{rad}^{avg}	equal to $\frac{2}{\pi^2}\rho c P_r \lambda_c (\frac{f}{f_c})^{1/2}$		
	r	equal to $\frac{V_1}{n_1}\frac{n_3}{V_3} + 1$ (asymptotic value)		
	S	surface area		
	S_3	equal to $2(ab+ac+bc)$		
	$S_p(\omega)$	exterior space average power spectrum of pressure with the structure removed		
	$\overline{S_p^i(\omega)}$	interior space average power spectrum of pressure, ignoring acoustic reactance and neglecting cross acceptance functions		
	V_1	volume of room with modal density n_1		
	V_3	volume of room with modal density n_3, equal to abc		
	x, y, z	rectangular coordinates		
	$\bar{x}$	variable point on surface of the structure		
	x_o, x_n	displacement at the origin and point n of the structure, respectively		
	$\bar{Y}_{mn}$	equal to $\omega_{mn}^2[1 - (\frac{\omega}{\omega_{mn}})^2 + j2\zeta_{mn}\frac{\omega}{\omega_{mn}}]$		
	r	weight density of panel		

RELEVANT RESULTS	REMARKS OR MISCELLANEOUS
SEA Approach – Wide Band Analysis $$NR = 10 \log_{10} \frac{\langle p_1^2 \rangle}{\langle p_3^2 \rangle} = \frac{R_{mech}^{avg} + R_{rad}^{avg}}{r \, R_{rad}^{avg}}$$ **Integral Equation Approach – Narrow Band Analysis** The following relation was used to compute the narrow band noise reduction for the box in a reverberant acoustic field ignoring acoustic reactance and cross acceptance functions. $$\frac{\overline{S_p^1(\omega)}}{S_p(\omega)} = \frac{2\rho^2 \omega^4 g^2}{\pi^4 \gamma^2 h^2 g^2} \sum_{M,N} \sum_{P,Q,r} \frac{\epsilon_p \epsilon_q \epsilon_r C_{Pq}^2 D_{Mq}^2 j_M^2(\omega) \, j_N^2(\omega)}{|\nabla_{MN}|^2 (\lambda_{P,q,r}^2 - k^2)^2}$$ $$II = \log_{10} \frac{A_p \eta_p}{h^2} \begin{cases} < 3 & \text{Resonance transmission theory applicable} \\ > 4.5 & \text{Nonresonant modes predominate, forced wave theory applicable} \\ 3 < II < 4.5 & \text{Resonant and nonresonant modes may be equally significant transmitters} \end{cases}$$	1. The results are applicable to small enclosures; hence the effects of coupling between structural modes induced by the acoustics of the internal fluid should be considered. Statistical energy analysis assumes that there is no modal coupling. 2. For most practical engineering package sizes and panel thicknesses, the results indicate that induced modal coupling as well as the effective mass loading are small and can be ignored, except near the cavity modal frequencies. At these frequencies the coupling induces a panel resonance and antiresonance not normally present in the uncoupled response. Unless the transmission at or near one of these frequencies is desired to high accuracy, the effect can be ignored in noise reduction computations. 3. At low frequencies cross acceptance functions can be neglected. At high frequencies some inaccuracy is introduced by neglecting the cross acceptance functions. Moreover, including them in a narrow band estimate is computationally inaccurate. The existence of cross terms implies that the panel modes are not truly statistically independent, but may be very nearly so for the frequency range under consideration. 4. In the high frequency regime, the nonresonant noise reduction is essentially a smooth, slowly varying function. 5. Large, thin, heavily damped panels tend to respond in a nonresonant fashion. The results present a nondimensional parameter II called the "participation factor," defined for flat aluminum panels, to estimate the predominance of resonance or nonresonance panel response prior to transmission studies. For II > 3 caution should be exercised in using statistical energy analysis.

REFERENCE	AUTHORS NOTATION		THEORETICAL APPROACH	MAJOR ASSUMPTIONS AND LIMITATIONS
7 (Cont.d)	a	ad hoc damping coefficient		
	Δf_s	incremental frequency for mode s (Hz)		
	$\Delta \omega$	incremental circular frequency in radians/sec		
	δ_s	logarithmic decrement for mode s, equal to $\frac{1}{n} \ln \frac{x_o}{x_n}$		
	$d\sigma$	element of surface area		
	$\epsilon_p, \epsilon_q, \epsilon_r$	equal to 1 for p, q, r = o. equal to 2 for p,q,r > o		
	ζ_s	equivalent viscous damping on a modal basis, i.e., hypothetical percentage of critical damping for mode s		
	η_p	panel loss factor, equal to $\frac{R_{mech}}{\omega M_p} = \frac{1}{Q}$ in a modal average sense, i.e., average loss factor over the modes considered over a band of frequencies		
	η_s	hypothetical structural damping coefficient or factor for mode s, equal to $2\zeta_s\left(\frac{\omega}{\omega_s}\right)$ and therefore at resonance equal to $2\zeta_s = \frac{1}{Q_s}$		
	λ_c	critical wavelength		
	$\lambda^2_{p,q,r}$	square of cavity eigenvalue, equal to $\left(\frac{p\pi}{a}\right)^2 + \left(\frac{q\pi}{b}\right)^2 + \left(\frac{r\pi}{c}\right)^2$; p, q, r = 0, 1, 2		
	$\partial \nu$	differential length normal to surface of structure, pointing into the cavity		
	$\bar{\xi}_s$	modal coordinate, where bar indicates its complex nature		
	Π	participation factor		
	ρ	density of air		
	$\Psi_s(\bar{x})$	in vacuo structural modes (or eigenfunction) equal to $\sin \frac{m\pi y}{b} \sin \frac{n\pi z}{c}$; m,n = 1, 2, 3		
	ω	circular frequency; band center frequency (radians/sec)		
	ω_s	circular resonance frequency for mode s in radians/sec		
	ω_{mn}	circular resonance frequency for mode mn in radians/sec		
13, 14	a	acceleration	Statistical Energy Analyses	1. The calculation of the response of a single mode is significant; that is the modal Q's are high (structural damping produces no coupling between the modes).
	c	speed of sound		
	$\eta_R(\omega)$	modal density of the large room and is equal to $\frac{\omega^2 V}{2\pi^2 c^3}$		2. Coupling between acoustic and structural modes is weak and linear. Only sets of structural and acoustic modes covering the same frequency band are coupled. Each mode in the set of structural modes is equally coupled to each mode in the set of acoustic modes over the band, i.e., a single structural mode interacts with many acoustic modes.
	$<p^2>$	mean square acoustic response		
	R_{rad}	radiation resistance of the structure or structure to room coupling resistance		
	$S_a(\omega)$	acceleration spectral density of the structure evaluated by multiplying the mean square acceleration per structural mode by the number of modes in a band 1-cycle wide		3. The acoustic field is reverberant or diffuse, i.e., uniform distribution in angle of uncorrelated modes in a frequency band so that the modal density or sound intensity is independent of angle and position for that band. The acoustic spectrum is nearly flat over a frequency band exceeding the modal bandwidth.
	$S_p(\omega)$	is the spectral density of the mean square acoustic pressure in the room equal to $\frac{<p^2>}{\Delta\omega}$		4. The response is multimodal.
	V	volume of the room		5. Modal amplitudes are statistically independent in the sense that the total response energy in each finite frequency band is assumed equal to the sum of the response energies of the resonant modes contained within that band; the reverberant field assures this property at sufficiently high frequencies, i.e., for large modal densities.
	β_r	damping coefficient equal to $\omega\eta_R$		
	η_R	dissipation loss factor of room		6. Equipartition of modal energies, i.e., all modes within a frequency band have equal mean energy.
	ρ	ambient density of fluid		
	ω	circular frequency		7. Room to structure coupling loss factor is much smaller than the dissipation loss factor of the room.
	$\Delta\omega$	frequency band		
15	A_p	panel area (a × b)	For low frequencies: Simple pressure-volume displacement relationship.	1. For low frequency computation C_p of clamped plate is restricted to plate aspect ratios greater than 1.5.
	a, b, c	dimensions of box enclosure with b and a being the width and height of the flexible panel respectively, and c the depth dimension of the box normal to the panel		2. Intermediate and high frequency computations for a simply supported plate include the assumptions and limitations inherent to the statistical energy method of analysis.
	C_b	acoustic compliance of interior free volume, equal to $\frac{V_b}{\rho c_a^2}$	For high frequencies: statistical energy methods.	
	C_p	acoustic compliance of panel, equal to $10^{-3}A_p^3 F(\alpha)/D$		3. Plate critical frequency is higher than the first acoustic resonance frequency of the enclosure.
	c_a	speed of sound in air		
	c_ℓ	longitudinal wave velocity in panel material		
	D	panel bending rigidity, equal to $\frac{c_p c_\ell^2 h^3}{12}$		

10

RELEVANT RESULTS	REMARKS OR MISCELLANEOUS
$$\frac{S_p(\omega)}{S_a(\omega)} = \frac{<p^2>}{<a^2>} = \left(\frac{\rho}{c}\right)\left(\frac{R_{rad}}{\beta_r}\right)[2\pi^2\eta_R(\omega)]^{-1} = \frac{R_{rad}}{\eta_R} \cdot \frac{\rho c^2}{V\omega^3}$$	1. The result is the power spectrum ratio resulting from the interaction of a reverberant acoustic field with either 'a) a single structural mode or (b) many structural modes, i.e., reverberant field of structural vibration. It refers to direct excitation by external random forces with consequent generation, via the vibrating structure, of a reverberant acoustic field in a large room. 2. The statistical energy method ignores nonresonant modal energy which may be significant when damping is not sufficiently light. 3. The results should be applied to cases where all structural modes in the frequency band of interest are uniformly coupled to all room modes in the band. If differently excited or differently coupled modes occur in the band, one must divide them into subsets of like modes, and apply the results to each subset separately using properly modified modal density expressions.
1. <u>Low Frequencies</u> (both panel and enclosed volume are stiffness controlled) $$NR = 20\log\frac{p}{p_b} = 20\log\left(1 + \frac{C_b}{C_p}\right)$$ 2. <u>Intermediate Frequencies</u> (panel is resonant and volume is stiff) a. For transmission due to one mode in a frequency band, i.e., for a single volume-displacing mode in $\Delta\omega$ (For largest dimension αa; if largest dimension βa then multiply by $(a/\beta)^8$) $$NR = 10\log\frac{<p^2>}{<p_b^2>} = 10\log\frac{3\pi^8\beta^2}{2^{13}a^4}\left(\frac{f}{f_a}\right)^8\left(\frac{c_a}{c_l}\right)^2\left(\frac{a}{h}\right)^2\Gamma^2\frac{\Delta\omega}{\omega}\eta_p$$ Lower limiting envelope	1. The results are applicable to a <u>small</u> enclosure. 2. The results do not include the effect of the cavity (back pressure) on panel modes and frequencies. 3. At very low frequencies both wall and enclosed volume are stiffness controlled. It is assumed that the first in vacuo panel mode has a resonance frequency lower than the first acoustic cavity resonance of the box volume. At intermediate frequencies this means that the acoustic wavelength is greater than the flexural wavelength at the first panel resonance. This requires the critical frequency of the panel (the frequency where the bending wavespeed equals the speed of sound) to lie above the lowest acoustic resonance frequency (assumption 3). Thus, a range exists, starting from the fundamental natural frequency of the panel and ending prior to

11

REFERENCE		AUTHORS NOTATION	THEORETICAL APPROACH	MAJOR ASSUMPTIONS AND LIMITATIONS
15 (Cont'd)	$F(a)$	function determining effect of aspect ratio on panel stiffness, plotted for simply supported and clamped plates in the reference		
	f	frequency		
	f_a	frequency of first volume resonance		
	f_c	critical frequency of panel		
	h	panel thickness		
	k	acoustic wavenumber		
	k_p	panel bending wavenumber		
	M_p	mass of panel		
	NR	noise reduction		
	n_b	modal density of box interior		
	n_p	modal density of panel in radian frequency equal to $\dfrac{\sqrt{3}\,A_p}{2\pi h c_i}$		
	n_R	modal density of room		
	P	panel perimeter, equal to $2(a+b) = 2a(1+a)$		
	p	external sound pressure		
	$<p^2>$	mean square pressure in incident reverberant field in a bandwidth $\Delta\omega$		
	p_b	internal sound pressure		
	R_{in}	transverse-point impedance equal to $\left[\left(\dfrac{4}{\sqrt{3}}\right)\rho_p c_i h^2\right]$		
	R_{rad}	radiation resistance of a panel equal to $\dfrac{2}{\pi^2}\rho c_a P\lambda_c\left(\dfrac{f}{f_c}\right)^{1/2}$ for an octave or more below f_c		
	R_{rad}^{int}	radiation resistance of panel due to interior of enclosure, i.e., looking into the box interior, equal to $\left(\dfrac{4}{\pi^2}\right)\rho c_a P\lambda_c\left(\dfrac{f}{f_c}\right)^{1/2}$		
	r	modal-density ratio, equal to $\dfrac{V_R}{n_R}\dfrac{n_b}{V_b} = 1 + \dfrac{3}{2}\dfrac{a\beta + a + \beta}{\beta}\dfrac{f_a}{f}$ $+ \dfrac{3}{2\pi}\dfrac{a(1+a+\beta)}{\beta}\left(\dfrac{f_a}{f}\right)^2$ (asymptotic form)		
	T	reverberation time		
	V_b	interior volume		
	V_R	room volume		
	Γ	ratio of material parameters equal to $2\pi\sqrt{3}\left(\dfrac{c_a}{c_i}\right)\left(\dfrac{\rho_p}{\rho}\right)$		
	$\Delta\omega$	noise bandwidth		
	a	panel aspect ratio, equal to $\dfrac{b}{a}$		
	β	ratio of box depth to height, equal to $\dfrac{c}{a}$		
	η_b	loss factor for box interior, expressible by $\eta_b = \dfrac{2.2}{fT}$		
	η_p	panel loss factor		
	λ_c	acoustic wavelength at critical frequency equal to $\dfrac{c_a}{f_c}$		
	ρ	density of air		
	ρ_p	panel-material density		
	τ	panel-transmission coefficient		
	ω	radian frequency		
	$<\ >$	symbol for time average operation or mean square quantity in a bandwidth $\Delta\omega$		
16, 17	a, b, c	length, width and depth of the flexible panel lying along x-, y- and z respectively	Vibration of flexible wall represented by doubly infinite Fourier series leads to determination of acoustic velocity potential in box from which the back pressure is computed and included as a generalized force in generalized equations of motion for the modes.	1. Velocity potential expressible as a separable function of the three space variables. The form assumed satisfies the acoustic boundary conditions at the walls.
	$a_{nm}^{(r',s')}$	Fourier coefficients of motion of panel vibrating in the $r's'$th mode		
	c_a	speed of sound		2. The boundary conditions do not allow for absorption at the walls.
	I	identity of matrix		
	K	stiffness matrix		3. Treats only volume displacing modes of vibration which would be the only modes of vibration to be excited by plane acoustic waves normally incident upon the flexible wall and are probably most affected by the cavity — they comprise one quarter of the possible modes of the system and are quite uncoupled to the other three independent types of modes. These modes are symmetric about the panel center lines in both x- and y-directions and only involve even values of m and n.
	$K_{rs}, K_{rs}^{(r',s')}$	direct and cross acoustic (generalized) stiffness, respectively. If the quantity is positive the cavity acts as a stiffness; if the quantity is negative it acts as a virtual mass.		
	M	mass matrix		
	M_{rs}	generalized mass		
	m, n	mode numbers		
	p	acoustic pressure in interior of box		
	p_{back}	cavity acoustic pressure acting on the flexible panel		4. Fluid loading and radiation impedance of fluid external to the box is considered negligible.
	$\bar{p}_o$	scalar mean square pressure at some reference point x_o, y_o on the panel		
	$q_{rs}, q_{r's'}$	generalized coordinates of the panel mode defined by rs and $r's'$ respectively, equal to $w_{rs}e^{i(\omega t - \psi_{rs})}$ and $w_{r's'}e^{i(\omega t - \psi_{r's'})}$ respectively		

RELEVANT RESULTS	REMARKS OR MISCELLANEOUS
b. For transmission, at higher frequencies, due to several volume-displacing modes in a frequency band $\Delta\omega$ (For largest dimension αa; if largest dimension βa then multiply by $\left(\frac{a}{\beta}\right)^a$) $NR \Big|_{\substack{\text{average value}}} = 10 \log \frac{<p^2>}{<p_b^2>} = \frac{\pi^a \beta^2}{128\, a^3 (1+a)^2}\ \Gamma^{-2} \eta_p \left(\frac{f}{f_a}\right)^a$	the fundamental frequency of the cavity, in which the panel behaves in a resonant fashion and the box volume acts like a stiffness. Since the incident (driving) acoustic wavelength exceeds the box dimensions we may assume the incident sound field at intermediate frequencies continues (as at low frequencies) to apply an essentially uniform pressure to the panel face. At <u>high</u> frequencies, extending upward from the natural frequency of the fundamental cavity mode, the panel dimensions exceed both the acoustic and flexural wavelengths. To satisfy the boundary conditions both "forced wave or mass controlled response" and "free wave or resonance response" of the panel exist, the former usually governing the NR at frequencies well above the first acoustic cavity mode and below the critical frequency.
3. High Frequencies, $f > f_a$ (panel and acoustic space have resonant behavior) $NR = 10 \log \frac{<p^2>}{<p_b^2>} \Big|_{\substack{\text{resonant or free wave panel vibrations}}} = \frac{1}{4\pi} k^3 V_b\, \eta_b\, \eta_p\, \frac{\omega M_p R_{in}}{R_{rad} R_{rad}^{int}} \left[\frac{V_b\, \eta_n}{\eta_b\, V_n}\right]$ $\sim \frac{\omega \eta_p M_p}{r R_{rad}}$ The approximation is based on the assumption that interior acoustic losses are entirely due to panel vibration, thereby yielding equal modal energy (thermal equilibrium) between panel and interior acoustic modes. $\cong \frac{3\Gamma \eta_p}{8(1+a)r} \left[\frac{c_a}{c_i}\ \frac{a}{h}\ \frac{2a\sqrt{3}}{\pi}\right]^{1/2} \left(\frac{f}{f_a}\right)^{1/2}$ Assuming further that frequencies lie an octave or more below the critical frequency.	
4. <u>High Frequencies</u>, $f > f_a$ (panel and acoustic wave have nonresonant forced wave behavior) $NR = 10 \log \frac{<p^2>}{<p_b^2>} \Big|_{\substack{\text{nonresonant or forced wave panel vibration}}} = 4\pi \left(\frac{\beta}{a}\right) \eta_b\, r \left(\frac{f}{f_a}\right)$	
1. **Cavity Acoustic Potential and Pressure** $\Phi = i\omega w_{r's'}\, e^{i(\omega t - \psi_{r's'})} \sum_{n=0}^{\infty} \sum_{m=0}^{\infty} \frac{a_{nm}^{(r's')} \cosh (\mu_{nm} z)}{\mu_{nm} \sinh (\mu_{nm} z)} \cos\left(\frac{n\pi x}{a}\right) \cos\left(\frac{m\pi y}{b}\right)$ $p = -\rho\, \frac{\partial\Phi}{\partial t}\ ;\ p_{back} = \left(-\rho\, \frac{\partial\Phi}{\partial t}\right)_{z=c}$ **2.** <u>Equations of Panel Vibration in Terms of in vacuo Modes</u> $w_p (x, y, t) = \sum_{r=1}^{r} \sum_{s=1}^{s} q_{rs} \sin\left(\frac{r\pi x}{a}\right) \sin\left(\frac{s\pi y}{b}\right)$ where $q_{rs} = w_{rs} e^{i\omega t}$ and ω are determined from the set of equations	**1.** The effect of the cavity on wall vibration is due to the back pressure. The analysis includes this effect, in terms of direct or cross acoustic stiffness*, of a closed backing cavity on the free vibrations of a bounding flexible panel; the effect results in the modification of <u>in vacuo</u> values of panel natural frequency and mode shape, i.e., the cavity produces direct or cross acoustic stiffness or inertial coupling of the various panel modes (see Notation for $k_{nm}^{(r's)}$. Thus the combination of panel and cavity modifies both the panel vibrations and cavity acoustics. **2.** The analysis shows that when the acoustic stiffness is of the same order as or greater than the panel stiffness (e.g., light or flexible panels and shallow cavities) there is very heavy coupling and large changes occur in the fundamental natural frequency of the panel and, to a lesser extent, in the overtone frequencies. The mode shapes are also considerably altered. However, when the acoustic stiffness is considerably less than the panel stiffness (e.g., heavy or stiff panels and relatively deep cavities) the coupling is light and the panel vibrations are negligibly affected by the cavity. For this case the acoustic field in the box can be calculated directly from the (unmodified) <u>in vacuo</u> vibrations of the panel.

13

REFERENCE	AUTHORS NOTATION		THEORETICAL APPROACH	MAJOR ASSUMPTIONS AND LIMITATIONS
16, 17 (Cont'd)	$r, s; r', s'; \ell, \tilde{s}$	mode numbers		5. Simply supported panel is considered to be vibrating freely in a mode consisting of a limited sum of modified in vacuo panel modes and the damping is zero. The modified modes include the stiffness or virtual mass effect of the backing cavity.
	t	time		
	$w_p(x,y,t)$	amplitude distribution of panel, equal to $\sum_{r=1}^{\bar{r}} \sum_{s=1}^{\bar{s}} w_{rs} \sin \frac{r\pi x}{a} \sin \frac{s\pi y}{b} e^{j(\omega t - \Psi_{rs})}$		
	$w_{rs}, w_{r's'}$	amplitude of the plate eigenfunction for the rs and r's' modes respectively		
	x, y, z	rectangular coordinates for the box cavity system, with one corner of the box at the origin and the flexible panel at $z = c$.		
	x_o, y_o	reference point on panel		
	μ_{nm}	equal to $\pi^2 \left[\left(\frac{n}{a}\right)^2 + \left(\frac{m}{b}\right)^2 \right] - \frac{\omega^2}{c_a^2}$		
	ρ	density of fluid in cavity		
	Φ	acoustic velocity potential		
	$\Psi_{rs}, \Psi_{r's'}$	phase lag between the motion in mode rs or r's' and the harmonic force which is causing the motion		
	ω	circular (or radian) frequency		
18	A_w	total area of the box walls	Statistical Energy Analysis	1. Broadband random excitation.
	A_{wj}	area of the box wall j		2. Assumptions inherent to Statistical Energy Analysis. In particular the structural-acoustic model of the complex dynamic system pertains to (a) a linear system with small losses, (b) loosely and conservatively coupled subsystems whose modes can be approximated by the modes of nondissipative uncoupled subsystems, (c) a reverberant field of vibration by which it is meant that the modes within the subsystems and frequency bands are temporally uncorrelated, i.e., are statistically independent, and have equal mean energy, or have equipartitioned energy, (d) wide-band excitation under which each mode accepts most of its energy in a narrow band around its resonance frequency. For stationary random conditions the mean kinetic and potential energies in each mode are equal to each other. Then ignoring results for individual modes the mean spectrum of energy stored in, and power for, the subsystem is obtained as a space-time average of the modal energies and power, additionally averaged over the many modes contained in the frequency band Δf (where $\Delta f \ll \omega$, the band center frequency). The system power and energy is the sum of the powers and energies in the subsystems.
	b	pertaining to box		
	c	speed of sound in air		
	c_w	speed of sound in box plate when all walls are of the same material and of equal thickness		
	c_{wj}	speed of sound in box wall j		
	C_j	wall compliances (ratios of displaced volume to pressure)		
	f	frequency, band center frequency		
	f_{cj}	critical frequency of box wall j in air, equal to $\sqrt{3} c^2 / \pi h_j c_{wj}$		
	h	box wall thickness when all walls are of equal thickness		
	h_j	thickness of box wall j		
	I_r, I_s	mean sound intensity incident upon the box walls and in the enclosed space respectively, i.e., incident and enclosed spectral density of sound power per unit area, averaged over Δf and space		
	L	sum of all box-edge lengths		
	L_{wj}	perimeter of box wall j		
	NR	noise reduction provided by box, ratio of mean-square sound pressures at a location before and after introduction of isolating system		
	n_r, n_s, n_{wj}	average modal density of room, box interior and wall j respectively		
	p_r, p_s	sound pressure in box enclosure and incident pressure in outside room (expected for a rigid box to be within 1 dB of the acoustic pressure on the box surface) respectively		
	r	pertaining to the subsystem r or to room		
	S_b^p, S_r^p, S_s^p	spectral density of equivalent pressure, averaged over time and Δf for box, room and space enclosed by the box respectively		
	V	volume, usually of box		
	w	pertaining to subsystem w or to box walls		
	$\Delta f, \Delta \omega$	averaging frequency band in hertz and radians, respectively		
	η_s^s	loss factor in enclosed space dominated by viscous and thermal losses at the boundary (losses due to internal absorption of the air are considered negligible), equal to $\frac{s_m c A_w}{4 \omega V}$ where $s_m = 18 \times 10^{-6} f^{1/2}$ at room temperature		
	η_b	total wall loss factor, approximately equal to $\eta_{wj}^{wj} + \eta_{wj}^r$: measured loss factor		
	$\eta_{wj}^{wj}, \eta_{wj}^r$	internal loss factor due to dissipation in wall j and coupling loss factor associated with unidirectional flow of energy from wall j to the outside room, respectively		
	μ	modal density correction factor equal to $1 + \frac{A_w c}{8 f V} + \frac{L c^2}{32 \pi f^2 V}$		
	ρ	density of air		
	ρ_w	density of wall material where all walls are of the same material		
	ρ_{wj}	density of material of wall j		
	τ	wall-transmission coefficient		
	ω	radian frequency		

14

TABLE 1 – VIBRO-ACOUSTIC RESPONSE AND NOISE REDUCTION OF A FINITE CLOSED PANEL-CAVITY SYSTEM SUBJECT TO VARIOUS TYPES OF PANEL EXCITATION

RELEVANT RESULTS	REMARKS OR MISCELLANEOUS
$$(-M_{rs}\omega^2 + K_{rs})\,q_{rs} + \sum_{r'=1}^{i}\sum_{s'=1}^{i} K_{rs}^{r's'}\,q_{r's'} = 0$$ or in Matrix form $$[M^{-1}K - \omega^2 I]\{q\} = 0$$ **3. Noise Reduction for Simply Supported Panel-Cavity System when the Panel is Subjected to Harmonically Varying Sound Pressures** $$NR = 20\log_{10}\left|\frac{\dot{p}_o}{p_{back}}\right|$$	3. NR is a function of the plate position chosen for the determination of back pressure and the frequency. The quantity $\left|\frac{p_o}{p_{back}}\right|$ is found from the solution of matrix equations given in the reference. 4. Only the steady state part of the general solution is found here and is used in analyzing the free oscillation of the panel-cavity system. This is not correct since the transient part of the general solution should have been used in this instance. * Cross acoustic stiffness implies that motion in one mode of vibration gives rise to generalized forces in other modes so that the original in vacuo modes are now stiffness coupled. The generalized force is proportional to the generalized displacement of the panel modes of vibration and is therefore regarded as an acoustic stiffness.
1. Low Frequencies (at frequencies below the lowest resonances the box panels and the enclosed air act as pure stiffnesses) $$NR = \left|\frac{p_r}{p_s}\right|^2 = \left[1 + \frac{V}{\rho c^2}\sum C_j\right]^2$$ **2. Intermediate Frequencies** (at frequencies extending from the lowest box panel resonance to somewhat below the lowest acoustic resonance, the air in the box still acts like a pure stiffness closely coupled to the walls but the walls exhibit resonant behavior) a. Noise Reduction at Single-Wall Resonances $$NR = \frac{S_r^p}{S_o^p} = \frac{\pi\Delta f}{2f}\left(\eta_{wj}^{wi} + \eta_{wj}'\right)\left[\frac{3\pi^3\rho_{wj}A_{wj}V}{8\rho h_j c^2 c_{wj}^2}\right]^2$$ b. Noise Reduction in Multimodal Bands $$NR = \frac{S_r^p}{S_s^p} = \omega\eta_b\left[\frac{\pi f^2 V}{c^3}\right]^2\left[\sum_{1}^{3} n_{wj}(\eta_{wj}')^2\right]^{-1}$$ $$= 6\left[\sum_{1}^{3}\frac{L_{wj}^2}{A_{wj}!}\right]^{-1}\eta_b\left[\frac{\pi^3 f^3\rho_w V}{\rho c^2 c_w}\right]^2$$ For all walls of same material and of equal thickness **3. High Frequencies** (at frequencies well above the fundamental panel and acoustic resonances, several panels as well as several acoustic modes lie within the considered frequency bands) $$NR = \frac{S_r^p}{S_s^p} = \frac{n_w\eta_b}{\mu\sum\eta_{wj}'n_{wj}}\left[1 + \frac{n_s\eta_s^5}{\sum\eta_{wj}n_{wj}}\right]$$ **4. Classical Transmission Theory** (Forced waves only) $$NR = \frac{I_R}{I_s} = 1 + \frac{4\omega\eta_s^t V}{cA_w'}$$ For walls of equal transmission coefficient	1. Although all walls of box are flexible in general the results can be applied as a special case to a box with all walls rigid except one. Moreover, for the case of single-wall resonances, all panels whose resonances lie outside the frequency band considered can be considered as rigid over the band. If two opposite box panels vibrate at or near their common resonance frequency and move symmetrically in phase with each other the problem can be reduced to a single nonrigid wall by considering half the volume. 2. Results for intermediate and high frequencies are applicable to a single nonrigid box wall treated as a baffled hinged plate for modes well below the critical frequency f_{cj} of the wall. 3. The classical wall transmission theory takes into account only <u>forced</u> waves as they would appear in a wall of infinite extent. The results for this theory are expected to be valid at high frequencies, where the box panels extend over many flexural wavelengths and the interior space encompasses many acoustic wavelengths. In a range one or two octaves below the critical frequency this theory for the prediction of NR was in better agreement with experiment than the present theory for high frequencies. 4. The transmission behavior of a box at a given frequency is shown to depend on the relation of this frequency to the lowest panel and acoustic resonance frequencies and the critical frequency of the walls. Theory and experiment show that near the lowest panel resonances the pressure in the box may considerably exceed that in the incident sound field. 5. The results obtained from vibration and sound measurements on rectangular aluminum boxes were found to agree reasonably well with theoretical predictions based on various models applicable in different frequency regions.

15

REFERENCE	AUTHORS NOTATION		THEORETICAL APPROACH	MAJOR ASSUMPTIONS AND LIMITATIONS
19	A	amplitude of the transverse velocity of the vibrating wall	Normal Mode Analysis	1. Waves on the wall $f(y,z)$ are unaffected by the sound pressures inside the room.
	a,b,c	room dimensions in x,y,z direction		2. The solution is derived for a room without losses. The losses in the room are introduced in the final solution in the form of complex wave numbers.
	c_o	speed of sound in air		
	f	frequency		3. Only the steady state solution is treated.
	$f(y,z)$	standing wave on wall, equal to $A \cos k_y y \, k_z z$		
	k	acoustic wave number		
	$k_{\ell mn}$	wave number of the ℓmn th mode of the room, equal to $\left[\left(\frac{\ell\pi}{a}\right)^2 + \left(\frac{m\pi}{b}\right)^2 + \left(\frac{n\pi}{c}\right)^2\right]^{\frac{1}{2}}$		
	k_y, k_z	wave numbers of the wave on the wall		
	ℓ,m,n	mode numbers for the room		
	p	sound pressure		
	$<p^2>_{av}$	average of $<p^2>$ for different standing waves on the wall where $<p^2>$ is the space average of $|p^2|$ i.e., $<p^2> = \frac{1}{V}\int_v |p^2| \, dV$		
	T	reverberation time, equal to $6.9/\delta$		
	V	volume of the rectangular room		
	θ	angle between the $\omega_{\ell mn}$-vector and the x-axis; thus $\cos\theta = \frac{\ell\frac{c_o\pi}{a}}{\omega_{\ell mn}}$		
	δ	loss factor of the room		
	ρ_o	density of air		
	ω	equal to $2\pi f$		
	$\omega_{\ell mn}$	equal to $c_o k_{\ell mn}$		
20	a,b	panel dimensions along the x and y axes, respectively	Statistical Energy Methods	1. Assumptions inherent to the Statistical Energy Method but does not assume that either (a) many acoustic modes couple with an individual structural mode even if the modal density ratio is high, or (b) the acoustic field is diffuse.
	c_o	speed of sound in air		
	c_e	speed of flexural waves		
	C_L	speed of longitudinal waves in the panel material		
	f	frequency		
	f_c	critical frequency		
	h	panel thickness		
	I_1	$\simeq \frac{3\left(\frac{f}{f_c}\right)\left(1+\frac{f}{f_c}\right)}{8\left[(\beta_r + \beta_m)\beta_m\right]^{\frac{1}{2}}} I$; $I_2 \simeq \frac{\omega_m^2}{8\left[(\beta_r + \beta_m)\beta_m\right]^{\frac{1}{2}}} I$		
	I_3	$\simeq \frac{(f/f_c)(1+1/f_c)}{8\omega^2\left[(\beta_r + \beta_m)\beta_m\right]^{\frac{1}{2}}} I$; $I_4 \simeq \frac{1}{8\left[(\beta_r + \beta_m)\beta_m\right]^{\frac{1}{2}}}$		
	I	$= \tan^{-1}\left[\frac{\Delta\omega}{\left[(\beta_r + \beta_m)\beta_m\right]^{\frac{1}{2}}}\right] - \tan^{-1}\left[\frac{(\beta_r + \beta_m)}{\left[(\beta_r + \beta_m)\beta_m\right]^{\frac{1}{2}}}\right]$		
	k_p	panel wave number $\frac{2\pi f}{c_e}$		
	k_r	acoustic wave number $\frac{2\pi f}{c_o}$		
	m	an integer or a panel mode subscript		
	n,p,q	integers		
	R_{rad}	radiation resistance		
	r	an integer or an acoustic mode subscript		
	s	area of panel equal to ab		
	V	fluid volume equal to abc		
	x	position vector		
	x,y,z	cartesian rectangular system coordinates		
	β_m, β_r	half power bandwidth of mode m, mode r		
	ϵ	q/n for $q<n$ or p/m for $p<m$		
	ϵ_m	equal to $S^{-1}\int_s \Phi_m^2(x)\,dx$		
	ϵ_r	equal to $V^{-1}\int_v \Psi_r^2(x)\,dx$		
	θ	modal energy/unit mass		
	ρ	density of fluid		
	Φ	panel eigenfunction		
	Ψ	acoustic eigenfunction		
	ω	circular frequency		

16

RELEVANT RESULTS	REMARKS OR MISCELLANEOUS
Average Sound Radiation from a wall with Standing Bending Waves of Sinusoidal Shape (i.e., $f(y,z) = A \cos k_y y \cos k_z z$) $$\frac{\langle p^2 \rangle_{av}}{\langle v^2 \rangle} \approx 0.8 \; \frac{\rho_o^2 c_o^2}{2ab \cos\theta} = \frac{0.4}{\pi} \frac{\rho_o^2 c_o^2 \omega}{\delta\ell} \ell_{mn} \; ; \quad \text{for } \frac{\Gamma \cos\theta}{a} > 0.08$$ and $\cos\theta$ not too small.	1. The results are for the frequency range above coincidence. 2. In the frequency range above coincidence, where $k_y^2 + k_z^2 < \frac{\omega_o^2}{c_o^2} = k^2$ or $c_{wall} > c_o$, for a given standing wave on the wall, i.e., given ω, k_y, k_z, the sound pressure in the room is built up of very few modes with resonance frequency lying close to ω. For in this range the coupling, in a limited frequency interval, of the room waves to the wall waves in the y and z directions is significant only for the very few room modes for which $m\pi < k_y b < (m+1)\pi$ and $n\pi < k_z c < (n+1)\pi$. 3. The analysis indicates that above coincidence the radiation from a standing wave of sinusoidal shape on the wall in a room is on the average very nearly the same as the radiation from the same wave into a semi-infinite space. 4. The solution derived does not satisfy all the boundary conditions. Hence it is not strictly correct although it is useful for an understanding of the panel-room problem.
1. Simply Supported Panel-Subcritical Frequency Range a. $R_{rad} \approx \left[\frac{128}{\pi^5} \rho h C_L (a+b) \right] \left(\frac{f}{f_c} \right)^{\frac{1}{2}} ; \quad f < 0.25 f_c$ b. $R_{rad} = \frac{64 \rho h C_L (a+b)}{\pi^5} \left[\frac{\sin^{-1} \left(\frac{f}{f_c} \right)^{\frac{1}{2}}}{1 - \frac{f}{f_c}} + \tan \left\{ \sin^{-1} \left(\frac{f}{f_c} \right)^{\frac{1}{2}} \right\} \right] ; \quad \frac{f}{f_c} < 0.9$ Note: (a) is a simplification of (b) for the frequency range given for (a). **2. Simply Supported Panel-Subcritical Frequency Range** $R_{rad} = \left(\frac{156}{\pi^5} \right) \left(1 - \frac{f_c}{f} \right)^{-\frac{1}{2}} \rho c_o ab \simeq 0.5 \left(1 - \frac{f_c}{f} \right)^{-\frac{1}{2}} \rho c_o ab$ **3. Clamped Panel** a. $(R_{rad})_{clamped} = 2 (R_{rad})_{simply \; supported} ; \quad$ for edge modes $k_1 \ll k_2$ or $k_2 \ll k_1$ b. $(R_{rad})_{clamped} \approx (R_{rad})_{simply \; supported} ; \quad$ for $k_1 \simeq k_2$ **4. Simply Supported Plate-Non-proximate Modal Coupling at Subcritical Frequencies** $R_{rad} = \frac{4(a+b)\rho c_o^2}{\epsilon_r \epsilon_m \pi^4} \left[\frac{\left(\frac{f}{f_c} \right)^{\frac{1}{2}} \beta_m}{\omega_m} I_1 + \frac{\left(\frac{f}{f_c} \right)^{\frac{1}{2}} \beta_m}{\pi \omega_m^2} I_2 + \left(\frac{f}{f_c} \right)^{\frac{1}{2}} \beta_r \omega_m I_3 + \frac{\left(\frac{f}{f_c} \right)^{\frac{1}{2}} \beta_r}{\pi \omega_m^2} I_4 \right]$	1. Since the acoustic field is not treated as diffuse, the theory is now applicable to the case where the enclosure dimension-acoustic wavelength ratio is not large. 2. A lower limiting frequency is found above which the model average subcritical acoustic radiation efficiency is equal to that of a baffled simply-supported panel radiating into a free field but below which the radiation efficiency falls below the free-field values; the latter is explained by non-proximate mode coupling theory described below. This limit is important for small box volumes, i.e., where the dimensions of the containing vessel are not large compared to the wavelength. At supercritical frequencies the radiation efficiency is found to be equal to half that of a freely radiating panel. The lower limiting frequency is confirmed by measurements. The experimental results give qualitative, but not universally good quantitative results. 3. For subcritical frequencies which correspond to the condition $k_p > k_r (= \omega/c_o)$ the the best acousto-structural coupling occurs for $p < \frac{ak_r}{\pi}$ when $p = m \pm 1$, $q = \epsilon n$ and for $q < \frac{bk_r}{\pi}$ when $q = n \pm 1$, $p = \epsilon m$, where $\epsilon < 1$ (see Figure 2 of Reference paper). We describe these acoustic modes as having proximate mode coupling to the individual structural mode considered. Such mode pairs are both close in natural frequency—the difference in the frequencies of the interacting (i.e., coupled) modes is less than half the sum of the half power bandwidths—and have the best available wave component match in either the x or y directions, i.e., the coupling factor is a maximum by virtue of both wavelength matching in one direction and natural frequency proximity. The structural modes are referred to as "edge modes" in the analysis of free-field radiation, i.e., these modes are well coupled. 4. For supercritical frequencies which correspond to the condition $k_p < k_r \left(= \frac{\omega}{c_o} \right)$ the maximum coupling dominating the frequency range corresponds to $p = m \pm 1$, $q = n \pm 1$. Modes having $p = m \pm 1$, $q = n \pm 3$ and vice versa contribute about 25% of the total coupling with the contributions from all other modal couplings being negligible (see Figure 3 of Reference paper). 5. Result 1(a) agrees closely with those of Reference 25 for "reverberant" field vibration of a baffled panel. Result 2 does not agree with any previous estimates of supercritical radiation resistance for baffled panels, or with the analytical results of Reference 19 for a similar box system. It yields half the previously reported 100% radiation efficiency for baffled panels. Result 3 indicates that clamped plate radiation damping is approximately 3 dB greater than that of the simply supported plate for $(f/f_c) < 0.5$. The factor decreases as (f/f_c) approaches unity and is equal to unity or zero dB at supercritical frequencies, i.e., the radiation damping of a clamped plate exceeds the simply supported value by a factor varying from about 3 dB at low frequencies to zero at the critical frequency and above. 6. To the results for proximate modal coupling are added result 4 for non-proximate modal coupling. The latter result is for a frequency band in which the center frequency lies below that estimated and also experimentally shown to be the lower limit for maximum proximate coupling. In this band no acoustic modes have natural frequencies close enough to that of a typical structural mode in a band to give proximate modal coupling. In other words, for those frequency bands of analysis for which the average number of acoustic modes having maximum proximate coupling to the structural modes in the frequency band of analysis is less than unity, it is necessary to consider coupling between acoustic and structural modes for which the natural frequencies are further apart than half the sum of their halfpower bandwidths. Figure 4 of the Reference paper shows the lattice points of acoustic modes which have natural frequencies within an analysis

REFERENCE	AUTHORS NOTATION		THEORETICAL APPROACH	MAJOR ASSUMPTIONS AND LIMITATIONS
20 (Cont'd)				
21	$C(\omega)$	relative correction factor for equivalent reverberant field, equal to $10 \log \dfrac{S_{p_r}(\omega) / S_{w_r}(\omega)}{S_p(\omega) / S_w(\omega)}$	Defines the spectral intensity of an equivalent reverberant field which produces the same structural response as does excitation by boundary layer turbulence.	Existence of reverberant field equivalent to turbulence field.
	c	ambient speed of sound		
	f	excitation frequency		
	NR	noise reduction for boundary layer excitation		
	NR_r	noise reduction for reverberant field excitation, equal to $10 \log \dfrac{S_{p_i}(\omega)}{p_{ref}^2}$		
	$N(f)$	total number of modes		
	$n(f)$	modal density of internal acoustic field		
	p_{ref}^2	mean square of the reference pressure, equal to $0.0002 \frac{dynes}{cm^2}$		
	Q_{ac}	magnification (or resonant amplification) factor of an acoustic mode		
	$\bar{S}, S_i$	total absorbing surface area, equal to ΣS_i and i^{th} absorbing surface respectively		
	S_t	transmitting area		
	$S_p(\omega), S_{p_r}(\omega)$	external pressure spectral densities for turbulent boundary layer noise field and for equivalent reverberant field, respectively		
	$S_{p_i}(\omega)$	space average spectral density of the internal pressure		
	$S_w(\omega), S_{w_r}(\omega)$	space average displacement spectral densities for turbulence boundary layer noise field and for equivalent reverberant field, respectively		
	$SL(\omega)$	true external turbulence pressure spectrum level, equal to $10 \log \dfrac{S_p(\omega)}{p_{ref}^2}$		
	$SL_i(\omega)$	space average internal pressure spectrum level, equal to $10 \log \dfrac{S_{p_i}(\omega)}{p_{ref}^2}$		
	$\bar{a}$	average (random incidence) absorption coefficient for several surfaces equal to $\dfrac{(\Sigma a_i S_i)}{\Sigma S_i}$		
	a_i	absorption coefficient for area S_i		
	Δf	frequency bandwidth		
	$\bar{\tau}_{ow}$	overall transmission coefficient of the structure through the transmitting area S_t		
22	a, b, c	room dimensions in the x, y, z directions respectively where b, c also represent the panel dimensions	General solution of Wave Equation with Inhomogeneous Boundary Conditions, based on modal theory	1. Panel and room damping are excluded in the analysis—but can be accounted for in the results by replacing the panel and room eigen-frequencies by a complex quantity.
	B_{mn}^{qr}	coupling coefficient between room modes m, n and panel modes q, r, equal to $\dfrac{4}{\pi^2} \dfrac{4qr}{(m^2 - q^2)(n^2 - r^2)}$. This can be viewed as consisting of two distinct parts, coupling coefficient $\dfrac{2}{\pi} \dfrac{2q}{(m^2 - q^2)}$ in the y-direction and a coupling coefficient $\dfrac{2}{\pi} \dfrac{2r}{(n^2 - r^2)}$ in the z-direction		2. Simply supported panel (note: with suitable modification the general solution can be applied to all types of panel edge conditions).
	c_g, c_{gr}	velocity of bending wave in panel		3. Amplitude of pressure difference on the panel is a function of panel and room modes including the phase difference between the pressures on the two surfaces of the panel.
	C_L	velocity of longitudinal wave in panel		
	c_o	velocity of sound in air		
	D	modulus of rigidity		
	$E_{mn}^{qr}(a)$	function equal to $\dfrac{1}{\omega_{qr}^2 - \omega^2} \dfrac{B_{mn}^{qr} \cosh\left(\frac{x}{c_o}\sqrt{\omega_{mn}^2 - \omega^2}\right)}{\sqrt{\omega_{mn}^2 - \omega^2} \sinh\left(\frac{a}{c_o}\sqrt{\omega_{mn}^2 - \omega^2}\right)} f_2(y, z)$		
	$\bar{E}_{mn}^{qr}(a)$	function equal to $\omega^3 E_{mn}^{qr}(a)$; see "Results"		

RELEVANT RESULTS	REMARKS OR MISCELLANEOUS

REMARKS OR MISCELLANEOUS (upper section):

bandwidth centered on the natural frequency of a typical structural mode, but not within the bandwidth for proximate coupling.

7. The analysis shows that it is not necessarily correct to assume that many acoustic modes couple with an individual structural mode even if the modal density ratio is high. Consequently, the statistical energy equations for the production of an acoustic field, response to acoustic excitation, and the difference between coupled and uncoupled loss factors, must be corrected as described in the reference paper when the mechanical loss factors are of the same order as the radiation loss factors.

1. Result 1 defines an equivalent field which replaces boundary layer turbulence, yet produces identical structural responses; i.e., identical displacement power spectral densities. This concept is particularly useful in simulating fluctuating pressure environments when studying transmission loss characteristics, i.e., noise reduction, since the theory for the latter is often determined for an external reverberant sound field driving the structure.

2. In results 1, 2, and 3 the correction factor $C(\omega)$ has the value necessary to correct the noise reduction, computed for reverberant field excitation, so that it corresponds to the actual noise reduction for the true or boundary layer excitation. Thus, $NR\Big|_{Boundary\ layer} \cong NR = NR_r - C(\omega)$. The value of $C(\omega)$ may be computed from the printout provided by the program (in the reference paper) of the ratios $\frac{S_{p_r}(\omega)}{S_{p_r}(\omega)}$ and $\frac{S_w(\omega)}{S_w(\omega)}$

Although this ratio can be computed over the entire frequency range the following practical range is suggested as a rough criteria for the frequency range: compute $C(\omega)$ from the program listing from approximately twice the panel fundamental frequency to the highest frequency of interest.

3. The noise reduction NR_r for reverberant field excitation is computed by either the modal approach or the diffuse field approach. The former approach considers the modal response of the internal acoustic field and an expression for the noise reduction is obtained by a modal summation; see reference paper for analytical details. However, at high frequencies where the modal density is high this involves lengthy computations, even for a computer, so that it is preferable to simplify the approach in this region and use more conventional methods for computing noise reduction. This can be done if the modal density is sufficiently high—of the order of 10 modes per bandwidth or more—so that the sound field can be considered to be uniform both in space and spectral content, i.e., NR_r is computed for a diffuse internal sound field. Result 3 gives the frequency at which the modal density requirement is satisfied.

RELEVANT RESULTS (upper section):

1. <u>Equivalent reverberant field expressed as a dB ratio of the exciting pressures</u>

$$10 \log \frac{S_p(\omega)}{S_w(\omega)}\Bigg|_{Reverberant} = 10 \log \frac{S_w(\omega)}{S_p(\omega)}\Bigg|_{Boundary\ layer} - 10 \log \frac{S_w(\omega)}{S_p(\omega)}\Bigg|_{Reverberant}$$

$$= 10 \log \frac{\dfrac{S_w(\omega)}{S_p(\omega)}}{\dfrac{S_w(\omega)}{S_{p_r}(\omega)}} = 10 \log \frac{\dfrac{S_{p_r}(\omega)}{S_w(\omega)}}{\dfrac{S_p(\omega)}{S_w(\omega)}} = C(\omega)$$

where $S_{w_r}(\omega) = S_w(\omega)$ by definition

2. <u>Space average Density inside the fuselage</u>

$$S_{p_i}(\omega) = S_p(\omega) \frac{S_p(\omega)}{S_{p_i}(\omega)} = S_p(\omega) \frac{S_{p_i}(\omega)}{S_{p_r}(\omega)} \left[\frac{\dfrac{S_{p_r}(\omega)}{S_w(\omega)}}{\dfrac{S_p(\omega)}{S_w(\omega)}} \right]$$

or in dB form

$$SL_i(\omega) = SL(\omega) - NR_r + C(\omega)$$

3. <u>Noise Reduction for Boundary Layer Noise Excitation</u>

$$NR = NR_r - C(\omega)$$

where $NR_r = 10 \log \left[1 + \frac{\bar{a}\hat{s}}{\bar{\tau}_{sw} s_t} \right]$ is applicable for diffuse internal sound

fields when

$$n(f) \cdot \Delta f = \left[\frac{dN}{df} \right] [\Delta f] = \left[\frac{4\pi^2 f^2 V}{\pi c^3} \right] \cdot \left[\frac{f}{Q_{ac}} \right] > 10$$

or

$$f > c \left[\frac{10 Q_{ac}}{4\pi V} \right]^{1/3}$$

RELEVANT RESULTS (lower section):

<u>Transmission Loss</u>

$$\frac{(p_1)_t^2}{(p_2)_t^2} = \left\{ 1 + \frac{\rho h \omega}{2 \rho_o c_o} \left[\sum_{\substack{q=1, r=1 \\ m=1, n=1}}^{\infty} (\bar{i}_{mn}(a))^2 \right] \right\}^{\frac{1}{2}}$$

where

$$(\bar{i}_{mn}(a))^2 = \frac{1}{4}(\bar{E}_{oo}(a))^2 + \frac{1}{2}(\bar{E}_{mo}(a))^2 + \frac{1}{2}(\bar{E}_{on}(a))^2 + (\bar{E}_{mn}(a))^2,$$

$$\bar{E}_{mn}(a) = \omega^3 E_{mn}(a)$$

$$= \frac{1}{(\omega_{qr}/\omega)^2 - 1} \frac{B_{mn} \cosh\left(\frac{a}{c_o}\sqrt{\omega_{mn}^2 - \omega^2}\right)}{\sqrt{(\omega_{mn}/\omega)^2 - 1} \sinh\left(\frac{a}{c_o}\sqrt{\omega_{mn}^2 - \omega^2}\right)}$$

$$\bar{K}_{mn}(a) = \frac{1}{4} B_{oo} \bar{E}_{oo}(a) + \frac{1}{2} B_{mo} \bar{E}_{mo}(a) + \frac{1}{2} B_{on} \bar{E}_{on}(a) + B_{mn} \bar{E}_{mn}(a).$$

and for steady state vibration

$$\langle p_1 \rangle_t^2 - \langle p_r \rangle_t^2 = \langle p_2 \rangle_t^2.$$

REMARKS OR MISCELLANEOUS (lower section):

1. The general solution given here explains the occurrence of the phenomenon of coincidence for a finite panel. It also explains the radiation of sound energy into the cavity below and above coincidence. The energy transmitted to the room can be supplied by resonant or by non-resonant modes and is most effective at frequency range above coincidence, i.e., for modes for which the forced frequency exceeds the room eigenfrequency. This chiefly governs the transmission at high frequencies. Modes for which the room eigenfrequency exceeds the forced frequency produce poorer sound transmission. At lower frequencies a large number of modes fall in the latter category and hence produce little acoustic pressure in the room. Moreover, the radiation of energy takes place only by certain specific combinations of room modes, i.e., certain room mode-panel mode combinations do not couple at all. For those that couple the coupling coefficient is a maximum when the panel modes are closest to the room modes, i.e., when $m = q \pm 1$ and $r = n \pm 1$.

2. Maximum sound transmission, or minimum transmission loss, occurs when the room eigenvector is at the grazing angle of incidence, i.e., grazes the flexible panel, under conditions of maximum coupling and panel resonance. More precisely, the sound transmission loss will be a minimum when the expression for $\frac{\langle p_1 \rangle_t^2}{\langle p_2 \rangle_t^2}$ given in the results becomes minimum, i.e., when the expression $\bar{E}_{mn}(a)$ becomes maximum. This will occur when (1) B_{mn} = maximum, i.e., $m = q \pm 1$, $n = r \pm 1$, (2) $\omega_{qr} = \omega$ and (3) $\omega_{mn} = \omega_{omn} = \omega$. When these conditions are satisfied, the

REFERENCE	AUTHORS NOTATION		THEORETICAL APPROACH	MAJOR ASSUMPTIONS AND LIMITATIONS
22 (Cont'd)	$f_2(y,z)$	equal to $\cos \frac{m\pi y}{b} \cos \frac{n\pi z}{c}$		
	h	panel thickness		
	$\hat{I}_{mn}(a), \overline{K}_{mn}(a)$	functions defined in "Results"		
	$k_{\ell mn}$	eigenvalue or wave number in the room		
	k_{qr}	eigenvalue or wave number in the panel		
	ℓ, m, n	room modes		
	p_2	acoustic pressure in room at wall $x = a$		
	p_i	incident acoustic pressure on the panel		
	p_{rs}	reflected and scattered pressure on the surface of incidence		
	q, r	panel modes		
	x, y, z	rectangular coordinates		
	κ	radius of gyration		
	ρ	density of plate material		
	ρ_o	density for air		
	ω	forced angular frequency		
	ω_c	critical coincidence angular frequency		
	$\omega_{\ell mn}$	eigen angular frequency for room modes ℓ, m, n equal to $c_o \left[\left(\frac{\ell\pi}{a} \right)^2 + \left(\frac{m\pi}{b} \right)^2 + \left(\frac{n\pi}{c} \right)^2 \right]^{1/2}$		
	$\omega_{mn} \equiv \omega_{omn}$	eigen angular frequency equal to $c_o \left[\left(\frac{m\pi}{b} \right)^2 + \left(\frac{n\pi}{c} \right)^2 \right]^{1/2}$		
	ω_{qr}	eigen angular frequency for panel modes q, r, equal to $\pi^2 \left(\frac{D}{\rho h} \right)^{1/2} \left[\left(\frac{q}{b} \right)^2 + \left(\frac{r}{c} \right)^2 \right]$		
23	θ_{mn}	coupling coefficient between room modes (m,n) and panel modes (q,r)	Solution of wave equation by double finite Fourier cosine transform and Laplace transform	1. Acoustically hard walls
	a, b, c	room dimensions in the x-, y- and z-directions, respectively		2. Simply supported panel
	c_L	velocity of longitudinal waves in the panel		3. Pressure at plate may be represented by sine series expansion
	c_o	velocity of sound in air		
	f_c	critical coincident frequency		
	h	thickness of panel		
	j	$\sqrt{-1}$		
	l, m, n	room modes		
	P_1	acoustic pressure on the surface of incidence		
	P_2	acoustic pressure within the cavity		
	P_{1qr}	modal pressure on the surface of incidence		
	P_{2qr}	modal pressure within the cavity at the panel surface		
	q, r	panel modes		
	t	time		
	V	velocity of panel motion		
	x, y, z	model coordinates		
	$Z_{mn}(0)$ cavity	cavity impedance of an (m,n) cavity mode at the surface of the panel looking towards the back wall		
	Z_{qr} panel	panel impedance of the (q,r) panel mode		
	$\alpha(t)$	$(1/c_o)\sqrt{\omega_{mn}^2 - \omega^2}$		
	δ	panel material damping, given by complex modulus measurement		
	ρ	density of panel material		
	ω	forced angular frequency		
	ω_{mn}	$c_o \sqrt{(m\pi/b)^2 + (n\pi/c)^2}$, the eigen-angular frequency for room mode (m,n)		
	ω_{qr}	eigen-angular frequency for panel mode (q,r)		
	$\langle \rangle_t^s$	space-time average		

RELEVANT RESULTS	REMARKS OR MISCELLANEOUS

RELEVANT RESULTS

1. Cavity Acoustic Pressure

$$P_2(x,y,z,t) = \sum_{\substack{q=1,\,r=1 \\ m=0,n=0}}^{\infty} K.K'.P_{1qr} \frac{B_{mn}[Z_{mn}(0)\text{ cavity}]\cosh\,[(a-x)\,a(t)]}{[Z_{mn}(0)\text{ cavity} + Z_{qr}\text{ panel}]\cosh\,[sa(t)]}$$

$$\times \cos\left(\frac{m\pi}{b}\,y\right)\cos\left(\frac{n\pi}{c}\,z\right)e^{j\omega t},$$

where

$K = 0.5$ for $m = 0$, $K = 1$ for $m > 0$;
$K' = 0.5$ for $n = 0$, $K' = 1$ for $n > 0$.

2. Pressure at Cavity Surface

$$P_2(0,y,z,t) = \sum_{q=1,\,r=1}^{\infty} P_{2qr}\sin\left(\frac{q\pi}{b}\,y\right)\sin\left(\frac{r\pi}{c}\,z\right)$$

3. Noise Reduction for Simply Supported Plate-Cavity System When the Panel Is Subjected to Harmonically Varying Sound Pressures

$$NR = \frac{<P_1^2>_t}{<P_2^2>_t} \cdot \frac{1}{\displaystyle\sum_{\substack{m=0,n=0 \\ q=1,r=1}}^{\infty} K.K'\left(\frac{16}{q r \pi}\right)^2\left|\frac{B_{mn}Z_{mn}(0)\text{ cavity}}{Z_{mn}(0)\text{ cavity} + Z_{qr}\text{ panel}}\right|^2}$$

4. Mean Square Velocity Pressure Ratio

$$\frac{<V^2>_t}{<P_1^2>_t} = \sum_{\substack{m=0,n=0 \\ q=1,r=1}}^{\infty} K.K'\left(\frac{16}{q r \pi}\right)^2\left|\frac{B_{mn}}{Z_{mn}(0)\text{ cavity} + Z_{qr}\text{ panel}}\right|^2$$

REMARKS OR MISCELLANEOUS

amplitude of flexural waves is maximum. This situation is called critical coincidence and the frequency at which it occurs is called the critical coincidence frequency ω_c.

3. The condition of maximum coupling can be approximated by taking $m \approx q$, $n \approx r$. Then $\left(\frac{m}{b}\right)^2 + \left(\frac{n}{c}\right)^2 \approx \left(\frac{q}{b}\right)^2 + \left(\frac{r}{c}\right)^2$ or $k_{omn} \approx k_{qr}$. Hence, $\frac{\omega_{mn}}{c_o} = \frac{\omega_{qr}}{c_{qr}} = \frac{\omega_{qr}}{c_B}$ or $c_o = c_B$ at critical coincidence. Moreover for a simply supported panel,

$\omega_{omn} = \omega_{qr} = \kappa C_L\,k_{qr}^2 = \kappa C_L\left(\frac{\omega_{qr}}{c_o}\right)^2$ at critical coincidence, so that the critical coincidence frequency is denoted by $\omega_c = \frac{c_o^2}{\kappa C_L}$. The angle of incidence affects the amplitude of the transmitted wave but does not affect the coincidence frequency.

4. The results also show that subsequent coincidences occur for room resonances with $\ell = 1, 2, 3 \ldots$ at frequencies higher than the critical coincidence frequency. These higher coincidence frequencies are referred to as coincidence frequencies. Thus in general, coincidence occurs when (1) B_{mn} is maximum, (2) $\omega_{qr} = \omega$ and (3) $\omega_{lmn} = \omega$, $\ell = 0, 1, 2 \ldots$. For the special case of coincidence where the wave vector is at the grazing angle, i.e., $\ell = o$, we have critical coincidence and the amplitude at subsequent coincidences diminishes according to $\frac{1}{c_o\frac{\ell\pi}{a}}$, that is, with increasing values of ℓ.

5. Additional analysis shows (see Figures 3 and 4 of the reference paper) that above critical coincidence, i.e., the high frequency response, under conditions of maximum coupling, $\omega_{qr} > \omega_{omn} > \omega_c$, and panel resonances $\omega_{qr} > \omega_c$ corresponding to $c_{qr} \equiv c_B > c_o$, and also for most cases of non-resonance operation, the sound pressure will be high as ω is raised. This means that the transmission loss $\frac{<p_1>_t^2}{<p_2>_t^2}$ will assume minimum values periodically. Conversely at frequencies below critical coincidence the maximum coupling condition is governed by $\omega_{qr} < \omega_{omn} < \omega_c$. The panel resonance $\omega_{qr} < \omega_c$ and $c_{qr} \equiv c_B < c_o$. Therefore $\omega < \omega_{omn}$ for a large number of modes and so at all panel resonances under the maximum coupling condition. The results given show that the response of the room will be increasingly poor as the magnitude of $\frac{a}{c_o}\sqrt{\omega_{mn}^2 - \omega^2}$ increases. Near and also away from critical coincidence, panel-room mode combinations which do not necessarily satisfy the condition of maximum coupling ($k_{omn} \approx k_{qr}$) may also provide significant contributions to the room pressure response.

1. Treats steady state harmonic solution only.

2. The transmission of sound through a finite plate-cavity system is governed by three factors: B_{mn}, $Z_{mn}(0)$ cavity, Z_{qr} panel.

3. For a particular mode combination, if panel damping exceeds fluid damping and $Z_{mn}(0)$ cavity $\gg \rho_A\left(\frac{\omega_{qr}}{\omega}\right)\omega_{qr}\,\delta$ then $<P_2^2>_t^i > <P_1^2>_t^i > <P_1^2>_t^i$ which represents a negative transmission loss.

4. At panel resonance $\omega = \omega_{qr}$, the transmission of sound is independent of cavity impedance, i.e., Z_{qr} panel $= 0$, and is wholly dependent on B_{mn}.

5. At cavity resonance, $\omega = \omega_{mn}$, the standing wave relationship, $\left(\frac{\ell\pi}{a}\right)^2 + \left(\frac{m\pi}{b}\right)^2 + \left(\frac{n\pi}{c}\right)^2 = \left(\frac{\omega}{c_o}\right)^2$, $\ell = 0, 1, 2 \ldots$, is satisfied and $Z_{mn}(0)$ cavity $= \infty$. The transmission of sound is independent of panel impedance and is controlled by B_{mn}.

6. For the cavity "off" resonance, when $Z_{mn}(0)$ cavity $= 0$ the effect of the cavity on the vibration is small and the transmission loss is high for the cavity mode concerned.

7. Coincidence is a simultaneous combination of the foregoing effects in that it occurs when (1) Z_{qr} panel $= 0$ (i.e., $\omega_{qr} = \omega$), (2) $Z_{mn}(0)$ cavity $= \infty$, (3) B_{mn} is a maximum (i.e., $m = q \pm 1$, $n = r \pm 1$). At this condition $<P_2^2>_t^i \to <P_1^2>_t^i$ and $V \to 0$. Many coincident frequencies exist, the fundamental being given by $f_c \approx \frac{\sqrt{3}\,C_o^2}{\pi C_L h}$.

8. Theoretical results compare favorably with both experimental results and predictions of other investigators.

TABLE 2 — IDENTIFICATION OF KEY RESULTS AND COMPARISON WITH DAVIES RESULTS

Note: For the various mode classifications, special cases for J_R^{mnqr} and J_x^{mnqr} are given in the text subsequent to the equations cited. In general, a special case is compared with the corresponding Davies result.

A. Half-Space Coupling Coefficients $\bar{J}^{mnqr} = J_x^{mnqr} + iJ_R^{mnqr}$

Mode Classification	Corre-sponding Figure	J_R^{mnqr}	J_x^{mnqr}	Agreement with Davies Result (See Appendix F)
I. TWO Y-EDGE MODES				
(a) $k_m, k_q > k; k_n = k_r < k$	12a	Equation (69b)	Equation (69c)	Good
(b) $k_m \neq k_q > k; k_n \neq k_r < k$	12b	Equation (69d)	Equation (69d)	↑
(c) $k_m = k_q > k; k_n = k_r < k$	12c	Equation (70c)	Equation (70d)	
(d) $k_m, k_q > k; k_n, k_r < k$	12b	Equation (71)	Equation (72)	
II. TWO CORNER MODES				
(a) $k_m, k_q > k; k_n, k_r > k$	- - -	Equation (73b)		
(b) $k_m, k_q > k; k_n = k_r > k$	12d		Equation (74)	Good
III. Y-EDGE ACOUSTICALLY FAST (AF) MODES				Good for J_R^{mnqr}. Poor for J_x^{mnqr} when ka>>1 and considering one mnqr mode, but good when considering several modes; see section 3 of Appendix F.
(a) $k_m, k_n k_r < k; k_q > k$	12e	Equation (80)	Equation (81)	
IV. Y-EDGE-CORNER MODES				Good for J_R^{mnqr}. Poor for J_x^{mnqr}, but good if Davies report has typographical error and $k_r^2 >> k_q^2$; see section 4 of Appendix F.
(a) $k_m, k_q > k; k_n < k; k_r > k$	12f	Equation (82)	Equation (83)	
V. TWO ACOUSTICALLY FAST (AF) MODES				
(a) $k_m, k_n, k_q, k_r < k$ and $k_q \geq k_m; k_r \geq k_n$	12g, h (special cases)	Equation (86g)	Equation (90)	Good
VI. TWO EDGE MODES				Good for J_R^{mnqr}. Davies does not give comparable term for J_x^{mnqr}, hence no comparison can be made.
(a) $k_m, k_n, k_q, k_r < k; k_{mn}^2, k_{qr}^2 > k^2$	12i, j (special cases) 12j	Equation (91d)	Equation (94)	

B. Cavity Coefficients i^{mnqr} for Almost Hard and Hard Walls

Equation (106)

C. Final Analytical Results (Working Equations) Programmed for Digital Computer

1. Equation (118) — Cross Spectral Density of Plate Displacement.
2. Equation (119) — Cross Spectral Density of Pressure in the Cavity.
3. Equation (121) — Spectral Density of Power Radiated into Half-Space.
4. Equation (123) — Cross Spectral Density of Pressure in the Half-Space.

1. Response of a plate to harmonic excitation.

2. Response of a plate to random excitation.

3. Cross-spectral density of the acoustic pressure in a cavity shaped like a rectangular parallelepiped; one of its surfaces is bounded by the plate and the other five are treated as hard or almost hard walls.

4. Spectral density of the (complex) power generated by the plate-cavity system in the semi-infinite half-space representing the region above the plate and away from the cavity.

5. Cross-spectral density of the acoustic pressure radiated by the plate-cavity system into half-space.

6. Spectral density of the (complex) power radiated by the plate cavity system into the cavity.

Note that all solutions are in terms of an excitation function and other quantities not yet explicitly represented or determinable. We observe also that the solutions for the plate response is the solution to the fundamental modal equation developed in this appendix.

Appendix B — Treats the explicit solution for the spectral quantities mentioned above which requires (among other things) evaluation of the half-space and cavity coupling coefficients; a more precise description of this requirement is given in the statement preceding and subsequent to Equations (44) and (45). This appendix presents an evaluation (1) of the joint and cross-coupling coefficients for the half-space, $\bar{J}^{mnmn}$ and $\bar{J}^{mnqr}$, respectively and (2) of the joint and cross-coupling coefficients for the cavity, $\bar{I}^{mnmn}$ and $\bar{I}^{mnqr}$, respectively. For the half-space, the right-hand side of the equation $\bar{J}^{mnmn} = J_x^{mnmn} + i J_R^{mnmn}$ represents the auto-reactive and resistive coupling components of $\bar{J}^{mnmn}$, respectively whereas the right-hand side of $\bar{J}^{mnqr} = J_x^{mnqr} + i J_R^{mnqr}$ represents the cross-reactive and resistive coupling components of $\bar{J}^{mnqr}$, respectively. For a simply supported plate and M=0, Equations (53) and (54) give the integral formulation to be solved to determine these quantities. The integral, which is of the form utilized by Davies,[9, 10] was evaluated for all possible intermodal combinations by contour integration using the Cauchy residue theorem; the results are identified in Table 2. For the cavity involving a simply supported plate, almost hard walls and hard walls, and M=0, the results for $\bar{I}^{mnqr}$ (which include qr=mn) are given by Equation (106) and are also cited in Table 2.

Appendix C — Presents a derivation of the cross-spectral density and wavenumber frequency spectrum of the turbulence (blocked) pressure by means of a Fourier transform of the cross-

correlation function for the turbulence pressure devised by Maestrello from semiempirical data.[1,12]* Joint and cross acceptances are then defined in terms of integral formulations of these spectral quantities and the plate modes. The acceptances are then evaluated for the low wavenumber region, considerably removed from the convection region, and it is shown that the cross acceptances are negligible. Hence only the joint acceptances need be considered in the computations of the vibroacoustic response.

Appendix D – Presents a derivation (the contributions of cross acceptances are ignored) of Items 2 through 6 listed above under Appendix A, where now the solutions for the spectral quantities are given in terms of quantities used in defining (or representing) the explicit turbulence excitation function cited in the preceding discussion and where all quantities are now known or determinable from preceding analyses. The working expression for the cross-spectral density of the pressure in the half-space (Item 5 of Appendix A) is derived for the far field only. However, a general expression for the cross-spectral density of near- and far-field pressures in the half-space is also presented. For the near-field results, this expression requires additional extensive evaluation which is beyond the scope of the present report.

Appendix E – Discusses the extension of the foregoing theory (1) to clamped-clamped plates for M=0 and (2) to both simply supported and clamped-clamped plates for M>0.

Appendix F – Shows that the intermodal coupling coefficients derived here are more complete, general, and exact than those derived by Davies and that in nearly all cases, they can be reduced to his first-order results as a special case; see commentary in Table 2.
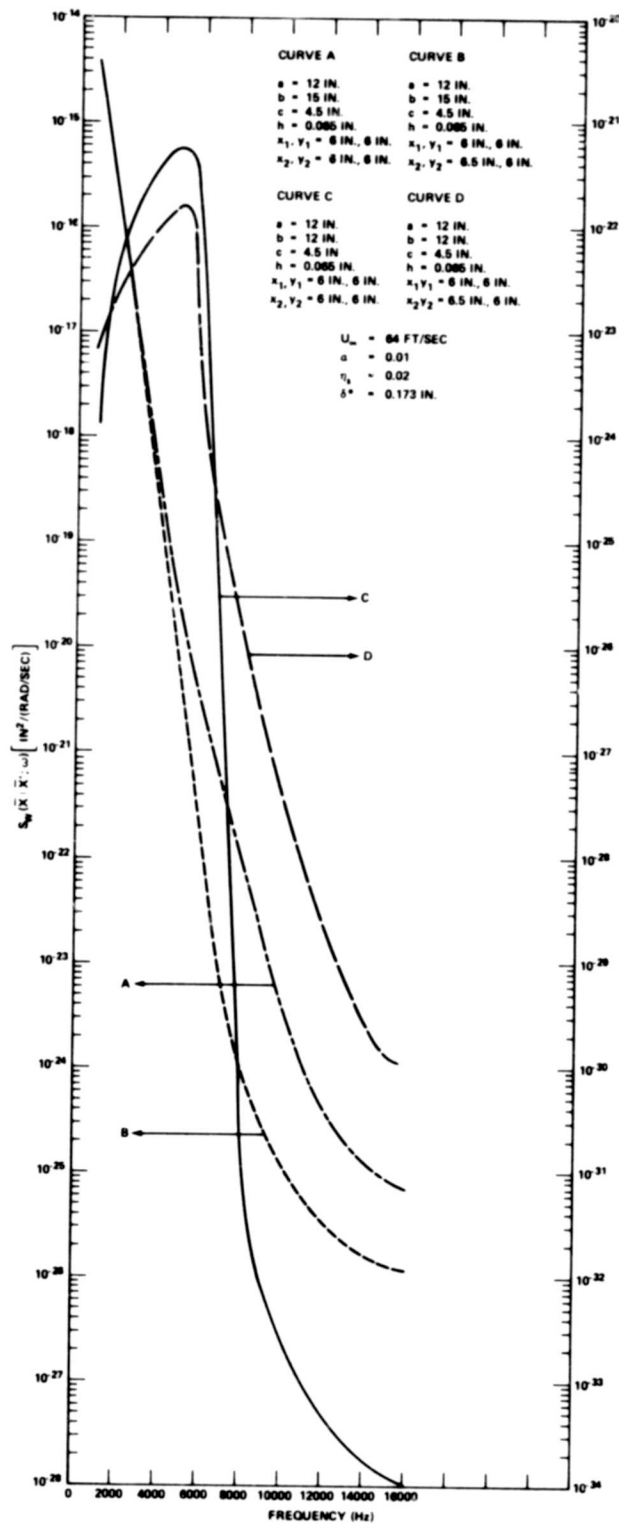
Appendix G – Discusses and presents the computer program which mechanizes four equations (given at the end of Table 2) corresponding to Items 2 through 5 in Appendix A. A derivation of the fluid-loaded mode resonances is also presented and includes the effects of the fluid in the half-space and in the cavity.

COMPUTATIONAL RESULTS

The limited computer results presented here were obtained by Bolt Beranek and Newman, Inc. The results indicated proper functioning of the computer program for the data used. However, a comprehensive evaluation of plate-cavity system performance awaits more extensive numerical calculations using the program.

Figures 2 through 5 are plots of typical sample computer results for the vibroacoustic response, i.e., spectral quantities, for turbulence-excited plate-cavity systems. The turbulent

---

*In contrast to the Maestrello evaluation for the cross spectrum, the present results include the effects of convection in both the x- and y-directions. Thus, Equation (112b) is a function of k_y as well as of k_x and ω.

CURVE A

a = 12 IN.
b = 15 IN.
c = 4.5 IN.
h = 0.065 IN.
x_1, y_1 = 6 IN., 6 IN.
x_2, y_2 = 6 IN., 6 IN.

CURVE B

a = 12 IN.
b = 15 IN.
c = 4.5 IN.
h = 0.065 IN.
x_1, y_1 = 6 IN., 6 IN.
x_2, y_2 = 6.5 IN., 6 IN.

CURVE C

a = 12 IN.
b = 12 IN.
c = 4.5 IN.
h = 0.065 IN.
x_1, y_1 = 6 IN., 6 IN.
x_2, y_2 = 6 IN., 6 IN.

CURVE D

a = 12 IN.
b = 12 IN.
c = 4.5 IN.
h = 0.065 IN.
$x_1 y_1$ = 6 IN., 6 IN.
$x_2 y_2$ = 6.5 IN., 6 IN.

U_∞ = 64 FT/SEC
α = 0.01
η_s = 0.02
δ^* = 0.173 IN.

$S_w(\bar{x}, \bar{x}'; \omega) \left[\text{IN}^2/(\text{RAD/SEC}) \right]$

FREQUENCY (Hz)

Note: (For Curves A, B use scale on left; for Curves C, D use scale on right.)

Figure 2 — Magnitudes of Cross-Spectral Density of Plate Displacement between Points x_1, y_1 and x_2, y_2 and Power Spectral Density of Plate Displacement at Points $x_1 = x_2$, $y_1 = y_2$, versus Frequency

25

a = 12 IN.

b = 12 IN.

c = 4.5 IN.

h = 0.065 IN.

υ_∞ = 64 FT/SEC

a = 0.01

η_s = 0.02

δ^* = 0.173 IN.

THE CURVE REPRESENTS THE APPROXIMATE RESULTS FOR EACH OF THE FOLLOWING 2 PAIRS OF POINTS

x_1, y_1, z_1 = 6 IN., 6 IN., 3 IN; x_2, y_2, z_2 = 6 IN., 6 IN., 3 IN.

x_1, y_1, z_1 = 6 IN., 6 IN., 3 IN; x_2, y_2, z_2 = 5.5 IN., 6 IN., 3 IN.

$$\frac{\left(1\,\frac{lb}{in^2}\right)^2}{\frac{rad}{sec}} = \frac{2\pi \left(\frac{lb}{in^2}\right)^2}{Hz} = \frac{2\pi \times 47.54 \times 10^6 \left(\frac{newtons}{meter^2}\right)^2}{Hz} = 298.55 \times 10^6 \frac{\left(\frac{newtons}{meter^2}\right)^2}{Hz}$$

Hence for $|S_{p_i}(\bar{\xi}\,|\,\bar{\xi}';\omega)| = 10^{-6} \frac{\left(\frac{lb}{in^2}\right)^2}{\frac{rad}{sec}} = 298.55 \frac{\left(\frac{newtons}{meter^2}\right)^2}{Hz}$,

and a 1 cycle bandwidth

$$\text{S.P.L.}\Big|_{1\,Hz\,band} = 10 \log \left[\frac{|S(\bar{\xi},\bar{\xi}';\omega)|}{p_{ref}^2}\right]_{1\,Hz\,band} db \, // \, p_{ref}^2 = 1\mu P_a^2 = (10^{-6})^2 \left(\frac{newtons}{meter^2}\right)^2$$

$$= 10 \log \frac{298.55}{10^{-12}} = 120 \log 298.55 = 297 \, db$$

Similarly for $|S_{p_i}(\bar{\xi}\,|\,\bar{\xi}';\omega)| = 10^{-7} \frac{\left(\frac{lb}{in^2}\right)^2}{\frac{rad}{sec}}$ the $\text{S.P.L.}\Big|_{1\,Hz\,band}$ = 272 db
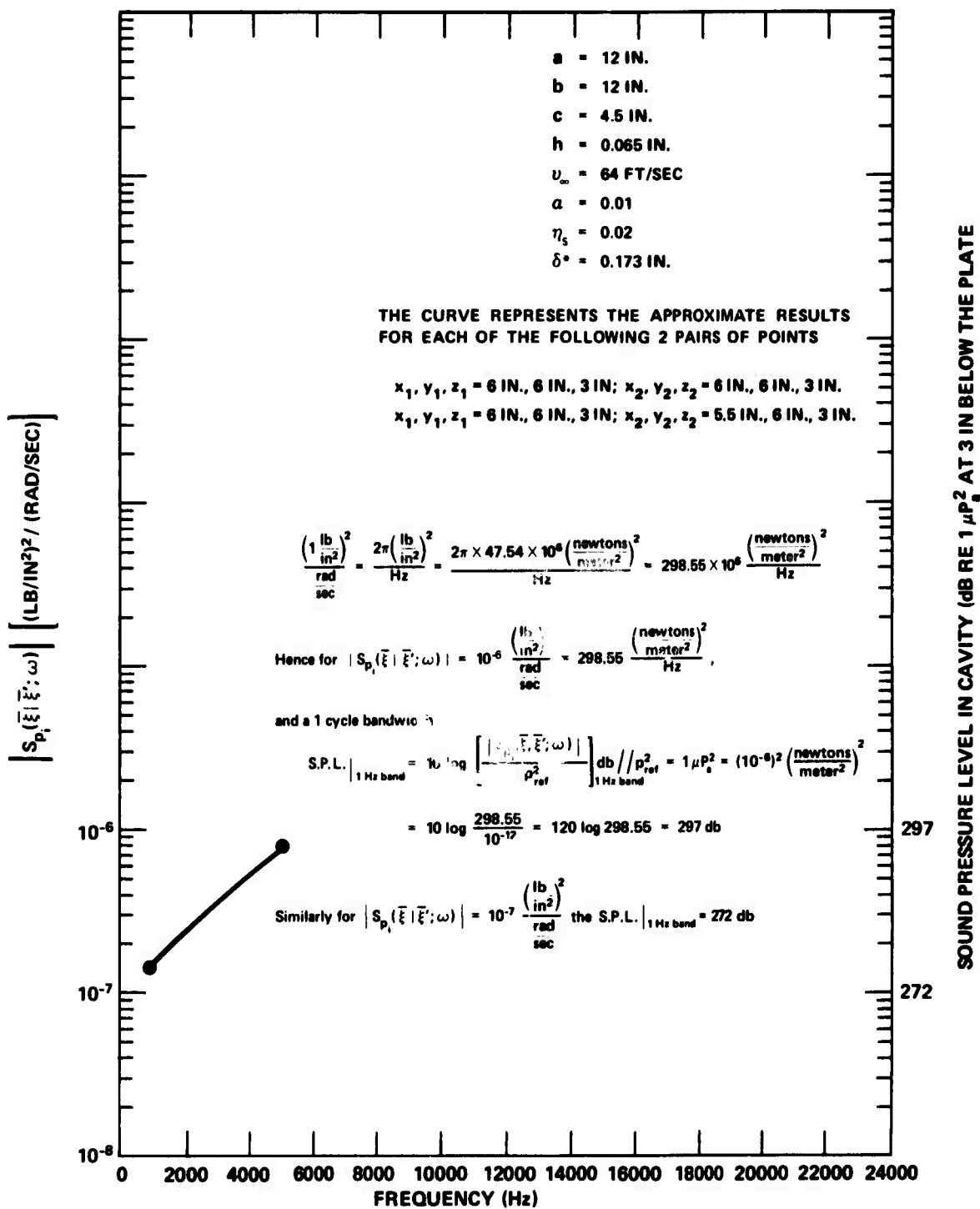
Figure 3 — Magnitudes of Cross-Spectral Density and Power Spectral Density of Cavity Acoustic Pressure versus Frequency
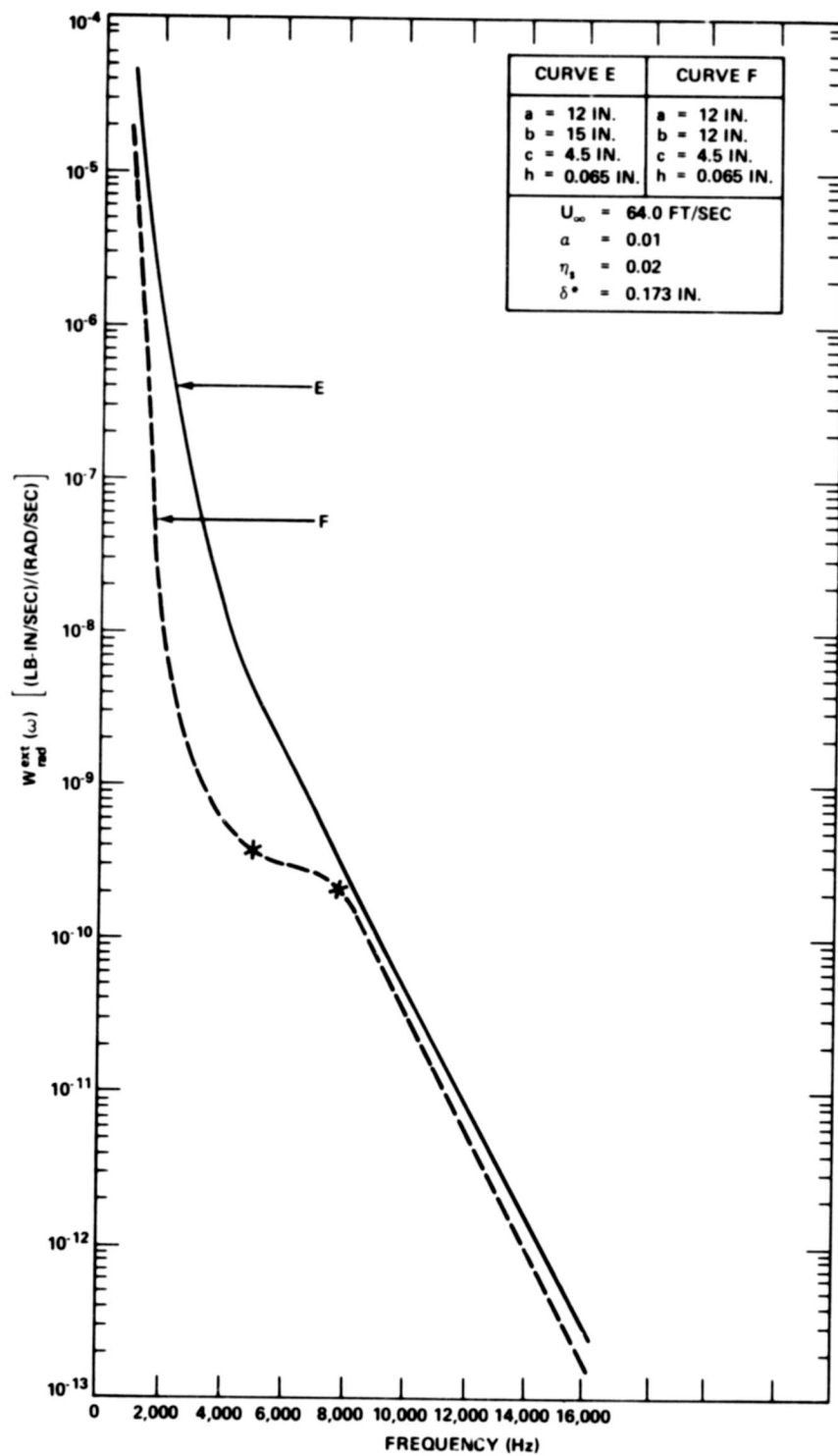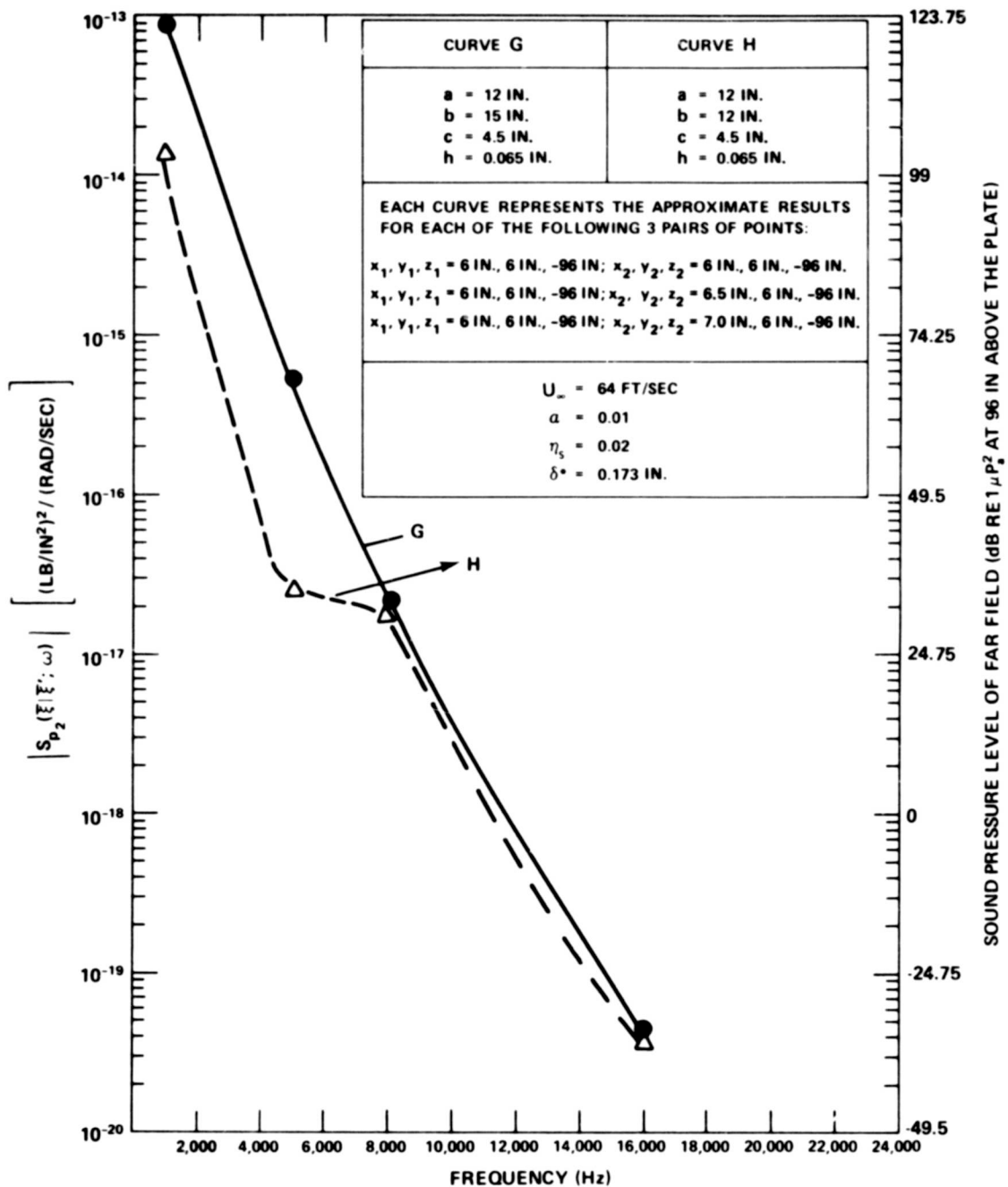
26

Figure 4 – Magnitude of Complex-Spectral Density of Radiated Power versus Frequency

27

Figure 5 – Magnitudes of Cross-Spectral Density of Far-Field Acoustic Pressure between Points x_1, y_1, z_1 and x_2, y_2, z_2 and Power Spectral Density of Far-Field Acoustic Pressure at $x_1 = x_2$, $y_1 = y_2$, $z_1 = z_2$, versus Frequency

SEE NOTE FIG. 3

28

boundary layer input data used can be obtained from either Appendix B of Reference 1 or from Reference 12, and other pertinent input data are specified on the figures. The two plate-cavity systems shown in Figures 2, 4 and 5 differ only in the width b; see Figure 1. Only narrow-band results are treated.

In Figure 2, the magnitudes of the cross-spectral density and the power spectral density of the plate displacement are represented by Curves B, D and A, C, respectively. The single curve shown in Figure 3 approximately represents the magnitudes of both the cross-spectral density and the power spectral density acoustic pressures for almost hard walls. In Figure 4, the magnitudes of the complex spectral density of power radiated into the distant field of the half-space above the plate are represented by Curves E and F. In Figure 5, the magnitudes of the cross-spectral density and the power spectral density of acoustic pressure in the distant far field of the half-space above the plate are represented by Curves H and G, respectively.

As shown in Appendix G, the foregoing spectral quantities are generally complex numbers consisting of a real or "coincident-spectral" term and an imaginary or "quadrature-spectral" term. Each spectral quantity may also be expressed in complex polar notation in terms of its magnitude and phase angle. Comparison of the "co" and "quad" data for the aforementioned spectral quantities for pressures and displacements shows that the numerical values for the former are considerably greater than those for the latter;* hence, the plotted curves (Figures 2, 3, and 5) for the magnitudes of the spectral quantities are virtually equal in magnitude to the "co" terms. The sample results presented were obtained with the program and are preliminary. Other additional (but limited) data output were obtained. Part D of Appendix G gives the program output which relates to the results presented here.

EVALUATION

1. Theoretical Results

The results of the present analytical study culminating in the development of a computer program represent:

1.   More complete, general, and exact solutions for the half-space intermodal co-efficients of a water-loaded rectangular plate in a baffle than those obtained by Davies.

2.   An extension of the work of earlier investigators on plate-cavity systems subject to turbulence and other excitation (see Table 1 and the Bibliography) to include the effects of any combination of dense and light fluids internal and external to the system on the vibration and radiation response. In general, it has been shown how present analysis

---

*The converse is true for the radiated and reactive power.

for simply supported plates and M=0 can be extended to plates with clamped-clamped (and other end) supports and M>0; for example, applicability to clamped-clamped plates and M=0 is quite easily made in accordance with the procedure given in Appendix E.

3.   A computer tool for calculating the vibroacoustic spectral quantities of a water-loaded plate-cavity system. Of particular interest is the potential use of the program to perform studies of effects due to the variation of parameters. Such studies are useful to the designer for achieving good judgment values relative to (a) the sensitivity of the vibroacoustic response associated with design changes, i.e., changes in the geometry and physical parameters of the system and (b) optimum system design for meeting vibroacoustic requirements.

2. Computational Results

A comparison of the magnitude of the plate displacement cross-spectral density (Curves B and D of Figure 2) indicates that all other dimensions being the same, the peak for

$$\left| S_w(\bar{x}|\bar{x}'; \omega) \right|_{b=15 \text{ in}}$$

is greater than the peak for
$$\bar{x} = x_1, y_1$$
$$\bar{x}' = x_2, y_2$$

$$\left| S_w(\bar{x}|\bar{x}'; \omega) \right|_{b=12 \text{ in}}$$

The trends for the curves on the right of the peaks indicate the decay with increasing frequency of S_w as computed for a selected number of resonant modes. A comparison of the magnitudes of the plate displacement power spectral density (Curves A and C of Figure 2) indicates that similar results prevail for $\bar{x} = \bar{x}'$ (or, equivalently, $x_1 = x_2$, $y_1 = y_2$).

However, the significance of the curves may be more apparent that real in view of the following. The program searches for those modes whose fluid-loaded resonances lie close to the excitation frequency, e.g., 1000 Hz. More precisely, we select those modes whose bandwidths, corresponding to the half-power points, encompass the excitation frequency. Therefore since a severely limited number (4) of excitation frequencies was considered, i.e., 1000, 5000, 8000, and 16,000 Hz, the curves in Figure 2 may not represent the essentially true magnitudes, locations, and sharpnesses of the peaks as well as the true general characteristics (i.e., response amplitude versus frequency) for S_w. Another effect may also lead to false conclusions. A resonance mode for the square plate could have a node near the position selected for the computation of the response. This could contribute to a relatively small response at that position. It is clear therefore that we must be careful not to make general inferences based on the specific results displayed by Figure 2. Additional frequency and spatial data are necessary for proper evaluation of the response. Analogously, this statement obtains for Figures 3 to 5.

The limited data in Figure 3 indicate that the magnitudes of the cross-spectral density and power spectral density of cavity acoustic pressure are nearly equal for the spatial coordinates of the observation points $(x_1, y_1, z_1; x_2, y_2, z_2)$ given on the figure.

In Figure 4, the magnitudes of the complex spectral density of radiated power, Curves E and F, decrease rapidly with frequency; Curve F decreases more rapidly at first but approaches Curve E at higher frequencies. Thus, at frequencies below 5000 Hz, the power radiated by the plate-cavity system of width b=15 in. may be greater than an order of magnitude than that for the system of width b=12 inches. Above 8000 Hz, however, the power radiated by both plate-cavity systems is nearly the same; note that the geometries for the plate-cavity systems used here and in Figure 2 correspond and that other parameters are the same.

Figure 5 indicates the magnitudes of the cross-spectral density and power spectral density of the far-field pressure, Curves G and H.

In sum, the limited numerical data obtained by use of the computer program do not permit a comprehensive evaluation of the plate-cavity system at the present time. Hence, although the foregoing curves are indicative of the types of data that can be obtained from the computer, they are not analyzed for general character, import, and practical significance.

CONCLUSIONS

1. For turbulence-excited plate-cavity systems, the analysis and computer program presented here permit the computation of the cross-spectral density and/or power spectral density of (a) the plate displacement, (b) the cavity acoustic pressure, and (c) the acoustic pressure in the distant far field of the half-space. The program also permits computation of the spectral density of power radiated in the half-space above the plate. Additional spectral quantities for the complex acoustic power in the cavity and for the near-field acoustic pressure above the plate can be computed by programming the completed (i.e., existing) analytical results for the former and analytically evaluating the general formulation devised here for the latter as well as developing a corresponding computer program.

2. The half-space intermodal coefficients for a water-loaded rectangular plate in a baffle evaluated here by contour integration are more complete, general, and exact than the first-order approximate evaluations by Davies.

3. With further development, the analysis and computer program are directly useful in the design of a water-loaded trough.

In summary, the present study has achieved its chief objectives involving the investigation of the basic physical mechanisms associated with (1) plate-acoustic field interaction for a fluid-loaded plate cavity system and (2) the contribution of turbulence excitation to the flow-

induced noise internal and external to a fluid-loaded plate-cavity system. A comprehensive evaluation of system performance awaits more extensive numerical calculations from the computer program.

RECOMMENDATIONS

Based on the results of the present study it is recommended that:

1. The computer program be used to obtain an adequate amount of numerical data for the response and radiation of a plate-cavity system excited by boundary layer turbulence. The data should be displayed as curves and tables in a form suitable for significant physical interpretation. For example, displays indicating the number and types of significantly radiating modes, the role and significance of intermodal coupling and damping, optimum plate-cavity system design, and sensitivity of vibroacoustic response to changes in geometry and physical parameters would be of interest.

2. The spectral density of the complex acoustic power in the cavity should be programmed and numerical results obtained from the program for display and interpretation.

3. The cross-spectral density of the pressure in the near field should be obtained by evaluating Equation (122). To obtain the near-field result, integrals involving the product of the half-space Green function with the characteristic modes of the plate have to be evaluated for various types of modes. These integrals reduce to the forms given by Equation (125) which should be solvable by contour integration techniques for all of the various types of modes which will exist. Thus, Equation (125) requires evaluation for x- and y-type edge modes, corner modes, and acoustically fast (AF) modes as well as all possible combinations of these modes. The analytical results should be programmed and computer runs made to obtain and display numerical results that will yield significant interpretations for the fundamental mechanisms involved and for design purposes.

ACKNOWLEDGMENTS

---

* See References 8 and 11.

APPENDIX A

DERIVATION OF BASIC EQUATIONS

The six sections of this appendix present integral equations for:

A1. The response of a plate* to harmonic excitation.

A2. The response of a plate* to random excitation.

A3. The cross-spectral density of the acoustic pressure in a cavity shaped like a rectangular parallelepiped; one surface of the cavity is bounded by the plate and the other five are treated as hard or nearly hard walls.

A4. The spectral density of the (complex) power generated by the plate-cavity system in the half-space representing the region above the plate and away from the cavity.

A5. The spectral density of the (complex) power radiated by the plate-cavity system system into half-space.

A6. The spectral density of the (complex) power radiated by the plate-cavity system into the cavity. Under consideration is a thin, flat, flexible, isotropic, rectangular, finite plate with either simply supported or clamped-clamped structural boundaries contiguous with a rigid infinite baffle. The fluids at the boundaries of both sides of the plate, external and internal to the plate-cavity system, may consist of any combination of heavy and light fluid media.

A1. PLATE RESPONSE TO HARMONIC EXCITATION

Figure 6 illustrates the kinematic relationship between the coordinates of a fixed (S) and moving (S') frame of reference; S' moves the fluid medium with a steady velocity $\overline{V}$ with respect to S. The transformation of the coordinates for a plane wave traveling in a direction specified by the vector wavenumber $\overline{k}$ is given by (see Chapter 11 of Morse and Ingard[24])

$$\overline{r} = \overline{r}' + \overline{V}t, \ t = t'$$

where the unprimed quantities are measured by an observer at rest in the "laboratory coordinates" and the primed quantities are measured by an observer moving with the system.

The equations governing the acoustic field in the coordinate system S' which is *comoving* with (or stationary with respect to) the fluid are

Continuity equation $\qquad \dfrac{\partial \delta}{\partial t'} + \rho \sum_i \dfrac{\partial u_i}{\partial x_i'} = 0$

Momentum equation $\qquad \rho \dfrac{\partial u_i}{\partial t'} = -\dfrac{\partial p_2}{\partial x_i'}$

---

*The flexible plate is one surface of a plate-cavity system described below.
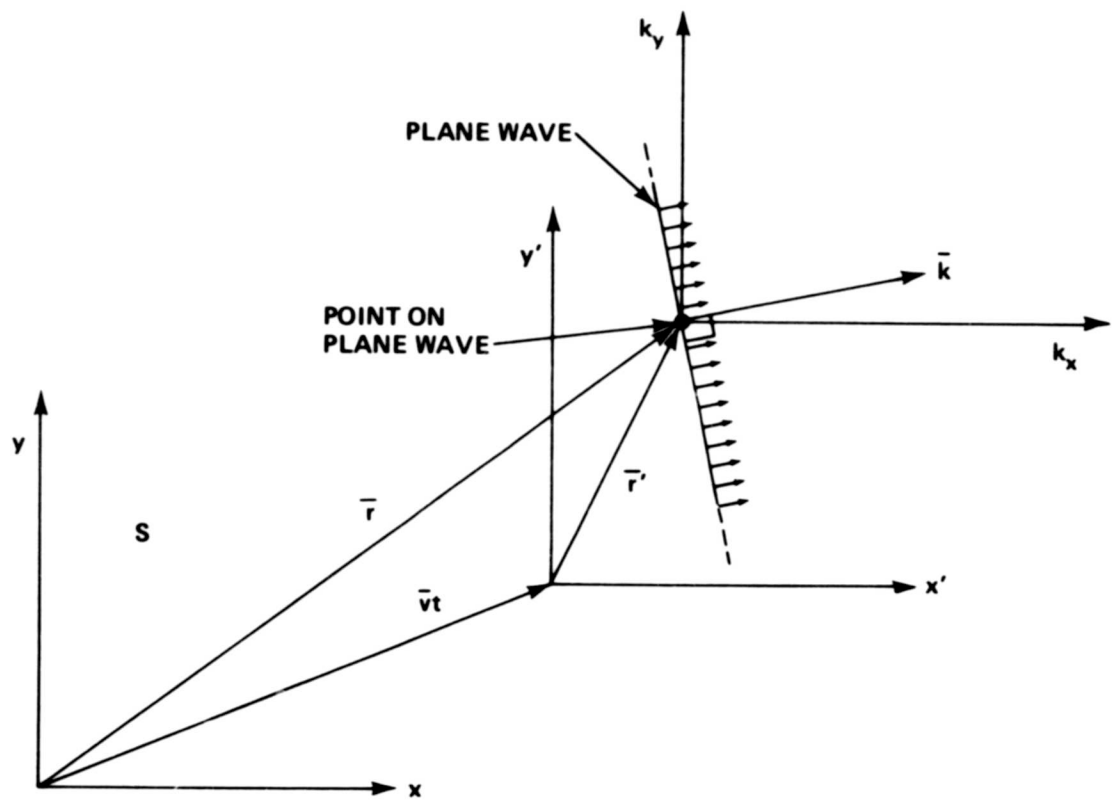
Note: ($\bar{r}$ and $\bar{r}'$ represent the coordinates in S and S' respectively for a plane wave travelling along $\bar{k}$)

Figure 6 – Kinematic Relationship between Coordinates of a Fixed (S) and Moving (S') Frame of Reference

Equation of state
$$p_2 = c_o^2 \, \delta$$

where p_2 = the pressure change caused by sound (the acoustic pressure)
ρ = the equilibrium density of the fluid and
δ = the small increase in density produced by sound.

The subscript i refers to x, y, and z, respectively. Thus, if V_i represents the components of the fluid steady velocity, the transformation of coordinates from the comoving system S' to the laboratory system S is given by

$$x_i = x'_i + V_i t', \ t = t', \quad \bar{V} = const$$

For any function of space and time, $f(x, t)$

$$\frac{\partial f}{\partial x'_i} = \frac{\partial f}{\partial x_i} \frac{\partial x_i}{\partial x'_i} + \frac{\partial f}{\partial t} \frac{\partial t}{\partial x'_i} = \frac{\partial f}{\partial x_i}$$

since $\frac{\partial x_i}{\partial x'_i} = 1, \frac{\partial t}{\partial x'_i} = 0.$ Hence $\frac{\partial}{\partial x'_i} = \frac{\partial}{\partial x}$

However, in accordance with the form of the continuity equation

$$\frac{\partial f}{\partial t'} = \frac{\partial f}{\partial t} \frac{\partial t}{\partial t'} + \sum_i \frac{\partial f}{\partial x_i} \frac{\partial x_i}{\partial t'} = \frac{\partial f}{\partial t} + \sum_i V_i \frac{\partial f}{\partial x_i}$$

or

$$\frac{\partial}{\partial t'} = \frac{\partial}{\partial t} + \sum_i V_i \frac{\partial}{\partial x_i} = \frac{\partial}{\partial t} + \bar{V} \cdot \nabla$$

since $\frac{\partial t}{\partial t'} = 1, \frac{\partial x_i}{\partial t'} = \bar{V}$

We observe that whereas the space derivatives are invariant under transformation, the time derivative is not. Thus, in the *stationary* frame S, the continuity and momentum equations are written as follows in terms of laboratory coordinates; in addition we repeat the equation of state

Continuity equation
$$\left(\frac{\partial}{\partial t} + \bar{V} \cdot \nabla \right) \delta + \rho \sum_i \frac{\partial u_i}{\partial x_i} = 0$$

Momentum equation
$$\rho \left(\frac{\partial}{\partial t} + \bar{V} \cdot \nabla \right) u_i = -\frac{\partial p_2}{\partial x_i}$$

Equation of state
$$p_2 = c_o^2 \, \delta$$

Combining the equations of state and continuity, we have

$$\frac{1}{c_o^2}\left(\frac{\partial}{\partial t} + \bar{V}\cdot\nabla\right)p_2 = -\rho\,\sum_i \frac{\partial u_i}{\partial x_i}$$

Multiplying both sides of this equation by the operator $\frac{\partial}{\partial t} + \bar{V}\cdot\nabla$, interchanging the summation and operator, and then using the momentum equation, we derive the convected wave equation

$$\frac{1}{c_o^2}\left(\frac{\partial}{\partial t} + \bar{V}\cdot\nabla\right)^2 p_2 = -\rho\,\sum_i \frac{\partial}{\partial x_i}\left(\frac{\partial}{\partial t} + \bar{V}\cdot\nabla\right)u_i = \sum_i \frac{\partial^2 p_2}{\partial x_i^2} = \nabla^2 p_2$$

Several forms for the wave equation, in laboratory coordinates for a fluid with steady velocity $\bar{V}$, are

$$\frac{1}{c_o^2}\left(\frac{\partial}{\partial t} + \bar{V}\cdot\nabla\right)^2 p_2 = \nabla^2 p_2 \tag{1a}$$

$$\frac{1}{c_o^2}\left(\frac{\partial}{\partial t} + \sum_i V_i\frac{\partial}{\partial x_i}\right)^2 p_2 = \nabla^2 p_2 \tag{1b}$$

$$\frac{1}{c_o^2}\left(\frac{\partial^2 p_2}{\partial t^2} + 2\sum_i V_i\frac{\partial}{\partial t}\frac{\partial p_2}{\partial x_i} + \sum_i V_i V_j\frac{\partial^2 p_2}{\partial x_i \partial x_j}\right) = \nabla^2 p_2 \tag{1c}$$

For assumed harmonic time dependence of the form $e^{-i\omega t}$

$$p_2(x_i, t) = p_2(x_i)\,e^{-i\omega t}\;,\;\frac{\partial p_2(x_i, t)}{\partial t} = -i\omega p_2(x_i, t),\;\frac{\partial^2 p_2(x_i, t)}{\partial t^2} = -\omega^2 p_2(x_i, t)$$

Thus $\frac{\partial}{\partial t} \to -i\omega$ and

Equation (1a) becomes

$$\frac{1}{c_o^2}(-i\omega + \bar{V}\cdot\nabla)^2 p_2 = \nabla^2 p_2$$

Expanding this equation, we have

$$\nabla^2 p_2 + \frac{\omega^2}{c_o^2}[1 + \frac{2i}{\omega}\bar{V}\cdot\nabla - (\frac{\bar{V}\cdot\nabla}{\omega})^2]\,p_2 = 0$$

or

$$\nabla^2 p_2 + \frac{\omega^2}{c_o^2}(1 + \frac{i}{\omega}\bar{V}\cdot\nabla)^2 p_2 = 0$$

36

For a fluid velocity parallel to the x-axis, $\bar{V} = V\hat{i}$ and $\bar{V} \cdot \nabla = V \frac{\partial}{\partial x}$. In this case Equation (1) becomes

$$\nabla^2 p_2 + \frac{\omega^2}{c_0^2} \left(1 + \frac{i}{\omega} V \frac{\partial}{\partial x}\right)^2 p_2 = 0$$

or

$$\nabla^2 p_2 + \left(\frac{\omega}{c_0} + \frac{i}{c_0} V \frac{\partial}{\partial x}\right)^2 p_2 = 0$$

or

$$\nabla^2 p_2 + \left(k + i M \frac{\partial}{\partial x}\right)^2 p_2 = 0; \quad M = \frac{V}{c_0}$$

or

$$\nabla^2 p_2 + L^2 p_2 = 0 \tag{2}$$

where L is an operator defined by

$$L = k + i M \frac{\partial}{\partial x} \tag{3}$$

The acoustic velocity $\bar{u}(x, y, z, t)$ is defined in S' in terms of the (acoustic) velocity potential $\psi(x, y, z, t)$ by

$$\bar{u} = \nabla \psi$$

The corresponding acoustic pressure is

$$p_2 = \rho \frac{\partial \psi}{\partial t'} = \rho \left(\frac{\partial}{\partial t} + \bar{V} \cdot \nabla\right) \psi = \rho \left(-i\omega + V \frac{\partial}{\partial x}\right) \psi = -i\rho c_0 \left(k + iM \frac{\partial}{\partial x}\right) \psi$$
$$= -i\rho c_0 L \psi \tag{4}$$

Inserting Equation (4) into Equation (2) yields

$$\nabla^2 \psi + L^2 \psi = \nabla^2 \psi + \left(k + i M \frac{\partial}{\partial x}\right)^2 \psi = 0$$

or

$$\frac{\partial^2 \psi}{\partial x^2} + \frac{\partial^2 \psi}{\partial y^2} + \frac{\partial^2 \psi}{\partial z^2} + k^2 \psi + 2ikM \frac{\partial \psi}{\partial x} - M^2 \frac{\partial^2 \psi}{\partial x^2} = 0$$

Thus ψ satisfies the following equation in cartesian (x,y,z) space

$$(1-M^2)\frac{\partial^2 \psi}{\partial x^2} + \frac{\partial^2 \psi}{\partial y^2} + \frac{\partial^2 \psi}{\partial z^2} + 2i\,k\,M\frac{\partial \psi}{\partial x} + k^2\,\psi = 0 \tag{5}$$

Now $\psi\,(x,y,z)$ may be expressed in terms of its Fourier transform* $\Psi\,(k_x,k_y,z)$

$$\psi\,(x,y,z) = \left(\frac{1}{2\pi}\right)^2 \int\limits_{-\infty}^{\infty} \int\limits_{-\infty}^{\infty} \Psi\,(k_x,k_y,z)\,e^{i\,(k_x x + k_y y)}dk_x\,dk_y \tag{5a}$$

Hence, taking the Fourier transform of each of the terms in Equation (5) with

$$\psi\,(x,y,z) \equiv \psi\,(\bar{x},z) \rightarrow \Psi\,(k_x,k_y,z)$$

$$\{\bar{x}\} \equiv \{x,y\}$$

we get

$$(M^2-1)\,k_x^2\,\Psi - k_y^2\,\Psi + \frac{d^2 \Psi}{dz^2} + 2i\,kM\,(ik_x)\,\Psi + k^2\,\Psi = 0$$

Thus Ψ satisfies the following equation in wavenumber (k_x,k_y) and z-space

$$\frac{d^2 \Psi}{dz^2} + \zeta^2\,\Psi = 0 \tag{6}$$

where

$$\zeta^2 = k^2 + (M^2-1)\,k_x^2 - 2k\,Mk_x - k_y^2 \tag{7}$$

We observe that for $M=0$, $\zeta^2 \rightarrow k^2 - k_x^2 - k_y^2 = k_z^2$. Hence, for any value of M, ζ replaces and comprehends as a special case (for $M=0$) the wavenumber k_z. If we choose the positive value of ζ to represent outgoing waves with $e^{-i\omega t}$ dependence, then we write the solution to Equation (6) as**

$$\Psi\,(k_x,k_y,z) = \Omega\,(k_x,k_y)\,e^{i\zeta z} \tag{8}$$

The boundary conditions at the fluid-plate interface require the equality of particle and normal plate velocity. Therefore,

$$\bar{u}\,|_{z=0} = \nabla\psi\,|_{z=0}$$

---

*The general form for the Fourier transform and its inverse used here is

$$f(\bar{x},t) = \frac{1}{(2\pi)^3} \int\limits_{-\infty}^{\infty} \int\limits_{-\infty}^{\infty} f(\bar{k},\omega)\,e^{i(\bar{k}\cdot\bar{x} + \omega t)}\,d\bar{k}\,d\omega;\ f\,(\bar{k},\omega) = \int\limits_{-\infty}^{\infty} \int\limits_{-\infty}^{\infty} f(\bar{x},t)\,e^{-i(\bar{k}\cdot\bar{x} + \omega t)}\,dx\,dt$$

where $\{\bar{x}\} = \{x,y\}$, $d\bar{x} = dx\,dy$, $\{\bar{k}\} = \{k_x,k_y\}$, $d\bar{k} = dk_x\,dk_y$

**In Equation (8), $e^{i\zeta z}$ represents the phase and decay in the half-space. Here for $z > 0$, we choose the positive value of ζ *and conversely*. However, for the present, we do not specify a positive coordinate system (i.e., direction of +z) for the plate; this is defined later for the plate-cavity system following Equation (16).

and in S' space, since $\frac{\partial}{\partial t'} = \frac{\partial}{\partial t} + \bar{V} \cdot \nabla = \frac{\partial}{\partial t} + V \frac{\partial}{\partial x}$, the vector relation

$$\bar{u}\big|_{z=0} = \frac{\partial \bar{w}}{\partial t'} = \left(\frac{\partial}{\partial t} + V \frac{\partial}{\partial x}\right) \bar{w}\big|_{z=0} = \left(-i\omega + V \frac{\partial}{\partial x}\right) \bar{w}\big|_{z=0} = -ic_0 \left(k + iM \frac{\partial}{\partial x}\right) \bar{w}\big|_{z=0}$$

$$= -ic_0 \; L\bar{w}\big|_{z=0} \qquad\qquad \text{on plate}$$

$$= 0 \qquad\qquad\qquad\qquad \text{off plate}$$

and the corresponding scalar relation is

$$\frac{d\psi}{dz}\bigg|_{z=0} = -i \, c_0 \; L\bar{w}\big|_{z=0} \qquad\qquad \text{on plate; zero otherwise}$$

The Fourier transform relationship obtained from this equation is then equated to the derivative $\frac{d\Psi}{dz}$ obtained from Equation (8). Thus

$$\frac{d\Psi}{dz}\bigg|_{z=0} = i \, c_0 \; \hat{LW}\big|_{z=0} = i \, \zeta \; \Psi\big|_{z=0}$$

where $\hat{LW} = \mathcal{F}(Lw)$. Note that z in frame S is equal to z' in frame S'. From this equation and Equation (8)

$$\Psi\big|_{z=0} = -\frac{c_0 \, \hat{LW}}{\zeta}\bigg|_{z=0} = \Omega \, (k_x, k_y)$$

Thus Equation (8) becomes

$$\Psi \, (k_x, k_y, z) = -\frac{c_0 \, \hat{LW}}{\zeta} \, e^{i\zeta z} \tag{9}$$

where in frame S'

$$\hat{LW}(k_x, k_y) = \int_0^a \int_0^b L'w \, (x', y') \, e^{-i(k_x x' + k_y y')} \, dx' \, dy' \tag{10}$$

$$L' = k + i \, M \frac{\partial}{\partial x'} \tag{11}$$

we perceive that $\hat{LW}$ is independent of z.

Using Equations (9) and (10) in conjunction with Equation (5a), we find

$$\psi(x, y, z) = \left(\frac{1}{2\pi}\right)^2 \int_{-\infty}^{\infty} \int_{-\infty}^{\infty} \Psi(k_x, k_y, z) \, e^{i(k_x x + k_y y)} \, dk_x \, dk_y$$

$$= \left(\frac{1}{2\pi}\right)^2 \int_{-\infty}^{\infty} \int_{-\infty}^{\infty} \left[\frac{-c_0 \, \hat{LW}}{\zeta} \, e^{i\zeta z}\right] e^{i(k_x x + k_y y)} \, dk_x \, dk_y$$

$$= -\frac{c_0}{(2\pi)^2} \int_{-\infty}^{\infty} \int_{-\infty}^{\infty} \frac{e^{i(k_x x + k_y y)}}{\zeta} \, e^{i\zeta z} \, dk_x \, dk_y \int_0^a \int_0^b L'w(x', y') \bullet$$

$$e^{-i(k_x x' + k_y y')} \, dx' \, dy'$$

39

$$= -\frac{c_o}{(2\pi)^2} \int_0^a \int_0^b dx'\, dy' \int_{-\infty}^{\infty} \int_{-\infty}^{\infty} L'w(x', y') \frac{e^{i[k_x(x-x') + k_y(y-y') + \zeta z]}}{\zeta} dk_x\, dk_y$$

$$= -\frac{c_o}{4\pi^2} \int_0^a \int_0^b G_p^o(\bar{x}, z|\bar{x}', o)\, L'w(x',y')\, dx'\, dy' \tag{12}$$

where the Green function for the half-space is

$$G_p^o(\bar{x}, z|\bar{x}', z') \equiv G_p^o(x, y, z|x', y', z') = \int_{-\infty}^{\infty} \int_{-\infty}^{\infty} \frac{e^{i[k_x(x-x') + k_y(y-y') + \zeta(z-z')]}}{\zeta} dk_x\, dk_y \tag{13}$$

and from Equation (7)

$$\zeta = \sqrt{k^2 + (M^2 - 1)k_x^2 - 2k\,Mk_x - k_y^2}$$

We now evaluate G_p^o in closed form for $M = \dfrac{V}{c_0} < 1$. To facilitate the evaluation, it will be convenient to change the form of Equation (13).

Therefore let

$$\xi = \sqrt{1 - M^2}\, k_x + \kappa M, \quad \kappa = \frac{k}{\sqrt{1-M^2}}, \quad u = \frac{x-x'}{\sqrt{1-M^2}}$$

where k_x and ξ range from $-\infty$ to ∞. Then

$$\zeta = \sqrt{\kappa^2(1-M^2) + (M^2-1)k_x^2 - 2\kappa M\sqrt{1-M^2}\, k_x - k_y^2}$$

$$= \sqrt{-[\kappa^2 M^2 + 2\kappa M\sqrt{1-M^2}\, k_x + (\sqrt{1-M^2})^2 k_x^2] + \kappa^2 - k_y^2}$$

$$= \sqrt{-(\kappa M + \sqrt{1-M^2}\, k_x)^2 + \kappa^2 - k_y^2}$$

$$= \sqrt{(\kappa^2 - \xi^2) - k_y^2} = i\sqrt{k_y^2 - (\kappa^2 - \xi^2)} = i\sqrt{k_y^2 + (\xi^2 - \kappa^2)}$$

where the positive algebraic sign for i has been chosen since, by definition, $+i$ represents the direction of outgoing waves; see footnote below Equation (8). Also
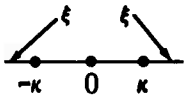
$$dk_x = \frac{d\xi}{\sqrt{1-M^2}}$$

40

Equation (13) may now be written for $z' = 0$ as

$$G_p^o (\bar{x}, z|\bar{x}', 0) = \int_{-\infty}^{\infty} \int_{-\infty}^{\infty} \frac{e^{i\left[\frac{(\xi-\kappa M)}{\sqrt{1-M^2}}(x-x') + k_y(y-y') + \xi z\right]}}{i\sqrt{k_y^2 + (\xi^2-\kappa^2)}} dk_x\, dk_y$$

$$= \frac{-ie^{-i\kappa Mu}}{\sqrt{1-M^2}} \int_{-\infty}^{\infty} e^{i\xi u}\left[\int_{-\infty}^{\infty} \frac{e^{-z\sqrt{k_y^2 + (\xi^2-\kappa^2)}}}{\sqrt{k_y^2 + (\xi^2-\kappa^2)}} e^{i k_y(y-y')} dk_y\right] d\xi$$

The integrand of the inner integral has square root type branch points at

$k_y^{1,2} = \pm\sqrt{\kappa^2-\xi^2}$. Then

for $\xi \leq -\kappa$ and $\xi \geq \kappa$, $k_y^{1,2} = \pm i\sqrt{\xi^2-\kappa^2}$ and

for $-\kappa < \xi < \kappa$, $k_y^{1,2} = \pm\sqrt{\kappa^2-\xi^2}$

Hence the integral for G_p^o consists of the following three components:

$$G_p^o = \frac{-ie^{-i\kappa Mu}}{\sqrt{1-M^2}}\left[\int_{-\infty}^{-\kappa} g_1(\xi)e^{i\xi u}\, d\xi + \int_{-\kappa}^{\kappa} g_2(\xi)e^{i\xi u}\, d\xi + \int_{\kappa}^{\infty} g_1(\xi)e^{i\xi u}\, d\xi\right]$$

where

$$\int_{-\infty}^{\infty} \frac{e^{-z\sqrt{k_y^2 + (\xi^2 - \kappa^2)}}}{\sqrt{k_y^2 + (\xi^2 - \kappa^2)}} e^{ik_y(y-y')}\, dk_y = \begin{cases} g_1(\xi) \text{ for } \xi^2 > \kappa^2 \\ g_2(\xi) \text{ for } \xi^2 < \kappa^2 \end{cases}$$

To evaluate $g_1(\xi)$ and $g_2(\xi)$, consider the following identity (page 710 in Gradshteyn and Ryzhik[25]). This identity and its Fourier transform will be used to obtain the closed form expression for G_p^o ($M < 1$); see Maestrello and Linden.[26]

$$I_1 = \int_{-\infty}^{\infty} e^{-itx} H_0^{(2)}(r\sqrt{a^2 - t^2})\, dt = \frac{2ie^{-ia\sqrt{r^2+x^2}}}{\sqrt{r^2+x^2}} \tag{14a}$$

[r and x real, $-\pi < \arg\sqrt{a^2-t^2} \leq 0$, $-\pi < \arg a \leq 0$]

Also, from the Fourier integral theorem

$$2i \left[\frac{1}{2\pi} \int_{-\infty}^{\infty} \frac{e^{-ia\sqrt{r^2 + x^2}}}{\sqrt{r^2 + x^2}} e^{itx} \, dx \right] = H_0^{(2)} \left(r\sqrt{a^2 - t^2} \right)$$

or

$$I_2 = \int_{-\infty}^{\infty} \frac{e^{-ia\sqrt{r^2 + x^2}}}{\sqrt{r^2 + x^2}} e^{itx} \, dx = - i\pi \, H_0^{(2)} \left(r\sqrt{a^2 - t^2} \right)$$

[r real or pure imaginary and x real, $-\pi < \arg \sqrt{a^2 - t^2} \leqslant 0$, $-\pi < \arg a \leqslant 0$]

Case 1: $\xi^2 > \kappa^2$

In equation (14b) we set

$$r = \pm\sqrt{\xi^2 - \kappa^2}, \; a = -iz, \; x = k_y, \; t = y - y'$$

then

$$g_1(\xi) = I_2 = -i\pi \, H_0^{(2)} \left(\pm\sqrt{\xi^2 - \kappa^2} \cdot \sqrt{-z^2 - (y-y')^2} \right)$$

$$= -i\pi \, H_0^{(2)} \left(\pm i \, R\sqrt{\xi^2 - \kappa^2} \right)$$

where

$$R = \sqrt{z^2 + (y-y')^2}$$

For convergence of $g_1(\xi)$, we require that $\lim_{\xi \to \infty} H_0^{(2)} \to 0$. Thus, we select only the solution $g_1(\xi)$ with the negative algebraic sign in the argument

$$g_1(\xi) = -i\pi \, H_0^{(2)} \left(-iR\sqrt{\xi^2 - \kappa^2} \right) = -i\pi \, H_0^{(2)} \left(-R\sqrt{\kappa^2 - \xi^2} \right)$$

We observe that, as required, both r and x are real. We require also that

$-\pi < \arg \sqrt{(-iz)^2 - (y-y')^2} = \arg (\pm iR) \leqslant 0$ and $-\pi < \arg(-iz) \leqslant 0$ Since $R > 0$, this require-
ment is met only for the minus sign preceding iR and for $z > 0$. Thus, we note that for these
conditions, $g_1(\xi)$ will converge since

$$\lim_{k_y \to \infty} \frac{e^{-z\sqrt{k_y^2 + (\xi^2 - \kappa^2)}}}{\sqrt{k_y^2 + (\xi^2 - \kappa^2)}} = 0 \text{ for } z > 0. \text{ Also since } \sqrt{\xi^2 - \kappa^2} > 0, \text{ then } -\pi < \arg(-iR) \leqslant 0$$

implies $-\pi < \arg(-iR\sqrt{\xi^2 - \kappa^2}) \leqslant 0$, confirming the fact that for this case,

$$\lim_{\xi \to \infty} H_0^{(2)} \left(-iR\sqrt{\xi^2 - \kappa^2} \right) = 0.$$

42

Case 2: $\kappa^2 > \xi^2$

In Equation (14b) we set

$$r = \pm\sqrt{\xi^2 - \kappa^2} = \pm i\sqrt{\kappa^2 - \xi^2}, \quad a = -iz, \quad x = k_y, \quad t = y-y'$$

Then

$$g_2(\xi) = I_2 = -i\pi\, H_0^{(2)}\left(\pm i\sqrt{\kappa^2 - \xi^2} \cdot i\sqrt{z^2 + (y-y')^2}\right)$$

$$= -i\pi\, H_0^{(2)}\left(\mp R\sqrt{\kappa^2 - \xi^2}\right)$$

Following reasoning similar to that above for $g_1(\xi)$, we choose the negative algebraic sign for the argument of $H_0^{(2)}$.

Hence

$$g_1(\xi) = g_2(\xi) = -i\pi\left(-R\sqrt{\kappa^2 - \xi^2}\right)$$

and

$$G_p^0(\bar{x},z|\bar{x}',0) = \frac{-\pi e^{-i\kappa M u}}{\sqrt{1 - M^2}} \int_{-\infty}^{\infty} H_0^{(2)}\left(-R\sqrt{\kappa^2 - \xi^2}\right) e^{i\xi u}\, d\xi$$

Letting $u = -u'$, $u^2 = (u')^2$ in this equation and then evaluating the integral by using Equation (14a) with*

$$r = -R, \quad a^2 = \kappa^2, \quad a = \pm\kappa, \quad t = \xi, \quad x = u'$$

we obtain the closed-form solution for $G_p^0(\bar{x},z|\bar{x}',0)$:

$$G_p^0(\bar{x},z|\bar{x}',0) = \frac{-\pi e^{i\kappa M u'}}{\sqrt{1 - M^2}}\, 2i\, \frac{e^{-i\,(\pm\kappa\sqrt{R^2 + (u')^2})}}{\sqrt{R^2 + (u')^2}}$$

The $-\kappa$ shown in the parentheses is chosen to ensure an outward-traveling wave, i.e., $e^{i\kappa\sqrt{}}$ represents an outgoing wave. Thus, letting $u' \to -u$

$$G_p^0(x,y,z|x',y',0) = \frac{-2\pi i}{\sqrt{1 - M^2}}\, \frac{e^{i\kappa\,(\sqrt{u^2 + R^2} - M u)}}{\sqrt{u^2 + R^2}} \qquad ; \quad M < 1 \qquad (15)$$

where

$$u = \frac{x - x'}{\sqrt{1 - M^2}}, \quad \kappa = \frac{k}{\sqrt{1 - M^2}}, \quad R^2 = z^2 + (y - y')^2$$

---

*The substitutions represent a change in the symbols used in Equation (14a). Once made, the actual value of

$$u = -u' = \frac{x - x'}{\sqrt{1 - M^2}}$$

Because of panel vibration, the pressure in the half-space above the panel, obtained from Equations (4) and (12) is, on interchanging the operator L and the integrals*

---

*Equation (16) is a general expression for $p_2(\bar{x},z)$. For a *clamped-clamped plate* this expression can be reduced as follows. Let

$$I = \int_0^a \int_0^b L G_p^o \, L'w\,(x',y')\,dx'dy' = \int_0^b \left[\int_0^a k\, G_p^o \, L'w\, dx' + iM \int_0^a \frac{\partial}{\partial x}\, G_p^o \, L'w\, dx' \right] dy'$$

Now from Equation (13), $\dfrac{\partial G_p^o}{\partial x} = -\dfrac{\partial G_p^o}{\partial x'}$, so that integrating the second integral in brackets by parts

$$u = L'w,\ dv = \frac{\partial G_p^o}{\partial x'},\ dx',\ v = G_p^o,\ du = \frac{\partial}{\partial x'}\, L'w\, dx'$$

we get

$$I = \int_0^b \left[\int_0^a k\, G_p^o \, L'w\, dx' - iM \int_0^a L'w \frac{\partial G_p^o}{\partial x'}\, dx' \right] dy'$$

$$= \int_0^b \left\{ \int_0^a k\, G_p^o \, L'w\, dx' - iM \left[\left. G_p^o \, L'w \right|_0^a - \int_0^a G_p^o \frac{\partial}{\partial x'}\, L'w\, dx' \right] \right\} dy'$$

where

$$\left. G_p^o \, L'w \right|_0^a = G_p^o\,(x,y,z|a,y',0) \left[k w(a,y') + iM \frac{\partial w}{\partial x'}\,(a,y') \right] - G_p^o\,(x,y,z|0,y',0) \left[k w(0,y') + iM \frac{\partial w(0,y')}{\partial x'} \right]$$

$$= 0 \text{ for clamped-clamped plate since } w(a,y') \equiv \frac{\partial w(a,y')}{\partial x'} \equiv w(0,y') \equiv \frac{\partial w(0,y')}{\partial x'} \equiv 0$$

Hence

$$I = \int_0^b \int_0^a \left[k\, G_p^o \, L'w + iM\, G_p^o \frac{\partial}{\partial x'}\, L'w \right] dx'dy' = \int_0^b \int_0^a G_p^o \left(k + iM \frac{\partial}{\partial x'} \right) L'w\, dx'dy'$$

$$= \int_0^a \int_0^b G_p^o \, L'^2 w\, dx'dy'$$

Thus for a *clamped-clamped plate*

$$p_2(\bar{x},z) = \frac{i\rho c_0^2}{4\pi^2} \int_0^a \int_0^b G_p^o\,(x,y,z|x',y',0)\, L'^2 w\,(x',y')\, dx'dy'$$

(compare with Equation (16)).

44

$$p_2(\bar{x},z) = \frac{i\rho c_0^2}{4\pi} \int_0^a \int_0^b L\, G_p^0\,(\bar{x},z|\bar{x}',0)\, L'w\,(\bar{x}',y')\, dx'dy' \qquad (16)$$

where w is defined as positive in the positive z direction.

For the vibrating plate in three-dimensional compressible flow, we consider two pressure fields, namely, (1) the internal (cavity) pressure field $p^i(\bar{x}')$, acting on the plate and (2) the external pressure field, $p^0(\bar{x}')$, acting on the plate. This external field consists of two superimposed parts: (a) the blocked pressure field, $p_{b\ell}(\bar{x}')$, which in the present problem, will be the turbulent pressure field on the streamside of a rigid plate, presumed known from measurements and mathematically formulated in statistical terms, and (b) the external acoustic pressure field, $p_2(\bar{x}')$ due to the plate motion. The plate motion is now treated.

Consider a plate-cavity system, see Figure 1; note w is now defined to be positive *inward*, in the direction of positive z, i.e., the half-space (including the upper surface of the plate) occupies all points x, y, $-\infty < z < 0$ and the cavity (including the lower surface of the plate) occupies all points x, y, $0 < z < c$. For harmonic excitation, the plate response is given in terms of the plate Green function G and the total pressure acting on the plate by

$$w(\bar{x}) = \int_{A_p} G\,(\bar{x}|\bar{x}';\omega)\, [p^0(\bar{x}') - p^i\,(\bar{x}')]\, d\bar{x}'$$

$$= \int_{A_p} G\,(\bar{x}|\bar{x}';\omega)[p_{b\ell}(\bar{x}') + p_2\,(\bar{x}') - p^i(\bar{x}')]\, d\bar{x}' \qquad (17)$$

because $p^0(\bar{x}') = p_{b\ell}(\bar{x}') + p_2\,(\bar{x}')$.

The pressure in the cavity is given in terms of the cavity Green function G_p and the derivative of the internal (cavity) pressure with respect to the normal

$$p^i(\bar{x}') = - \int_{A_p} G_p\,(\bar{x}|\bar{x}';\omega)\frac{\partial p^i(\bar{x})}{\partial \nu}\, d\bar{x}$$

Now if $\phi(\bar{x},z,t) = \phi(\bar{x},z)\, e^{-i\omega t}$ is the velocity potential in the cavity space with fluid density ρ_c, then at the plate boundary where z = 0

$$p^i(\bar{x},t) = \rho_c\, \frac{\partial\phi(x,t)}{\partial t} = \rho_c\, \left[-i\omega\phi(\bar{x})\, e^{-i\omega t}\right]$$

and

$$\frac{\partial p^i(\bar{x},t)}{\partial \nu} = -i\rho_c \omega \frac{\partial \phi(\bar{x})}{\partial \nu} e^{-i\omega t}$$

Since the boundary conditions for the velocity are (note fluid particle velocity is $-\nabla \phi$ in cavity and is $\nabla \psi$ in half-space outside of the cavity)

$$\frac{\partial \phi(\bar{x},t)}{\partial \nu} = -\dot{w}(\bar{x},t) = -\frac{\partial w}{\partial t}(\bar{x},t) = - \left[-i\omega w(\bar{x}) e^{-i\omega t} \right] \quad \text{on plate}$$
$$= 0 \qquad\qquad\qquad\qquad \text{off plate}$$

then

$$\frac{\partial \phi(\bar{x})}{\partial \nu} = i\omega w(\bar{x}) \text{ on plate}$$

$$= 0 \qquad \text{off plate}$$

and

$$\frac{\partial p^i(\bar{x})}{\partial \nu} = \rho_c \omega^2 w(\bar{x})$$

Hence, the resulting pressure in the cavity is

$$p^i(\bar{x}') = - \rho_c \omega^2 \int_{A_p} G_p(\bar{x}|\bar{x}'; \omega) \, w(x) \, dx \qquad (18)$$

Using the principle of reciprocity, $G_p^o(\bar{x}, z|\bar{x}', o) = G_p^o(\bar{x}', o|\bar{x}, z)$, the pressure on the panel ($z=o$) adjacent to the half-space as obtained from Equation (16) is*

$$p_2(\bar{x}') \equiv p_2(\bar{x}', o) \equiv p_2(x', y', o) = \frac{+i\rho c_o^2}{4\pi^2} \int_0^a \int_0^b L' \, G_p^o(x', y', o|x, y, o) L w(x, y) \, dx \, dy$$

Expanding the plate displacement in terms of its *in vacuo* mode shapes

$$w(\bar{x}) = \sum_s \bar{\xi}_s \psi^s(\bar{x}); \quad \bar{\xi}_s = \bar{\xi}_s(\omega) \qquad (19)$$

Substituting Equation (19) into Equation (17), multiplying by $m\psi^r(\bar{x})$ and integrating with respect to $\bar{x}$ over the panel area, we obtain

$$M_r \xi_r \int_{A_p} \int_{A_p} m\psi^r(\bar{x}) G(\bar{x}|\bar{x}'; \omega) \left[p_{b\ell}(\bar{x}') + p_2(\bar{x}') - p_i(\bar{x}') \right] d\bar{x} \, d\bar{x}' \qquad (20)$$

---

*$G_p^o(x', y', o|x, y, o)$ is defined by Equation (15) with z=o and R=(y-y').

where $M_r = \displaystyle\int_{A_p} m\, \psi^s(\bar{x})\, \psi^r(\bar{x}) d\bar{x}$ is the modal mass.

The plate Green function is*

$$G(\bar{x}|\bar{x}') = \sum_s \frac{\psi^s(\bar{x})\, \psi^s(\bar{x}')}{M_s \bar{Y}_s} \tag{21}$$

where

$$\bar{Y}_s = \omega_s^2 \left[1 - \left(\frac{\omega}{\omega_s}\right)^2 - i\eta_s\right] \tag{22}$$

Substituting Equation (21) into Equation (20) and performing the integration with respect to $\bar{x}$ gives

$$M_r \bar{\xi}_r - \frac{M_r}{M_r \bar{Y}_r} \int_{A_p'} \psi^r(\bar{x}') \left[p_{b\ell}(\bar{x}') + p_2(\bar{x}') - p_i(\bar{x}')\right] d\bar{x}' = 0$$

or

$$-\bar{Y}_r M_r \bar{\xi}_r + \Gamma^r_{p_2} - \Gamma^r_{p_i} = -\Gamma^r_{p_{b\ell}} \tag{23}$$

---

*The modal equation for the plate is[27, 28]

$$M_s[\omega_s^2 - \omega^2 - i2\zeta_s \omega_s \omega]\, \xi_s(\omega) = M_s \omega_s^2 \left[1 - \left(\frac{\omega}{\omega_s}\right)^2 - i2\zeta_s \frac{\omega}{\omega_s}\right]\xi_s(\omega)$$

$$= M_s \omega_s^2 \left[1 - \left(\frac{\omega}{\omega_s}\right)^2 - i\eta_s\right]\xi_s(\omega)$$

$$= M_s Y_s(\omega)\xi_s(\omega) = \int_{A_p} p(x)\psi^s(x)dx$$

where $p(\bar{x}) = p^o(x) - p^i(x)$ and $\eta_s = 2\zeta_s \dfrac{\omega}{\omega_s}$

Then

$$G(x|x';\omega) = w(x)\Big|_{p(x)=\delta(x-x')} \equiv w(x;\omega)\Big|_{p(x)=\delta(x-x')} = \sum_s \xi_s(\omega)\psi^s(x)\Big|_{p(x)=\delta(x-x')} = \sum_s \left(\frac{\displaystyle\int_{A_p}\delta(x-x')\psi^s(x)dx}{M_s Y_s(\omega)}\right)\psi^s(x)$$

$$= \sum_s \frac{\psi^s(x)\,\psi^s(x')}{M_s Y_s}$$

which is Equation (21)

47

In Equation (23) define

$$\Gamma^r_{P_{b\ell}} = \int_{A'_p} \psi^r(\bar{x}') \, p_{b\ell}(\bar{x}') \, d\bar{x}' \tag{24}$$

and

$$\Gamma^r_{P_2} = \int_{A'_p} \psi^r(\bar{x}') \, p_2(\bar{x}') \, d\bar{x}'$$

$$= \frac{i\rho c_o^2}{4\pi^2} \int_{A'_p} \psi^r(x') \int_{A_p} L' \, G^o_p(\bar{x}'|x) L \sum_s \bar{\xi}_s \, \psi^s(\bar{x}) \, d\bar{x} \, dx'$$

$$= -\rho \omega^2 \sum_s J^{rs} \xi_s \tag{25}$$

and

$$\Gamma^r_{P_i} = \int_{A'_p} \psi^r(\bar{x}') \, p^i(\bar{x}') d\bar{x}'$$

$$= -\rho_c \, \omega^2 \int_{A'_p} \psi^r(\bar{x}') \int_{A_p} G_p(x|\bar{x}') \sum_s \bar{\xi}_s \, \psi^s(\bar{x}) \, d\bar{x} \, d\bar{x}'$$

$$= -\rho_c \omega^2 \sum_s \bar{I}^{rs} \xi_s \tag{26}$$

where

$$\bar{J}^{rs} = \frac{-i}{4\pi^2 k^2} \int_{A'_p} \int_{A_p} \psi^r(x') \, L' \, G^o_p(x'|\bar{x}) L \, \psi^s(\bar{x}) \, dx \, d\bar{x}' \tag{27}$$

and

$$I^{rs} = \int_{A'_p} \int_{A_p} \psi^r(\bar{x}) \, G_p(x|\bar{x}') \, \psi^s(x') \, dx \, dx' \tag{28}$$

Here, $G^o_p(x',y',o|x,y,o)$ is the upper half-space Green function at the surface of the plate and $G_p = G_p(x,y,o|x',y',o)$ is the cavity Green function at the surface of the plate.

48

Substituting Equations (25) and (26) into Equation (23), we obtain the *fundamental modal equation* *

$$\left[-M_r \bar{Y}_r + \omega^2 (\rho_c \bar{I}^{rr} - \rho \bar{J}^{rr})\right] \bar{\xi}_r + \sum_{s \neq r} \omega^2 (\rho_c \bar{I}^{rs} - \rho \bar{J}^{rs}) \bar{\xi}_s = -\Gamma^r_{p_{b\ell}} \qquad (29)$$

which can be expressed in the simpler form

$$\bar{a}_{rr} \bar{\xi}_r + \sum_{s \neq r} \bar{a}_{rs} \bar{\xi}_s = -\Gamma^r_{p_{b\ell}} \qquad (30)$$

where the $\bar{a}_{rs}$'s are the *intermodal coupling coefficients;* $\bar{a}_{rr}$ and $\bar{a}_{rs}$ are the *auto* and *cross* terms respectively given by

$$\bar{a}_{rr} = -M_r \bar{Y}_r + \omega^2 (\rho_c \bar{I}^{rr} - \rho \bar{J}^{rr})$$

$$\bar{a}_{rs} = \omega^2 (\rho_c \bar{I}^{rs} - \rho \bar{J}^{rs})$$

A2. RESPONSE TO RANDOM EXCITATION

The Fourier transform of the *truncated* random displacement of the plate $W_T(\bar{x}, \omega)$ is related to the Fourier transform of the *truncated* random exciting blocked pressure at the surface $P_{b\ell_T}(\bar{x}, \omega)$ (compare with Equation (17)) by[7]

$$W_T(\bar{x}, \omega) = \int_{A'_p} G(x|\bar{x}';\omega) \left[P_{b\ell_T}(\bar{x}', \omega) + P_{2_T}(\bar{x}', \omega) - P_{i_T}(\bar{x}', \omega) \right] d\bar{x}' \qquad (31)$$

where the transforms are defined over the interval $-\frac{T}{2} < t < \frac{T}{2}$. By analogy with Equations (18) and (16), the internal and external fields are respectively given by

$$P_{i_T}(\bar{x}', \omega) = -\rho_c \omega^2 \int_{A_p} G_p(\bar{x}|\bar{x}';\omega) W_T(\bar{x}, \omega) dx \qquad (32)$$

$$P_{2_T}(\bar{x}', \omega) = \frac{i\rho c_0^2}{4\pi^2} \int_{A_p} L' G_p^0(x|\bar{x}';\omega) L W_T(x, \omega) d\bar{x} \qquad (33)$$

---

*For a cavity containing a vacuum, $\rho_c = 0$. Hence terms in $\bar{I}^{rr}$ and $\bar{I}^{rs}$ vanish for this case.

Equations (31) through (33) can be solved to yield*

$$W_T(\bar{x},\omega) = -\sum_{r,t} \psi^r(\bar{x})\, \bar{a}_{rt}\, \Gamma^t_{p_{b\ell_T}}(\omega) \qquad (34)$$

where

$$\bar{a}_{rt} = \frac{\bar{A}_{tr}}{\det(\bar{a}_{tr})} \qquad (35)$$

$\bar{A}_{tr}$ is the cofactor of the element $\bar{a}_{tr}$ in the determinant $\det(\bar{a}_{tr})$ where $\bar{a}_{tr}$ is the modal matrix obtained by truncating the modal series in Equation (30).

The cross-spectral density of the plate displacement is defined by

$$S_w(\bar{x}|\bar{x}';\omega) = \lim_{T\to\infty}\; \frac{2}{T} W_T(\bar{x},\omega)\, W_T^*(\bar{x}',\omega) \qquad (36)$$

Substituting Equation (34) into Equation (36) and using the definition of $\Gamma^t_{p_{b\ell_T}}(\omega)$ as defined by analogy with Equation (24)

$$S_w(\bar{x}|\bar{x}';\omega) = \sum_r \sum_t \sum_\ell \sum_n \bar{a}_{rt}\, \bar{a}^*_{\ell n}\, \psi^r(\bar{x})\, \psi^\ell(\bar{x}')$$

$$\cdot \int_{A'_p} \int_{A_p} \psi^t(\bar{x})\, \psi^n(\bar{x}')\, \lim_{T\to\infty} \frac{2}{T} P_{b\ell_T}(\bar{x},\omega)\, P^*_{b\ell_T}(\bar{x},\omega)\, d\bar{x}\, d\bar{x}'$$

$$= \sum_r \sum_t \sum_\ell \sum_n \bar{a}_{rt}\, a^*_{\ell n}\, \psi^r(\bar{x})\, \psi^\ell(\bar{x}')$$

$$\cdot \int_{A'_p} \int_{A_p} \int_{P_{b\ell}} (\bar{x}|\bar{x}';\omega)\, \psi^t(\bar{x})\, \psi^n(\bar{x}')\, d\bar{x}\, d\bar{x}' \qquad (37)$$

---

*In Equations (19) and (30), let S→r and r→t. Then Equation (30) written as

$$\bar{a}_{tt}(\omega)\bar{\xi}_r(\omega) + \sum_{r\neq t} \bar{a}_{tr}(\omega)\,\bar{\xi}_r(\omega) = \sum_{r,t} \bar{a}_{tr}(\omega)\bar{\xi}_r(\omega) = -\Gamma^t_{p_{b\ell_T}}(\omega)$$

has the solution[29]

$$\bar{\xi}_r = -\sum_{r,t} a_{rt}\, \Gamma^t_{p_{b\ell_T}}$$

and Equation (19) has the corresponding solution

$$W_T(\bar{x},\omega) = -\sum_{r,t} \psi^r(\bar{x})\, a_{rt}\, \Gamma^t_{p_{b\ell_T}}$$

where $\bar{a}_{rt} = \dfrac{\bar{A}_{tr}}{\det(\bar{a}_{tr})}.$

50

where

$$S_{p_{b\ell}}(\bar{x}|\bar{x}', \omega) = \lim_{T \to \infty} \frac{2}{T} P_{b\ell_T}(\bar{x}, \omega) P^*_{b\ell_T}(\bar{x}',\omega)$$

represents the cross-spectral density of the blocked pressure, i.e., turbulence pressure. The spectral density of plate displacement is obtained by letting $\bar{x}' \to \bar{x}$.

A3. CROSS-SPECTRAL DENSITY OF THE ACOUSTIC PRESSURE IN A CAVITY

The cross-spectral density of the cavity pressure is defined by

$$S_{p_i}(x|x'; \omega) = \lim_{T \to \infty} \frac{2}{T} P_{i_T}(x, \omega) P^*_{i_T}(x', \omega)$$

Substituting Equation (32) into this equation with

$$S_{p_i}(\bar{x}''|\bar{x}'''; \omega) = \rho_c^2 \omega^4 \int_{A'_p} \int_{A_p} G^*_p(x|x''; \omega) G_p(x'|x'''; \omega) \lim_{T \to \infty} \frac{2}{T} W_T(x,\omega) W^*_T(x',\omega)\, dx\, dx'$$

Let $\bar{x}'' \to \bar{\xi}$ and $\bar{x}''' \to \bar{\xi}'$ then

$$S_{p_i}(\bar{\xi}|\bar{\xi}'; \omega) = \rho_c^2 \omega^4 \int_{A'_p} \int_{A_p} G^*_p(x|\xi; \omega) G_p(x'|\xi'; \omega) S_w(x|x'; \omega)\, dx\, dx' \tag{38}$$

An alternative method of derivation is given by Pope.[7]

Substituting the expression for S_w given by Equation (37) into Equation (38) gives the expression for the cross-spectral density of the pressure at any two points in the cavity in terms of the cross-spectral density of the external blocked pressure and the cavity Green function.

A4. SPECTRAL DENSITY OF (COMPLEX) POWER RADIATED TO THE HALF-SPACE

The cross-spectral density of pressure p_{2_T} at position x with velocity v_T at position x' is defined by

$$S_{p_2 v}(x|x'; \omega) = \lim_{T \to \infty} \frac{2}{T} P_{2_T}(x,\omega) V^*_T(x',\omega) \tag{39}$$

where P_{2_T} and V_T are the Fourier transforms of the truncated random quantities. Now

$$v_T(x,t) = \frac{d}{dt} w_T(x,t)$$

51

so the Fourier transform*

$$V_T(\bar{x},\omega) = i\omega W_T(\bar{x},\omega), \qquad V_T^*(\bar{x},\omega) = -i\omega W_T^*(\bar{x},\omega)$$

and from Equation (33) with $L' \equiv L \equiv k$ for $M=0$ and letting $\bar{x}' \to \bar{x}$, $\bar{x} \to \bar{x}''$ and $G_p^0(\bar{x}''|\bar{x};\omega) = G_p^0(\bar{x}|\bar{x}'';\omega)$, we get

$$p_{2_T}(\bar{x},\omega) = \frac{i\rho\omega^2}{(2\pi)^2} \int_{A_p''} G_p^0(\bar{x}|\bar{x}'';\omega)\, W_T(\bar{x}'',\omega)\, d\bar{x}''$$

Hence Equation (39) is

$$S_{p_2 v}(\bar{x}|\bar{x}';\omega) = \frac{\rho\omega^3}{(2\pi)^2}\left\{\lim_{T\to\infty}\frac{2}{T}\left(\int_{A_p''} G_p^0(\bar{x}|\bar{x}'';\omega)\,W_T(\bar{x}'',\omega)d\bar{x}''\right) W_T^*(\bar{x}',\omega)\right\}$$

$$= \frac{\rho\omega^3}{(2\pi)^2} \int_{A_p''} G_p^0(\bar{x}|\bar{x}'';\omega)\,\lim_{T\to\infty}\frac{2}{T}\,W_T(\bar{x}'',\omega)\,W_T^*(\bar{x}',\omega)\,dx''$$

$$= \frac{\rho\omega^3}{(2\pi)^2} \int_{A_p''} G_p^0(\bar{x}|\bar{x}'';\omega)\,S_w(\bar{x}''|\bar{x}';\omega)\,d\bar{x}'' \qquad (40)$$

The spectral density or spectrum of power being radiated to the half-space by the panel is obtained by letting $\bar{x}' \to x$ and by integrating $S_{p_2 v}(\bar{x};\omega)$ over the panel area

$$W_{rad}^{ext}(\omega) = \int_{A_p} S_{p_2 v}(\bar{x};\omega)\,d\bar{x} \qquad (41)$$

---

*

$$V_T(\bar{x},\omega) = \mathcal{F}\left(\frac{dw_T}{dt}\right) = \int_{-\infty}^{\infty}\frac{dw_T}{dt}e^{-i\omega t}\,dt.$$ We integrate this expression by parts letting $u = e^{-i\omega t}$,

$$du = -i\omega e^{-i\omega t}\,dt,\; dv = \frac{dw_T}{dt}\,dt,\; v = w_T \text{ so that } \int_{-\infty}^{\infty}\frac{dw_T}{dt}e^{-i\omega t}\,dt = w_T e^{-i\omega t}\Big|_{-\infty}^{\infty} - \int_{-\infty}^{\infty} -i\omega w_T e^{-i\omega t}\,dt.$$

But $w_T e^{-i\omega t}\Big|_{-\infty}^{\infty} \to 0$ since $w_T \to 0$ at $\pm\infty$. Hence $\int_{-\infty}^{\infty}\frac{dw_T}{dt}e^{-i\omega t}\,dt = +i\omega \int_{-\infty}^{\infty} w_T e^{-i\omega t}\,dt$ or

$$\mathcal{F}\left(\frac{dw_T}{dt}\right) = +i\omega\mathcal{F}(w_T).$$

Equation (41) is a complex quantity, the real part of which represents the real power.* Substitution of Equations (37) and (40) into Equation (41) (letting $\bar{x}' \to \bar{x}$ and the dummy variable $\bar{x}'' \to \bar{x}'$ in Equation (40) or $G_p^o (\bar{x}|\bar{x}'';\omega) \to G_p^o (\bar{x}|\bar{x}';\omega)$ and $S_w (\bar{x}''|\bar{x}';\omega) \to S_w (\bar{x}'|\bar{x};\omega) \equiv S_w (\bar{x}|\bar{x}';\omega))$ gives

$$W_{rad}^{ext} (\omega) = \frac{\rho \omega^3}{(2\pi)^2} \sum_{r,t,\ell,n} a_{rt} \, \bar{a}_{\ell n}^* \int_{A_p'} \int_{A_p} G_p^o (\bar{x}|\bar{x}') \, \psi^r(\bar{x}) \, \psi^\ell(\bar{x}') \, d\bar{x}d\bar{x}'$$

$$\cdot \int_{A_p''} \int_{A_p'''} S_{p_w} (\bar{x}''|\bar{x}''';\omega) \, \psi^t(\bar{x}'') \, \psi^n(\bar{x}''') \, dx''d\bar{x}''' \qquad (42)$$

The total power generated in a band $\Delta\omega$ is

$$\Pi_{rad}^{ext}\bigg|_{\Delta\omega} = \int_{\Delta\omega} W_{rad}^{ext} (\omega) \, d\omega$$

A5. CROSS-SPECTRAL DENSITY OF PRESSURE IN THE HALF-SPACE

In analogy with Equation (38)

$$S_{p_2} (\xi|\xi';\omega) = \frac{\rho^2 \omega^4}{(2\pi)^4} \int_{A_p} \int_{A_p'} G_p^{o*} (\bar{x}|\xi;\omega) \, G_p^o (\bar{x}'|\xi';\omega) \, S_w (\bar{x}|\bar{x}';\omega) \, d\bar{x}d\bar{x}' \qquad (43a)$$

A6. SPECTRAL DENSITY OF (COMPLEX) POWER RADIATED INTO THE CAVITY

The cross-spectral density of pressure p_i at position $\bar{x}$ with velocity v_T at position $\bar{x}'$ is

$$S_{p_i v} (x|x';\omega) = \lim_{T \to \infty} \frac{2}{T} P_{i_T} (x,\omega) \, V_T^* (x',\omega) \qquad (43b)$$

where P_{i_T} and V_T are the Fourier transforms of the truncated random quantities. Now

$$v_T (\bar{x},t) = \frac{d}{dt} w_T (\bar{x},t)$$

so the Fourier transform

$$V_T(\bar{x},\omega) = i\omega W_T(\bar{x},\omega), \qquad V_T^*(\bar{x},\omega) = -i\omega W_T^*(\bar{x},\omega)$$

and from Equation (32), first letting $\bar{x}' \to x$, $x \to x''$ and then $G_p(x''|\bar{x};\omega) = G_p(x|x'';\omega)$, we get

---

*In Equation (41) $W_{rad}^{ext} (\omega)$ represents both the real and reactive power generated in the half-space.

$$p_{i_T}(\bar{x},\omega) = -\rho_c \omega^2 \int_{A_p''} G_p(\bar{x}|\bar{x}'';\omega) W_T(\bar{x}'';\omega) d\bar{x}''$$

Hence

$$S_{p_i v}(\bar{x}|\bar{x}';\omega) = \lim_{T\to\infty} \frac{2}{T}(-i\omega) P_{i_T}(\bar{x};\omega) W_T^*(\bar{x}';\omega)$$

$$= i\rho_c \omega^3 \lim_{T\to\infty} \frac{2}{T} \left(\int_{A_p''} G_p(\bar{x}|\bar{x}'';\omega) W_T(\bar{x}'';\omega) d\bar{x}'' \right) W_T^*(\bar{x}';\omega) d\bar{x}''$$

$$= i\rho_c \omega^3 \int_{A_p''} G_p(\bar{x}|\bar{x}'';\omega) S_w(\bar{x}''|\bar{x}';\omega) d\bar{x}'' \qquad (43c)$$

The spectral density of power radiated into the cavity is obtained by letting $\bar{x}' \to \bar{x}$ and by integrating $S_{p_i v}(\bar{x};\omega)$ over the panel area.

$$W_{rad}^{int}(\omega) = \int_{A_p} S_{p_i v}(\bar{x};\omega) d\bar{x} \qquad (43d)$$

Equation (43d) is a complex quantity, the real part of which represents the real power (see footnote to sentence below Equation (41)).

Substitution of Equations (37) and (43c) into (43d) (letting $\bar{x}' \to \bar{x}$ and the dummy variables $\bar{x}'' \to \bar{x}'$ in Equation (43c) or $G_p(\bar{x}|\bar{x}'';\omega) \to G_p(\bar{x}|\bar{x}';\omega)$ and $S_w(\bar{x}''|\bar{x}';\omega) \to S_w(\bar{x}'|\bar{x};\omega) \equiv S_w(\bar{x}|\bar{x}';\omega)$ gives

$$W_{rad}^{int}(\omega) = i\rho_c \omega^3 \sum_{r,t,\ell,n} a_{rt} \bar{a}_{\ell n}^* \int_{A_p} \int_{A_{p'}} G_p(x|\bar{x}') \psi^r(\bar{x}) \psi^\ell(\bar{x}') d\bar{x}d\bar{x}'$$

$$\cdot \int_{A_p''} \int_{A_p'''} S_{p_{b\ell}}(\bar{x}''|\bar{x}''') \psi^t(\bar{x}'') \psi^n(\bar{x}''') d\bar{x}''d\bar{x}''' \qquad (43e)$$

The total power generated in a band $\Delta\omega$ is

$$\Pi_{rad}^{int}\bigg|_{\Delta\omega} = \int_{\Delta\omega} W_{rad}^{int}(\omega) d\omega$$

54

APPENDIX B

EVALUATION OF THE INTERMODAL
COUPLING COEFFICIENTS

From Equation (30), the *intermodal coupling coefficients* consist of *auto terms* $\bar{a}_{rr}$ and *cross terms* $\bar{a}_{rs}$. The auto terms $\bar{a}_{rr}$ are expressed in terms of the *joint coupling coefficients* of the cavity $\bar{I}^{rr}$ and of the half-space $\bar{J}^{rr}$, in accordance with Equation (44) below. The cross terms $\bar{a}_{rs}$ are expressed in terms of the *cross coupling coefficients* of the cavity $\bar{I}^{rs}$ and of the half-space $\bar{J}^{rs}$, in accordance with Equation (45) below*

$$\bar{a}_{rr} = - M_r \bar{Y}_r + \omega^2 (\rho_c \bar{I}^{rr} - \rho \bar{J}^{rr}) \tag{44}$$

$$\bar{a}_{rs} = \omega^2 (\rho_c \bar{I}^{rs} - \rho \bar{J}^{rs}) \tag{45}$$

The intermodal coupling coefficients $\bar{a}_{rr}$, $\bar{a}_{rs}$ must be evaluated to obtain the *intermodal receptances* $\bar{a}_{rt}$ from Equation (35). The evaluation of the intermodal receptances is required for the solution of Equations (37), (38), (42) and (43).

B1. CALCULATION OF THE HALF-SPACE COEFFICIENTS $\bar{J}_{rr}$, $\bar{J}_{rs}$

In marine applications, the free-stream velocity is low so that, approximately, M = O. For this case $L = k + iM\frac{\partial}{\partial x} \longrightarrow k$, $L' = k + iM \frac{\partial}{\partial x'} \longrightarrow k$, and from Equation (27),

$$\bar{J}^{rs} = \frac{-i}{4\pi^2} \int_{A_p'} \int_{A_p} \psi^r (\bar{x}') G_p^0 (\bar{x}'|\bar{x}) \psi^s (\bar{x}) \, d\bar{x} \, d\bar{x}' \quad ; \quad M = 0 \tag{46}$$

where $G_p^0 (\bar{x}'|\bar{x}) \equiv G_p^0 (x', y', o \mid x, y, z)\Big|_{z=o} = G_p^0 (\bar{x}|\bar{x}')$ is the half-space Green function at the surface of the plate. Thus, from Equation (15) with M = 0 letting $\kappa \to k$, $u \to \eta = x - x'$, $R \to \mu = y - y'$:

$$G_p^0 (\bar{x}|\bar{x}') \equiv G_p^0 (\bar{x}'|\bar{x}) = \frac{-2\pi i \, e^{ikr}}{r} \quad ; \quad M = 0 \tag{47}$$

where $r = \sqrt{(x - x')^2 + (y - y')^2} = \sqrt{\eta^2 + \mu^2}$

The Fourier transform of $G_p^0 (\bar{x}|\bar{x}')$ is defined by

---

*The joint coupling coefficients for the half-space $\bar{J}^{rr}$ represents the auto resistive and reactive coupling. Similarly, the cross coupling coefficient, $\bar{J}^{rs}$, represents the cross resistive and reactive coupling

$$G_p^o(k_x, k_y) = \int_{-\infty}^{\infty} \int_{-\infty}^{\infty} G_p^o(\bar{x}|\bar{x}') e^{-i(k_x\eta + k_y\mu)} d\eta \, d\mu \qquad (48a)$$

where $G_p^o(\bar{x}|\bar{x}') = G_p^o(\eta, \mu)$

Thus

$$G_p^o(\bar{x}|\bar{x}') = \frac{-2\pi i e^{ikr}}{r} = \frac{1}{(2\pi)^2} \int_{-\infty}^{\infty} \int_{-\infty}^{\infty} G_p^o(k_x, k_y) e^{i(k_x\eta + k_y\mu)} dk_x dk_y \quad ; \quad M = 0 \qquad (48b)$$

and therefore

$$G_p^o(k_x, k_y) = -2\pi i \int_{-\infty}^{\infty} \int_{-\infty}^{\infty} \frac{e^{ik\sqrt{\eta^2 + \mu^2}}}{\sqrt{\eta^2 + \mu^2}} e^{-i(k_x\eta + k_y\mu)} d\eta d\mu$$

$$= -2\pi i \int_{-\infty}^{\infty} e^{-ik_y\mu} \left[\int_{-\infty}^{\infty} \frac{e^{ik\sqrt{\eta^2 + \mu^2}}}{\sqrt{\eta^2 + \mu^2}} e^{-ik_x\eta} d\eta \right] d\mu$$

Using the *inverse* Fourier transform of Gradshteyn and Ryzhik[25] (see formula 6.616.4 on page 710 of their book), the integral within the brackets is evaluated to $\frac{\pi}{i} H_0^{(2)}(\mu\sqrt{k^2 - k_x^2})$ so that

$$G_p^o(k_x, k_y) = -(2\pi)^2 \int_{-\infty}^{\infty} H_0^{(2)}\left(\mu\sqrt{k^2 - k_x^2}\right) e^{-ik_y\mu} d\mu$$

$$= \frac{-(2\pi)^2}{\sqrt{k^2 - (k_x^2 + k_y^2)}} \quad ; \quad M = 0$$

where the last result is obtained *directly* ftom the above referenced formula.

We can easily confirm this result for $G_p^o(k_x, k_y)$ as follows. From Equation (8),

$\Psi = \Omega(k_x, k_y) e^{i\zeta z}\big|_{z>0} = \Omega(k_x, k_y) e^{i(-\zeta)(z)}\big|_{z<0}$. For the chosen plate-cavity coordinate system, the half-space represents the region of $-z$ or $z<0$. Hence for an outgoing wave, we require the quantity $-\zeta$ or $\zeta<0$. Thus, comparing Equations (48b) and (13) with $z \equiv z' \equiv 0$ we get

$$G_p^o(k_x, k_y)\bigg|_{M=0} = \frac{(2\pi)^2}{-\zeta}\bigg|_{M=0} = \frac{-(2\pi)^2}{\sqrt{k^2 - (k_x^2 + k_y^2)}} \quad ; \quad M = 0$$

56

where the quantity ζ in Equation (7) is preceded by a negative sign. Substituting the integral expression for $G_p^o(\bar{x}|\bar{x}')$ into equation (46), we get*

$$\bar{J}^{rs} = \frac{-i}{(2\pi)^4} \int_{-\infty}^{\infty} \int_{-\infty}^{\infty} G_p^o(k_x, k_y) S_s(k_x, k_y) S_r^*(k_x, k_y) \, dk_x dk_y \qquad (49)$$

where

$$S_s(k_x, k_y) = \int_0^a \int_0^b \psi^s(x', y') e^{-i(k_x x' + k_y y')} \, dx' dy' \qquad (50)$$

and

$$S_r^*(k_x, k_y) = \int_0^a \int_0^b \psi^r(x, y) e^{+i(k_x x + k_y y)} \, dx \, dy \qquad (51)$$

For a *simply supported plate*,** let $s = (m, n)$ and $r = (q, r)$ represent the mode numbers for two modes. The corresponding mode shapes for the plate are given by

$$\psi^s(\bar{x}) \equiv \psi_{mn}(x, y) = \sin k_m x \sin k_n y$$

$$\psi^r(\bar{x}) \equiv \psi_{qr}(x, y) = \sin k_q x \sin k_r y \qquad (52a,b)$$

where

$$k_m = \frac{m\pi}{a}, \quad k_n = \frac{n\pi}{b}, \quad k_q = \frac{q\pi}{a}, \quad k_r = \frac{r\pi}{b}$$

Substituting Equation (52a) into (50) and Equation (52b) into (51) and performing the integrations, we get

---

*The result for $G_p^o(k_x, k_y)$ is further substantiated by use of the general relation between $J^{rs} = \bar{J}^{mnqr}$ and Davies radiation coefficient R_{mnqr} (see first footnote to Appendix F). $J^{mnqr} = \frac{-i}{\omega\rho} R_{mnqr}$ where $\bar{J}^{mnqr}$ is given by Equation (49) and R_{mnqr} is given by Equation (B16) of References 4 and 5; to account for the fact that S_s and S_r^* defined here and in equation (B16) are complex conjugates of each other we set $i = -i$ in the relation.

**See Appendix E for method of solution for clamped plates.

57

$$S_s \equiv S_{mn}(k_x, k_y) = \frac{k_m k_n [(-1)^m e^{-ik_x a}-1] [(-1)^n e^{-ik_y b}-1]}{(k_x^2 - k_m^2)(k_y^2 - k_n^2)}$$

$$S_r^* \equiv S_{qr}^*(k_x, k_y) = \frac{k_q k_r [(-1)^q e^{+ik_x a} - 1] [(-1)^r e^{ik_y b} -1]}{(k_x^2 - k_q^2)(k_y^2 - k_r^2)} \tag{52c,d}$$

Hence for a simply supported plate

$$S_{mn}S_{qr}^* = \frac{k_m k_n k_q k_r [1+(-1)^{q+m}-(-1)^m e^{-ik_x a}-(-1)^q e^{ik_x a}][1+(-1)^{n+r}-(-1)^n e^{-ik_y b}-(-1)^r e^{ik_y b}]}{(k_x^2-k_m^2)(k_x^2-k_q^2)(k_y^2-k_n^2)(k_y^2-k_r^2)}$$

Consider

$$N = [1 + (-1)^{q+m} - (-1)^m e^{-ik_x a} - (-1)^q e^{ik_x a}]$$

Case 1: q odd, m odd; q + m even

$$(-1)^{q+m} = 1, \ (-1)^m = -1 = (-1)^q$$

$$\therefore N = 2[1 - (-1)^m \cos k_x a]$$

Case 2: q even, m even; q + m even

$$(-1)^{q+m} = 1, \ (-1)^m = 1 = (-1)^q$$

$$\therefore N = 2[1 - (-1)^m \cos k_x a]$$

Case 3: q odd, m even; q + m odd

$$(-1)^{q+m} = -1, \ (-1)^m = 1, \ (-1)^q = -1, \ (-1)^m = -(-1)^q$$

$$\therefore N = [e^{ik_x a} - e^{-ik_x a}] = 2i \sin k_x a$$

Case 4: q even, m odd; q + m odd

$$(-1)^{q+m} = -1, \ (-1)^m = -1, \ (-1)^q = 1, \ (-1)^m = -(-1)^q$$

$$\therefore N = -[e^{-ik_x a} - e^{ik_x a}] = -2i \sin k_x a$$

Similar results pertain for the n, r mode numbers in the second bracket of the numerator in the expression for $S_{mn} S_{qr}^*$.

We now take account of the fact that $G_p^0 (k_x, k_y) = \dfrac{-(2\pi)^2}{\sqrt{k^2 - (k_x^2 + k_y^2)}}$ is an even function in k_x and k_y and that terms involving sines of the wave numbers (Cases 3 and 4) will vanish as the integrations for $\overline{J}^{mnqr}$ given by Equation (49) are performed over the infinite intervals. Furthermore, m and q, and n and r must have the same parity; that is, either both are even or both are odd, otherwise $\overline{J}^{mnqr} \equiv 0$.

Thus the only permissible combinations for the odd and even mode numbers are (o = odd, e = even)

$$m, n, q, r = \begin{cases} o & o & o & o \\ o & e & o & e \\ e & o & e & o \\ e & e & e & e \end{cases} \quad ; \quad \begin{array}{l} m + q = e \\ n + r = e \end{array}$$

and we conclude that only panel modes of similar form are coupled by the cavity so that each mode is thus coupled to at most only one-quarter of all of the other modes.

In view of the requirement of parity, we can write

$$S_{mn}S_{qr}^* = \frac{4 \, k_m \, k_n \, k_q \, k_r \, [1 - (-1)^m \cos k_x a] \, [1 - (-1)^n \cos k_y b]}{(k_x^2 - k_m^2) \, (k_x^2 - k_q^2) \, (k_y^2 - k_n^2) \, (k_y^2 - k_r^2)} \tag{52e}$$

Hence Equation (49) becomes

$$\overline{J}^{mnqr} = \frac{i}{(2\pi)^4} \int_{-\infty}^{\infty} \int_{-\infty}^{\infty} \frac{(2\pi)^2}{(k^2 - k_x^2 - k_y^2)^{1/2}} \, \frac{4 \, k_m \, k_n \, k_q \, k_r \, [1 - (-1)^m \cos k_x a] \, [1 - (-1)^n k_y b]}{(k_x^2 - k_m^2) \, (k_x^2 - k_q^2) \, (k_y^2 - k_n^2) \, (k_y^2 - k_r^2)} \, dk_x dk_y$$

or, equivalently,

$$\overline{J}^{mnqr} = \frac{i \, K_1 \, I}{\pi^2} \tag{53}$$

where

$$K_1 = k_m k_n k_q k_r$$

and

$$I = \int_{-\infty}^{\infty} \int_{-\infty}^{\infty} \frac{[1 - (-1)^m \cos k_x a] \, [1 - (-1)^n \cos k_y b] \, dk_x \, dk_y}{(k_y^2 - k_m^2) \, (k_x^2 - k_q^2) \, (k_y^2 - k_n^2) \, (k_y^2 - k_r^2) \, (k^2 - k_x^2 - k_y^2)^{\frac{1}{2}}} \tag{54}$$

Equation (54) is of the *form utilized by Davies*[9].* In subsequent analyses, we shall be concerned with calculating the real and imaginary parts of Equation (54) and therefore of Equation (53).

$$\bar{J}^{mnqr} = J_X^{mnqr} + i \, J_R^{mnqr} \tag{55}$$

where J_X^{mnqr} is the reactive component and J_R^{mnqr} is the radiation component of the inter-modal coupling coefficient $\bar{J}^{mnqr}$. In Equation (54) let $k_x = a$, $k_y = \beta$; then

$$I = \int_{-\infty}^{\infty} \left[\int_{-\infty}^{\infty} \frac{[1 - (-1)^m \cos a \, a] \, d a}{(a^2 - k_m^2) \, (a^2 - k_q^2) \, (k^2 - a^2 - \beta^2)^{\frac{1}{2}}} \right] \frac{[1 - (-1)^n \cos b \, \beta]}{(\beta^2 - k_n^2) \, (\beta^2 - k_r^2)} \, d\beta$$

$$= \int_{-\infty}^{\infty} I_1(\beta) \, \frac{[1 - (-1)^n \cos b \, \beta]}{(\beta^2 - k_n^2) \, (\beta^2 - k_r^2)} \, d\beta \tag{56a}$$

where

$$I_1(\beta) = \int_{-\infty}^{\infty} \frac{[1 - (-1)^m \cos a \, a]}{(a^2 - k_m^2) \, (a^2 - k_q^2) \, (k^2 - a^2 - \beta^2)^{\frac{1}{2}}} \, da \tag{56b}$$

The denominator of the integrand in equation (56b) is two-sheeted with square-root type branch points at

$$a_b^{1,2} = \pm \sqrt{k^2 - \beta^2}$$

and poles at

$$a = \pm k_m, \quad a = \pm k_q$$

Figure 7 shows the locus of $a_b^{1,2}$ as β ranges from $-\infty$ to ∞ . Possible configurations of the branch cuts for various values of β are shown in Figure 8a. The preferred configurations are shown in Figure 8b; the real and imaginary parts of $\bar{J}^{mnqr}$ are naturally separated by using these cuts. Now we observe that

$$\int_{-\infty}^{\infty} e^{iaa} \, f(a) \, da = \int_{-\infty}^{\infty} \cos aa \, f(a) \, da$$

---

*The equivalence between Davies results and the present results for $\bar{J}^{mnqr}$ is shown in Appendix F.

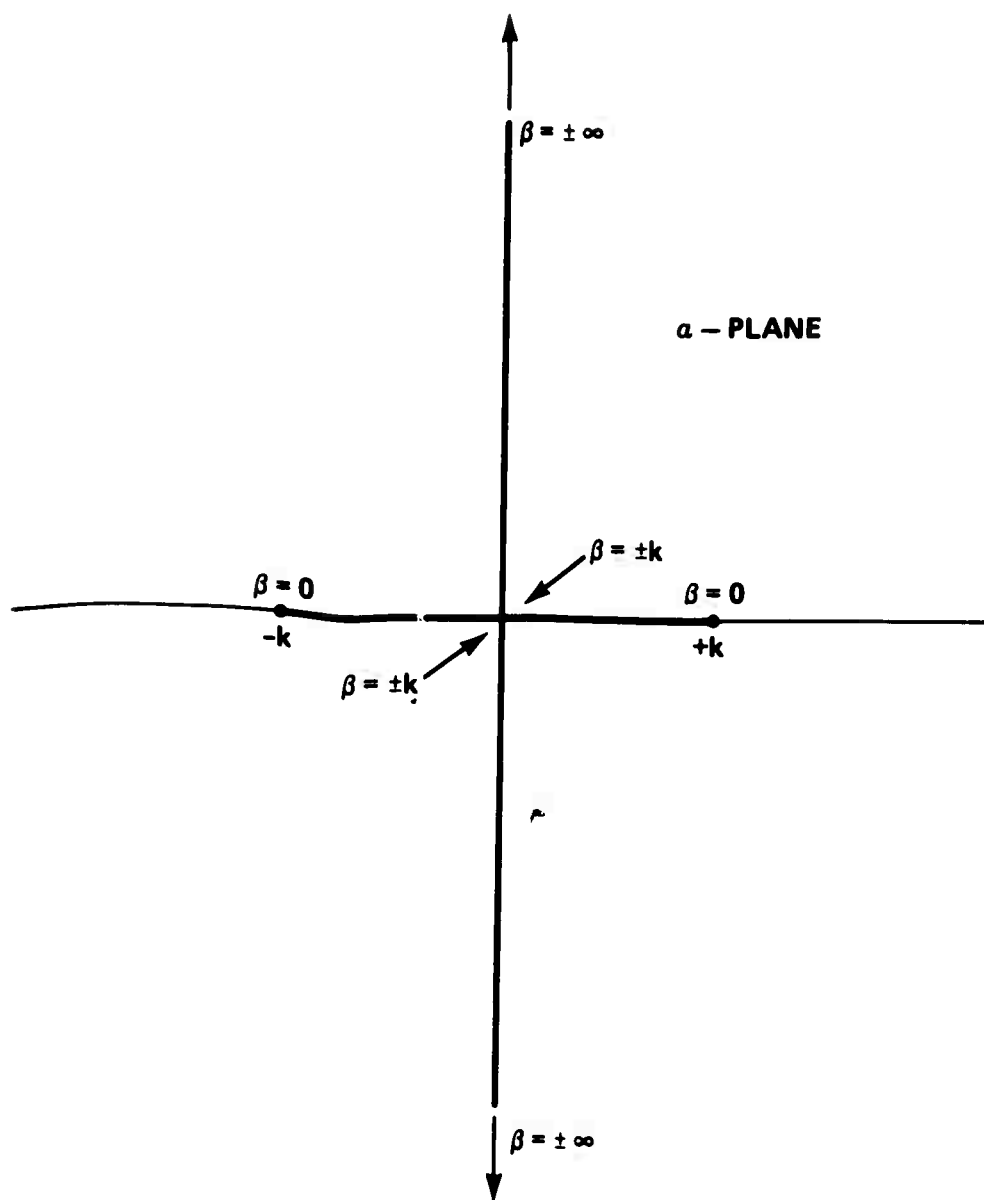Figure 7 — Locus of $a_b^{1,2}$

In the figure:

$\beta = \pm \infty$

$a - \text{PLANE}$

$\beta = \pm k$

$\beta = 0$

$\beta = 0$

$-k$

$+k$

$\beta = \pm k$
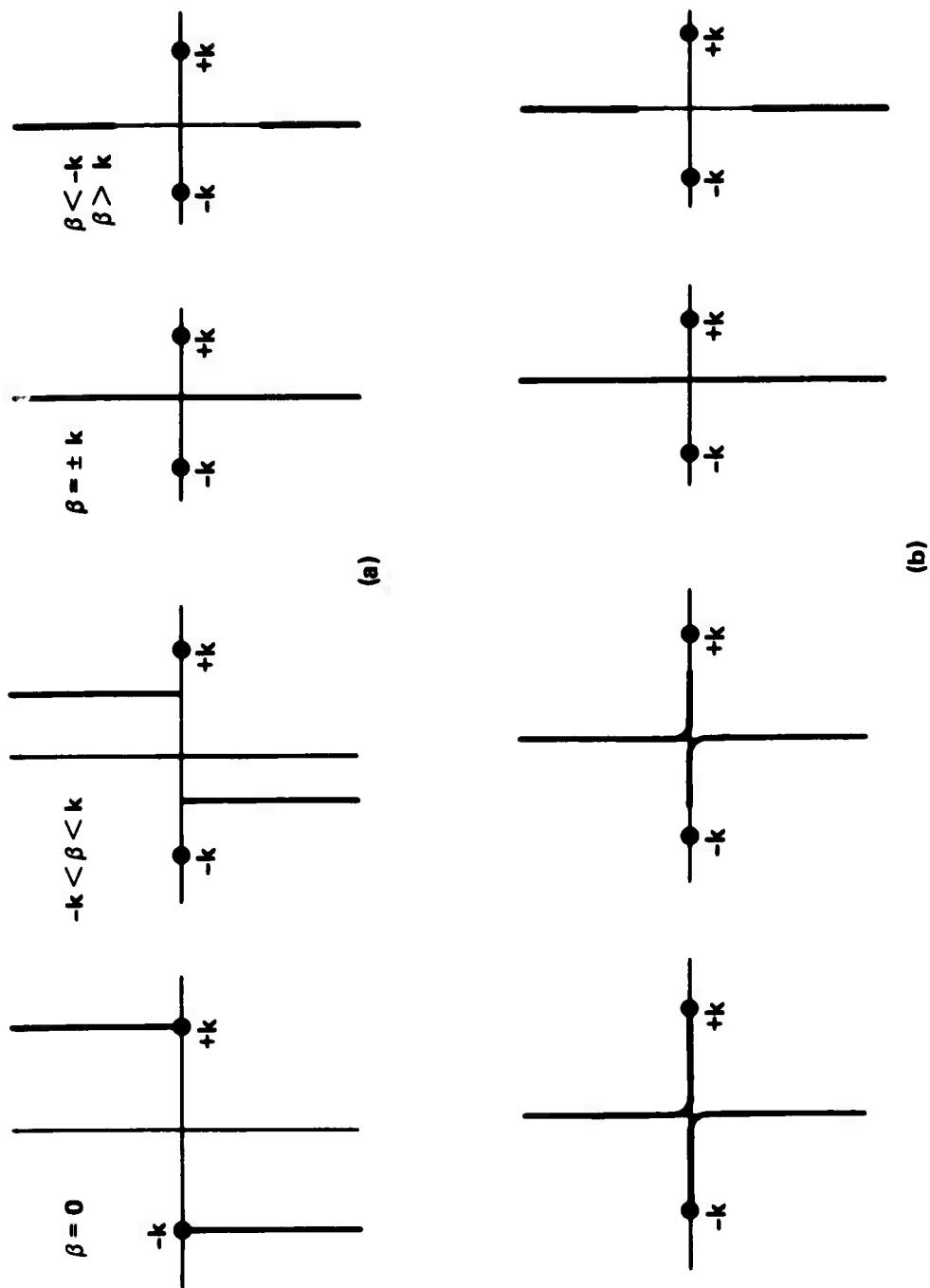
$\beta = \pm \infty$

Figure 8 – Representation of Branch Points and Cuts in the α-plane

for even f (a). Therefore, we consider equation (56b) in the form

$$I_1\ (\beta) = \int_{-\infty}^{\infty} \frac{[1 - (-1)^m\ e^{ia a}]\ da}{(a^2 - k_m^2)\ (a^2 - k_q^2)\ (k^2 - a^2 - \beta^2)^{\frac{1}{2}}} \tag{57}$$

and represent the infinite integral as that portion of a contour integral corresponding to a path along the real axis. The contour is closed in the upper half-plane. Note that $I_1(\beta)$ will evaluate to two different functions of β according to the value of β. The values of $I_1(\beta)$ for which the branch points lie on the positive and negative imaginary lines are designated Case 1, and the values of $I_1(\beta)$ for which the branch points lie on the positive and negative real lines are designated as Case 2.

To begin, consider a case with k_m, k_q > k, m ≠ q and m + q even. The branch points and cuts and the location of the poles are shown in Figure 9. Now consider the encirclement of the poles and the selection of the branch of the square root.

$$\zeta = (k^2 - a^2 - \beta^2)^{\frac{1}{2}} \tag{58}$$

Since we are working in the space $z<0$ and the radiated pressure is of the form $e^{i\zeta z}$, ζ must have a negative imaginary part* for large (real) a with the integration contour shown in Figure 10. Consider Case 2. Application of the Cauchy residue theorem gives for the integral of the contour which completely encloses the poles $\pm k_m$, $\pm k_q$:

$$\int_{\Gamma_1} + \int_{\Gamma_2} + \int_{C_\rho} + \int_{\Gamma_3} + \int_{\Gamma_4} + \int_{C_{R_2}} + \int_{\Gamma_{-x}} + \int_{\Gamma_5} + \int_{\Gamma_6} + \int_{C_\rho} + \int_{\Gamma_x} + \int_{\Gamma_7} + \int_{\Gamma_8} + \int_{C_{R_1}}$$

$$= 2\pi i \sum \text{Residues} = 2\pi i\ [\text{Res}\ (k_m) + \text{Res}\ (k_q)]$$

where the integrand for these integrals is that of Equation (57).

Now**

$$\int_{C_\rho} \to 0 \text{ as } \rho \to 0$$

---

*So that the pressure will decay with distance from the plate.

**Let $a = a_1 + \rho e^{i\phi}$, $a^2 = a_1^2 + 2\rho a_1\ e^{i\phi} + \rho^2\ e^{i2\phi}$; $da = i\rho e^{i\phi} d\phi$

Then for the circle C_ρ, we have $\int_{C_\rho} = \int_{\pi}^{-\pi} \frac{[1 - (-1)^m\ e^{ia a_1}]\ da}{(a^2 - k_m^2)\ (a^2 - k_q^2)\ (a_1^2 - a^2)}$

$$= \int_{\pi}^{-\pi} \frac{[1 - (-1)^m\ e^{ia(a_1 + \rho e^{i\phi})}]\ [i\rho\ e^{i\phi}\ d\phi]}{(a_1^2 + 2\rho a_1\ e^{i\phi} + \rho^2\ e^{i2\phi}-k_m^2)\ (a_1^2 + 2\rho a_1\ e^{i\phi} + \rho^2\ e^{i2\phi}-k_q^2)\ (a_1^2 - a_1^2 - 2\rho a_1\ e^{i\phi}-\rho^2 e^{i2\phi})^{\frac{1}{2}}}$$

Now $e^{ia\ (a_1 + \rho e^{i\phi})} = e^{ia a_1}\cdot e^{ia\rho(\cos \phi + i \sin \phi)} = e^{ia a_1}\ e^{ia\rho \cos \phi} e^{-a\rho \sin \phi}$

Thus as $\rho \to 0$, the integrand tends to

$$\frac{i\rho[1 - (-1)^m\ e^{ia a_1}]\ e^{i\phi}}{(a_1^2 - k_m^2)\ (a_1^2 - k_q^2)\ (b\rho^{\frac{1}{2}})} = \frac{i\rho^{\frac{1}{2}}\ [1 - (-1)^m\ e^{ia a_1}]\ e^{i\phi}}{(a_1^2 - k_m^2)\ (a_1^2 - k_q^2)\ b}\quad , b \text{ complex}$$

Therefore, $\lim_{\rho \to 0} \int_{C_\rho} = 0$ independent of the limits for ϕ; hence the same results are obtained for $\int_\pi^0 [\ ] da$ around branch point $-a$.

63

CASE 1

$\beta < -k, \beta > k$

a – PLANE

$a_1 = i \sqrt{\beta^2 - k^2}$

$-k_q$ $-k_m$ $-k$ k k_m k_q

$a_2 = -i \sqrt{\beta^2 - k^2}$

CASE 2

$-k < \beta < k$

a – PLANE

$a_1 = \sqrt{k^2 - \beta^2}$

$-k_q$ $-k_m$ $-k$ k k_m k_q

$a_2 = -\sqrt{k^2 - \beta^2}$
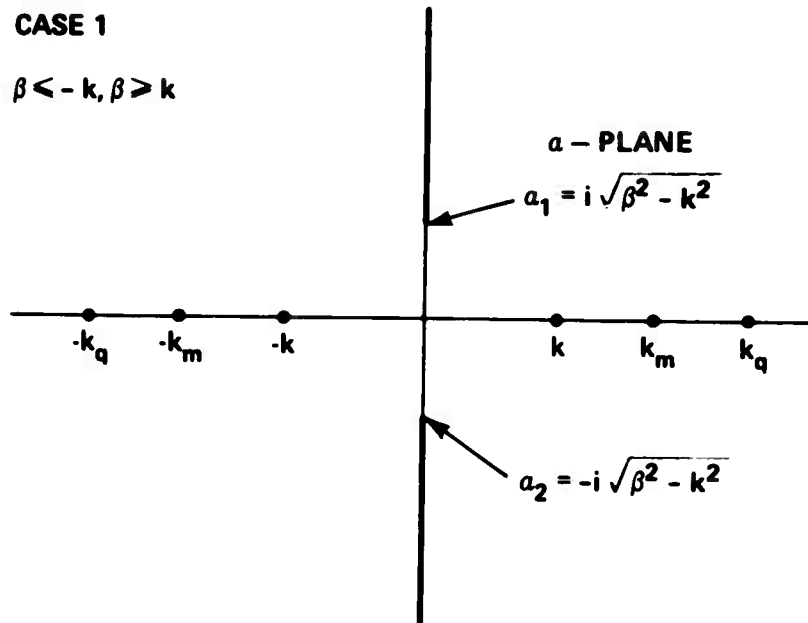
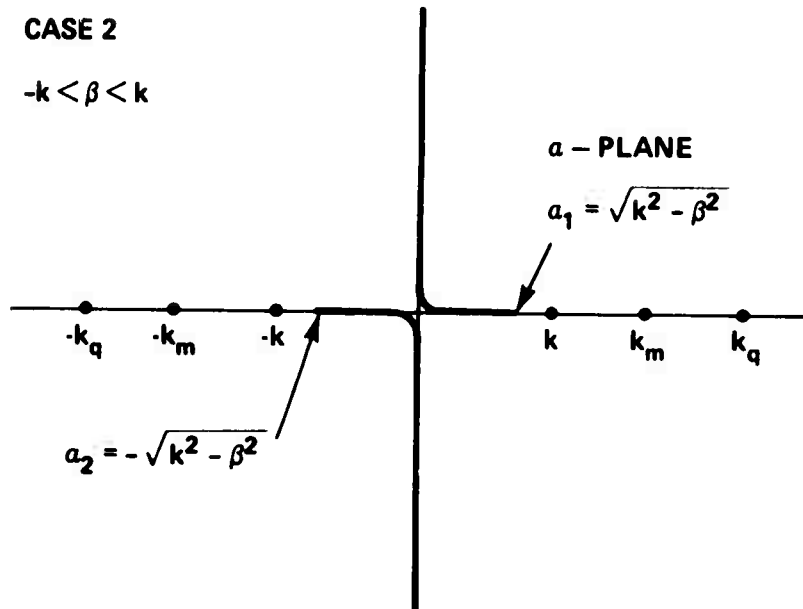Figure 9 – Branch Points and Cuts in the a-plane: k_m, $k_q > k$, $k_m \neq k_q$

64

Figure 10 – Case 2 Integration Contour: $k_q > k_m > k > a_1$
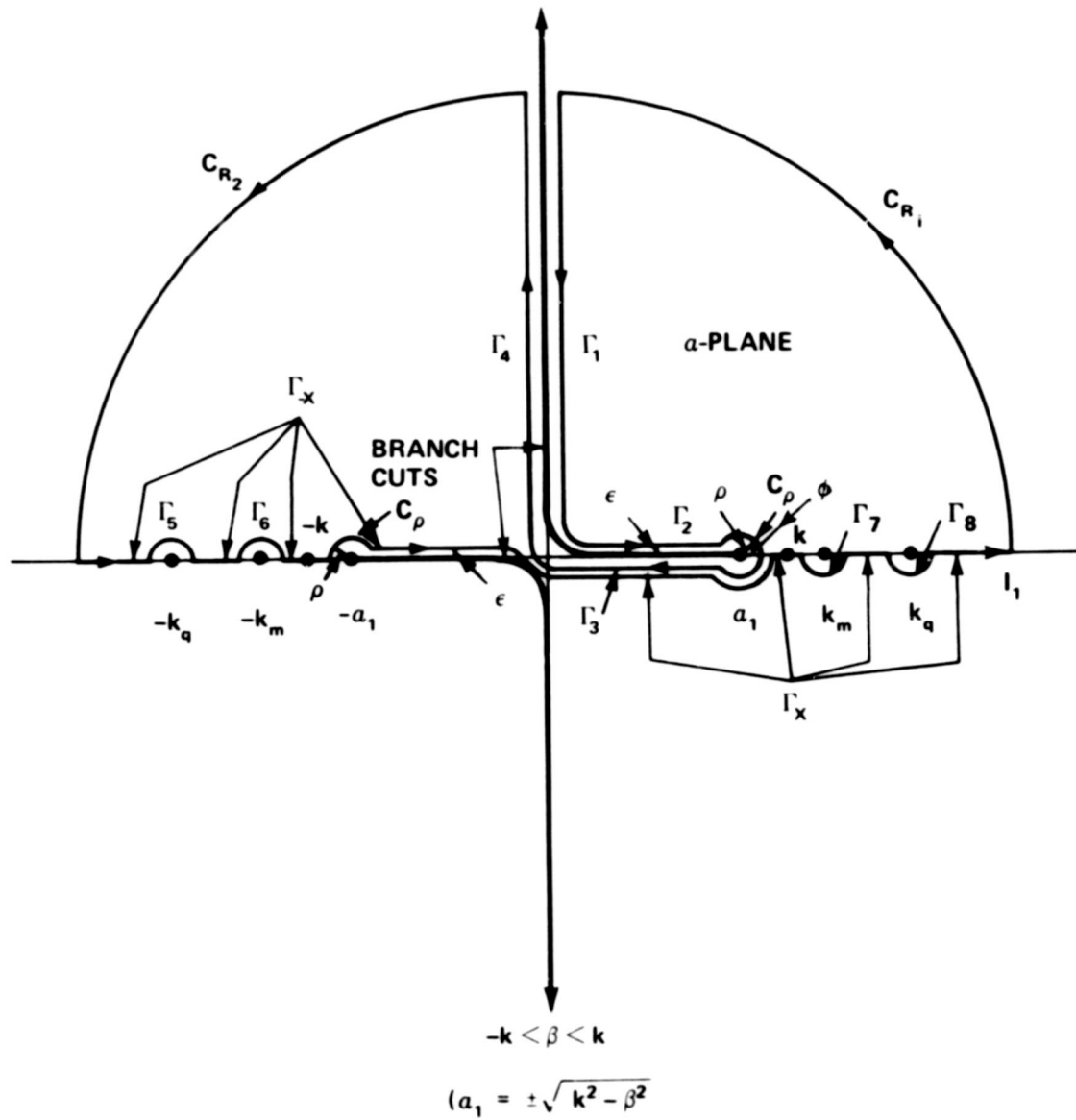
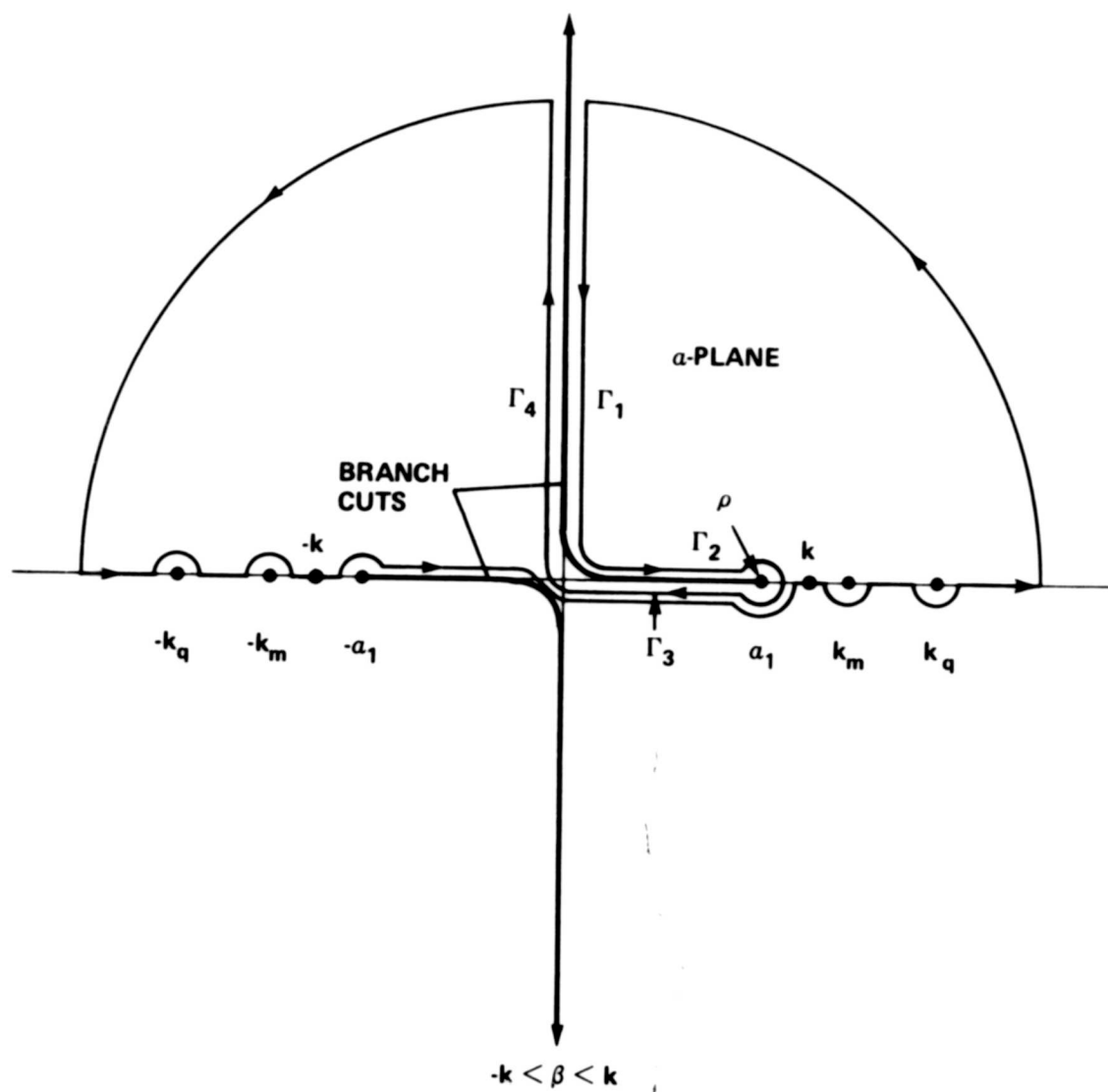$$-k < \beta < k$$

$$(a_1 = \pm\sqrt{k^2 - \beta^2}$$

Figure 10a

65

a-PLANE

Γ_4 Γ_1

BRANCH
CUTS

-k

ρ

Γ_2 k

-k_q -k_m -a_1

Γ_3 a_1 k_m k_q

-k < β < k

Figure 10 b

$$\int_{C_{R_1}} \equiv \int_{C_{R_2}} \to 0 \text{ as } R \to \infty \text{ where } R \text{ is the radius of the arcs } C_{R_1}, C_{R_2}$$

$$\int_{\Gamma_5} = -\pi i \operatorname{Res}(-k_q)$$

$$\int_{\Gamma_6} = -\pi i \operatorname{Res}(-k_m)$$

$\left. \begin{array}{l} \\ \\ \\ \end{array} \right\}$ due to negative sense of the integral for the contour encircling , $-k_m$, $-k_q$

$$\int_{\Gamma_7} = \pi i \operatorname{Res}(+k_m)$$

$$\int_{\Gamma_8} = \pi i \operatorname{Res}(+k_q)$$

$\left. \begin{array}{l} \\ \\ \\ \end{array} \right\}$ due to positive sense of the integral for the contour encircling , $+k_m$, $+k_q$

Hence the principal value of $I_1(\beta)$ is

$$P[I_1(\beta)] = \int_{\Gamma_{-x}} + \int_{\Gamma_{+x}} = 2\pi i [\operatorname{Res}(k_m) + \operatorname{Res}(k_q)] + \pi i [\operatorname{Res}(-k_m) + \operatorname{Res}(-k_q) + \operatorname{Res}(k_m) + \operatorname{Res}(k_q)]$$

$$- \left(\int_{\Gamma_1} + \int_{\Gamma_2} + \int_{\Gamma_3} + \int_{\Gamma_4} \right)$$

For *simplication in notation*, let $\int_{\Gamma_i} \longrightarrow \Gamma_i$. Then the preceding equation is written as

$$P[I_1(\beta)] = \pi i [\operatorname{Res}(k_m) + \operatorname{Res}(k_q)] + \pi i [\operatorname{Res}(-k_m) + \operatorname{Res}(-k_q)] - (\Gamma_1 + \Gamma_2 + \Gamma_3 + \Gamma_4) \qquad (59)$$

where for the pole at $a = k_m$,

$$\operatorname{Res}(k_m) = \left. \frac{[1 - (-1)^m e^{ia\alpha}]}{(a + k_m)(a^2 - k_q^2)(a_1^2 - a^2)} \right|_{a = k_m} = \frac{[1 - (-1)^m e^{ik_m a}]}{2k_m (k_m^2 - k_q^2)(a_1^2 - k_m^2)} = 0$$

since $1 - (-1)^m e^{ik_m a} = 1 - (-1)^m e^{im\pi} = 1 - (-1)^{2m} = 0$

Therefore, for the *simple poles* in Equation (59)

$$\operatorname{Res}(k_m) \equiv \operatorname{Res}(-k_m) \equiv \operatorname{Res}(k_q) \equiv \operatorname{Res}(-k_q) = 0$$

and

$$P[I_1(\beta)] = - (\Gamma_1 + \Gamma_2 + \Gamma_3 + \Gamma_4)$$

The representation for each line integral is now determined for the proper branch of ζ. To determine this branch let

$$\zeta = \sqrt{k^2 - a^2 - \beta^2} = \gamma^{\frac{1}{2}}$$

or

$$\gamma = (k^2 - \beta^2) - a^2 = a_1^2 - a^2 = \gamma_x + i\gamma_y$$

The two branches of $\zeta = \gamma^{\frac{1}{2}}$ are

$$\gamma^{\frac{1}{2}} = \left| (k^2 - \beta^2) - a^2 \right|^{\frac{1}{2}} e^{i\frac{1}{2}\theta_p}$$

$$\gamma^{\frac{1}{2}} = \left| (k^2 - \beta^2) - a^2 \right|^{\frac{1}{2}} e^{i\frac{1}{2}(\theta_p + 2\pi)} = - \left| (k^2 - \beta^2) - a^2 \right|^{\frac{1}{2}} e^{i\frac{1}{2}\theta_p}$$

where

$$\theta_p = \tan^{-1} \frac{\gamma_y}{\gamma_x}$$

Along I_1 $a = x - i\epsilon$ (see Figure 10). Let $x > a_1$; then

$$\gamma = a_1^2 - a^2 = a_1^2 - x^2 + \epsilon^2 + i2\epsilon x$$

$$= - [x^2 - (a_1^2 + \epsilon^2)] + i2\epsilon x = re^{i\epsilon_\theta} \; ; \; x > a_1$$

γ PLANE
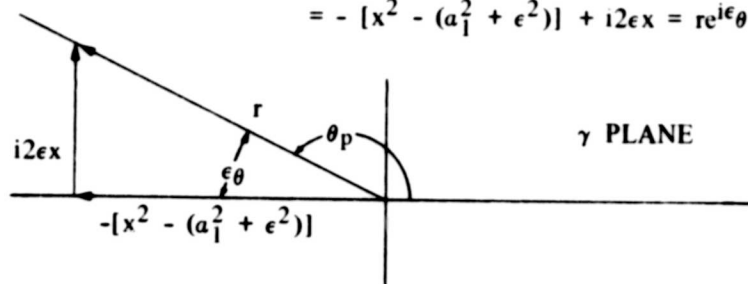
where

$$r = \sqrt{[x^2 - (a_1^2 + \epsilon^2)]^2 + (2\epsilon x)^2} \approx x^2 - a_1^2$$

$$\epsilon_\theta = \tan^{-1} \frac{\gamma_y}{\gamma_x} = \tan^{-1} \frac{2\epsilon x}{x^2 - (a_1^2 + \epsilon^2)} \approx \tan^{-1} \frac{2\epsilon x}{x^2 - a_1^2}$$

$$\theta_p = \pi - \epsilon_\theta \approx \pi$$

Therefore, the branch for $\zeta = \gamma^{1/2}$ is potentially either represented by

$$\gamma^{1/2} = (x^2 - a_1^2)^{1/2} \, e^{i\frac{\pi}{2}} = + i(x^2 - a_1^2)^{1/2}, \quad \text{branch } k=0$$

or by

$$\gamma^{1/2} = (x^2 - a_1^2)^{1/2} \, e^{i\frac{1}{2}(\pi + 2\pi)} = - (x^2 - a_1^2)^{1/2} \, e^{i\frac{\pi}{2}} = - (x^2 - a_1^2)^{1/2}, \quad \text{branch } k=1$$

Since $\zeta = \gamma^{1/2}$ must have a *negative* imaginary part, we select the second branch, (k=1) as the proper branch to use in determining Γ_1, Γ_2, Γ_3 and Γ_4.

Thus, the proper branch along I_1 is given by

$$\zeta = - i (x^2 - a_1^2)^{1/2} \quad ; \quad x > a_1$$

For Γ_3, $a = x - i\epsilon$ where $x < a_1$. Then

$$\gamma = a_1^2 - a^2 = a_1^2 - (x^2 - i2\epsilon x - \epsilon^2) \approx (a_1^2 - x^2) + i2\epsilon x$$
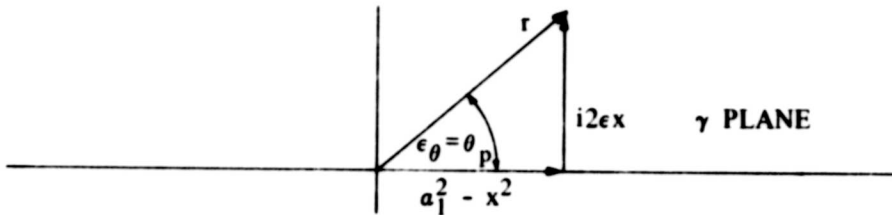
On branch k=1, $\zeta = \gamma^{1/2} \approx (a_1^2 - x^2)^{1/2} \, e^{i\frac{1}{2}(\tan^{-1}\frac{2\epsilon x}{a_1^2 - x^2} + 2\pi)} \approx - [a_1^2 - x^2]^{1/2}; \quad x < a_1$

For Γ_2, $a = x + i\epsilon$ where $x < a_1$. Then

$$\gamma = a_1^2 - a^2 = [(a_1^2 + \epsilon^2) - x^2] - i2\epsilon x \approx (a_1^2 - x^2) - i2\epsilon x$$

69

On branch k=1, $\zeta = \gamma^{1/2} \approx (a_1^2 - x^2)^{1/2} e^{i\frac{1}{2}\left[\left(2\pi - \tan^{-1}\frac{2\epsilon x}{a_1^2 - x^2}\right) + 2\pi\right]} \approx (a_1^2 - x^2) e^{i\frac{1}{2}(4\pi)}$

$$= + [a_1^2 - x^2]^{1/2} \; ; x < a_1$$

For Γ_1, $a = \epsilon + iy$

$$\gamma = a_1^2 - a^2 = a_1^2 + y^2 - \epsilon^2 - i2\epsilon y \approx a_1^2 + y^2 - i2\epsilon y$$

On branch k=1,

$$\zeta = \gamma^{1/2} = (a^2 + y^2)^{1/2}\, e^{i\frac{1}{2}[2\pi - \epsilon_\theta + 2\pi]} \approx + [a_1^2 + y^2]^{1/2}$$
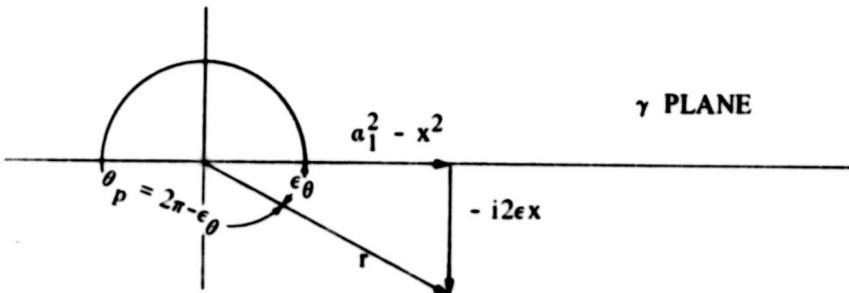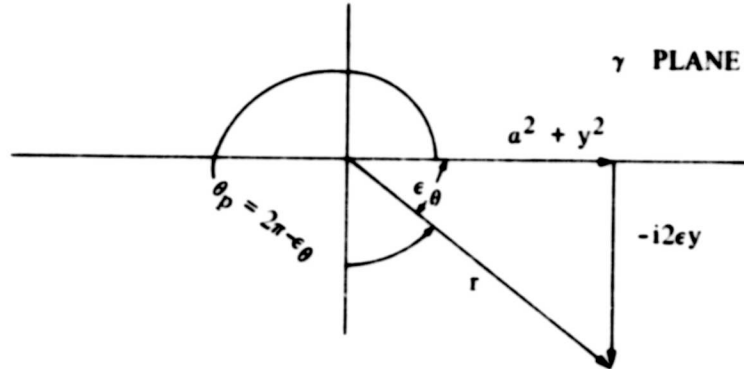
For Γ_4, $a = -\epsilon + iy$

$$\gamma = a_1^2 - a^2 = a_1^2 + y^2 - \epsilon^2 + i2\epsilon y \approx a_1^2 + y^2 + i2\epsilon y$$
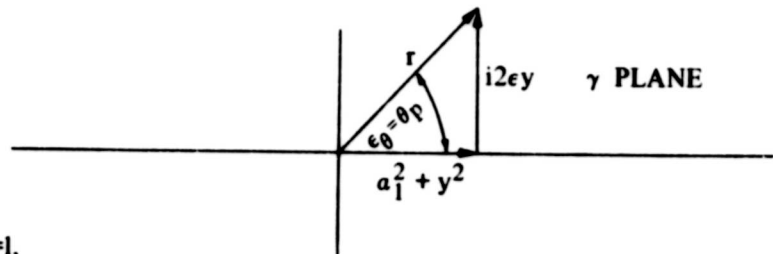
On branch k=1,

$$\zeta = \gamma^{1/2} = (a_1^2 + y^2)^{1/2}\, e^{i\frac{1}{2}\left(\tan^{-1}\frac{2\epsilon y}{a_1^2 + y^2} + 2\pi\right)} \approx - [a_1^2 + y^2]^{1/2}$$

We recall that in Equation (59), $\Gamma_i \equiv \displaystyle\int_{\Gamma_i}$ where the integrand of the integrals for all i is that given by Equation (57). Hence substituting the above results* for a and ζ into the integrand for each Γ_i, we get

*$a = iy$, $da = idy$ for Γ_1 and Γ_4. $a = x$, $da = dx$ for Γ_2 and Γ_3.

70

$$\Gamma_1 = i \int_{\infty}^{0} \frac{[1 - (-1)^m e^{-ay}] \, dy}{(y^2 + k_m^2)(y^2 + k_q^2)(a_1^2 + y^2)^{\frac{1}{2}}}$$

$$\Gamma_2 = \int_{0}^{a_1} \frac{[1 - (-1)^m e^{iax}] \, dx}{(x^2 - k_m^2)(x^2 - k_q^2)(a_1^2 - x^2)^{\frac{1}{2}}}$$

$$(60)$$

$$\Gamma_3 = \int_{a_1}^{0} \frac{[1 - (-1)^m e^{iax}] \, dx}{(x^2 - k_m^2)(x^2 - k_q^2)[-(a_1^2 - x^2)^{\frac{1}{2}}]}$$

$$\Gamma_4 = i \int_{0}^{\infty} \frac{[1 - (-1)^m e^{-ay}] \, dy}{(y^2 + k_m^2)(y^2 + k_q^2)[-(a_1^2 + y^2)^{\frac{1}{2}}]}$$

Thus, with the vanishing of the simple poles and the combining of Γ_2 and Γ_3 as well as Γ_1 and Γ_4, Equation (59) reduces to

$$P[I_1(\beta)] = -(\Gamma_1 + \Gamma_2 + \Gamma_3 + \Gamma_4)$$

$$(61)$$

$$= -2P \int_{0}^{a_1} \frac{[1-(-1)^m \cos ax] \, dx}{(x^2-k_m^2)(x^2-k_q^2)(a_1^2-x^2)^{\frac{1}{2}}} + 2i \left[\int_{0}^{\infty} \frac{[1-(-1)^m e^{-ay}] \, dy}{(y^2+k_m^2)(y^2+k_q^2)(a_1^2+y^2)^{\frac{1}{2}}} + P \int_{0}^{a_1} \frac{(-1)^m \sin ax \, dx}{(x^2-k_m^2)(x^2-k_q^2)(a_1^2-x^2)^{\frac{1}{2}}} \right]$$

Since k_m, $k_q > k > a_1$ or k_m^2, $k_q^2 \gg a_1^2$, then in the first and third integrals, k_m and k_q lie outside the range of integration defined by the limits 0, a_1. The principal contribution to these integrals comes from the region $x \rightarrow a_1$. Hence for k_m^2, $k_q^2 \gg a_1^2$, the first integral in Equation (61) is approximated by

$$\frac{1}{(k_m^2-a_1^2)(k_q^2-a_1^2)} P \left[\int_{0}^{a_1} \frac{dx}{(a_1^2-x^2)^{\frac{1}{2}}} - (-1)^m \int_{0}^{a_1} \frac{\cos ax \, dx}{(a_1^2-x^2)^{\frac{1}{2}}} \right] = \frac{1}{(k_m^2-a_1^2)(k_q^2-a_1^2)} \left[\frac{\pi}{2} - (-1)^m \frac{\pi}{2} J_0(aa_1) \right]$$

and the third integral is approximated by

$$\frac{(-1)^m}{(k_m^2 - a_1^2)(k_q^2 - a_1^2)} P \int_{0}^{a_1} \frac{\sin ax \, dx}{(a_1^2 - x^2)^{\frac{1}{2}}} = \frac{(-1)^m}{(k_m^2 - a_1^2)(k_q^2 - a_1^2)} \sum_{i=0}^{\infty} \frac{(-1)^i (aa_1)^{2i+1}}{[(2i+1)!]^2}$$

71

where in evaluating the integrals we have used formulas from Korn and Korn,[30] (Equation (164) on page 942) and Gradshteyn and Ryzhik[25] (Equations 3.753.1 and 3.753.2 on page 419).

Thus, with the above approximations, we have for

Case 2:

$$P[I_1(\beta)] \equiv I_1^{mq} \ (\beta:\beta < k) = \frac{-\pi \ [1 - (-1)^m \ J_0 \ (aa_1)]}{(k_m^2 - a_1^2) \ (k_q^2 - a_1^2)}$$

$$+ 2i \left\{ \int_0^\infty \frac{[1 - (-1)^m \ e^{-ay}] \ dy}{(y^2 + k_m^2) \ (y^2 + k_q^2) \ (a_1^2 + y^2)^{1/2}} + \frac{1}{(k_m^2 - a_1^2) \ (k_q^2 - a_1^2)} \sum_{i=0}^\infty \frac{(-1)^{i+m} \ (aa_1)^{2i+1}}{[(2i+1)!]^2} \right\}$$

(62)

We now turn our attention to Case 1 for which the branch points lie on the positive and negative imaginary axes. Since k_m, $k_q > k$, $m \neq q$, and $m + q$ are even, the branch points and cuts and locations of the poles are shown in Figure 9 (Case 1) and the integration contour is shown in Figure 11. Application of the Cauchy residue theorem (in a manner similar to that for Case 2) yields for Case 1 $(\beta \leq -k, \ \beta \geq k)$ the following integral form for Equation (57).* Again the residues for the simple poles shown in Figure 11 vanish.

Case 1:

$$P[I_1(\beta)] \equiv I_1^{mq} \ (\beta:\beta > k) = - (\Gamma_1 + \Gamma_2) = + 2i \int_{a_1'}^\infty \frac{[1 - (-1)^m \ e^{-ay}] \ dy}{(y^2 + k_m^2) \ (y^2 + k_q^2) \ (y^2 - a_1'^2)^{1/2}}$$

(63)

where $a_1' = \sqrt{\beta^2 - k^2} = i\sqrt{k^2 - \beta^2} = ia_1$; $a_1'^2 = - a_1^2$

We observe that for Case 1, $P[I_1(\beta)]$ is purely reactive, i.e., imaginary.

To summarize, we have reduced Equation (57) or, equivalently, Equation (56b), to two expressions given by Cases 1 and 2 above corresponding to two different values of β. Thus, we have reduced that part of Equation (54) which involves integration with respect to k_x ($\equiv a$) to two expressions. Further, the limits for the two corresponding integrals for

---

*Note that the path is identical for Γ_2 in Figure 11 and Γ_4 in Figure 10 and that the path for Γ_1 is also identical in both figures. Hence the results for Γ_4 and Γ_1 in Equation (60) apply here if we replace the integral limit o by a_1' and the integrand variable a_1^2 by $-a_1'^2$, in accordance with the position of the branch point in Figure 11. With the preceding changes, combining Γ_4 and Γ_1 in Equation (60) yields a result for $P[I_1 \ (\beta)]$ analogous to the second integral in Equation (61).

Figure 11 – Case 1 Integration Contour: $k_q > k_m > k$

$$l_1(\beta) = -(\Gamma_1 + \Gamma_2)$$
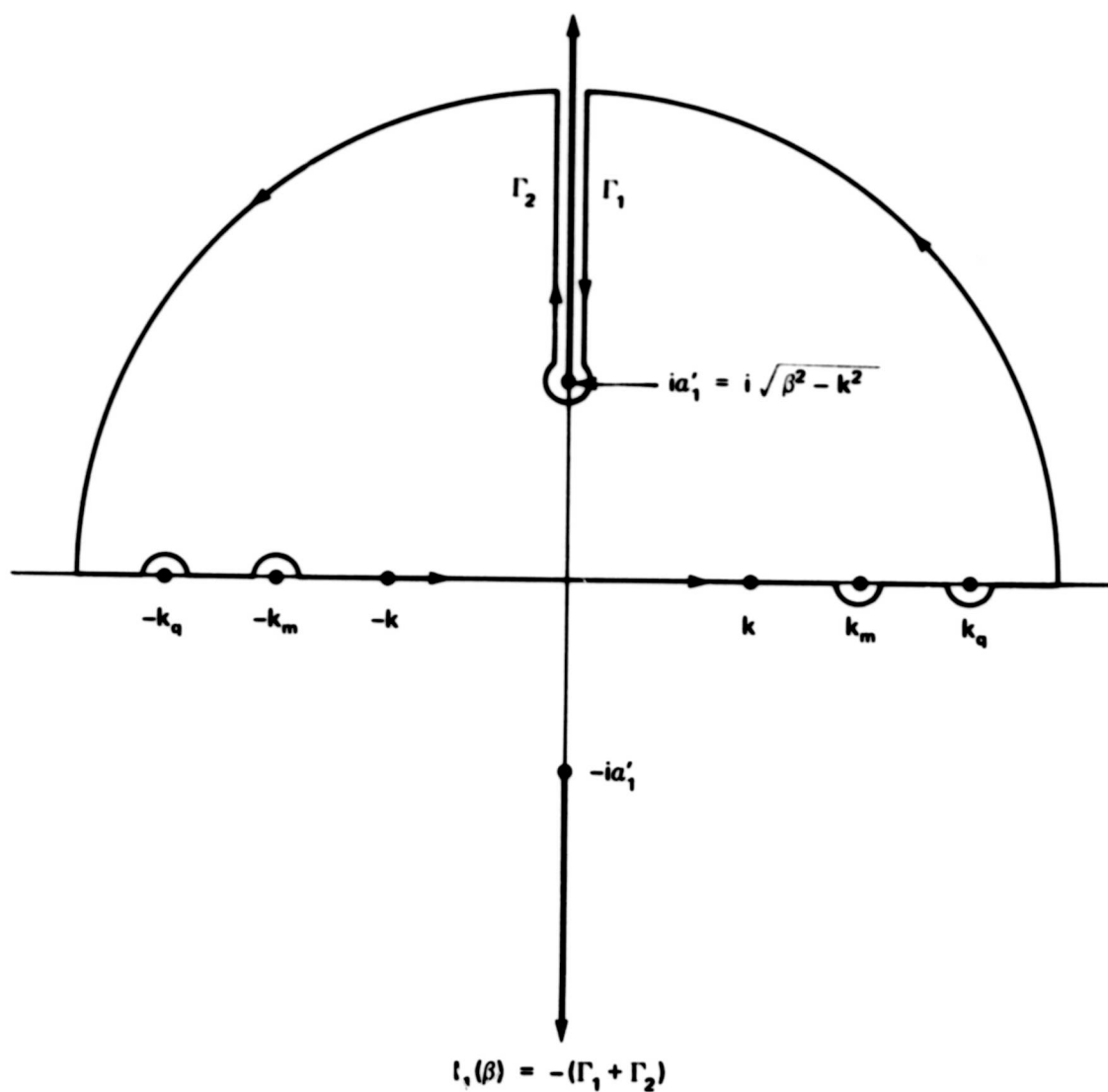
$$(a_1' = \sqrt{\beta^2 - k^2} = i\sqrt{k^2 - \beta^2} = ia_1;\ \text{from Pope}[8])$$

73

$k_y (\equiv \beta)$ now representing Equation (54) must conform to the corresponding ranges for β required for Cases 1 and 2. With these considerations, Equation (53) together with (54) is written, with $k_y \to \beta$, as

$$\bar{J}^{mnqr} = \frac{2iK_1}{\pi^2} \left\{ \int_k^\infty \frac{[1-(-1)^n \cos b\beta]}{(\beta^2-k_n^2)(\beta^2-k_r^2)} I_1^{mq}(\beta:\beta>k)\,d\beta + \int_0^k \frac{[1-(-1)^n \cos b\beta]}{(\beta^2-k_n^2)(\beta^2-k_r^2)} I_1^{mq}(\beta:\beta<k)\,d\beta \right\} \quad (64)$$

Equation (64) represents the *basic working expression* for evaluating the intermodal coupling coefficients. The coefficients are evaluated for plate wavenumbers above and below the acoustic wavenumber k.

Our immediate objective is to determine the radiation component J_R^{mnqr} and reactive component J_x^{mnqr} of the half-space coupling coefficient $\bar{J}^{mnqr}$ for all the possible combinations of (self- or cross-coupled) modes that exist in wavenumber space. The modal classification scheme for illustrating the location of the modes in wavenumber space relative to the acoustic wavenumber is an extension of that presented by Maidanik.[31] Appendix F indicates the general relationship between J_R^{mnqr}, J_x^{mnqr} and the radiation coefficients S_{mnqr}, T_{mnqr} derived by Davies [9] and presents a comparison of the corresponding analytical results derived here and by Davies for these quantities.

I. Edge Modes

(a) *Two Y-edge modes, k_m, $k_q > k$, $k_n = k_r < k$*

The modal classification scheme for the case k_m, $k_q > k$, $k_n = k_r < k$ is shown in Figure 12a. We use the following approximation[32]

$$\left. \frac{1-(-1)^n \cos b\beta}{(\beta^2-k_n^2)(\beta^2-k_r^2)} \right|_{n=r} \simeq \frac{\pi b}{4 k_n^2} \delta(\beta - k_n) \quad (65)$$

When Equation (65) is substituted into (64) with $\beta = k_n = k_r < k$, only the second term of Equation (64) is applicable. The result is

$$\bar{J}^{mnqn} = \frac{2 i k_n^2 k_m k_q}{\pi^2} \left(\frac{\pi b}{4 k_n^2} \right) I_1^{mq} (k_n:k_n<k) \quad (66a)$$

where $I_1^{mq} (k_n:k_n<k)$ is given by Equation (62) with $a_1^2 = k^2 - \beta^2 \to k^2 - k_n^2$.

Thus,

$$
\bar{j}^{mnqn} = \frac{i}{2\pi} \frac{k_m k_q}{2\pi} b \left[\frac{-\pi \, [1 - (-1)^m \, J_0 \, (a\sqrt{k^2 - k_n^2})]}{(k_m^2 + k_n^2 - k^2)(k_q^2 + k_n^2 - k^2)} \right]
$$

$$
- \frac{k_m k_q}{\pi} b \left\{ \left[\left(\sum_{i=0}^{\infty} \frac{(-1)^{i+m} \, (a\sqrt{k^2 - k_n^2})^{2i+1}}{[(2i+1)!]^2} \right) \left(\frac{1}{(k_m^2 + k_n^2 - k^2)(k_q^2 + k_n^2 - k^2)} \right) \right. \right.
$$

$$
\left. \left. + \int_0^\infty \frac{[1 - (-1)^m \, e^{-ay}] \, dy}{(y^2 + k_m^2)(y^2 + k_q^2)(k^2 - k_n^2 + y^2)^{\frac{1}{2}}} \right] \right\} \tag{66b}
$$

Note that the first term of this equation is imaginary and the last two terms are real.

To complete the solution for $\bar{J}^{mnqn}$, we evidently require the solution of the integral in Equation (66b) which is represented as the sum of four integrals

$$
\int_0^\infty \frac{[1 - (-1)^m \, e^{-ay} \, dy]}{(y^2 + k_m^2)(y^2 + k_q^2)(k^2 - k_n^2 + y^2)^{\frac{1}{2}}} = \int_0^k \frac{dy}{(y^2 + k_m^2)(y^2 + k_q^2)(k^2 - k_n^2 + y^2)^{\frac{1}{2}}}
$$

$$
+ \int_k^\infty \frac{dy}{(y^2 + k_m^2)(y^2 + k_q^2)(k^2 - k_n^2 + y^2)^{\frac{1}{2}}} - (-1)^m \int_0^k \frac{e^{-ay} \, dy}{(y^2 + k_m^2)(y^2 + k_q^2)(k^2 - k_n^2 + y^2)^{\frac{1}{2}}}
$$

$$
- (-1)^m \int_k^\infty \frac{dy}{(y^2 + k_m^2)(y^2 + k_q^2)(k^2 - k_n^2 + y^2)^{\frac{1}{2}}} \tag{66c}
$$

For the first and third integrals on the right-hand side, $0 < y < k$, whereas for the second and fourth integrals on that side, $k < y < \infty$.

Now for the first integral, $0 < y < k < k_m < k_q$. Therefore, both $y^2 + k_m^2 \approx k_m^2$ and $y^2 + k_q^2 \approx k_q^2$ lie outside the region of integration. Hence,[33]

$$
\int_0^k \frac{dy}{(y^2 + k_m^2)(y^2 + k_q^2)(k^2 - k_n^2 + y^2)^{\frac{1}{2}}} \approx \frac{1}{k_m^2 k_q^2} \int_0^k \frac{dy}{(k^2 - k_n^2 + y^2)^{\frac{1}{2}}} \approx \frac{1}{k_m^2 k_q^2} \ln\left(\frac{k + \sqrt{2k^2 - k_n^2}}{\sqrt{k^2 - k_n^2}} \right) \tag{67}
$$

For the second integral on the right-hand side of Equation (66c), $k < y$ so that $k^2 - k_n^2 < y^2$. Therefore $(k^2 - k_n^2 + y^2)^{1/2} \approx y$. Hence, expanding the approximate integrand in partial fractions* and integrating term by term yields

$$\int_k^\infty \frac{dy}{(y^2+k_m^2)(y^2+k_q^2)y} = -\frac{1}{k_m^2(k_q^2-k_m^2)}\int_k^\infty \frac{y\,dy}{(y^2+k_m^2)} - \frac{1}{k_q^2(k_m^2-k_q^2)}\int_k^\infty \frac{y\,dy}{(y^2+k_q^2)} + \frac{1}{k_m^2 k_q^2}\int_k^\infty \frac{dy}{y}$$

$$= -\frac{\ln(k_m^2+y^2)}{2k_m^2(k_q^2-k_m^2)}\Bigg|_k^{\displaystyle\lim_{y\to\infty}} - \frac{\ln(k_q^2+y^2)}{2k_q^2(k_m^2-k_q^2)}\Bigg|_k^{\displaystyle\lim_{y\to\infty}} + \frac{\ln y}{k_m^2 k_q^2}\Bigg|_k^{\displaystyle\lim_{y\to\infty}}$$

$$= \lim_{y\to\infty}\left[-\frac{\ln y^2}{2k_m^2(k_q^2-k_m^2)} - \frac{\ln y^2}{2k_q^2(k_m^2-k_q^2)} + \frac{1}{k_m^2 k_q^2}\ln y \right]$$

$$+ \left[\frac{\ln(k_m^2+k^2)}{2k_m^2(k_q^2-k_m^2)} + \frac{\ln(k_q^2+k^2)}{2k_q^2(k_m^2-k_q^2)} - \frac{1}{k_m^2 k_q^2}\ln k \right]$$

where for the upper limit only we have taken $k_m^2 + y^2 \approx y^2$ and $k_q^2 + y^2 \approx y^2$. Letting $\ln y^2 = 2\ln y$, factoring out a $\ln y$, and using a common denominator for the remaining terms in the first bracket, we find that this bracket vanishes and the result is

$$\int_k^\infty \frac{dy}{(y^2+k_m^2)(y^2+k_q^2)y} = \frac{1}{k_q^2-k_m^2}\left[\frac{1}{2k_m^2}\ln(k_m^2+k^2) - \frac{1}{2k_q^2}\ln(k_q^2+k^2) \right] - \frac{1}{k_m^2 k_q^2}\ln k \qquad (68)$$

---

* $$\frac{1}{(y^2+k_m^2)(y^2+k_q^2)y} = \frac{1}{(y+ik_m)(y-ik_m)(y+ik_q)(y-ik_q)y} = \frac{A}{y+ik_m} + \frac{B}{y-ik_m} + \frac{C}{y+ik_q} + \frac{D}{y-ik_q} + \frac{E}{y}$$

Multiplying, in turn, each side of the last two equations by the denominators of the constants A, B, etc., and evaluating the equations at the root of the denominator under consideration, we find $A = B =$

$$\frac{-1}{2k_m^2(k_q^2-k_m^2)}, \quad C = D = \frac{-1}{2k_q^2(k_m^2-k_q^2)}, \quad E = \frac{1}{k_m^2 k_q^2}$$

For the third and fourth integrals on the right-hand side of the unnumbered equation preceding Equation (67), we expand $e^{-ay} = 1 - ay + \ldots$. Here e^{-ay} is approximated with sufficient accuracy by

$$
e^{-ay} = \begin{cases} 1 - ay & ay < 1 \text{ or } y < \dfrac{1}{a} \\[2ex] 0 & a, > 1 \text{ or } y > \dfrac{1}{a} \end{cases}
$$

For the region of integration, $y > k$ or $ay > ak$. Hence if $ak > \pi$, then $ay > \pi$ and consequently by the foregoing approximation for e^{-ay}, the fourth integral vanishes and the third integral is written as the sum of two terms, the second of which also vanishes because of the above approximation.*

Thus,

$$
\int_0^k \frac{e^{-ay} dy}{(y^2+k_m^2)(y^2+k_q^2)(k^2-k_n^2+y^2)^{1/2}} = \int_0^{\frac{1}{a}} \frac{(1-ay)dy}{(y^2+k_m^2)(y^2+k_q^2)(k^2-k_n^2+y^2)^{1/2}}
$$

$$
+ \int_{\frac{1}{a}}^k \frac{(o)\, dy}{(y^2+k_m^2)(y^2+k_q^2)(k^2-k_n^2+y^2)^{1/2}} \approx \frac{1}{k_m^2 k_q^2} \int_0^{\frac{1}{a}} \frac{dy}{(k^2-k_n^2+y^2)^{1/2}}
$$

$$
- \frac{a}{k_m^2 k_q^2} \int_0^{\frac{1}{a}} \frac{y\, dy}{(k^2-k_n^2+y^2)^{1/2}} \approx \frac{1}{k_m^2 k_q^2} \left\{ \ln \left(\frac{\frac{1}{a} + \sqrt{k^2-k_n^2+\left(\frac{1}{a}\right)^2}}{\sqrt{k^2-k_n^2}} \right) \right.
$$

$$
\left. - a \left[\left(k^2-k_n^2+\left(\frac{1}{a}\right)^2\right)^{1/2} - (k^2-k_n^2)^{1/2} \right] \right\} \tag{69a}
$$

where we have used the Dwight tables[33] to evaluate the integrals leading to Equation (69a).

Equations (67), (68), and (69a), which are all real quantities, are now combined and substituted for the integral in Equation (66b) to complete the solution of $\bar{J}^{mnqn}$. Equating the real and imaginary parts of $\bar{J}^{mnqn} = J_x^{mnqn} + i J_R^{mnqn}$ given by Equation (55) to that given by Equation (66b), including the above-mentioned substitution for the integral in this equation, we get

$$
J_R^{mnqn} = \frac{-b\, k_m k_q \left[1 - (-1)^m\, J_o\left(a\sqrt{k^2-k_n^2}\right) \right]}{2(k_{mn}^2-k^2)(k_{qn}^2-k^2)} \tag{69b}
$$

---

*Clearly since only the first integral on the right-hand side of the following equation obtains, then $y < \frac{1}{a} < k$ or $ay < 1 < ak$ for this integral.

$$J_x^{mnqn} = \frac{-b}{\pi k_m k_q} \left\{ \ln\left(\frac{k+\sqrt{2k^2-k_n^2}}{k\sqrt{k^2-k_n^2}}\right) + \frac{1}{2(k_q^2-k_m^2)} \left[k_q^2 \ln(k_m^2+k^2) - k_m^2 \ln(k_q^2+k^2)\right] \right.$$

$$- (-1)^m \left\{ \ln\left(\frac{\frac{1}{a} + \sqrt{k^2-k_n^2+\left(\frac{1}{a}\right)^2}}{\sqrt{k^2-k_n^2}}\right) - a \left[\left(k^2-k_n^2+\left(\frac{1}{a}\right)^2 - (k^2-k_n^2)^{1/2}\right)\right] \right\}$$

$$\left. + \frac{k_m^2 k_q^2}{(k_{mn}^2-k^2)(k_{qn}^2-k^2)} \sum_{i=0}^{\infty} \frac{(-1)^{i+m} \left(a\sqrt{k^2-k_n^2}\right)^{2i+1}}{[(2i+1)!]^2} \right\} \tag{69c}$$

where $k_{mn} = (k_m^2+k_n^2)^{1/2}$, $k_{qn} = (k_q^2+k_n^2)^{1/2}$

Some special cases for the previous results are now presented.

(1)   In the limit, $k_n = k_r \ll k$

$$J_R^{mnqn} \rightarrow \frac{-b\, k_m k_q\, [1 - (-1)^m J_o\,(a\,k)]}{2(k_m^2-k^2)(k_q^2-k^2)}$$

since $J_o\,(a\sqrt{k^2-k_n^2}) < 1$, J_R^{mnqn} is always negative.

(2)   In the limit, $k_n = k_r \ll k$ and k_m, $k_q \gg k$

$$J_R^{mnqn} \rightarrow \frac{-b\, [1 - (-1)^m J_o\,(a\,k)]}{2 k_m k_q}$$

(3)   In the high frequency limit, $a\,k \gg \pi$, $J_o\,(a\,k) \ll 1$ the foregoing case reduces to

$$J_R^{mnqn} \rightarrow \frac{-b}{2 k_m k_q}$$

(4)   In the limit, $k_q > k_m$, $k_q^2 \gg k_m^2$, k_n sufficiently small so that $k^2-k_n^2 \approx k^2$ and observing that $\frac{1}{a} < k$

$$J_x^{mnqn} \rightarrow \frac{-b}{\pi k_m k_q} \left[\ln(1 + \sqrt{2}\,)\frac{k_m}{k} + (-1)^m\, k\, a\right]$$

where $\frac{k_m}{k} = \frac{m\pi}{ka}$. For $k_m \gg k$, i.e., for sufficiently large values of m, the first term in the bracket will predominate. In this case

$$J_x^{mnqn} \to \frac{-b}{\pi k_m k_q} \ln \left[(1 + \sqrt{2}) \frac{k_m}{k} \right]$$

For two x-type edge modes with k_n, $k_r > k$, $k_m = k_q < k$, Equations (71) (72) hold with $m \leftrightarrow n$, $q \leftrightarrow r$, and $a \leftrightarrow b$, i.e., symmetrical results obtain.

(b) *Two Y=edge modes.* $k_m \neq k_q > k$, $k_n \neq k_r < k$

This case is shown in Figure 12b. The delta function approximation given by Equation (65) shows that for $k_n \neq k_r$ the $\bar{J}^{mnqr}$'s vanish. Hence,

$$J_R^{mnqr} \equiv J_x^{mnqr} \equiv 0 \qquad \text{for } n \neq r \tag{69d}$$

(c) *Two Y-edge modes,* $k_m = k_q > k$, $k_n = k_r < k$

This case is shown in Figure 12c. From Equation (57) (which is equivalent to Equation (56b)), with $k_m = k_q$,

$$I_1(\beta) = \int_{-\infty}^{\infty} \frac{[1 - (-1)^m e^{i a a}] \, da}{(a^2 - k_m^2)^2 (k^2 - a^2 - \beta^2)^{\frac{1}{2}}} = \int_{-\infty}^{\infty} \frac{[1 - (-1)^m e^{i a a}] \, da}{(a + k_m)^2 (a - k_m)^2 (k^2 - a^2 - \beta^2)^{\frac{1}{2}}}$$

Following a procedure similar to that which led to Equation (59) except that the poles at $\pm k_m$ and $\pm k_q$ in that equation now merge, we obtain

$$I_1(\beta) = \pi i [\text{Res}(k_m) + \text{Res}(-k_m)] - (\Gamma_1 + \Gamma_2 + \Gamma_3 + \Gamma_4) \tag{70a}$$

where $\text{Res}(\pm k_m)$ represent *second order poles* evaluated as follows. The integrand for $I_1(\beta)$ is written as

$$f(a, \beta) = \frac{[1 - (-1)^m e^{i a a}]}{(a + k_m)^2 (a - k_m)^2 (k^2 - a^2 - \beta^2)^{\frac{1}{2}}}$$

Now $f(a, \beta)$ has removable singularities at $a = \pm k_m$. To find the residue of the second order poles at $a = k_m$, let

$$\text{Res}(k_m) = \frac{df(a, \beta)}{da} \bigg|_{a = k_m} = \left[\frac{d}{da} \left(\frac{[1 - (-1)^m e^{i a a}]}{(a + k_m)^2 (k^2 - a^2 - \beta^2)^{\frac{1}{2}}} \right) \right]_{a = k_m}$$

$$= \frac{-i a}{4 k_m^2 (k^2 - k_m^2 - \beta^2)^{\frac{1}{2}}}$$

since

$$[1 - (-1)^m e^{i k_m a}] = 1 - (-1)^{2m} = 0 \text{ and } (-1)^{2m+1} = 0.$$

79

Similarly

$$\text{Res}(-k_m) = \left[\frac{d}{da}\left(\frac{[1 - (-1)^m \, e^{iaa}]}{(a-k_m)^2 \, (k^2-a^2-\beta^2)^{\frac{1}{2}}}\right)\right]_{a=-k_m}$$

$$= \frac{-ia}{4 k_m^2 \, (k^2-k_m^2-\beta^2)^{\frac{1}{2}}}$$

and

$$I_1(\beta) = - (\Gamma_1+\Gamma_2+\Gamma_3+\Gamma_4) + \frac{\pi a}{2k_m^2 \, (k^2-k_m^2-\beta^2)^{\frac{1}{2}}}$$

Now *for the case* $k_m = k_q$, the Case 2 solution for Equation (57) given by Equation (62)*, designated as $I_1^{mq}(\beta:\beta<k)$, is modified by letting $k_q \rightarrow k_m$ and adding the term representing $\pi i[\text{Res} (k_m) + \text{Res} (-k_m)]$ which is

$$+ \frac{\pi a}{2k_m^2 \, (k^2-k_m^2-\beta^2)^{\frac{1}{2}}}$$

which is imaginary for $\beta<k$, $k_m>k$. Hence

$$P[I_1(\beta)] = I_1^{mq}(\beta:\beta<k) \approx \frac{-\pi[1 - (-1)^m \, J_o \, (aa_1)]}{(k_m^2 - a_1^2)^2}$$

$$+2i\left\{\int_0^\infty \frac{[1 - (-1)^m \, e^{-ay}dy}{(y^2+h_m^2)^2 \, (a_1^2+y^2)^{\frac{1}{2}}} + \left[\frac{1}{(k_m^2-a_1^2)^2}\right]\sum_{i=o}^\infty \frac{(-1)^{i+m}(aa_1)^{2i+1}}{[(2i+1)!]^2}\right\}$$

$$+ \frac{\pi a}{2k_m^2 \, (k^2-k_m^2-\beta^2)^{\frac{1}{2}}} \qquad\qquad \text{for } k_m = k_q \qquad\qquad (70b)$$

where $a_1^2 = k^2-\beta^2$

Now from Equations (53), (54), (55) and (56a) with $n = r$ and $P[I_1(\beta)] = I_1^{mq}(\beta:\beta<k)$, we write

_____

*Equation (62), modified for $k_m = k_q$ as shown, is applicable because k_m, k_q still lie outside the range of integration. Otherwise, we would return to the general expression, Equation (61).

$$\bar{J}^{mnqr} = \bar{J}_X^{mnqr} + i\,\bar{J}_R^{mnqr} = \frac{i\,k_m k_n k_q k_r}{\pi^2} \int_{-\infty}^{\infty} \left. \frac{[1-(-1)^n \cos b\beta]}{(\beta^2-k_n^2)(\beta^2-k_r^2)}\right|_{n=r} I_1(\beta)\,d\beta$$

$$= \frac{i\,k_m k_n k_q k_r}{\pi^2} \left\{ 2\int_0^k \left. \frac{[1-(-1)^n \cos b\beta]}{(\beta^2-k_n^2)(\beta^2-k_r^2)}\right|_{n=r} I_1^{mq}\,(\beta:\beta<k)\,d\beta \right.$$

Hence for $m = q$, $n = r$ (using Equation (65)),

$$\bar{J}^{mnmn} = J_X^{mnmn} + i\,J_R^{mnmn} = \frac{i\,2k_m^2 k_n^2}{\pi^2}\left(\frac{\pi b}{4k_n^2}\right)\!\int_0^k \delta(\beta-k_n)\,I_1^{mq}\,(\beta:\beta<k)\,d\beta$$

where $I_1^{mq}\,(\beta:\beta<k)$ is given by Equation (70b). Performing the integration on the right-hand side of the above equation with $\beta \to k_n$, $a_1 = \sqrt{k^2-\beta^2} \to \sqrt{k^2-k_n^2}$ and equating imaginary terms, we get J_R^{mnmn} given by Equation (69b) with $q = m$. That is

$$J_R^{mnmn} = \frac{-b\,k_m^2}{2}\,\frac{[1-(-1)^m J_0(a\sqrt{k^2-k_n^2})]}{(k_m^2 + k_n^2 - k^2)^2} \tag{70c}$$

Equating real terms, we get the reactive component J_X^{mnqn} given by Equation (69c)* with $q = m$ and an additional contribution associated with the last term in Equation (70b) due to the second order pole occurring for $k_m = k_q$. That is**

---

*We recall that the quantity in quotes in Equation (70b) includes an integral which has already been evaluated. This quantity led to Equation (69c) which is applicable for n=r and m≠q. Hence when n=r and m=q, we append the contribution of the second order pole, given by the last term in Equation (70b) to (69c) to obtain J_X^{mnmn}.

**Note that for $k_m = k_q$, the second term in equation (69c) is indeterminate. We evaluate this term by writing

$$\frac{1}{2(k_q^2-k_m^2)}\,[k_q^2 \ln(k_m^2+k^2) - k_m^2 \ln(k_q^2+k^2)] = \frac{k_q^2 \ln(k_m^2+k^2) - k_m^2 \ln(k_m^2+k^2)\left(1+\dfrac{k_q^2-k_m^2}{k_m^2+k^2}\right)}{2(k_q^2-k_m^2)}$$

$$= \frac{(k_q^2-k_m^2)\ln(k_m^2+k^2) - k_m^2 \ln\left(1+\dfrac{k_q^2-k_m^2}{k_m^2+k^2}\right)}{2(k_q^2-k_m^2)}$$

$$\approx \frac{1}{2}\ln(k_m^2+k^2) - \frac{k_m^2}{2(k_q^2-k_m^2)} \cdot \frac{k_q^2-k_m^2}{k_m^2+k^2}$$

$$\approx \ln k_m - \frac{1}{2} \quad \text{for } k_m^2 \gg k^2$$

Note also that the approximation obtains because $\ln(1+x)\approx x$, $x<1$.

81

$$J_x^{mnmn} = \frac{-b}{\pi k_m^2} \left\{ \ln\left(\frac{k + \sqrt{2k^2 - k_n^2}}{k \sqrt{k^2 - k_n^2}}\right) + \ln k_m - \frac{1}{2} \right.$$

$$- (-1)^m \left\{ \ln\left(\frac{\frac{1}{a} + \sqrt{k^2 - k_n^2 + \left(\frac{1}{a}\right)^2}}{\sqrt{k^2 - k_n^2}}\right) - a \left[\left(k^2 - k_n^2 + \left(\frac{1}{a}\right)^2\right)^{\frac{1}{2}} - (k^2 - k_n^2)^{\frac{1}{2}} \right] \right\}$$

$$\left. + \frac{k_m^4}{(k_{mn}^2 - k^2)^2} \sum_{i=o}^{\infty} \frac{(-1)^{i+m} (a\sqrt{k^2 - k_n^2})^{2i+1}}{[(2i+1)!]^2} \right\} - \frac{A_p}{4(k_m^2 + k_n^2 - k^2)^{\frac{1}{2}}} \qquad (70d)$$

where the last term in Equation (70d) represents the second order contribution which is reactive*

Some special cases for the previous results are now presented

(1) For $k_m > k$, $k_m \gg k_n$, J_o $(a \sqrt{k^2 - k_n^2}) \ll 1$,

$$J_R \rightarrow \frac{-b}{2k_m^2}$$

(2) For $k_{mm}^2 = k_m^2 + k_n^2 \gg k^2$,

$$J_x^{mnmn} \rightarrow \frac{-A_p}{4k_{mn}}$$

For two x-type edge modes with $k_n = k_r > k$, $k_m = k_q < k$, Equations (70c,d) hold with m↔n, q↔r, a↔b.

(d) *Two Y-edge modes k_m, $k_q > k$; k_n, $k_r < k$.*

This is the general representation for two Y-edge modes which accounts for any combination of m=q or m≠q and n=r or n≠r. All of the preceding results for two Y-edge modes are special cases of this representation.

---

*The last term in Equation (70d) is obtained from the last term in Equation (70b) as follows. Let

$$\left. I_1^{mq} \right|_{\substack{\text{second order} \\ \text{pole contribution}}} = \frac{\pi a}{2k_m^2 (h^2 - k_m^2 - \beta^2)^{\frac{1}{2}}}$$

Then $\left. J_x^{mnmn} \right|_{\substack{\text{second order} \\ \text{pole contribution}}} = \frac{i \, 2k_m^2 k_n^2}{\pi^2} \left(\frac{\pi b}{4k_n^2}\right) \int_o^k \delta(\beta - k_n) \frac{\pi a d\beta}{2k_m^2(k^2 - k_m^2 - \beta^2)^{\frac{1}{2}}} = \frac{-Ap}{4k_m^2(k_m^2 + k_n^2 - k^2)^{\frac{1}{2}}}$

where we have let $(k^2 - k_m^2 - k_n^2)^{\frac{1}{2}} \rightarrow -i(k_m^2 + k_n^2 - k^2)^{\frac{1}{2}}$; see statement following Equation (58).

Generalizing, Equations (69b), (69d), and (70c) for representation by a single equation, we write

$$J_R^{mnqr} = \frac{-b k_m k_q [1 - (-1)^m J_o (a \sqrt{k^2 - k_n^2})]}{2(k_{mn}^2 - k^2)(k_{qn}^2 - k^2)} \delta_{nr} \tag{71}$$

and generalizing Equations (69c,d) and (70d) for representation by a single equation, we write

$$\begin{aligned}
J_x^{mnqr} = \frac{-b}{\pi k_m k_q} &\left\{ \left[\left\{ \ln \left[\frac{k + \sqrt{2k^2 - k_n^2}}{k \sqrt{k^2 - k_n^2}} \right] + \frac{1}{2(k_q^2 - k_m^2)} [k_q^2 \ln(k_m^2 + k^2) - k_m^2 \ln(k_q^2 + k^2)] \right\} \right. \right. \\
&- (-1)^m \left\{ \ln \left[\frac{\frac{1}{a} + \sqrt{k^2 - k_n^2 + \left(\frac{1}{a}\right)^2}}{\sqrt{k^2 - k_n^2}} \right] - a \left[\left(k^2 + k_n^2 + \left(\frac{1}{a}\right)^2\right)^{\frac{1}{2}} - (k^2 - k_n^2)^2 \right] \right\} \\
&+ \frac{k_m^2 k_q^2}{(k_{mn}^2 - k^2)(k_{qn}^2 - k^2)} \sum_{i=o}^{\infty} \frac{(-1)^{i+m} (a \sqrt{k^2 - k_n^2})^{2i+1}}{[(2i+1)!]^2} \left. \right] \delta_{nr} \\
&- \frac{1}{2(k_q^2 - k_m^2)} [k_q^2 \ln(k_m^2 + k^2) - k_m^2 \ln(k_q^2 + k^2)] \delta_{mq} \delta_{nr} \\
&\left. + (\ln k_m - \frac{1}{2}) \delta_{mq} \delta_{nr} \right\} - \frac{A_p \delta_{mq} \delta_{nr}}{4(k_m^2 + k_n^2 - k^2)^{\frac{1}{2}}} \tag{72}
\end{aligned}$$

where

$$\delta_{nr} = 1 \text{ for } n = r \qquad\qquad \delta_{mq} \delta_{nr} = 1 \text{ for } m = q, n = r$$
$$= o \text{ otherwise} \qquad\qquad\qquad = o \text{ otherwise}$$

For two x-type edge modes with k_n, $k_r > k$; k_m, $k_q < k$, Equations (71) and (72) hold with $m \leftrightarrow n$, $q \leftrightarrow r$, $a \leftrightarrow b$.

II. Corner Modes

(a) *Two corner modes, k_m, $k_q > k$; $k_n = k_r > k$*

Figure 12d shows the modal classification scheme for the case k_m, $k_q > k$; $k_n = k_r > k$. *If we use the approximation* given by Equation (65), then only $\beta = k_n = k_r$ will yield a value for $\bar{J}^{mnqr}$ in Equation (64). Thus, the approximation requires that $\beta > k$ and consequently

83

only the first integral in Equation (64), with integral limits for β ranging from k to ∞, obtains. For this case, Equations (64) and (65) give

$$\bar{J}^{mnqn} = \frac{2iK_1}{\pi^2} \int_k^\infty \frac{\pi b}{4k_n^2} \, \delta(\beta - k_n) \, I_1^{mq} \, (\beta:\beta > k) \, d\beta \tag{73a}$$

We observe that since $I_1^{mq} (\beta:\beta > k)$ represented by Equation (63) is a pure imaginary, then the δ function approximation leads to a null contribution for the resistance, i.e. $\bar{J}_R^{mnqn} = 0$. However, since $\bar{J}_R^{mnqr}$ actually does exist but is weak, we conclude that *for this particular case the δ function representation is a poor approximation* for the left-hand side of Equation (65). Hence we discard this approximation and the corresponding requirement that β be greater than k only and proceed to evaluate the general case k_n, $k_r > k$ (which includes both $k_n \neq k_r$ and, as a special case, $k_n = k_r$) for which the range of β is unrestricted, i.e., $\beta \gtrless k$. Hence we may now use the second integral in Equation (64) to obtain

$$J_R^{mnqr} = \frac{2K_1}{\pi^2} \, \mathrm{Re} \left[\int_0^k \frac{1 - (-1)^n \cos b\beta}{(\beta^2 - k_n^2)(\beta^2 - k_r^2)} \, I_1^{mq} \, (\beta:\beta < k) \, d\beta \right]$$

$$\simeq \frac{-4}{\pi^2 k_m k_n k_q k_r} \int_0^k \int_0^{\sqrt{k^2 - \beta^2} \approx k} \frac{[1 - (-1)^n \cos b\beta] \, [1 - (-1)^m \cos ax] \, dx \, d\beta}{(k^2 - \beta^2 - x^2)^{1/2}}$$

where we have used the first term of Equation (61) for $\mathrm{Re} \, P[I_1(\beta)] = \mathrm{Re} \, [I_1^{mq} \, (\beta:\beta < k)]$ with the upper limit $a_1 = \sqrt{k^2 - \beta^2} \approx k$ for $\beta < k$ or $\beta^2 \ll k^2 \ll k_n^2, k_r^2$. Since all the modal wavenumbers lie outside the range of integration, we have also made, for this case, the approximations $\beta^2 - k_n^2 \sim -k_n^2$, $\beta^2 - k_r^2 \sim -k_r^2$, $x^2 - k_m^2 \sim -k_m^2$, $x^2 - k_q^2 \sim -k_q^2$. The Davies[9] results of integrating the foregoing expression and confirmed through detailed evaluation by Leibowitz[5] are

$$J_R^{mnqr} = \frac{-2k}{\pi k_m k_n k_q k_r} \left\{ 1 - (-1)^m \frac{\sin ka}{ka} - (-1)^n \frac{\sin kb}{kb} - (-1)^{m+n} \frac{\sin k \sqrt{a^2 + b^2}}{k \sqrt{a^2 + b^2}} \right\} \tag{73b}$$

84

For the reactive term, we use the first integral of Equation (64) in conjunction with Equation (63):

$$J_x^{mnqr} = \frac{-4k_m k_n k_q k_r}{\pi^2} \int_k^\infty \left[\iint_{\sqrt{\beta^2-k^2}\approx 0}^\infty \frac{[1-(-1)^m e^{-ay}]\,dy}{(y^2+k_m^2)(y^2+k_q^2)(y^2-\beta^2+k^2)^{1/2}} \right] \frac{1-(-1)^n \cos b\beta}{(\beta^2-k_n^2)(\beta^2-k_r^2)}\,d\beta$$

where $a_1' = \sqrt{\beta^2-k^2} \approx 0$ is taken as the lower limit since $\beta > k$. For the reactive term, however, we can obtain the major contribution to the above integral by using the δ function approximation given by Equation (65). Thus for $k_n = k_r$, the preceding equation becomes

$$J_x^{mnqr} = \frac{-bk_m k_q}{\pi} \int_k^\infty \left[\int_0^\infty \frac{[1-(-1)^m e^{-ay}]\,dy}{(y^2+k_m^2)(y^2+k_q^2)(y^2-\beta^2+k^2)^{1/2}} \right] \delta(\beta-k_n)\,d\beta\,\delta_{nr}$$

$$= \frac{-bk_m k_q}{\pi} \int_0^\infty \frac{[1-(-1)^m e^{-ay}]\,dy}{(y^2+k_m^2)(y^2+k_q^2)(y^2-k_n^2+k^2)^{1/2}}\,\delta_{nr}$$

The integral is identical to that of Equation (66c) represented and previously evaluated as the sum of four integrals. The first and third integrals of the sum are respectively evaluated to Equations (67) and (69a) which are approximately zero for $0 < y < k < k_m$, k_n, k_q, k_r and $k_n > \frac{1}{a}$. The fourth integral of the sum has also been shown to vanish. Hence, the above integral $\int_0^\infty \rightarrow \int_k^\infty$ given by the second integral on the right-hand side of Equation (66c). Moreover, since $y^2 \gg k^2-k_n^2$, then, as before, $(y^2-k_n^2+k^2)^{1/2} \approx y$ and the result for $\int_k^\infty$ is given by Equation (68). Hence, generalizing

$$J_x = A\delta_{nr} + B\delta_{mq} - (A+B)\,\delta_{nr}\delta_{mq} + C\,\delta_{nr}\delta_{mq} \tag{74}$$

where

$$A = \frac{-b}{\pi k_m k_q} \left\{ -\ln k + \frac{1}{2(k_q^2-k_m^2)}\,[k_q^2 \ln(k_m^2+k^2) - k_m^2 \ln(k_q^2+k^2)] \right\} \tag{75}$$

85

$$B = \frac{-a}{\pi k_n k_r} \left\{ -\ln k + \frac{1}{2(k_r^2 - k_n^2)} \left[k_r^2 \ln(k_n^2 + k^2) - k_n^2 \ln(k_r^2 + k^2) \right] \right\} \qquad (76)$$

$$C = \frac{-A_p}{4(k_m^2 + k_n^2 - k^2)^{1/2}} + \frac{b}{\pi k_m^2} \left(\ln \frac{k}{k_m} + \frac{1}{2} \right) + \frac{a}{\pi k_n^2} \left(\ln \frac{k}{k_n} + \frac{1}{2} \right) \qquad (77)$$

where the right-hand side of Equation (74) reduces to the first term $A\delta_{nr}$ for $n = r$ or $n \neq r$ and $m \neq q$, and by symmetry to the second term $B\delta_{mq}$ for $m = q$ or $m \neq q$ and $n \neq r$, and to the fourth term $C\delta_{nr}\delta_{mq}$ for both $n = r$, $m = q$ or $n \neq r$, $m \neq q$. For this last case, we have a second order pole at $k_m = k_q$ which, as previously shown, yields the contribution given by the first term on the right-hand side of Equation (77). In addition, for this case ($k_m = k_q$, $k_n = k_r$), both Equations (75) and (76) are indeterminate. They respectively evaluate to the second and third terms given in parentheses in Equation (77) as shown by the footnote to Equation (70d).

III. Y-Edge - Acoustically Fast (AF) Modes

Figure 12e shows the *modal classification scheme for the case* k_m, k_n, $k_r < k$; $k_q > k$. We consider two cases $\beta > |k|$ and $\beta < |k|$.

<u>Case 1 – $\beta > |k|$</u>: The appropriate contour of integration is shown in Figure 13 with simple poles at $a = \pm k_m$, $a = \pm k_q$. Again, the real integral, Equation (57), is replaced by the contour integral. As before, integration in the a-plane over the contour yields Equation (63), i.e., Equation (63) is applicable for $\beta > |k|$ because the second term in Equation (61) is unchanged for $k_m < k$. Thus

$$I_1^{mq}(\beta:\beta > k) = + 2i \int_{a_1'}^{\infty} \frac{[1 - (-1)^m e^{-ay}] \, dy}{(y^2 + k_m^2)(y^2 + k_q^2)(y^2 - a_1'^2)^{1/2}} \qquad (78)$$

<u>Case 2 – $\beta < |k|$</u>: We treat two regions for β corresponding to two different regions for a_1.

(1) Suppose, $0 < a_1 = \sqrt{k^2 - \beta^2} < k_m$; see Figure 14. Then, $\sqrt{k^2 - k_m^2} < \beta < k$ Obviously integration in the a-plane over the contour given by Figures 14 and 10 yields the same results. Hence,

$$I_1^{mq}(\beta:\beta > \sqrt{k^2 - k_m^2}) \Bigg|_{\substack{k_m < k \\ k_q > k}} = I_1^{mq}(\beta:\beta < k) \Bigg|_{\substack{k_m > k \\ k_q > k}} = \text{r.h.s. of Equation (62)} \qquad (79a)$$

(2) Suppose $k_m < a_1 = \sqrt{k^2 - \beta^2} < k$; see Figure 15. Then $o < \beta < \sqrt{k^2 - k_m^2}$ and I_1^{mq} $(\beta : \beta < \sqrt{k^2 - k_m^2}$ is determined by integration over a contour encircling k_m and a_1 as shown in Figure 15. Thus, in analogy with Equation (59),

$$I_1^{mq} (\beta : \beta < \sqrt{k^2 - k_m^2}) = + \pi i \, [\text{Res}(-k_q) + \text{Res}(-k_m)] + \pi i \, [\text{Res}(k_q) + \text{Res}(k_m)] - (\Gamma_1 + \Gamma_2)$$

But for $k_m \neq k_q$

$$\text{Res}(-k_q) \equiv \text{Res}(-k_m) \equiv \text{Res}(k_q) \equiv \text{Res}(k_m) \equiv o$$

Hence

$$I_1^{mq} (\beta : \beta < \sqrt{k^2 - k_m^2}) = - (\Gamma_1 + \Gamma_2)$$

We now deform the contours* in Figure 15 to the one shown in Figure 16. Application of the Cauchy theorem to this contour gives (note that here Γ_1 includes the integral contributions for the path above the x-axis running from $y = \infty$ to $x = a_1$; Γ_2 includes the integral contribution for the path running from $y = \infty$ to $x = a_1$ but approaches a_1 along a path below the axis.

$$\Gamma_1 = i \int_\infty^o \frac{[1 - (-1)^m \, e^{-ay}] \, dy}{(y^2 + k_m^2)(y^2 + k_q^2)(a_1^2 + y^2)^{\frac{1}{2}}} + \int_0^{k_m - \rho} \frac{[1 - (-1)^m \, e^{iax}] \, dx}{(x^2 - k_m^2)(x^2 - k_q^2)(a_1^2 - x^2)^{\frac{1}{2}}}$$

$$+ \int_{C_\rho} \frac{[1 - (-1)^m \, e^{iax}] \, dx}{(x^2 - k_m^2)(x^2 - k_q^2)(a_1^2 - x^2)^{\frac{1}{2}}} + \int_{k_m + \rho}^{a_1} \frac{[1 - (-1)^m \, e^{iax}] \, dx}{(x^2 - k_m^2)(x^2 - k_q^2)(a_1^2 - x^2)^{\frac{1}{2}}}$$

We observe that the first integral on the right-hand side is identical to the first of Equations (60) and the sum of the following three integrals have the same form as for Γ_2 in Equation (60). In the limit as $\rho \to o$, the contribution of the third integral for the pole at k_m is $-\pi i \, \text{Res}(k_m)$ (due to the negative sense of the integral). But $\text{Res}(k_m) = o$. The contribution of $+a_1$ has previously been excluded from the integral since $\int_{C_{a_1}} = o$.

---

*Res $(\pm k_m)$, Res $(\pm k_q)$, and the contour integrals around $\pm a_1$ make no contribution to the contour integral. Hence we can conveniently exclude the points $-k_m$, $-k_q$, $-a$ in the upper left hand plane of the deformed figure and ignore the contributions of $+k_m$ and $+a_1$ in the following integral for Γ_1. Note that the path of the branch cut for the deformed contour runs from $i\infty$ to o on the imaginary axis and from o to a_1 on the real axis.

The contribution of the second and fourth integrals are combined so that $\displaystyle\int_0^{k_m-\rho}$

$+\displaystyle\int_{k_m+\rho}^{a_1} \rightarrow P_{k_m}\displaystyle\int_0^{a_1}$ where the principal value P_{k_m} excludes the pole at $x = k_m$.

Hence, as $\rho \rightarrow 0$

$$\Gamma_1 = -i\int_0^\infty \frac{[1-(-1)^m e^{-ay}]\,dy}{(y^2+k_m^2)(y^2+k_q^2)(y^2+a_1^2)^{1/2}} + P_{k_m}\int_0^{a_1}\frac{[1-(-1)^m e^{iax}]\,dx}{(x^2-k_m^2)(x^2-k_q^2)(a_1^2-x^2)^{1/2}}$$

Using similar reasoning for Γ_2, it follows that

$$\Gamma_1+\Gamma_2 = -i\int_0^\infty \frac{2[1-(-1)^m e^{-ay}]\,dy}{(y^2+k_m^2)(y^2+k_q^2)(a_1^2+y^2)^{1/2}} + P_{k_m}\int_0^{a_1}\frac{2[1-(-1)^m e^{iax}]\,dx}{(x^2-k_m^2)(x^2-k_q^2)(a_1^2-x^2)^{1/2}}$$

Note that for Γ_2, the form of the last two integrals of Equation (60) are applicable. Thus

$$I_1^{mq}\left(\beta:\beta<\sqrt{k^2-k_m^2}\right) = -(\Gamma_1+\Gamma_2) = +i\int_0^\infty \frac{2[1-(-1)^m e^{-ay}]\,dy}{(y^2+k_m^2)(y^2+k_q^2)(a_1^2+y^2)^{1/2}}$$

$$-P_{k_m}\int_0^\infty \frac{2[1-(-1)^m e^{iax}]\,dx}{(x^2-k_m^2)(x^2-k_q^2)(a_1^2-x^2)^{1/2}} \qquad (79b)$$

where P_{k_m} indicates the principal value of the integral with respect to $x = k_m$.

Substituting the contributions given by Equations (78) and (79a,b) into Equation (56a), we represent I as the sum of three integrals with respect to β. The integral limits for each of the component integrals are selected in accordance with the several arguments for I_1^{mq}. Thus

$$I = 2\int_0^{\sqrt{k^2-k_m^2}} \frac{1-(-1)^n\cos b\beta}{(\beta^2-k_n^2)(\beta^2-k_r^2)}\; I_1^{mq}\left(\beta:\beta<\sqrt{k^2-k_m^2}\right)\,d\beta$$

$$+2\int_{\sqrt{k^2-k_m^2}}^{k} \frac{1-(-1)^n\cos b\beta}{(\beta^2-k_n^2)(\beta^2-k_r^2)}\; I_1^{mq}\left(\beta:\beta>\sqrt{k^2-k_m^2}\right)\,d\beta$$

$$+ 2 \int_k^\infty \frac{1 - (-1)^n \cos b\beta}{(\beta^2 - k_n^2)(\beta^2 - k_r^2)} I_1^{mq} (\beta : \beta > k) \, d\beta$$

$$= 2 \int_0^{\sqrt{k^2 - k_m^2}} \frac{1 - (-1)^n \cos b\beta}{(\beta^2 - k_n^2)(\beta^2 - k_r^2)} \left[i \int_0^\infty \frac{2[1 - (-1)^m e^{-ay}] \, dy}{(y^2 + k_m^2)(y^2 + k_q^2)(a_1^2 + y^2)^{1/2}} \right.$$

$$\left. -P_{k_m} \int_0^{a_1} \frac{2[1 - (-1)^m e^{iax}] \, dx}{(x^2 - k_m^2)(x^2 - k_q^2)(a_1^2 - x^2)^{1/2}} \right] d\beta + 2 \int_{\sqrt{k^2 - k_m^2}}^k \frac{1 - (-1)^n \cos b\beta}{(\beta^2 - k_n^2)(\beta^2 - k_r^2)} \left[\frac{-\pi[1 - (-1)^m J_0(a_1)]}{(k_m^2 - a_1^2)(k_q^2 - a_1^2)} \right.$$

$$+ 2i \left\{ \int_0^\infty \frac{[1 - (-1)^m e^{-ay}] \, dy}{(y^2 + k_m^2)(y^2 + k_q^2)(a_1^2 + y^2)^{1/2}} + \frac{1}{(k_m^2 - a_1^2)(k_q^2 - a_1^2)} \sum_{i=0}^\infty \frac{(-1)^{i+m} (aa_1)^{2i+1}}{[(2i+1)!]^2} \right\} \right] d\beta$$

$$+ 2 \int_k^\infty \frac{1 - (-1)^n \cos b\beta}{(\beta^2 - k_n^2)(\beta^2 - k_r^2)} \left[2i \int_{a_1'}^\infty \frac{[1 - (-1)^m e^{-ay}] \, dy}{(y^2 + k_m^2)(y^2 + k_q^2)(y^2 - a_1'^2)^{1/2}} \right] d\beta \tag{79c}$$

where $a_1 = \sqrt{k^2 - \beta^2}$, $a_1' = \sqrt{\beta^2 - k^2}$

It is clear from Equations (53) and (55) that the real and imaginary quantities in the above equation respectively produce the radiation and reactive components, J_R^{mnqr} and J_x^{mnqr}, of $\bar{J}^{mnqr}$. Before determining these components from Equation (79c), we first establish two simple but significant results that will simplify the analysis.

(a) Let $k_n \neq k_r < k$. Then

$$I_1^{mq} (\beta : \beta < \sqrt{k^2 - k_m^2}) \approx I_1^{mq} (\beta : \beta > \sqrt{k^2 - k_m^2})$$

where $o < \beta < k$.

(b) Let $k_n = k_r < k$. Generally, $k_m^2 + k_n^2 < k^2$ or $k_n < \sqrt{k^2 - k_m^2}$. But, for $k_n = k_r$, the second integral of Equation (79c) requires that $\beta \to k_n > \sqrt{k^2 - k_m^2}$ which is contradicted by the general condition $k_n < \sqrt{k^2 - k_m^2}$. Hence the second integral cannot exist for $k_n = k_r$.

With these results, we now proceed to evaluate J_R^{mnqr} from the real parts of the integrals in Equation (79c). We observe that the real parts of $I_1^{mq} (\beta : \beta < \sqrt{k^2 - k_m^2})$,

I_1^{mq} $(\beta:\beta > \sqrt{k^2-k_m^2})$ are slowly varying functions of β which can be taken to be constant

in the neighborhood of the peaks of $I_{nr}(\beta) = \left. \dfrac{1 - (-1)^n \cos b\beta}{(\beta^2-k_n^2)(\beta^2-k_r^2)} \right|_{n \neq r}$. This will account

for the major contribution to J_R^{mnqr} for $n \neq r$. Also the function $I_{nr}(\beta)$ varies rapidly with β and, approximately, is equally positive and negative for the entire range of β. Hence, $R_e(I) = o$ for $k_n \neq k_r < k$ and from Equations (53) and (55)

$$J_R^{mnqr} \approx o \text{ for } n \neq r$$

Since the second integral in equation (79c) is not possible for $k_n = k_r$, then using the real part of the first integral,

$$\text{Re}(I) = 2 \int_0^{\sqrt{k^2-k_m^2}} \left(\frac{\pi b}{4k_n^2}\right) \text{Re}[I_1^{mq}(\beta:\beta < \sqrt{k^2-k_m^2})] \, \delta(\beta-k_n) \, d\beta$$

$$= \frac{-\pi b}{2k_n^2} \left(P_{k_m} \int_0^{\sqrt{k^2-k_n^2}} \frac{2[1 - (-1)^m \cos ax] \, dx}{(x^2-k_m^2)(x^2-k_q^2)(k^2-k_n^2-x^2)^{1/2}} \right)$$

where $\beta \to k_n < \sqrt{k^2-k_m^2}$.

Consider

$$P_{k_m} \int_0^{\sqrt{k^2-k_n^2}} \frac{2[1 - (-1)^m \cos ax] \, dx}{(x^2-k_m^2)(x^2-k_q^2)(k^2-k_n^2-x^2)^{1/2}} = \lim_{\rho \to 0} \int_0^{k_m-\rho} \frac{2[1 - (-1)^m \cos ax] \, dx}{(x^2-k_m^2)(x^2-k_q^2)(k^2-k_n^2-x^2)^{1/2}}$$

$$+ \lim_{\rho \to 0} \int_{k_m+\rho}^{\sqrt{k^2-k_n^2}} \frac{2[1 - (-1)^m \cos ax] \, dx}{(x^2-k_m^2)(x^2-k_q^2)(k^2-k_n^2-x^2)^{1/2}}$$

The first integral on the left-hand side evaluates approximately to

$$\lim_{\rho \to 0} \frac{2}{(k_m^2-k_q^2)(k^2-k_n^2-k_m^2)^{1/2}} \left[\int_0^{k_m-\rho} \frac{dx}{x^2-k_m^2} - (-1)^m \int_0^{k_m-\rho} \frac{\cos ax \, dx}{x^2-k_m^2} \right]$$

We obtain the principal value of the second term of the preceding equation near $x = k_m$

$$\lim_{\rho \to 0} (-1)^m \int_0^{k_m-\rho} \frac{\cos ax \, dx}{x^2-k_m^2} \approx (-1)^m \lim_{\rho \to 0} \cos(k_m-\rho)a \int_0^{k_m-\rho} \frac{dx}{x^2-k_m^2}$$

$$= (-1)^m \cos k_m a \lim_{\rho \to 0} \int_0^{k_m-\rho} \frac{dx}{x^2-k_m^2} = (-1)^{2m} \lim_{\rho \to 0} \int_0^{k_m-\rho} \frac{dx}{x^2-k_m^2}$$

$$= \lim_{\rho \to 0} \int_0^{k_m-\rho} \frac{dx}{x^2-k_m^2} = \int_0^{k_m} \frac{dx}{x^2-k_m^2}$$

Hence

$$\lim_{\rho \to 0} \int_0^{k_m-\rho} \frac{2[1 - (-1)^m \cos ax] \, dx}{(x^2-k_m^2)(x^2-k_q^2)(k^2-k_n^2-x^2)^{1/2}} \approx 0$$

and similarly

$$\lim_{\rho \to 0} \int_{k_m+\rho}^{\sqrt{k^2-k_n^2}} \frac{2[1 - (-1)^m \cos ax] \, dx}{(x^2-k_m^2)(x^2-k_q^2)(k^2-k_n^2-x^2)^{1/2}} \approx 0$$

Thus there is no contribution to the principal value of the integral from the pole at $x = k_m$.
Since $x = k_q$ lies outside the range of integration, it also produces no contribution.

There remain only the contributions from the square root singularity at $x = \sqrt{k^2-k_n^2}$. Thus, the original principal integral is rewritten as

$$\frac{2}{(k^2-k_q^2-k_n^2)} P_{k_m} \left\{ \int_0^{\sqrt{k^2-k_n^2}} \frac{dx}{(x^2-k_m^2)(k^2-k_n^2-x^2)^{1/2}} - (-1)^m \int_0^{\sqrt{k^2-k_n^2}} \frac{\cos ax \, dx}{(x^2-k_m^2)(k^2-k_n^2-x^2)^{1/2}} \right\}$$

We first show

$$P_{k_m} \int_0^{\sqrt{k^2-k_n^2}} \frac{dx}{(x^2-k_m^2)(k^2-k_n^2-x^2)^{1/2}} = 0$$

91

Now we treat the integral as improper at $x = k_m$ because this point lies within the region of integration* and we wish to exclude this point from that region. Since

$$\frac{1}{x^2 - k_m^2} = \frac{-1}{2k_m} \left(\frac{1}{x + k_m} - \frac{1}{x - k_m} \right)$$

we have

$$P_{k_m} \int_0^{a_1 = \sqrt{k^2 - k_n^2}} \frac{dx}{(x^2 - k_m^2)(a_1^2 - x^2)^{\frac{1}{2}}} = \frac{-1}{2k_m} \left[\int_0^{a_1} \frac{dx}{(x + k_m)(a_1^2 - x^2)^{\frac{1}{2}}} - \int_0^{a_1} \frac{dx}{(x - k_m)(a_1^2 - x^2)^{\frac{1}{2}}} \right]$$

The first integral need not be treated as improper since $x = -k_m$ lies outside the range of integration. Hence

$$= \frac{-1}{2k_m} \left[\int_0^{a_1} \frac{dx}{(x + k_m)(a_1^2 - x^2)^{\frac{1}{2}}} - \int_0^{k_m - \epsilon} \frac{dx}{(x - k_m)(a_1^2 - x^2)^{\frac{1}{2}}} - \int_{k_m + \epsilon}^{a_1} \frac{dx}{(x - k_m)(a_1^2 - x^2)^{\frac{1}{2}}} \right]$$

Now from Peirce[34]

$$\int \frac{dx}{v \sqrt{X}} = \frac{1}{\sqrt{k}} \ln \frac{2k + \beta v - 2b' \sqrt{kX}}{v}$$

where

$$X = a + bx + cx^2 \qquad v = a' + b'x \qquad q = 4ac - b^2 \qquad \beta = bb' - 2a'c$$

$$k = ab'^2 - abb' + ca'^2$$

For the first integral,

$$a = a^2 \qquad b = 0 \qquad c = -1$$

$$a' = k_m \qquad b' = 1 \qquad v = k_m + x$$

$$q = -4a^2 \qquad \beta = 2k_m \qquad k = a^2 - k_m^2$$

$$X = a^2 - x^2$$

---

*Since $x = k_m$ lies in the region of integration, the quantity $\frac{1}{x^2 - k_m^2}$ should not be placed outside the integral if a precise integration is desired.

For the second and third integrals,

$$a = a^2 \qquad b = 0 \qquad c = -1$$

$$a' = -k_m \qquad b' = 1 \qquad v = -k_m + x$$

$$q = -4a^2 \qquad \beta = -2k_m \qquad k = a^2 - k_m^2$$

$$X = a^2 - x^2$$

Hence the foregoing principal value is

$$\approx \frac{-1}{2k_m} \left(\frac{1}{\sqrt{a_1^2 - k_m^2}} \right) \left[\ln \frac{2(a_1^2 - k_m^2) + 2k_m(x + k_m) - 2\sqrt{(a_1^2 - k_m^2)(a_1^2 - x^2)}}{x + k_m} \Bigg|_0^{a_1} \right.$$

$$\left. - \ln \frac{2(a_1^2 - k_m^2) - 2k_m(x - k_m) - 2\sqrt{(a_1^2 - k_m^2)(a_1^2 - x^2)}}{x - k_m} \Bigg|_0^{k_m - \epsilon} \right.$$

$$\left. - \ln \frac{2(a_1^2 - k_m^2) - 2k_m(x - k_m) - 2\sqrt{(a_1^2 - k_m^2)(a_1^2 - x^2)}}{x - k_m} \Bigg|_{k_m + \epsilon}^{a_1} \right]$$

$$= \lim_{\epsilon \to 0} \left(\frac{-1}{2k_m} \right) \left(\frac{1}{\sqrt{a_1^2 - k_m^2}} \right) \left\{ \ln \frac{2a_1(a_1 + k_m)}{a_1 + k_m} - \ln \frac{2a_1^2 - 2a_1\sqrt{a_1^2 - k_m^2}}{k_m} \right.$$

$$\left. - \ln \frac{2(a_1^2 - k_m^2) + 2k_m\epsilon - 2\sqrt{(a_1^2 - k_m^2)[a_1^2 - (k_m - \epsilon)^2]}}{-\epsilon} \right.$$

$$\left. + \ln \frac{2a_1^2 - 2a_1\sqrt{a_1^2 - k_m^2}}{-k_m} - \ln \frac{2a_1(a_1 - k_m)}{a_1 - k_m} \right.$$

$$\left. + \ln \frac{2(a_1^2 - k_m^2) - 2k_m\epsilon - 2\sqrt{(a_1^2 - k_m^2)[a_1^2 - (k_m + \epsilon)^2]}}{\epsilon} \right\}$$

The first and fifth terms cancel, and the second and fourth combine to give $-\log(-1)$. The third and sixth terms are indeterminate as $\epsilon \to 0$, so

$$\simeq \lim_{\epsilon \to 0} \left(\frac{-1}{2k_m}\right)\left(\frac{1}{\sqrt{a_1^2-k_m^2}}\right)\left\{-\ln(-1)+\ln - \left[\frac{2(a_1^2-k_m^2)+2k_m\epsilon - 2\sqrt{(a_1^2-k_m^2)[a_1^2-(k_m-\epsilon)^2]}}{2(a_1^2-k_m^2)-2k_m\epsilon - 2\sqrt{(a_1^2-k_m^2)[a_1^2-(k_m+\epsilon)^2]}}\right]\right\}$$

We expand the square root in a series and obtain

$$\approx \lim_{\epsilon \to 0} \left(\frac{-1}{2k_m}\right)\left(\frac{1}{\sqrt{a_1^2-k_m^2}}\right) \; -\ln(-1)+\ln - \frac{2(a_1^2-k_m^2)+2k_m\epsilon-2a_1(a_1^2-k_m^2)\left[1-\frac{1}{2}\left(\frac{k_m-\epsilon}{a_1}\right)^2-\ldots\right]}{2(a_1^2-k_m^2)-2k_m\epsilon-2a_1(a_1^2-k_m^2)\left[1-\frac{1}{2}\left(\frac{k_m+\epsilon}{a_1}\right)^2-\ldots\right]}\bigg\}\bigg\}$$

$$\longrightarrow 0 \text{ as } \epsilon \to 0$$

Note that had we placed the term $\frac{1}{x^2-k_m^2}$ outside the integral, with x equal to the

square root singularity, then we would have obtained an integral $\displaystyle\int_0^{\sqrt{k^2-k_n^2}} \frac{dx}{(k^2-k_n^2-x^2)^{\frac{1}{2}}} = \frac{\pi}{2}$

instead of zero as obtained above for $\frac{1}{x^2-k_m^2}$ inside the integral. The $\frac{\pi}{2}$ result would

be an approximation similar to that obtained in the evaluation for k_m, $k_q > k$.
Now consider

$$P_{k_m}\left[-(-1)^m \int_0^{\sqrt{k^2-k_n^2}} \frac{2\cos ax \, dx}{(x^2-k_m^2)(x^2-k_q^2)(k^2-k_n^2-x^2)^{\frac{1}{2}}}\right]$$

Again k_q lies outside the range of integration and since, as previously shown, there is no

contribution from the pole at $x = k_m$ (also there is no indeterminancy from $\frac{\cos ax}{x^2-k_m^2}$ at

$x = k_m$) the above integral is written, as an approximation, with $\frac{1}{x^2-k_m^2}$ now appropriately

placed outside the integral where x equals the square root singularity. Thus, the integral
is written as

$$\frac{-2(-1)^m}{(k^2-k_m^2-k_n^2)(k^2-k_q^2-k_n^2)} \int_0^{\sqrt{k^2-k_n^2}} \frac{\cos ax \, dx}{(k^2-k_n^2-x^2)^{\frac{1}{2}}}$$

94

which evaluates to

$$\frac{-2\,(-1)^m}{(k^2-k_m^2-k_n^2)(k^2-k_q^2-k_n^2)} \; \frac{\pi}{2} \; J_0 \; (a \; \sqrt{k^2-k_n^2})$$

Hence

$$\text{Re (I)} = \frac{-\pi b}{2k_n^2} \left[\frac{-2\,(-1)^m}{(k^2-k_m^2-k_n^2)(k^2-k_q^2-k_n^2)} \; \frac{\pi}{2} \; J_0 \; (a \; \sqrt{k^2-k_n^2}) \right]$$

and from Equations (53) and (55)

$$J_R^{mnqn} = \frac{(-1)^m \, k_m k_q \, b}{2(k^2-k_m^2-k_n^2)(k^2-k_q^2-k_n^2)} \; J_0 \; (a \; \sqrt{k^2-k_n^2})$$

for $k_n = k_r$.

Therefore, in general for a Y-edge and an AF mode with k_m, k_n, k_r, $< k$; $k_q > k$

$$J_R^{mnqr} = \frac{(-1)^m \, k_m k_q \, b}{2(k^2-k_m^2-k_n^2)(k^2-k_q^2-k_n^2)} \; J_0 \; (a \; \sqrt{k^2-k_n^2}) \; \delta_{nr} \qquad (80)$$

We now evaluate the reactive component J_x^{mnqr}

For $k_n \neq k_r < k$ since $I_1^{mq} (\beta : \beta < \sqrt{k^2-k_m^2}) \approx I_1^{mq} (\beta : \beta > \sqrt{k^2-k_m^2})$, then the sum of the imaginary parts of the integrals in Equation (79c) is written

$$\mathcal{I}m(I) = \mathcal{I}m \; 2 \int_0^k \frac{1 - (-1)^n \cos b \, \beta}{(\beta^2-k_n^2)(\beta^2-k_r^2)} \; I_1^{mq} \; (\beta : \beta < k)$$

$$+ \mathcal{I}m \; 2 \int_k^\infty \frac{1 - (-1)^n \cos b \, \beta}{(\beta^2-k_n^2)(\beta^2-k_r^2)} \; I_1^{mq} \; (\beta : \beta > k)$$

$$\approx 0 \quad \text{for } n \neq r$$

Hence

$$J_x^{mnqr} \approx 0 \quad \text{for } n \neq r$$

95

Note that the first integral in the preceding equation is approximately zero for the reason previously discussed i.e., because $I_1^{mq}(\beta)$ is a slowly varying function of β and I_{nr} is approximately equally positive and negative over the range of β. The second integral is even smaller than the first because k_n, $k_r < k$ and $k < \beta < \infty$ for this integral.

Since, as previously shown, the second integral in Equation (79c) does not exist for $k_n = k_r$, then

$$\mathcal{I}m\,(I) = \mathcal{I}m\left\{ 2 \int_0^{\sqrt{k^2-k_m^2}} \frac{\pi b}{4k_n^2} \delta(\beta-k_n)\, I_1^{mq}\,(\beta:\beta < \sqrt{k^2-k_m^2})\, d\beta \right.$$

$$\left. + 2 \int_k^\infty \frac{\pi b}{4k_n^2} \delta(\beta-k_n)\, I_1^{mq}\,(\beta:\beta > k)\, d\beta \right\}$$

But the last integral is not possible since $k_n = k_r < \sqrt{k^2-k_m^2} < k$ and $\beta \to k_n < k$ which contradicts the requirement for the last integral that $\beta > k$. Hence we obtain from the first integral of Equation (79c)

$$\mathcal{I}m(I) = \frac{\pi b}{k_n^2} \int_0^{\sqrt{k^2-k_m^2}} \delta(\beta-k_n) \left\{ \int_0^\infty \frac{[1-(-1)^m e^{-ay}]\,dy}{(y^2+k_m^2)(y^2+k_q^2)(k^2-\beta^2+y^2)^{1/2}} + P_{k_m}\int_0^{\sqrt{k^2-\beta^2}} \frac{(-1)^m \sin ax\, dx}{(x^2-k_m^2)(x^2-k_q^2)(k^2\beta^2-x^2)^{1/2}} \right\} d\beta$$

$$= \frac{\pi b}{k_n^2} \left\{ \int_0^\infty \frac{[1-(-1)^m e^{-ay}]\,dy}{(y^2+k_m^2)(y^2+k_q^2)(y^2+k^2-k_n^2)^{1/2}} + P_{k_m}\int_0^{\sqrt{k^2-k_n^2}} \frac{(-1)^m \sin ax\, dx}{(x^2-k_m^2)(x^2-k_q^2)(k^2-k_n^2-x^2)^{1/2}} \right\}$$

$$= \frac{\pi b}{k_n^2} \left\{ \int_0^k \frac{dy}{(y^2+k_m^2)(y^2+k_q^2)(y^2+k^2-k_n^2)^{1/2}} + \int_k^\infty \frac{dy}{(y^2+k_m^2)(y^2+k_q^2)(y^2+k^2-k_n^2)^{1/2}} \right.$$

$$- \int_0^k \frac{(-1)^m e^{-ay}\,dy}{(y^2+k_m^2)(y^2+k_q^2)(y^2+k^2-k_n^2)^{1/2}} - \int_k^\infty \frac{(-1)^m e^{-ay}\,dy}{(y^2+k_m^2)(y^2+k_q^2)(y^2+k^2-k_n^2)^{1/2}}$$

$$\left. + P_{k_m}\int_0^{\sqrt{k^2-k_n^2}} \frac{(-1)^m \sin ax\, dx}{(x^2-k_m^2)(x^2-k_q^2)(k^2-k_n^2-x^2)^{1/2}} \right\}$$

We evaluate each integral of the preceding equation as follows:

(a) for $o < y < k$; $k_m < k < k_q$

$$\int_0^k \frac{dy}{(y^2+k_m^2)(y^2+k_q^2)(y^2+k^2-k_n^2)^{1/2}} \approx \frac{1}{k_q^2} \int_0^k \frac{dy}{(y^2+k_m^2)(k^2-k_n^2+y^2)^{1/2}}$$

$$\approx \frac{1}{k_q^2(k_m^2+k_n^2-k^2)} \int_0^k \frac{dy}{(k^2-k_n^2+y^2)^{1/2}}$$

$$= \frac{1}{k_q^2(k_m^2+k_n^2-k^2)} \ln\left(\frac{k+\sqrt{2k^2-k_n^2}}{\sqrt{k^2-k_n^2}}\right)$$

from Equation (67).

(b) for

$$\int_k^\infty \frac{dy}{(y^2+k_m^2)(y^2+k_q^2)(y^2+k^2-k_n^2)^{1/2}} \approx \int_k^\infty \frac{dy}{(y^2+k_m^2)(y^2+k_q^2)y}$$

$$\approx \frac{1}{k_q^2-k_m^2}\left[\frac{1}{2k_m^2} \ln (k_m^2+k^2) - \frac{1}{2k_q^2} \ln (k_q^2+k^2) - \frac{1}{k_m^2 k_q^2} \ln k\right]$$

from Equation (68)

(c) for $o < y < k$

$$\int_0^\infty \frac{e^{-ay}\,dy}{(y^2+k_m^2)(y^2+k_q^2)(y^2+k^2-k_n^2)^{1/2}} \approx \int_0^{\frac{1}{a}} \frac{(1-ay)\,dy}{(y^2+k_m^2)(y^2+k_q^2)(k^2-k_n^2+y^2)^{1/2}}$$

$$\approx \frac{1}{k_q^2} \int_0^{\frac{1}{a}} \frac{(1-ay)\,dy}{(y^2+k_m^2)(k^2-k_n^2+y^2)^{1/2}}$$

$$\approx \frac{1}{k_q^2(k_m^2+k_n^2-k^2)} \int_0^{\frac{1}{a}} \frac{(1-ay)\,dy}{(k^2-k_n^2+y^2)^{1/2}}$$

97

$$\approx \frac{1}{k_q^2(k_m^2+k_n^2-k^2)^{1/2}} \left\{ \ln \left(\frac{\frac{1}{a} + \sqrt{k^2-k_n^2+\left(\frac{1}{a}\right)^2}}{\sqrt{k^2-k_n^2}} \right) - a \left[\left(k^2-k_n^2+\left(\frac{1}{a}\right)^2\right)^{1/2} - \left(k^2-k_n^2\right)^{1/2} \right] \right\}$$

where we have followed Equation (69a) with $\int_0^k = \int_0^{\frac{1}{a}} + \int_{\frac{1}{a}}^k \approx \int_0^{\frac{1}{a}}$ since (as for the

derivation of Equation (69a)) $e^{-ay} = o$ for $y > \frac{1}{a}$. Also $\frac{1}{y^2+k_m^2} \longrightarrow \frac{1}{(k_m^2+k_n^2-k^2)}$ because

y is taken as the value at the square root singularity.

(d) for $k < y < \infty$

$$\int_k^\infty \frac{e^{-ay} \, dy}{(y^2+k_m^2)(y^2+k_q^2)(y^2+k^2-k_n^2)^{1/2}} \approx o$$

since the approximation $e^{-ay} = o$ for $y > k$; see derivation of Equation (69a).

(e) for $o < x < \sqrt{k^2-k_n^2} < k$; $k_m < k < k_q$

Referring to the last integral, we observe that

$$\lim_{x \to k_m} \frac{\sin ax}{x^2-k_m^2} = \frac{\sin k_m a}{x^2-k_m^2} = \frac{\sin m\pi}{x^2-k_m^2}$$

is indeterminate. Hence using the L'Hopital rule,

$$\lim_{x \to k_m} \frac{\frac{d}{dx}(\sin ax)}{\frac{d}{dx}(x^2-k_m^2)} = \lim_{x \to k_m} \frac{a \cos ax}{2x} = \frac{(-1)^m a}{2k_m} \ ,$$

a finite quantity.

Thus, $\frac{1}{x^2-k_m^2}$ can be taken outside the integral where x equals the value of the

square root singularity. Therefore,

$$P_{k_m} \int_0^{\sqrt{k^2-k_n^2}} \frac{(-1)^m \sin ax \, dx}{(x^2-k_m^2)(x^2-k_q^2)(k^2-k_n^2-x^2)^{1/2}} \approx \frac{(-1)^m}{(-k_q^2)(k^2-k_n^2-k_m^2)} P_{k_m} \int_0^{\sqrt{k^2-k_n^2}=a_1} \frac{\sin ax \, dx}{(k^2-k_n^2+x^2)^{1/2}}$$

$$\approx \frac{-(-1)^m}{k_q^2(k^2-k_n^2-k_m^2)} \sum_{i=0}^{\infty} \frac{(-1)^i (aa_1)^{2i+1}}{[(2i+1)!]^2}$$

using the approximation for the principal part of the integral $\int_0^{a_1} \frac{\sin ax \, dx}{(a_1^2-x^2)^{1/2}}$ given below

Equation (61) with $a_1^2 = k^2-k_n^2$.

Combining these results, we obtain

$$\mathcal{L}m(I) = \frac{\pi b}{k_n^2} \left\{ \frac{1}{k_q^2(k_m^2+k_n^2-k^2)} \left[\ln \left(\frac{k+\sqrt{2k^2-k_n^2}}{\sqrt{k^2-k_n^2}} \right) \right. \right.$$

$$- (-1)^m \left\{ \ln \left(\frac{\frac{1}{a}+\sqrt{k^2-k_n^2+\left(\frac{1}{a}\right)^2}}{\sqrt{k^2-k_n^2}} \right) - a \left[\left(k^2-k_n^2+\left(\frac{1}{a}\right)^2 \right)^{1/2} - (k^2-k_n^2)^{1/2} \right] \right\} \right]$$

$$+ \frac{1}{(k_q^2-k_m^2)} \left[\frac{1}{2k_m^2} \ln (k_m^2+k^2) - \frac{1}{2k_q^2} \ln (k_q^2+k^2) \right]$$

$$\left. - \frac{1}{k_m^2 k_q^2} \ln k - \frac{(-1)^m}{k_q^2(k^2-k_n^2-k_m^2)} \sum_{i=0}^{\infty} \frac{(-1)^i (a \sqrt{k^2-k_n^2})^{2i+1}}{[(2i+1)!]^2} \right\} \delta_{nr}$$

and from Equations (53) and (55),

$$J_x^{mnqr} = \frac{-k_m k_q b}{2\pi} \left\{ \frac{2}{k_q^2(k_m^2+k_n^2-k^2)} \left[\ln \left(\frac{k+\sqrt{2k^2-k_n^2}}{\sqrt{k^2-k_n^2}} \right) \right. \right.$$

$$- (-1)^m \left\{ \ln \left(\frac{\frac{1}{a}+\sqrt{k^2-k_n^2+\left(\frac{1}{a}\right)^2}}{\sqrt{k^2-k_n^2}} \right) - a \left[\left(k^2-k_n^2+\left(\frac{1}{a}\right)^2 \right)^{1/2} - (k^2-k_n^2)^{1/2} \right] \right\} \right]$$

99

$$+ \frac{2}{(k_q^2 - k_m^2)} \left[\frac{1}{2k_m^2} \ln(k_m^2 + k^2) - \frac{1}{2k_q^2} \ln(k_q^2 + k^2) \right]$$

$$\left. - \frac{2\ln k}{k_m^2 k_q^2} - \frac{2(-1)^m}{k_q^2 (k^2 - k_n^2 - k_m^2)} \sum_{i=0}^{\infty} \frac{(-1)^i (a \sqrt{k^2 - k_n^2})^{2i+1}}{[(2i+1)!]^2} \right\} \delta_{nr} \qquad (81)$$

Note if k_q, k_n, $k_r < k$; $k_m > k$ let $m \leftrightarrow q$

Some special cases for the previous results are now presented.

(1) For k_m^2, $k_n^2 = k_r^2 \ll k^2$, $k_q^2 \gg k^2$

$$J_R^{mnqn} \longrightarrow \frac{-(-1)^m k_m b}{2k^2 k_q} J_o(ka)$$

(2) For large ka, we have $J_o(ka) \approx \sqrt{\frac{2}{\pi ka}} \cos\left(ka - \frac{\pi}{4}\right)$ (see page 88 in Kinsler and Frey[35]) and therefore

$$J_R^{mnqn} \longrightarrow \frac{-(-1)^m b k_m}{\pi k^2 k_q} \left(\frac{\pi}{2ka}\right)^{1/2} \cos\left(ka - \frac{\pi}{4}\right)$$

(3) For k_m^2, k_n^2, $k_m^2 + k_n^2 \ll k^2 \ll k_q^2$; $\left(\frac{1}{a}\right)^2 \ll k^2$ and using the first term of the summation in Equation (81):

$$J_X^{mnqn} \longrightarrow \frac{-k_m k_q b}{2\pi} \left\{ \frac{2}{-k_q^2 k^2} [\ln(1 + \sqrt{2})] + \frac{2\ln k}{k_q^2 k_m^2} - \frac{2\ln k}{k_q^2 k_m^2} \right.$$

$$\left. - \frac{2(-1)^m}{k_q^2 k^2} (ka) \right\}$$

$$\longrightarrow \approx \frac{k_m b}{\pi k_q k^2} \ln 2.4 + \frac{(-1)^m (k_m b)(ka)}{\pi k_q k^2}$$

For an X-edge mode–AF mode, use Equations (80) and (81) with $m \leftrightarrow n$, $q \leftrightarrow r$, and $a \leftrightarrow b$.

100

IV   Y-Edge—Corner Modes

Figure 12f shows the modal classification scheme for the case k_m, $k_q > k$; $k_n < k$; $k_r > k$. The appropriate contours of integration are again Figures (10) and (11) (with simple poles at $a = \pm k_m$, $a = \pm k_q$) for $\beta < |k|$ and $\beta > |k|$, respectively. Hence, Equation (64) is applicable.

$$\overline{J}^{mnqr} = J_X^{mnqr} + i\, J_R^{mnqr}$$

$$= \frac{2iK_1}{\pi^2}\left[\int_0^k \frac{1-(-1)^n \cos b\beta}{(\beta^2-k_n^2)(\beta^2-k_r^2)}\, I_1^{mq}\,(\beta:\beta<k)d\beta + \int_k^\infty \frac{1-(-1)^n \cos b\beta}{(\beta^2-k_n^2)(\beta^2-k_r^2)}\, I_1^{mq}\,(\beta:\beta>k)d\beta\right.$$

where $I_1^{mq}\,(\beta:\beta<k)$ and $I_1^{mq}\,(\beta:\beta>k)$ are respectively given by Equations (62) and (63). Thus for $k_m \neq k_q > k$, the real term in Equation (62) gives

$$J_R^{mnqr} = \frac{-2k_m k_n k_q k_r}{\pi}\int_0^k \frac{1-(-1)^n \cos b\beta}{(\beta^2-k_n^2)(\beta^2-k_r^2)}\left[\frac{1-(-1)^m J_0\left(a\sqrt{k^2-\beta^2}\right)}{(k_m^2-k^2+\beta^2)(k_q^2-k^2+\beta^2)}\right]d\beta$$

For $k_r > k > k_n$ and k_m^2, $k_q^2 > k^2 > \beta^2$, let $\beta^2-k_r^2 \to -k_r^2$, $k_m^2-k^2+\beta^2 \to k_m^2$, $k_q^2-k^2+\beta^2 \to k_q^2$.
Then for $ka \gg \pi$ i.e., for high frequencies (neglecting the $J_0\,(a\sqrt{k^2-k_n^2})$ term),

$$J_R^{mnqr} \approx \frac{2k_n}{\pi k_r k_m k_q}\left[P\int_0^k \frac{d\beta}{\beta^2-k_n^2} + (-1)^n\, P\int_0^k \frac{\cos b\beta\, d\beta}{k_n^2-\beta^2}\right]$$

$$\approx \frac{2k_n}{\pi k_r k_m k_q}\left[\frac{1}{2k_n}\,\ln\,\frac{k-k_n}{k+k_n}\right]$$

$$\approx \frac{1}{\pi k_r k_m k_q}\,\ln\,\frac{k-k_n}{k+k_n} \tag{82}$$

neglecting $P\displaystyle\int_0^k \frac{\cos b\beta}{k_n^2-\beta^2}\,d\beta$.

If $k_n > k$; $k_r < k$, let $k_n \longleftrightarrow k_r$. Equation (82) also holds for $k_m = k_q$ since the second order pole at k_m makes no contribution to J_R^{mnmr}

Now for the reactive terms in Equations (62) and (63), it is convenient to write

$$J_x^{mnqr} = \frac{-2k_m k_n k_q k_r}{\pi} \left[\int_0^k \frac{[1 - (-1)^n \cos b\beta]}{(\beta^2 - k_n^2)(\beta^2 - k_r^2)} \mathscr{I}m \, [I_1^{mq}(\beta : \beta < k)] \, d\beta \right.$$

$$\left. + \int_k^\infty \frac{[1 - (-1)^n \cos b\beta]}{(\beta^2 - k_n^2)(\beta^2 - k_r^2)} \mathscr{I}m \, [I_1^{mq}(\beta : \beta > k)] d\beta \right] \approx o \text{ for } m \neq q$$

because $I_1^{mq}(\beta : \beta < k) \approx I_1^{mq}(\beta : \beta > k)$ are slowly varying functions of β. That is, these functions

vary slowly in the region of $\beta = k_n$ and $\beta = k_r$, $k_n \neq k_r$, where $\dfrac{1 - (-1)^n \cos b\beta}{(\beta^2 - k_n^2)(\beta^2 - k_r^2)}$ varies rapidly

and in (approximately) equal amounts in both the positive and negative directions. Hence the integrals equate approximately to zero.

However for m=q, we return to the general representation for $I_1^{mq}(\beta : \beta < k)$ given by Equation (57) rather than that given by Equation (62) which holds for simple poles only. We have previously shown in deriving Equation (70b) that the contribution to $I_1^{mq}(\beta : \beta < k)$ of the second order pole at $k_m = k_q$ is

$$\frac{\pi a}{2k_m^2 (k^2 - k_m^2 - \beta^2)^{1/2}}$$

Hence this term which is imaginary for $\beta < k$, $k_m > k$ is the sole contributor to J_x^{mnmr}

$$J_x^{mnmr} \approx \frac{-2k_m^2 k_n k_r}{\pi^2} \, P \int_0^k \frac{[1 - (-1)^n \cos b\beta]}{(\beta^2 - k_n^2)(\beta^2 - k_r^2)} \left[\frac{\pi a}{2k_m^2 (k_m^2 + \beta^2 - k^2)^{1/2}} \right] \, d\beta$$

Now for $k_r > k$, $\dfrac{1}{\beta^2 - k_r^2} \rightarrow \dfrac{-1}{k_r^2}$. Also $\beta < k$; $k_m > k$. Therefore

$$J_x^{mnmr} \approx \frac{k_n a}{\pi k_r k_m} \, P \int_0^k \frac{[1 - (-1)^n \cos b\beta]}{\beta^2 - k_n^2} \, d\beta$$

The integral has previously been evaluated in obtaining J_R^{mnqr} given by Equation (82). Therefore, using the results of the evaluation

$$J_x^{mnqr} = \frac{a}{2\pi k_r k_m} \, \ln \frac{k - k_n}{k + k_n} \, \delta_{mq} \tag{83}$$

10?

If $k_n > k$; $k_r < k$, let $k_n \longleftrightarrow k_r$.

Some special cases for the previous results are now presented.

(1) For $k_n^2 \ll k^2$, $\ln \dfrac{k - k_n}{k + k_n} = \ln \dfrac{1 - \dfrac{k_n}{k}}{1 + \dfrac{k_n}{k}} \doteq -\ln \dfrac{1 + \dfrac{k_n}{k}}{1 - \dfrac{k_n}{k}} \approx -2\dfrac{k_n}{k}$, using the first term of

the expansion $\ln \dfrac{1 + x}{1 - x} = 2 \displaystyle\sum_{i=1}^{\infty} \dfrac{x^{2i-1}}{2i-1}$ where $x^2 = \left(\dfrac{k_n}{k}\right)^2 \ll 1$. Hence

$$J_R^{mnqr} \longrightarrow \frac{-2k_n}{\pi k_r k_m k_q k}$$

which also obtains for $k_m = k_q$

(2) For $k_n^2 \ll k^2$, $\ln \dfrac{k - k_n}{k + k_n} \approx \dfrac{-2k_n}{k}$

$$J_x^{mnqr} \longrightarrow \frac{-k_n a}{\pi k_r k_m k} \, \delta_{mq}$$

For an X-edge mode-corner mode, k_n, $k_r > k$; $k_m < k$; $k_q > k$

$$J_R^{mnqr} = \frac{1}{\pi k_q k_n k_r} \, \ln \frac{k - k_m}{k + k_m} \tag{84}$$

$$J_x^{mnqr} = \frac{b}{2\pi k_q k_n} \, \ln \frac{k - k_m}{k + k_m} \, \delta_{nr} \tag{85}$$

If $k_m > k$; $k_q < k$, let $k_m \longleftrightarrow k_q$.

V   Two Acoustically Fast (AF) Modes

For the case of two AF modes, k_m, $k_n k_q$, $k_r < k$, we begin with the case $k_m = k_q < k$; $k_n = k_r < k$ for which the modal classification scheme is shown in Figure 12g. We can evaluate I for this case *directly* from the basic equation, given by Equation (56a), without resorting to contour integration. Thus for $k_m = k_q$, $k_n = k_r$

103

$$I = \int_{-\infty}^{\infty} \frac{[1 - (-1)^n \cos b\beta]}{(\beta^2 - k_n^2)^2} \left[\int_{-\infty}^{\infty} \frac{[1 - (-1)^m \cos a\alpha]\, d\alpha}{(\alpha^2 - k_m^2)^2 (k^2 - \alpha^2 - \beta^2)^{1/2}} \right] d\beta$$

$$\approx -4 \int_0^{\infty} I_{nn}(\beta) \left[\int_0^{\infty} \frac{I_{mm}(\alpha)\, d\alpha}{(k^2 - \alpha^2 - \beta^2)^{1/2}} \right] d\beta$$

$$\approx -4 \cdot \frac{\pi b}{4 k_n^2} \cdot \frac{\pi a}{4 k_m^2} \int_0^{\infty} \delta(\beta - k_n) \left[\int_0^{\infty} \delta(\alpha - k_m) \frac{d\alpha}{(k^2 - \alpha^2 - \beta^2)^{1/2}} \right] d\beta$$

$$\approx -\frac{\pi^2 A_p}{4 k_m^2 k_n^2} \int_0^{\infty} \delta(\beta - k_n) \frac{1}{(k^2 - k_m^2 - \beta^2)^{1/2}} \, d\beta$$

$$= \frac{-\pi^2 A_p}{4 k_m^2 k_n^2 (k^2 - k_m^2 - k_n^2)^{1/2}}$$

which is real since $k_m^2 + k_n^2 < k^2$. Note that the negative sign is chosen to precede $(k^2 - k_m^2 - k_n^2)^{1/2}$ for consistency with our sign convention.* In the derivation, $I_{nn}(\beta) = \frac{1 - (-1)^n \cos b\beta}{(\beta^2 - k_n^2)(\beta^2 - k_r^2)} \bigg|_{n=r}$

$$= \frac{1 - (-1)^n \cos b\beta}{(\beta^2 - k_n^2)^2} \bigg|_{n=r} \approx \frac{\pi b}{4 k_n^2} \, \delta(\beta - k_n) \text{ and similarly for } I_{mm}(\alpha)$$

Thus, from Equations (53) and (55)

$$J_R^{mnmn} = \frac{-A_p}{4(k^2 - k_m^2 - k_n^2)^{1/2}} \tag{86a}$$

We now consider two cases

Case 1 $\beta > |k|$: Figure 12h shows the modal classification scheme for the case $k_m \neq k_q < k$; $k_n = k_r < k$; $k_m^2 + k_n^2 < k^2$. The appropriate contour is for $\beta > |k|$ shown in Figure 17. The simple poles at $\pm k_m$ and $\pm k_q$ lie inside of k. Again we replace the real integral, Equation (57), by the contour integral. Integration in the α-plane over the contour yields Equation (63) as before. In other words, Equation (63) is applicable for $\beta > |k|$ because the

---

*For the half-plane, wherein $z < 0$, we precede $\zeta = (k^2 - \alpha^2 - \beta^2)^{1/2}$ with a minus sign.

second term in Equation (61) in unchanged for $k_m < k$. Thus Case 1 remains identical to the previous Case 1 for k_m, $k_q > k$ and $k_m < k$; $k_q > k$ given by Equations (63) and (78), respectively.

$$I_1^{mq}(\beta : \beta > k) = 2i \int_{a_1'}^{\infty} \frac{[1 - (-1)^m e^{-ay}] \, dy}{(y^2 + k_m^2)(y^2 + k_q^2)(y^2 - a_1'^2)^{1/2}} \qquad (86b)$$

Case 2 — $-k < \beta < k$: For $\beta < |k|$, we treat three regions for β corresponding to three different regions for a:

(1) Suppose $o < a_1 = \sqrt{k^2 - \beta^2} < k_m$; see Figure 18.

Then $\sqrt{k^2 - k_m^2} < \beta < k$

Obviously, integration in the a-plane over the contours given by Figure (18) and Figure (10) yield the same results. Hence

$$\left. I_1^{mq}(\beta : \beta > \sqrt{k^2 - k_m^2}) \right|_{\substack{k_m < k \\ k_q < k}} = \left. I_1^{mq}(\beta : \beta < k) \right|_{\substack{k_m > k \\ k_q > k}} = \text{r.h.s. of equation (62)} \qquad (86c)$$

(2) Suppose $k_m < a_1 = \sqrt{k^2 - \beta^2} < k_q$; see Figure 19.

Then $\sqrt{k^2 - k_q^2} < \beta < \sqrt{k^2 - k_m^2}$. Obviously, integration in the a-plane over the contours given by Figures 19 and 15 (with $k_q < k$) yield the same results, namely, those given by Equation (79b). Thus

$$I_1^{mq}(\beta : \sqrt{k^2 - k_q^2} < \beta < \sqrt{k^2 - k_m^2}) = +i \int_0^{\infty} \frac{2[1 - (-1)^m e^{-ay}] \, dy}{(y^2 + k_m^2)(y^2 + k_q^2)(y^2 + a_1^2)^{1/2}} - P_{k_m} \int_0^{a_1} \frac{2[1 - (-1)^m e^{iax}] \, dx}{(x^2 - k_m^2)(x^2 - k_q^2)(a_1^2 - x^2)^{1/2}}$$

$$(86d)$$

where $k_q < k$

(3) Suppose $k_q < a_1 = \sqrt{k^2 - \beta^2} < k$; see Figure 20.

Then $o < \beta < \sqrt{k^2 - k_q^2}$. Obviously, integration in the a-plane over the contours given by by Figures 20 and 15 (with $k_q < k$) yields the same results, namely, those given by Equation (79b) with the change $P_{k_m} \longrightarrow P_{k_m k_q}$ indicating the principal values with respect to both $x = k_m$ and $x = k_q$. Thus

$$I_1^{mq}(\beta:\beta< \sqrt{k^2-k_q^2}) = +i \int_0^\infty \frac{2[1-(-1)^m e^{-ay}]\,dy}{(y^2+k_m^2)(y^2+k_q^2)(y^2+a_1^2)^{\frac{1}{2}}} - P_{k_m k_q} \int_0^{a_1} \frac{2[1-(-1)^m e^{iax}]\,dx}{(x^2-k_m^2)(x^2-k_q^2)(a_1^2-x^2)^{\frac{1}{2}}}$$

$$(86e)$$

where $k_q < k$.

Substituting the contributions given by Equations (86b-e) into Equation (56a), we represent I as the sum of four integrals with respect to β. The integral limits for each of the component integrals are selected in accordance with the several arguments for I_1^{mq}. Thus

$$I = 2 \int_0^{\sqrt{k^2-k_q^2}} \frac{1-(-1)^n \cos b\beta}{(\beta^2-k_n^2)(\beta^2-k_r^2)} I_1^{mq}(\beta:\beta< \sqrt{k^2-k_q^2})$$

$$+ 2 \int_{\sqrt{k^2-k_q^2}}^{\sqrt{k^2-k_m^2}} \frac{1-(-1)^n \cos b\beta}{(\beta^2-k_n^2)(\beta^2-k_r^2)} I_1^{mq}(\beta: \sqrt{k^2-k_q^2} < \beta < \sqrt{k^2-k_m^2})$$

$$+ 2 \int_{\sqrt{k^2-k_m^2}}^{k} \frac{1-(-1)^n \cos b\beta}{(\beta^2-k_n^2)(\beta^2-k_r^2)} I_1^{mq}(\beta: \sqrt{k^2-k_m^2} < \beta < k)$$

$$+ 2 \int_k^\infty \frac{1-(-1)^n \cos b\beta}{(\beta^2-k_n^2)(\beta^2-k_r^2)} I_1^{mq}(\beta:\beta > k)$$

$$= 2 \int_0^{\sqrt{k^2-k_q^2}} \frac{1-(-1)^n \cos b\beta}{(\beta^2-k_n^2)(\beta^2-k_r^2)} \left[+i \int_0^\infty \frac{2[1-(-1)^m e^{-ay}]\,dy}{(y^2+k_m^2)(y^2+k_q^2)(a_1^2+y^2)^{\frac{1}{2}}} \right.$$

$$\left. - P_{k_m k_q} \int_0^{a_1} \frac{2[1-(-1)^m e^{iax}]\,dx}{(x^2-k_m^2)(x^2-k_q^2)(a_1^2-x^2)^{\frac{1}{2}}} \right] d\beta$$

$$+ 2 \int_{\sqrt{k^2-k_q^2}}^{\sqrt{k^2-k_m^2}} \frac{1-(-1)^n \cos b\beta}{(\beta^2-k_n^2)(\beta^2-k_r^2)} \left[+i \int_0^\infty \frac{2[1-(-1)^m e^{-ay}]\,dy}{(y^2+k_m^2)(y^2+k_q^2)(a_1^2+y^2)^{\frac{1}{2}}} \right.$$

$$
-P_{k_m} \int_0^{a_1} \frac{2\left[1-(-1)^m e^{iax}\right]dx}{(x^2-k_m^2)(x^2-k_q^2)(a_1^2-x^2)^{\frac{1}{2}}}\Bigg] d\beta
$$

$$
+2 \int_{\sqrt{k^2-k_m^2}}^{k} \frac{1-(-1)^n \cos b\beta}{(\beta^2-k_n^2)(\beta^2-k_r^2)} \left[\frac{-\pi\left[1-(-1)^m J_0(aa_1)\right]}{(k_m^2-a_1^2)(k_q^2-a_1^2)}\right.
$$

$$
+2i\left\{ \int_0^{\infty} \frac{\left[1-(-1)^m e^{-ay}\right]dy}{(y^2+k_m^2)(y^2+k_q^2)(a_1^2+y^2)^{\frac{1}{2}}} + \left[\frac{1}{(k_m^2-a_1^2)(k_q^2-a_1^2)} \sum_{i=0}^{\infty} \frac{(-1)^{i+m}(aa_1)^{2i+1}}{[(2i+1)!]^2}\right]\right\}\Bigg] d\beta
$$

$$
+2 \int_k^{\infty} \frac{1-(-1)^n \cos b\beta}{(\beta^2-k_n^2)(\beta^2-k_r^2)} \left[+2i \int_{a_1'}^{\infty} \frac{\left[1-(-1)^m e^{-ay}\right]dy}{(y^2+k_m^2)(y^2+k_q^2)(y^2-a_1'^2)^{\frac{1}{2}}}\right] d\beta \qquad (86f)
$$

It is clear from Equations (53) and (55) that the real and imaginary quantities in Equation (86f) respectively produce the radiation and reactive components J_R^{mnqr} and J_X^{mnqr}, of $\bar{J}^{mnqr}$. Before determining these components, we first extend some results found earlier and used in evaluating Equation (79c) for application to the present problem. Thus:

For $k_n \neq k_r < k$, I is negligibly small.

For $k_n \neq k_r < k$, the second, third and fourth integrals, (which respectively stipulate that $\beta > \sqrt{k^2-k_q^2}$, $\beta > \sqrt{k^2-k_m^2}$, and $\beta > k$) cannot exist because they contradict the general requirement that $k_q^2+k_r^2 < k^2$ and therefore that $\beta \rightarrow k_n = k_r < \sqrt{k^2-k_q^2} < k$, and the general requirement that $k_m^2+k_n^2 < k^2$ and therefore that $\beta \rightarrow k_n = k_r < \sqrt{k^2-k_m^2} < k$.

With these results, we now proceed to evaluate J_R^{mnqr}. Since I is negligibly small for $k_n \neq k_r < k$, $J_R^{mnqr} = 0$.

For $k_n = k_r < k$ with $0 < \beta < \sqrt{k^2 - k_q^2}$, the last three integrals of Equation (86f) vanish and

$$I = 2 \int_0^{\sqrt{k^2-k_q^2}} \left(\frac{\pi b}{4k_n^2}\right) \ I_1^{mq}(\beta:\beta< \sqrt{k^2-k_q^2})\delta(\beta-k_n)d\beta$$

$$= \frac{\pi b}{2k_n^2} \ I_1^{mq}(k_n:k_n< \sqrt{k^2-k_q^2})$$

$$= \frac{\pi b}{2k_n^2} \left[+i \int_0^\infty \frac{2[1 - (-1)^m e^{-ay}] \ dy}{(y^2+k_m^2)(y^2+k_q^2)(y^2+k^2-k_n^2)^{1/2}} - P_{k_m k_q} \int_0^{\sqrt{k^2-k_n^2}} \frac{2[1 - (-1)^m e^{iax}] \ dx}{(x^2-k_m^2)(x^2-k_q^2)(a_1^2-x^2)^{1/2}} \right]$$

Consider

$$\mathrm{Re}(I) = 2 \int_0^{\sqrt{k^2-k_q^2}} \left(\frac{\pi b}{4k_n^2}\right) \mathrm{Re}\,[I_1^{mq}(\beta:\beta< \sqrt{k^2-k_m^2})] \ \delta(\beta-k_n)d\beta$$

$$= \mathrm{Re}\left[\frac{-\pi b}{2k_n^2} \left(P_{k_m k_q} \int_0^{\sqrt{k^2-k_n^2}} \frac{2[1 - (-1)^m e^{iax}] \ dx}{(x^2-k_m^2)(x^2-k_q^2)(k^2-k_n^2-x^2)^{1/2}} \right) \right]$$

where $\beta \to k_n < \sqrt{k^2-k_q^2}$. Hence

$$\mathrm{Re}(I) = \frac{-\pi b}{k_n^2} \ P_{k_m k_q} \left[\int_0^{a_1 = \sqrt{k^2-k_n^2}} \frac{dx}{(x^2-k_m^2)(x^2-k_q^2)(a_1^2-x^2)^{1/2}} - (-1)^m \int_0^{a_1 = \sqrt{k^2-k_n^2}} \frac{\cos ax \ dx}{(x^2-k_m^2)(x^2-k_q^2)(a_1^2-x^2)^{1/2}} \right]$$

$$= \frac{-\pi b}{k_n^2} \left\{ \frac{1}{2k_m} \left[\int_0^{a_1} \frac{dx}{(x+k_m)(a_1^2-x^2)^{1/2}} - \int_0^{a_1} \frac{dx}{(x-k_m)(a_1^2-x^2)^{1/2}} \right] - \frac{1}{2k_q} \left[\int_0^{a_1} \frac{dx}{(x+k_q)(a_1^2-x^2)^{1/2}} \right. \right.$$

$$\left. - \int_0^{a_1} \frac{dx}{(x-k_q)(a_1^2-x^2)^{1/2}} \right] - (-1)^m P_{k_m k_q} \int_0^{a_1} \frac{\cos ax \ dx}{(x^2-k_m^2)(x^2-k_q^2)(a_1^2-x^2)^{1/2}}$$

108

where, using a partial fraction expansion,

$$\frac{1}{(x^2-k_m^2)(x^2-k_q^2)} = \frac{1}{k_q^2-k_m^2}\left[\frac{1}{2k_m}\left(\frac{1}{x+k_m}-\frac{1}{x-k_m}\right)-\frac{1}{2k_q}\left(\frac{1}{x+k_q}-\frac{1}{x-k_q}\right)\right]$$

the first principal integral has been written as the sum of four integrals. Following the derivation for Equation (80), it is clear that each of the brackets for the last integral equation has a value of zero; again using partial fractions and considering the value of the integral only at the square root singularity, therefore

$$\mathrm{Re}(I) = \frac{(-1)^m \pi b}{k_n^2}\, P_{k_m k_q}\int_0^{a_1}\frac{\cos ax\, dx}{(x^2-k_m^2)(x^2-k_q^2)(k^2-k_n^2-x^2)^{1/2}}$$

$$= \frac{(-1)^m \pi b}{k_n^2\,(k_m^2-k_q^2)}\left[\int_0^{a_1}\frac{\cos ax\, dx}{(x^2-k_m^2)(k^2-k_n^2-x^2)^{1/2}} - \int_0^{a_1}\frac{\cos ax\, dx}{(x^2-k_q^2)(k^2-k_n^2-x^2)^{1/2}}\right]$$

$$\approx \frac{(-1)^m \pi b}{k_n^2\,(k_m^2-k_q^2)}\left[\frac{1}{(k^2-k_m^2-k_n^2)}\int_0^{a_1}\frac{\cos ax\, dx}{(k^2-k_n^2-x^2)^{1/2}} - \frac{1}{(k^2-k_q^2-k_n^2)}\int_0^{a_1}\frac{\cos ax\, dx}{(k^2-k_n^2-x^2)^{1/2}}\right]$$

$$\approx \frac{(-1)^m \pi b}{k_n^2\,(k_m^2-k_q^2)}\left[\frac{k_m^2-k_q^2}{(k^2-k_m^2-k_n^2)(k^2-k_q^2-k_n^2)}\right]\frac{\pi}{2}\, J_0\left(a\sqrt{k^2-k_n^2}\right)$$

$$\approx \frac{(-1)^m \pi^2 b}{2k_n^2\,(k^2-k_m^2-k_n^2)(k^2-k_q^2-k_n^2)}\, J_0\left(a\sqrt{k^2-k_n^2}\right)$$

and from Equations (53) and (55)

$$J_R^{mnqn} = \frac{(-1)^m\, k_m k_q\, b}{2(k^2-k_m^2-k_n^2)(k^2-k_q^2-k_n^2)}\, J_0\left(a\sqrt{k^2-k_n^2}\right)$$

for $k_n = k_r$.

Therefore in general for two AF modes with $k_q \geq k_m$; $k_r \geq k_n$ and k_m, k_n, k_q, $k_r < k$

$$J_R^{mnqr} = A\delta_{nr} + B\delta_{mq} + C\delta_{mq}\delta_{nr} \tag{86g}$$

where

$$A = \frac{(-1)^m \, k_m k_q \, b}{2(k^2-k_m^2-k_n^2)(k^2-k_q^2-k_n^2)} \, J_0 \, (a \, \sqrt{k^2-k_n^2}) \qquad (87)$$

$$B = \frac{(-1)^n \, k_n k_r \, a}{2(k^2-k_m^2-k_n^2)(k^2-k_m^2-k_r^2)} \, J_0 \, (b \, \sqrt{k^2-k_m^2}) \qquad (88)$$

$$C = \frac{-A_p}{4(k^2-k_m^2-k_n^2)^{1/2}} \qquad (89)$$

We now evaluate the reactive component J_x^{mnqr}.

For $k_n \neq k_r < k$, since I is negligibly small, $J_x^{mnqr} = o$.

For $k_n = k_r < k$; $k_m = k_q < k$, I is real (see derivation leading to Equation (86a)) and therefore $J_x^{mnmn} = o$.

For $k_n = k_r < k$; $k_m \neq k_q < k$, since the last three integrals for β in Equation (86f) cannot exist, then for $o < \beta < \sqrt{k^2-k_q^2}$

$$\mathrm{Im}(I) = \mathrm{Im} \, 2 \int_o^k \left(\frac{\pi b}{4k_n^2}\right) I_1^{mq} \, (\beta : \beta < \sqrt{k^2-k_q^2}) \delta \, (\beta-k_n) d\beta$$

$$= \frac{\pi b}{2k_n^2} \int_o^{\sqrt{k^2-k_q^2}} \delta \, (\beta-k_n) \left[\int_o^\infty \frac{2[1 - (-1)^m \, e^{-ay}] \, dy}{(y^2+k_m^2)(y^2+k_q^2)(a_1^2+y^2)^{1/2}} + (-1)^m P_{k_m k_q} \int_o^{a_1} \frac{\sin \, ax \, dx}{(x^2-k_m^2)(x^2-k_q^2)(a_1^2-x^2)^{1/2}} \right] d\beta$$

The integrals within the bracket are similar to those integrals within the first bracket of Equation (79c): The only changes in Equation (79c) are $P_{k_m} \longrightarrow P_{k_m k_q}$ here and $k_q > k \longrightarrow k_q < k$ here. Hence the steps in evaluating Im(I) here are analogous to those used in obtaining Im(I) immediately preceding, and leading to, Equation (81) except that whereas previously the term $\frac{1}{y^2+k_q^2} \longrightarrow \frac{1}{k_q^2}$ was placed outside certain integrals, the corresponding term $\frac{1}{y^2+k_q^2} \longrightarrow \frac{1}{k_q^2+k_n^2-k^2}$ is now placed outside the integral because here y is evaluated

110

at the square root singularity of the term $\dfrac{1}{(k^2-k_n^2+y^2)^{1/2}}$. Hence we obtain the final

expression for J_x^{mnqn} directly from Equation (81), with appropriate modification (just cited), as

$$J_x^{mnqr} = \frac{-k_m k_q \, b}{2\pi} \left\{ \frac{2}{(k_q^2+k_n^2-k^2)(k_m^2+k_n^2-k^2)} \left[\ln\left(\frac{k+\sqrt{2k^2-k_n^2}}{\sqrt{k^2-k_n^2}}\right) -(-1)^m \left\{ \ln\left(\frac{\frac{1}{a}+\sqrt{k^2-k_n^2+\left(\frac{1}{a}\right)^2}}{\sqrt{k^2-k_n^2}}\right) \right. \right. \right.$$

$$\left. \left. \left. -a\left[\left(k^2-k_n^2+\left(\frac{1}{a}\right)^2\right)^{1/2}-(k^2-k_n^2)^{1/2}\right]\right\}\right] + \frac{2}{(k_q^2-k_m^2)}\left[\frac{1}{2k_m^2}\ln(k_m^2+k^2)-\frac{1}{2k_q^2}\ln(k_q^2+k^2)\right] \right.$$

$$\left. -\frac{2\ln k}{k_m^2 k_q^2} - \frac{2(-1)^m}{(k^2-k_n^2-k_q^2)(k^2-k_n^2-k_m^2)} \sum_{i=0}^{\infty} \frac{(-1)^i (a\sqrt{k^2-k_n^2})^{2i+1}}{[(2i+1)!]^2} \right\} \delta_{nr} \qquad (90)$$

For $k_q < k_m$ then $m \longleftrightarrow q$ and for $k_r < k_n$ then $n \longleftrightarrow r$.

Some special cases for the previous results are now presented

(1) For $k_m^2,\ k_n^2,\ k_q^2,\ k_r^2 \ll k^2$; $k_m^2 \neq k_q^2$ and for large ka

$$J_R^{mnqn} \longrightarrow \frac{(-1)^m k_m k_q \, b}{2k^4} \left(\frac{2}{\pi ka}\right)^{1/2} \cos\left(ka - \frac{\pi}{4}\right) \delta_{nr}$$

$$= \frac{(-1)^m k_m k_q \, b}{\pi k^4} \left(\frac{\pi}{2ka}\right)^{1/2} \cos\left(ka - \frac{\pi}{4}\right) \delta_{nr}$$

(2) For $k_m^2,\ k_n^2,\ k_m^2+k_n^2 \ll k^2$; $k_q^2,\ k_r^2,\ k_q^2+k_r^2 \ll k^2$; $\left(\dfrac{1}{a}\right)^2 \ll k^2$ and using the first term of the summation in equation (90)

$$J_x^{mnqn} \longrightarrow \frac{-k_m k_q \, b}{2\pi} \left\{ \frac{2}{k^4} [\ln(1+\sqrt{2}] + \frac{2(-1)^m (ak)}{k^4} \right\} \approx 0$$

VI   Two Edge Modes

For two edge modes, $k_m,\ k_n,\ k_q,\ k_r < k$; $k_{mn}^2,\ k_{qr}^2 > k^2$, we begin with the case $k_m = k_q < k$; $k_n = k_r < k$; $k_{mn}^2,\ k_{qr}^2 > k^2$ for which the modal classification scheme is shown

in Figure 12i. For this case, we can evaluate I *directly* from the basic equation given by Equation (56a) without resorting to contour integration. The equations used in evaluating I are therefore identical to those used for two AF modes (leading to Equation (86)) which has the final result (note that we use the negative imaginary part; see Equation (58))

$$I = \frac{\pi^2 A_p}{4 k_m^2 k_n^2 (k^2 - k_m^2 - k_n^2)^{1/2}} = \frac{i\pi^2 A_p}{4 k_m^2 k_n^2 (k_m^2 + k_n^2 - k^2)^{1/2}} \tag{91a}$$

Equation (91) is reactive (imaginary) because $k_m^2 + k_n^2 > k^2$

Hence, for this case $J_R^{mnmn} = 0$.

Next, consider the case $k_m \neq k_q < k$; $k_n = k_r < k$; k_{mn}^2, $k_{qr}^2 > k^2$ for which the modal classification scheme is shown in Figure 12j. In analogy with Equation (86f) for two AF modes,

where
$$\int_0^{\sqrt{k^2-k_q^2}} + \int_{\sqrt{k^2-k_q^2}}^{\sqrt{k^2-k_q^2}} + \int_{\sqrt{k^2-k_m^2}}^{k} + \int_k^{\infty} \longrightarrow \int_0^k + \int_k^{\infty}$$

here,* we have

$$I = 2 \int_0^k \frac{[1 - (-1)^n \cos b\beta]}{(\beta^2 - k_n^2)^2} I_1^{mq}(\beta:\beta < k)d\beta + 2 \int_0^k \frac{[1 - (-1)^n \cos b\beta]}{(\beta^2 - k_n^2)^2} I_1^{mq}(\beta:\beta > k)d\beta$$

By Equation (65), the second integral cannot exist for $k_n = k_r$ since $\beta \rightarrow k_n < k$. Hence

$$I = 2 \int_0^k \frac{[1 - (-1)^n \cos b\beta]}{(\beta^2 - k_n^2)^2} I_1^{mq}(\beta:\beta < k)d\beta = \frac{\pi b}{2k_n^2} I_1^{mq}(k_n:k_n < k)$$

$$= \frac{\pi b}{2k_n^2} \left\{ +i \int_0^{\infty} \frac{2[1 - (-1)^m e^{-ay}] \, dy}{(y^2 + k_m^2)(y^2 + k_q^2)(y^2 + k^2 - k_n^2)^{1/2}} - \int_0^{a_1 = \sqrt{k^2-k_n^2}} \frac{2[1 - (-1)^m e^{iax}] \, dx}{(x^2 - k_m^2)(x^2 - k_q^2)(k_n^2 - x^2)^{1/2}} \right. \tag{91b}$$

---

*Note that $k_m^2 + k_n^2 > k^2$ and $k_q^2 + k_r^2 > k^2$ or $k_n = k_r > \sqrt{k^2 - k_m^2}$ and $k_r = k_n > \sqrt{k^2 - k_q^2}$ Hence I_1^{mq} (β: $\sqrt{k^2 - k_q^2} < \beta < \sqrt{k^2 - k_m^2} < k$) can now exist so that we can appropriately represent the sum of the first three integrals as a single integral.

where again integration in the a-plane over the contour yields, as before, Equation (61) for $I_1^{mq}(\beta:\beta<k)$ where $\beta \rightarrow k_n$. Note that $P_{k_m k_q}$ has been dropped in the last integral because $k_q^2+k_n^2>k^2$ and $k_m^2+k_n^2>k^2$, so that $k_q > \sqrt{k^2-k_n^2} > x$; $k_m> \sqrt{k^2-k_n^2} >x$; i.e. k_m, k_q lie outside the range of integration and therefore $x^2-k_m^2 \sim -k_m^2$, $x^2-k_q^2 \sim -k_q^2$ Hence

$$\text{Re}(I) = \frac{\pi b}{2k_n^2} \int_0^{\sqrt{k^2-k_n^2}} \frac{2[1 - (-1)^m \cos ax]\, dx}{(x^2-k_m^2)(x^2-k_q^2)(k^2-k_n^2-x^2)^{1/2}} = \frac{\pi b}{k_n^2 k_m^2 k_q^2} \int_0^{\sqrt{k^2-k_n^2}} \frac{[1 - (-1)^m \cos ax]\, dx}{(k^2-k_n^2-x^2)^{1/2}}$$

$$= \frac{-\pi b}{k_n^2 k_m^2 k_q^2} \left(\frac{\pi}{2} [1 - (-1)^m J_0 (a \sqrt{k^2-k_n^2})] \right)$$

where the foregoing integral has been previously evaluated in connection with the first integral of Equation (61). Hence from Equations (53) and (55),

$$J_R^{mnqn} = \frac{-b}{2k_m k_q} [1 - (-1)^m J_0 (a \sqrt{k^2-k_n^2})] \tag{91c}$$

For the case $k_m \neq k_n \neq k_q \neq k_r<k$; k_{mn}^2, $k_{qr}^2>k^2$ with modal classification scheme represented by Figure (12k), $I = 2 \int_0^k \frac{[1 - (-1)^n \cos b\beta]}{(\beta^2-k_n^2)(\beta^2-k_r^2)} \Bigg|_{n \neq r} I_1^{mq}(\beta:\beta<k)d\beta$ is negligibly small so that

$$J_R^{mnqr} \approx 0 \quad \text{for } n \neq r, \ m \neq q$$

In general, therefore,

$$J_R^{mnqr} = A\delta_{nr} + B\delta_{mq} - (A+B)\delta_{nr}\delta_{mq} \tag{91d}$$

where

$$A = \frac{-b}{2k_m k_q} [1 - (-1)^m J_0 (a \sqrt{k^2-k_n^2})] \tag{92}$$

$$B = \frac{-a}{2k_n k_r} \left[1 - (-1)^n \, J_o \, (b \, \sqrt{k^2 - k_m^2}) \right] \tag{93}$$

We now evaluate the reactive component J_x^{mnqr}. Consider the contribution from Equation (91b) for $k_m \neq k_q < k$; $k_n = k_r < k$; k_{mn}^2, $k_{qr}^2 > k^2$:

$$I_m(I) = \frac{\pi b}{k_n^2} \left[\int_0^\infty \frac{[1 - (-1)^m \, e^{-ay}] \, dy}{(y^2 + k_m^2)(y^2 + k_q^2)(y^2 + k^2 - k_n^2)^{1/2}} + (-1)^m \int_0^{\sqrt{k^2 - k_n^2}} \frac{\sin ax \, dx}{(x^2 - k_m^2)(x^2 - k_q^2)(k^2 - k_n^2 - x^2)^{1/2}} \right]$$

The evaluation of the integrals yields a result for J_x^{mnqr} identical to that of Equation (90) except that (1) the coefficient of the first term within the braces of Equation (90),

$$\frac{2}{(k_q^2 + k_n^2 - k^2)(k_m^2 + k_n^2 - k^2)} \longrightarrow \frac{2}{k_q^2 k_m^2} \quad \text{here because now } k_q^2 > k^2 - k_n^2; \ k_m^2 > k^2 - k_n^2 \quad \text{and (2) the}$$

coefficient of the last term within the quotes $\dfrac{-2(-1)^m}{(k^2 - k_n^2 - k_q^2)(k^2 - k_n^2 - k_m^2)} \longrightarrow \dfrac{-2(-1)^m}{k_q^2 k_m^2}$ here

because $x^2 - k_m^2 \sim -k_m^2$; $x^2 - k_q^2 \sim -k_q^2$. Hence, *with inclusion of Equation (91a)*, the final general result is

$$J_x^{mnqr} = C\delta_{nr} + D\delta_{mq} - (C+D)\delta_{mq}\delta_{nr} + E\delta_{mq}\delta_{nr} \tag{94}$$

where

$$C = \frac{-b}{\pi k_m k_q} \left[\left\{ \ln \left(\frac{k + \sqrt{2k^2 - k_n^2}}{k \, \sqrt{k^2 - k_n^2}} \right) + \frac{1}{2(k_q^2 - k_m^2)} \, [k_q^2 \ln (k_m^2 + k^2) - k_m^2 \ln (k_q^2 + k^2)] \right\} \right.$$

$$\left. - (-1)^m \left\{ \ln \left(\frac{\frac{1}{a} + \sqrt{k^2 - k_n^2 + \left(\frac{1}{a}\right)^2}}{\sqrt{k^2 - k_m^2}} \right) - a \left[\left(k^2 - k_n^2 + \left(\frac{1}{a}\right)^2 \right)^{1/2} - (k^2 - k_n^2)^{1/2} \right] \right\} + \sum_{i=o}^\infty \frac{(-1)^{i+m} \left(a \, \sqrt{k^2 - k_n^2} \right)^{2i+1}}{[(2i+1)!]^2} \right] \tag{95}$$

$$D = \frac{-a}{\pi k_n k_r} \left[\left\{ \ln \left(\frac{k + \sqrt{2k^2 - k_m^2}}{k \, \sqrt{k^2 - k_m^2}} \right) + \frac{1}{2(k_r^2 - k_n^2)} \, [k_r^2 \ln (k_n^2 + k^2) - k_n^2 \ln (k_r^2 + k^2)] \right\} \right.$$

114

$$-(-1)^n \left\{ \ln\left(\frac{\frac{1}{b} + \sqrt{k^2-k_m^2 + \left(\frac{1}{b}\right)^2}}{\sqrt{k^2-k_m^2}}\right) - b\left[\left(k^2-k_m^2+\left(\frac{1}{b}\right)^2\right)^{\frac{1}{2}} - (k^2-k_m^2)^{\frac{1}{2}}\right]\right\}$$

$$\left. + \sum_{i=0}^{\infty} \frac{(-1)^{i+n}(b\sqrt{k^2-k_m^2})^{2i+1}}{[(2i+1)!]^2}\right] \tag{96}$$

$$E = \frac{-A_p}{4(k_m^2 + k_n^2 - k^2)^{\frac{1}{2}}} \tag{97}$$

B2.   EVALUATION OF THE CAVITY COEFFICIENTS $\bar{I}^{rr}$, $\bar{I}^{rs}$

For the cavity-induced coupling we require the solution of Equation (28):

$$\bar{I}^{rs} = \int_{A_p'} \int_{A_p} \psi^r(\bar{x}) \, G_p(\bar{x}|\bar{x}') \, \psi^s(\bar{x}') \, d\bar{x} \, d\bar{x}'$$

where $G_p(\bar{x}|\bar{x}') \equiv G_p(x,y,o|x',y',o;\omega)$ is the cavity Green function at the surface of the vibrating plate. For the coordinate system of Figure 1 with origin located at one corner as shown, we treat two cases: (a) almost hard walls and (b) hard walls; mathematical development for the latter is subsumed in the former.

Hence, following the analysis in Chapter 9 of Morse and Ingard[24] and Chapter 14 of Reference 37, Kinsler and Frey[35] the specific wall admittance for a cavity mode n ($n = a, \beta, \gamma$) for almost hard walls is:

$$\beta_n = \xi_n - i\sigma_n = \frac{\rho c}{z_n} = \frac{\rho c}{r_n + ix_n} = \frac{r_n - ix_n}{|z_n|^2} \quad ; \quad o < \beta_n < 1$$

where

ξ = specific wall conductance	σ_n = the specific wall susceptance
r_n = specific wall resistance	x_n = specific wall reactance
z_n = $\rho c\,(r_n + ix_n)$ is the specific wall impedance	

In the above equation, β_n may be taken as frequency-dependent through the parameters n. Assuming $x_n \approx o$ (or $r_n \gg x_n$)

$$\beta_n \approx \xi_n \approx \frac{1}{r_n} \approx \frac{a_n}{8} \tag{98}$$

where a_n is the wall absorption coefficient. Now assume that β_n is uniform and small (or $r_n \gg 1$) over all surfaces of the cavity including the panel, i.e., β_n is taken as a numerically small constant for all modes (frequencies). Since β_n is very small ($\beta_n \ll 1$), the cavity eigenfunctions can be assumed real, but the eigenvalues $\overline{\lambda}_n$ are complex. From Morse and Ingard[24] (Equations (9.4.8), (9.4.9), (9.4.31), and p. 572) the cavity Green function is*

$$G_p(\overline{\xi}|\overline{\xi}';\omega) = \sum_n^{\infty} \frac{\phi_n(\overline{\xi})\phi_n(\overline{\xi}')}{\left[\int_V \phi_n^2(\overline{\xi})dV\right](\overline{\lambda}_n^2 - k_c^2)} \tag{99}$$

where

$$\phi_n(\overline{\xi}) = \phi_{a,\beta,\gamma}(\overline{\xi}) = \cos\frac{a\pi x}{a}\cos\frac{\beta\pi y}{b}\cos\frac{\gamma\pi z}{c} \quad ; a,\beta,\gamma = 0,1,2\ldots. \tag{100}$$

$$\overline{\lambda}_n = \lambda_n - i\Lambda_n \tag{101}$$

$$\lambda_n = \left[\left(\frac{a\pi}{a}\right)^2 + \left(\frac{\beta\pi}{b}\right)^2 + \left(\frac{\gamma\pi}{c}\right)^2\right]^{\frac{1}{2}} \tag{102}$$

$$\Lambda_n = \frac{k_c a_n}{8\lambda_n}\left(\frac{\epsilon_a}{a} + \frac{\epsilon_\beta}{b} + \frac{\epsilon_\gamma}{c}\right) \tag{103}$$

$$\epsilon_a, \epsilon_\beta, \epsilon_\gamma = \begin{cases} 1 \text{ for } a, \beta, \gamma = o \\ 2 \text{ for } a, \beta, \gamma > o \end{cases} \tag{104}$$

For a, β, γ all equal to zero we take $\Lambda_n = o$

$$\int_V \phi_n^2 \, dV = \frac{V}{\epsilon_a\epsilon_\beta\epsilon_\gamma} = \frac{a \cdot b \cdot c}{\epsilon_a\epsilon_\beta\epsilon_\gamma} \tag{105a}$$

---

*In Equation (9.4.31) of Reference 24, let $K_n \to \overline{\lambda}_n$, $\eta_n \to \lambda_n$, $k \to k_c$, $\epsilon_{n_x} \to \epsilon_a$, $\epsilon_{n_y} \to \epsilon_\beta$, $\epsilon_{n_z} \to \epsilon_\gamma$, $l_x \to a$, $l_y \to b$,

$l_z \to c$, and $\beta_{x_o} = \beta_{x_1} = \beta_{y_o} = \beta_{y_1} = \beta_{z_o} = \beta_{z_1} = \beta_n = \xi_n = \frac{a_n}{8}$.

Substituting Equations (100), (101), and (105) into (99):

$$G_p(\bar{\xi}|\bar{\xi}';\omega) = \sum_{\alpha,\beta,\gamma=0}^{\infty} \frac{\epsilon_\alpha \epsilon_\beta \epsilon_\gamma}{V(\lambda_n^2 - k_c^2)} \cos\frac{\alpha\pi x}{a} \cos\frac{\beta\pi y}{b} \cos\frac{\gamma\pi z}{c} \cos\frac{\alpha\pi x'}{a} \cos\frac{\beta\pi y'}{b} \cos\frac{\gamma\pi z'}{c}$$

where $\bar{\lambda}_n^2 = (\lambda_n^2 - \Lambda_n^2) - i2\lambda_n\Lambda_n$. Substituting into the equation for G_p and rationalizing the denominator of the resulting equation*

$$G_p(\bar{\xi}|\bar{\xi}';\omega) = \frac{1}{V}\left\{ \sum_{\alpha,\beta,\gamma=0}^{\infty} \frac{\epsilon_\alpha \epsilon_\beta \epsilon_\gamma (\lambda_n^2 - \Lambda_n^2 - k_c^2)\cos\frac{\alpha\pi x}{a}\cos\frac{\beta\pi y}{b}\cos\frac{\gamma\pi z}{c}\cos\frac{\alpha\pi x'}{a}\cos\frac{\beta\pi y'}{b}\cos\frac{\gamma\pi z'}{c}}{(\lambda_n^2 - \Lambda_n^2 - k_c^2)^2 + 4\lambda_n^2\Lambda_n^2} \right.$$

$$\left. + i2 \sum_{\alpha,\beta,\gamma=0}^{\infty} \frac{\epsilon_\alpha \epsilon_\beta \epsilon_\gamma \lambda_n\Lambda_n \cos\frac{\alpha\pi x}{a}\cos\frac{\beta\pi y}{b}\cos\frac{\gamma\pi z}{c}\cos\frac{\alpha\pi x'}{a}\cos\frac{\beta\pi y'}{b}\cos\frac{\gamma\pi z'}{c}}{(\lambda_n^2 - \Lambda_n^2 - k_c^2)^2 + 4\lambda_n^2\Lambda_n^2} \right\} \qquad (105b)$$

Substitution of this equation into Equation (28) with $G_p(\bar{x}|\bar{x}') \equiv G_p(\bar{\xi}|\bar{\xi}')_{z,z'=0}$ gives for the coupled modes of a simply supported plate

$$\bar{I}^{rs}(\omega) = \bar{I}^{mnqr}(\omega) = \frac{1}{V}\int_{x'=0}^{a}\int_{y'=0}^{b} \sin\frac{m\pi x'}{a}\sin\frac{n\pi y'}{b}$$

$$\cdot\left\{\int_{x=0}^{a}\int_{y=0}^{b}\sum_{\alpha,\beta,\gamma=0}^{\infty}\left[\frac{\epsilon_\alpha\epsilon_\beta\epsilon_\gamma(\lambda_n^2-\Lambda_n^2-k_c^2)+i2\lambda_n\Lambda_n}{(\lambda_n^2-\Lambda_n^2-k_c^2)^2+4\lambda_n^2\Lambda_n^2}\right]\cos\frac{\alpha\pi x}{a}\cos\frac{\beta\pi y}{b}\right.$$

$$\left.\cos\frac{\alpha\pi x'}{a}\cos\frac{\beta\pi y'}{b}\sin\frac{q\pi x}{a}\sin\frac{r\pi y}{b}\,dx\,dy\right\}\,dx'\,dy'$$

---

*Alternatively, we may use (see page 1134 in Morse and Feshbach[36])

$$G_p(\bar{\xi}|\bar{\xi}';\omega) = \frac{-1}{A_p}\sum_{\alpha=0}^{\infty}\sum_{\beta=0}^{\infty}\epsilon_\alpha\epsilon_\beta\left[\frac{\cos\frac{\alpha\pi x}{a}\cos\frac{\beta\pi y}{b}}{k_{\alpha\beta}\sin k_{\alpha\beta}z}\right]$$

$$\cdot\cos\frac{\alpha\pi x'}{a}\cos\frac{\beta\pi y'}{b}\begin{cases}\cos k_{\alpha\beta}z\cos[k_{\alpha\beta}(c-z')] & ; \quad z'>z \\ \cos k_{\alpha\beta}z'\cos[k_{\alpha\beta}(c-z)] & ; \quad z'<z\end{cases}$$

where $k_{\alpha\beta}^2 = k^2 - \left(\frac{\alpha\pi}{a}\right)^2 - \left(\frac{\beta\pi}{b}\right)^2$

117

$$= \sum_{a,\beta,\gamma=0}^{\infty} \frac{\epsilon_a\epsilon_\beta\epsilon_\gamma(\lambda_n^2-\Lambda_n^2-k_c^2)+i2\lambda_n\Lambda_n}{(\lambda_n^2-\Lambda_n^2-k_c^2)+4\lambda_n^2\Lambda_n^2} \int_0^a \frac{\sin m\pi x'}{a} \cos \frac{a\pi x'}{a} \, dx'$$

$$\int_0^a \frac{\sin q\pi x}{a} \cos \frac{a\pi x}{a} \, dx \int_0^b \frac{\sin n\pi y'}{b} \cos \frac{\beta\pi y'}{b} \, dy' \int_0^b \frac{\sin r\pi y}{b} \cos \frac{\beta\pi y}{b} \, dy$$

Now

$$\int_0^a \frac{\sin m\pi x'}{a} \cos \frac{a\pi x'}{a} \, dx' = \begin{cases} \dfrac{1-\cos[(m+a)\pi]}{2\left[(m+a)\frac{\pi}{a}\right]} + \dfrac{1-\cos[(m-a)\pi]}{2\left[(m-a)\frac{\pi}{a}\right]} & ; \ m \neq a \\[4mm] 0 & ; \ m = a \end{cases}$$

and similarly for the other three integrals in the equation for $\bar{I}^{mnqr}$. Hence

$$\bar{I}^{mnqr}(\omega) = \frac{A_p^2}{16\pi^4 V} \sum_{a,\beta,\gamma=0}^{\infty} \frac{(\lambda_n^2-\Lambda_n^2-k_c^2)+i2\lambda_n\Lambda_n}{(\lambda_n^2-\Lambda_n^2-k_c^2)^2+4\lambda_n^2\Lambda_n^2} \ \epsilon_a\epsilon_\beta\epsilon_\gamma A_{ma}A_{n\beta}A_{qa}A_{r\beta} \qquad (106)$$

where

$$A_{ij} = \begin{cases} \left\{ \dfrac{1-\cos[(i+j)\pi]}{i+j} + \dfrac{1-\cos[(i-j)\pi]}{i-j} \right\} & ; \ i \neq j \\[4mm] 0 & ; \ i = j \end{cases} \qquad (107)$$

Equation (106) represents the cavity coupling coefficient for *almost hard walls*. For the case of hard walls $\beta_n = a_n = \Lambda_n = 0$ so that $\bar{\lambda}_n = \lambda_n$, the real eigenvalue. Thus the cavity coupling coefficient for *hard walls*, obtained from Equation (106) with $\Lambda_n = 0$, is

$$\bar{I}^{mnqr} = \frac{A_p^2}{16\pi^4 V} \sum_{a,\beta,\gamma=0}^{\infty} \frac{\epsilon_a\epsilon_\beta\epsilon_\gamma \ A_{ma}A_{n\beta}A_{qa}A_{r\beta}}{(\lambda_n^2-k_c^2)}$$

which is a real quantity. Note that m and q, and n and r must have the same parity (either both even or both odd), otherwise $\bar{I}^{mnqr} \equiv 0$.

118

Figure 12 – Modal Classification in Wavenumber Space
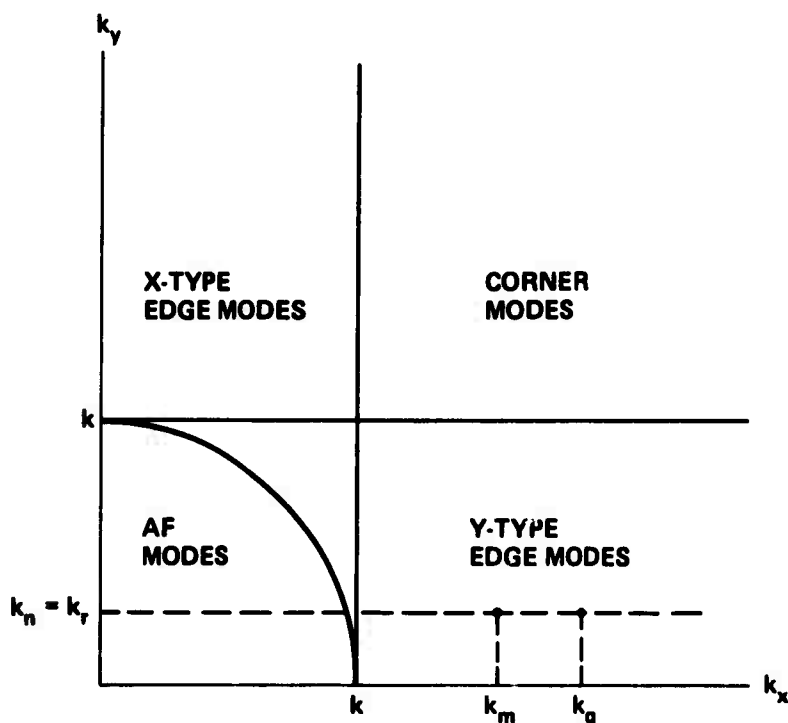
Figure 12a – Two Y-Edge Modes: $k_m, k_q > k$
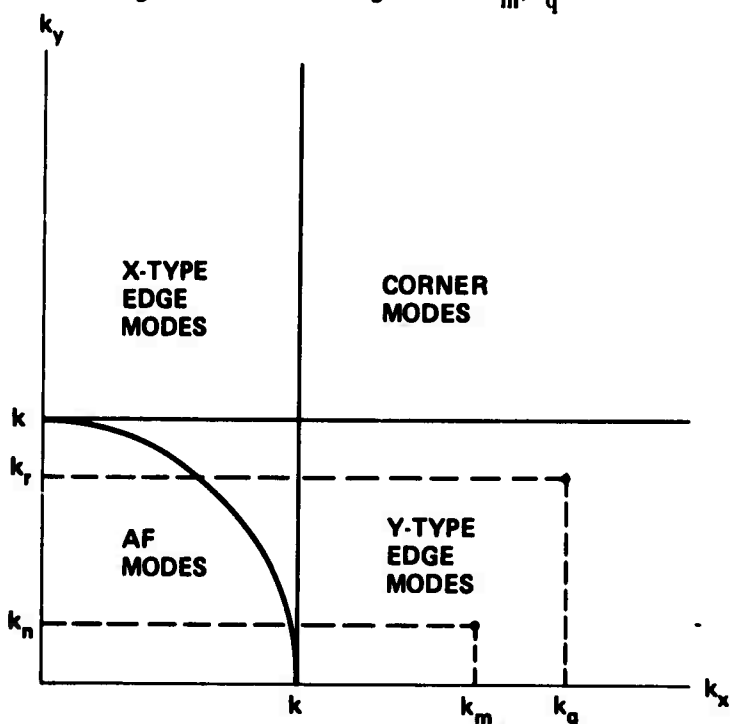
Figure 12b – Two Y-Edge Modes: $k_m \neq k_q > k$; $k_n \neq k_r < k$
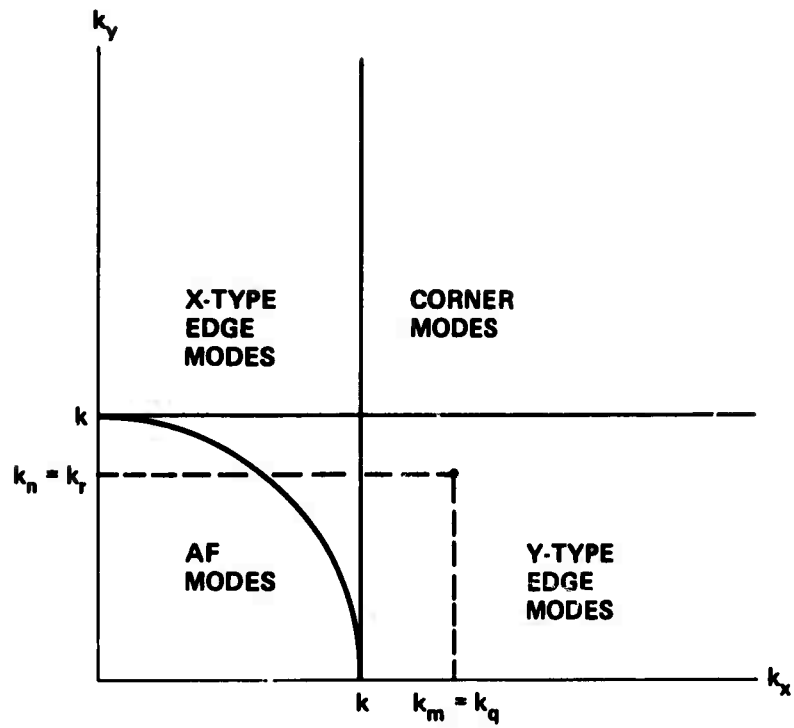
Figure 12c — Two Y-Edge Modes: $k_m = k_q > k$; $k_n = k_r < k$
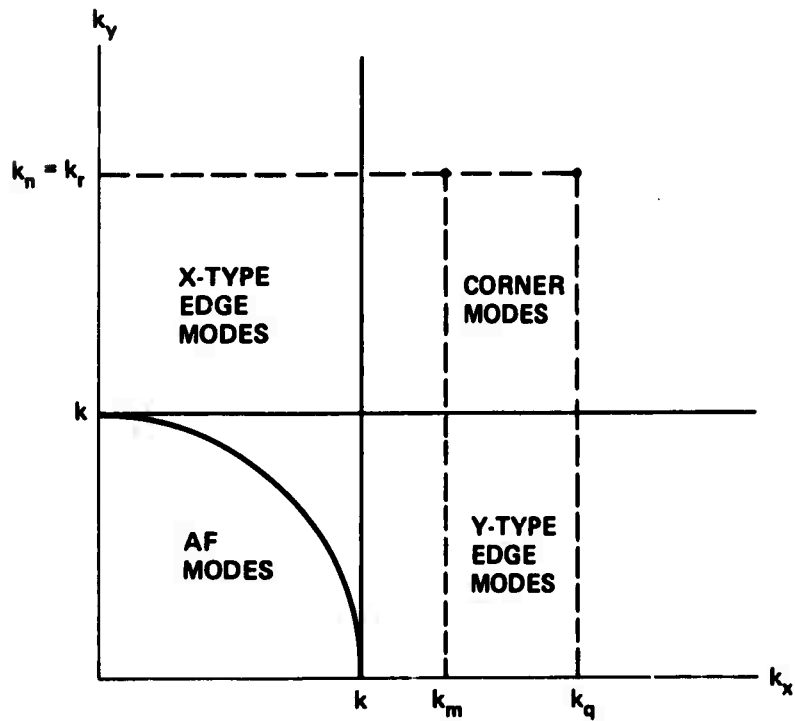
Figure 12d — Two Corner Modes: $k_m, k_q > k$; $k_n = k_r > k$
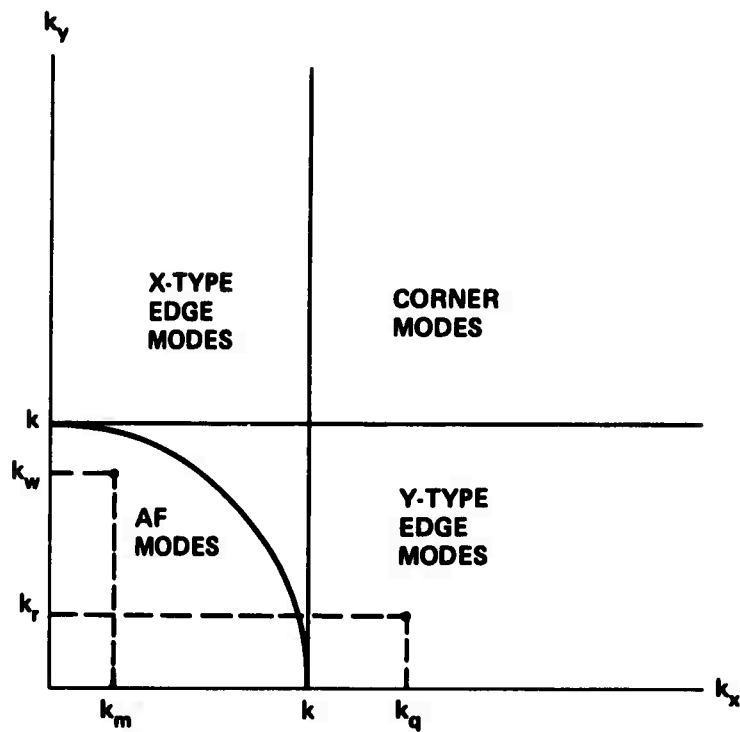
Figure 12e – Y-Edge-Acoustically Fast (AF) modes:
$k_m \, k_n, k_r < k; \, k_q > k$
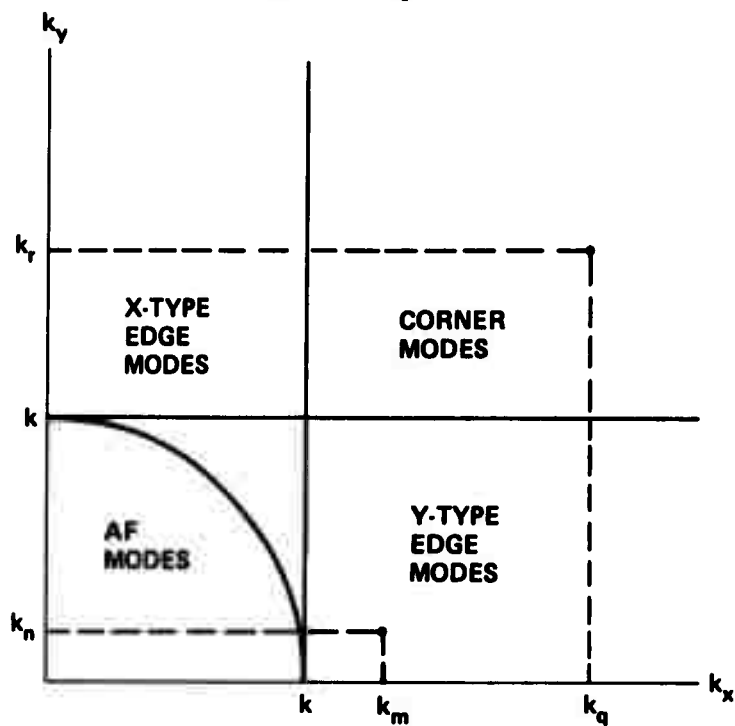
Figure 12f – Y-Edge-Corner modes: $k_m, k_q > k; \, k_n < k; \, k_r > k$

121
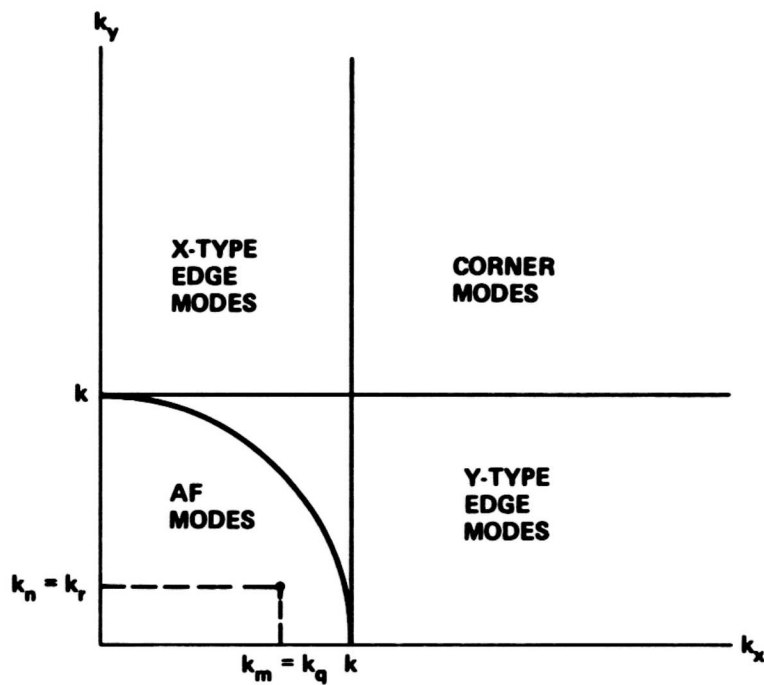
Figure 12g – Two Acoustically Fast Modes: $k_m = k_q < k$; $k_n = k_r < k$
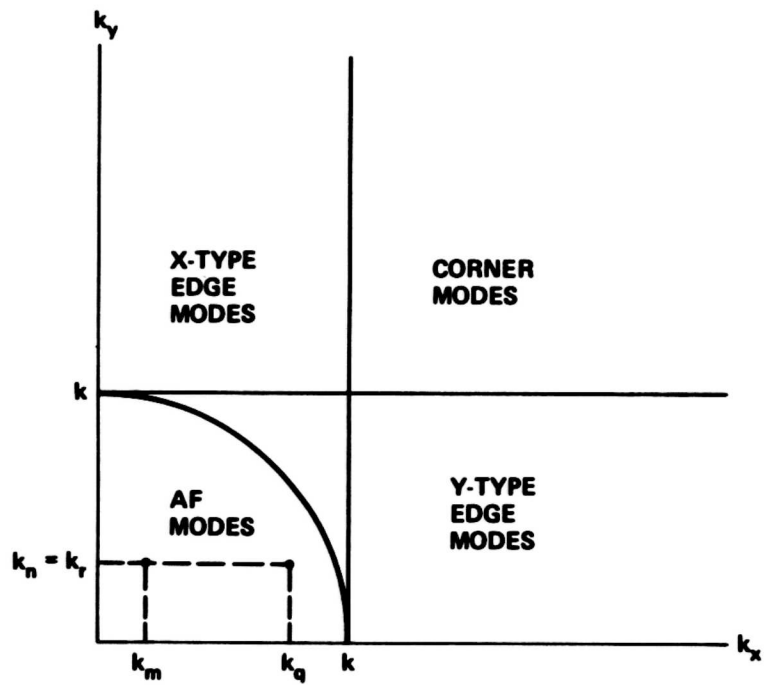
Figure 12h – Two Acoustically Fast Modes: $k_m \neq k_q < k$; $k_n = k_r < k$
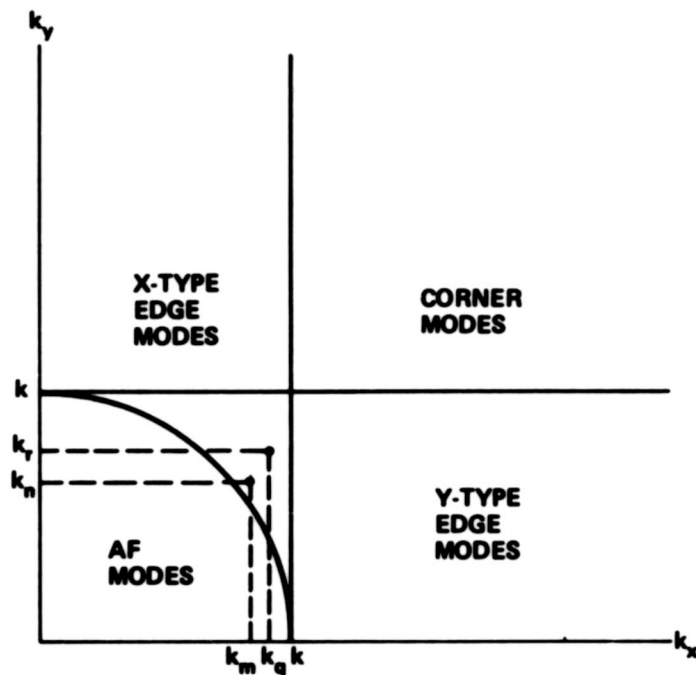
Figure 12i — Two Edge Modes: $k_m = k_q < k$; $k_n = k_r < k$; k_{mn}^2, $k_{qr}^2 > k^2$
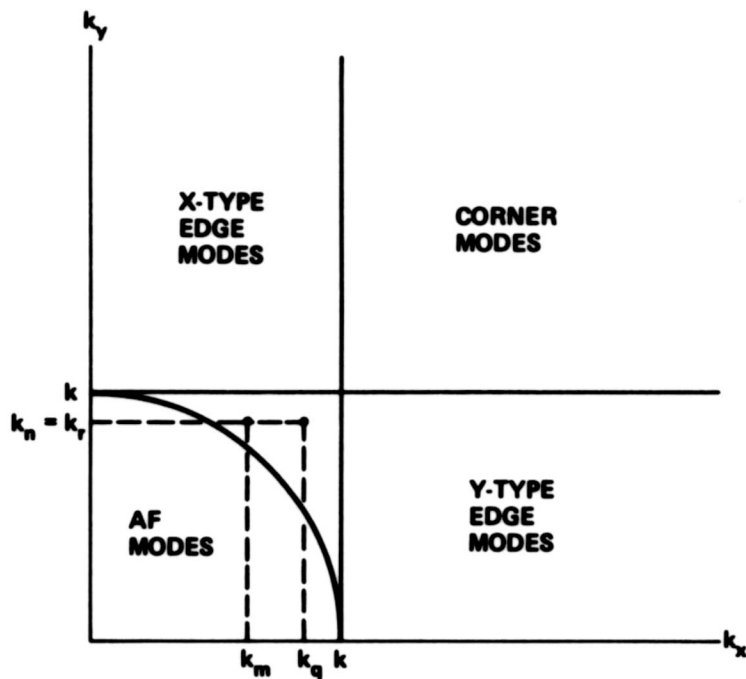
Figure 12j — Two Edge Modes: $k_m \neq k_q < k$; $k_n = k_r < k$; k_{mn}^2, $k_{qr}^2 > k^2$
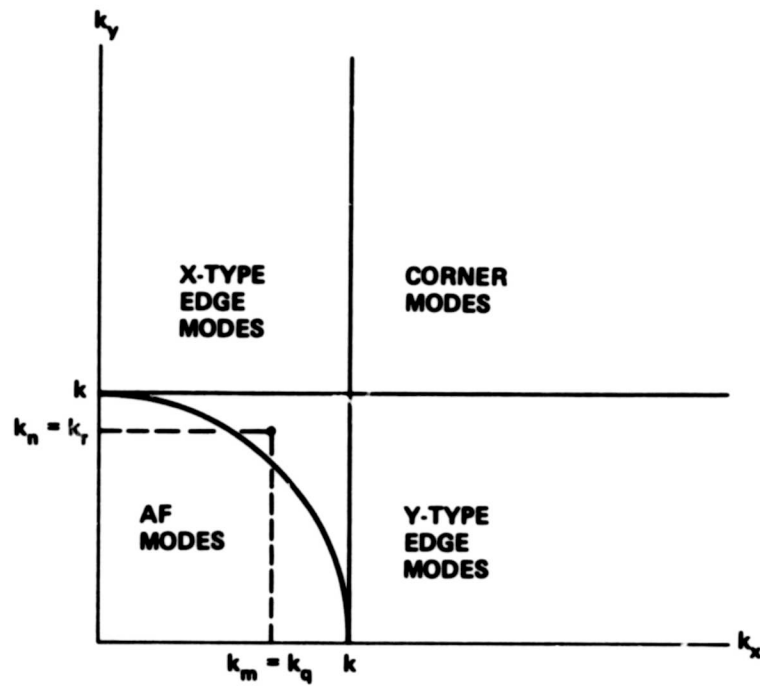
Figure 12k – Two Edge Modes: $k_m \neq k_n \neq k_q \neq k_r < k; k_{mn}^2, k_{qr}^2 > k2$
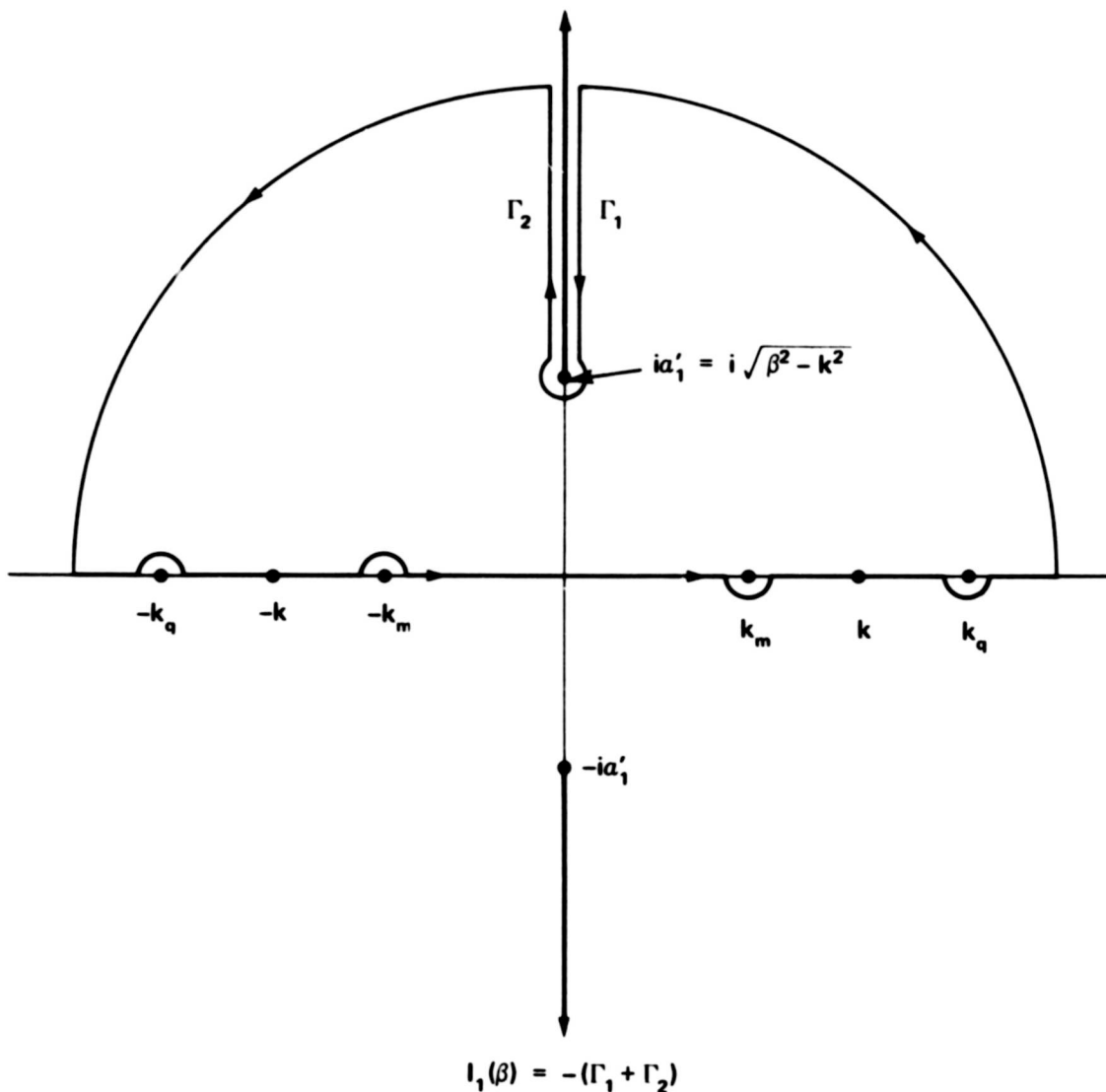
124

$$I_1(\beta) = -(\Gamma_1 + \Gamma_2)$$

(Contour of integration for Y-edge acoustically fast mode corresponding to Figure 12e)

Figure 13 — Case 1 Integration Contour for I_1^{mq} ($\beta : \beta > |k|$)
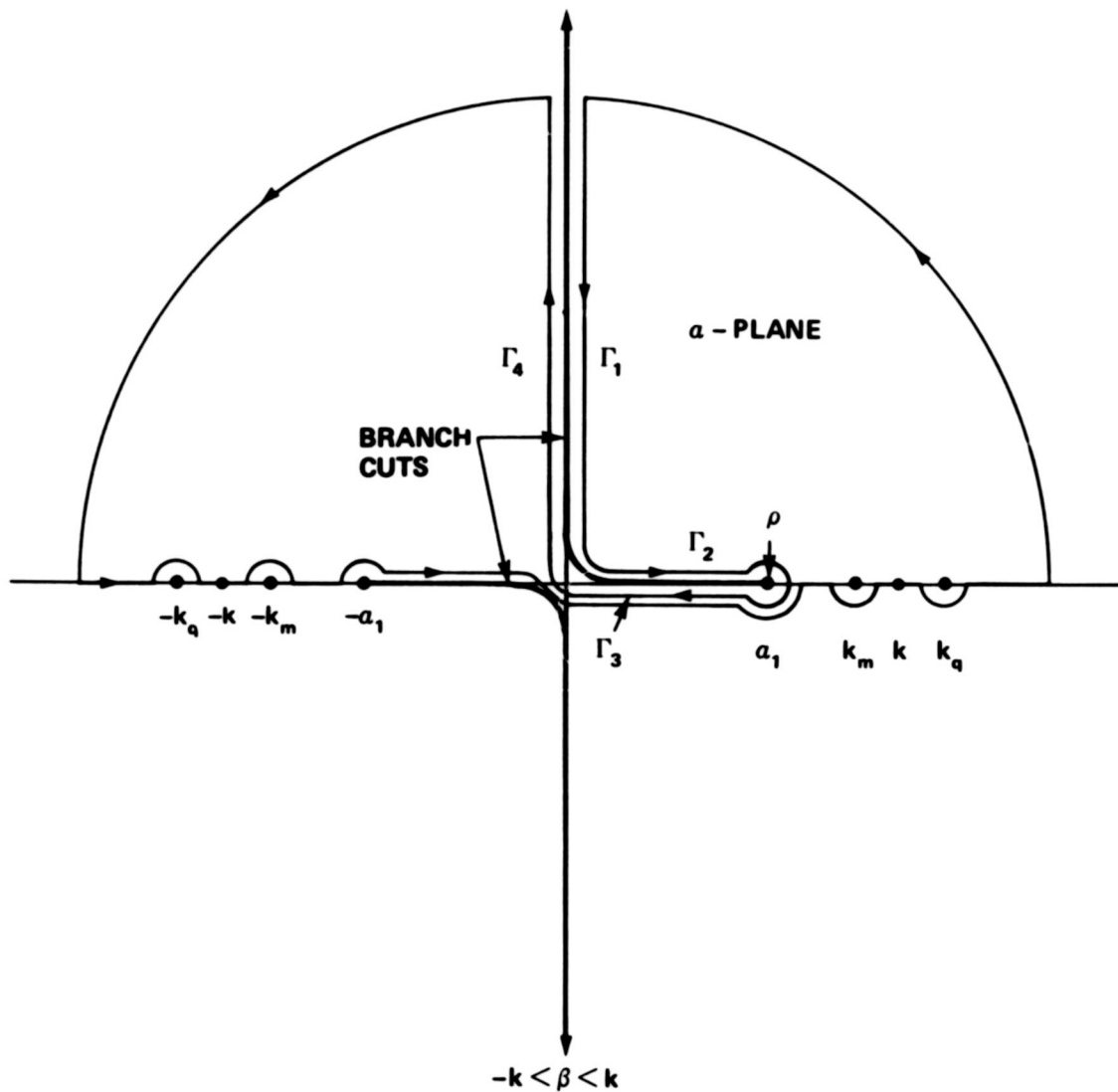
(Contour of integration for Y-edge acoustically fast mode corresponding to Figure 12e)

Figure 14 — Case Integration Contour for I_1^{mq} $(\beta{:}\sqrt{k^2-k_m^2} < \beta < k)$
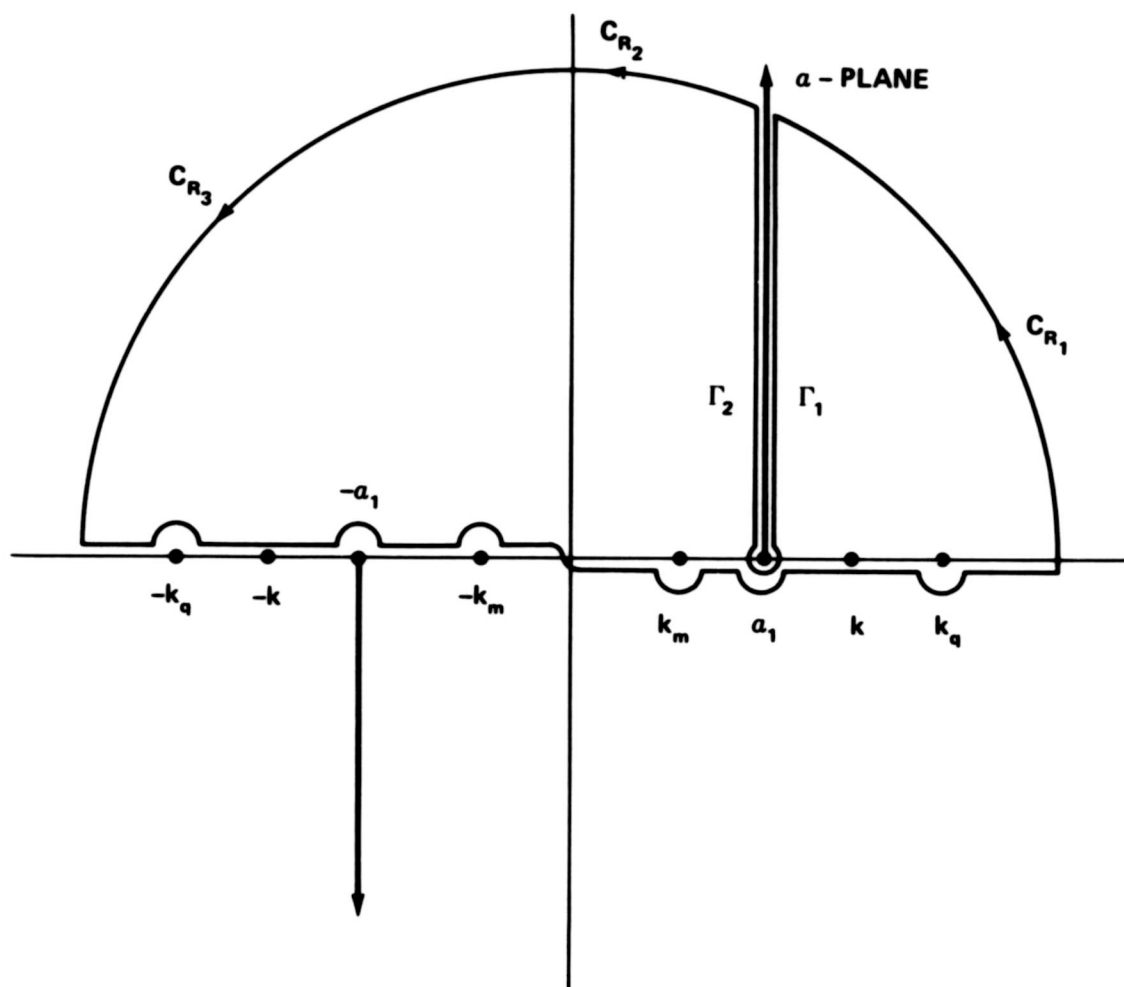
(Contour of integration for Y-edge acoustically fast mode corresponding to Figure 12e)

Figure 15 — Case 2 Integration Contour for I_1^{mq} $(\beta : \beta < \sqrt{k^2 - k_m^2})$
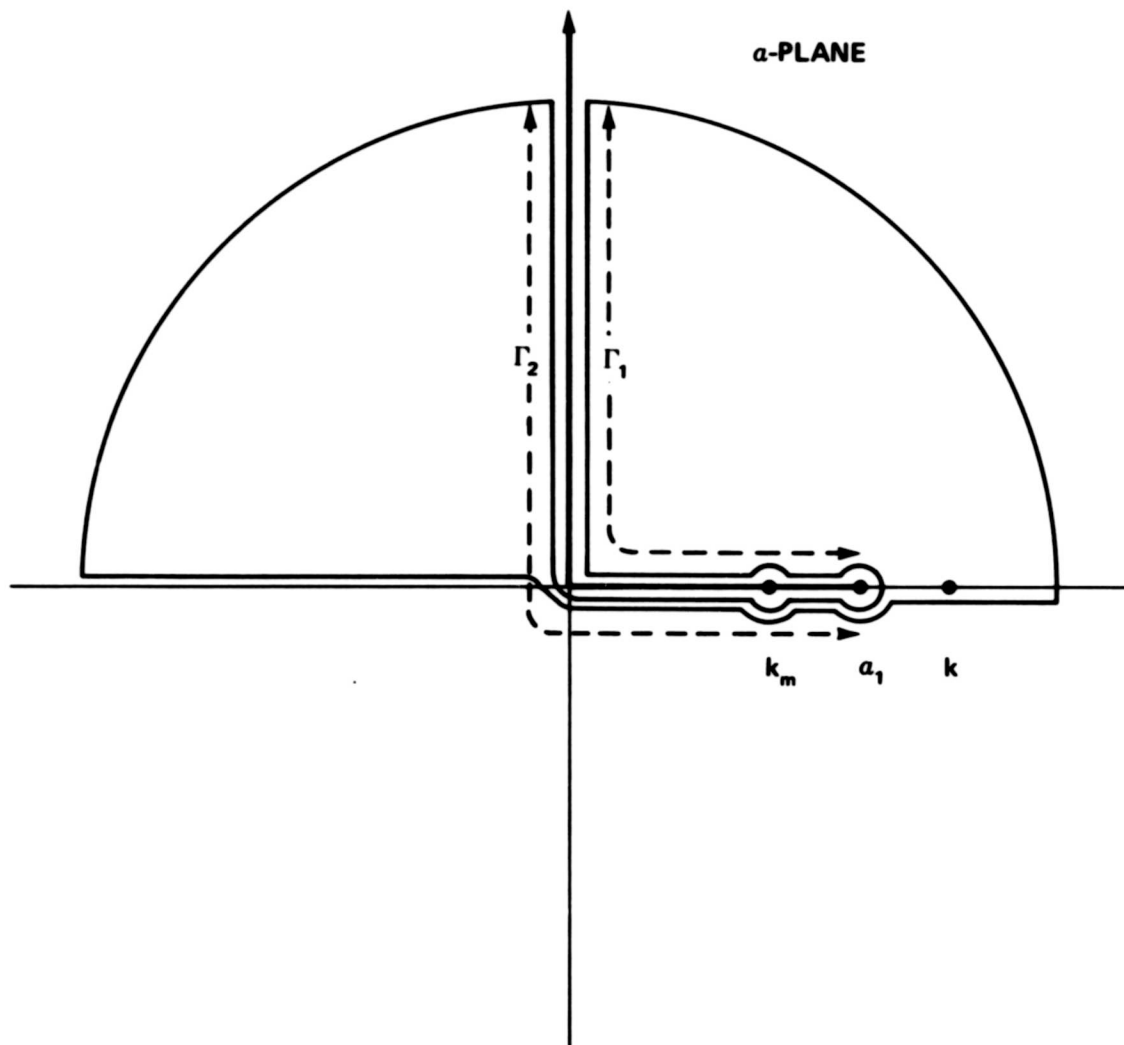
Figure 16 — Deformation of Contour in Figure 15
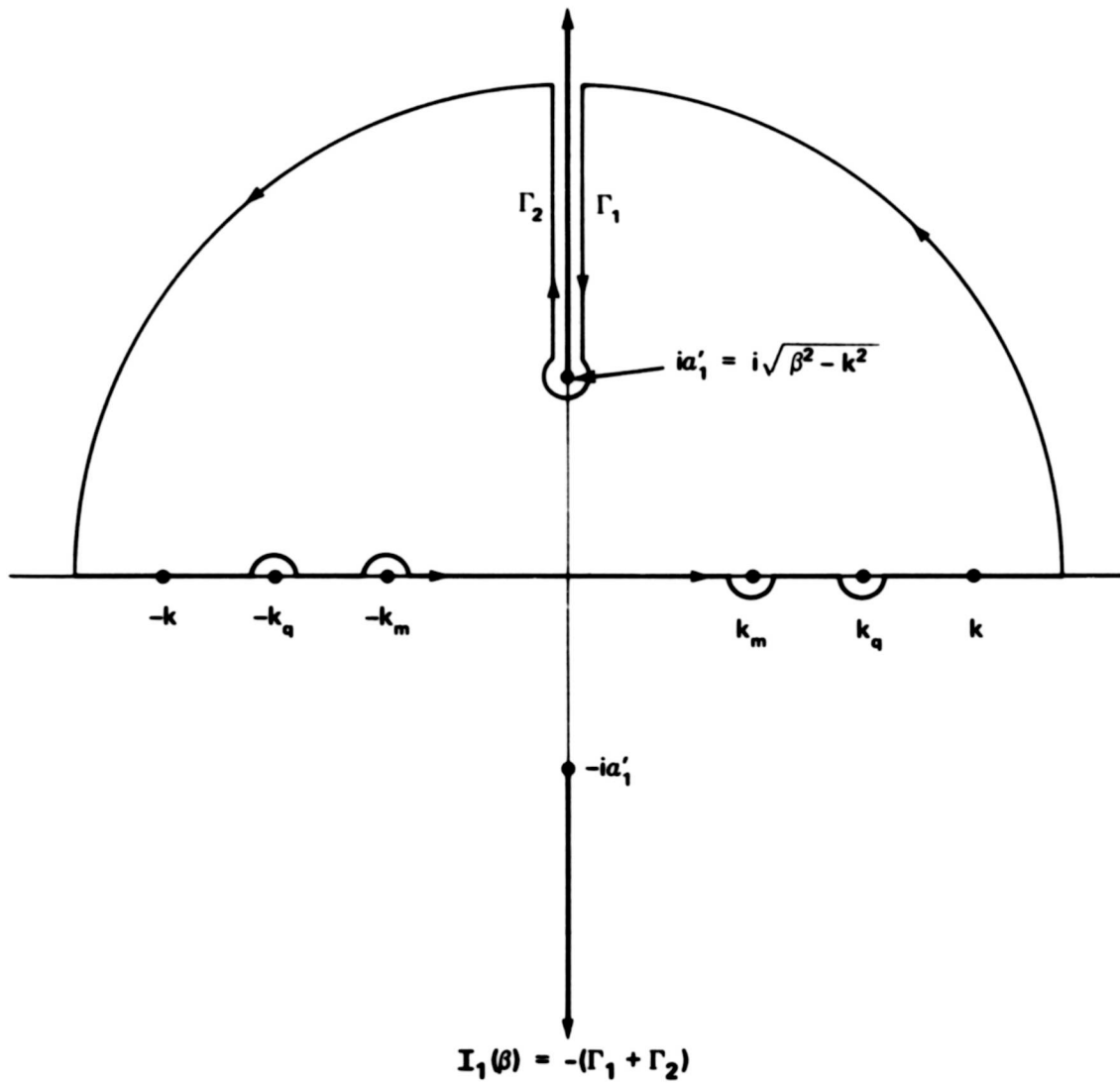
128

(Contour of integration for two acoustically fast modes corresponding to Figure 12h)

Figure 17 — Case 1 Integration Contour for I_1^{mq} ($\beta: \beta > |k|$)
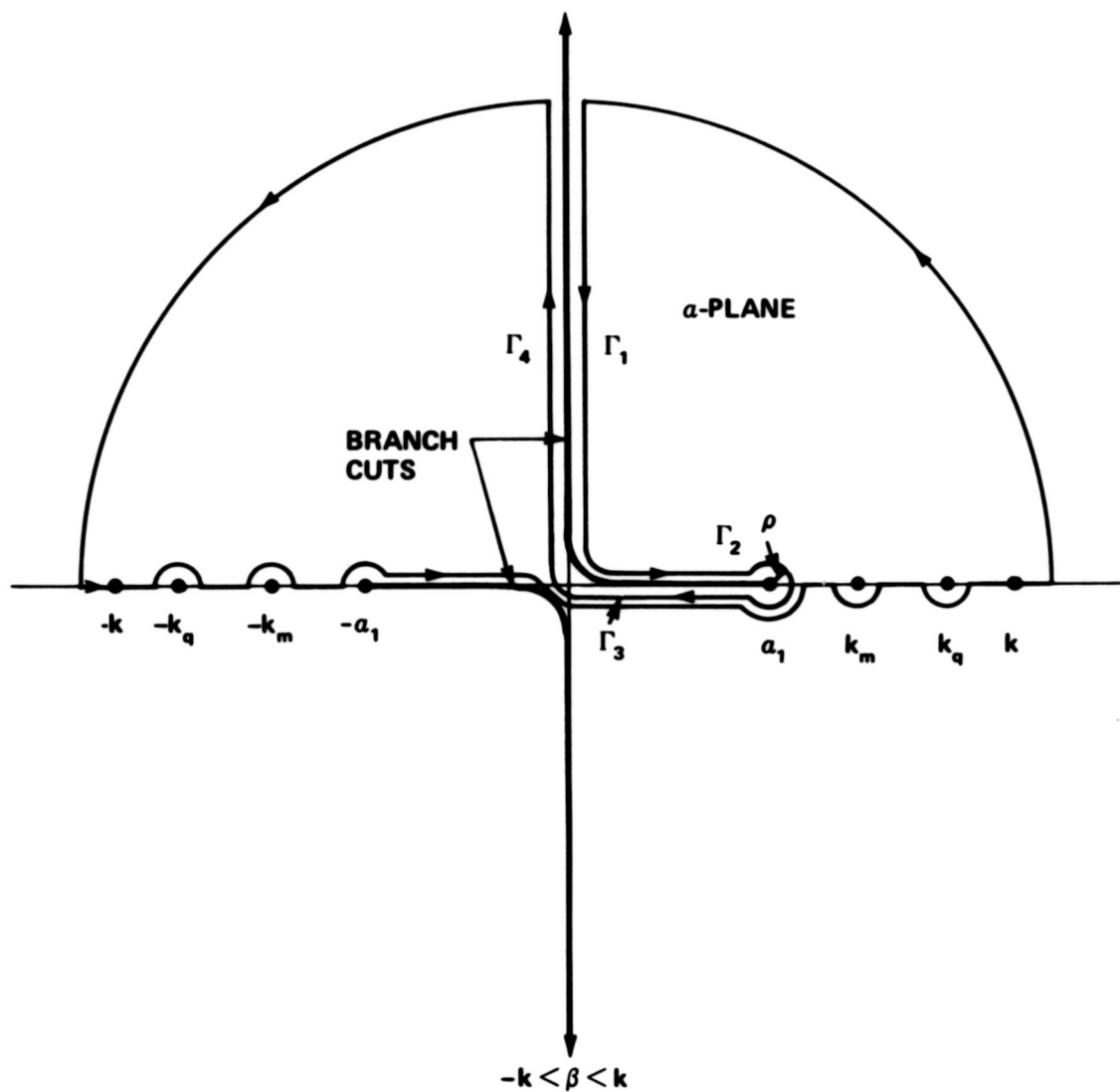
(Contour of integration for two acoustically fast modes corresponding to Figure 12h)

Figure 18 — Case 2 Integration Contour for $I_1^{mq}(\beta:\sqrt{k^2 - k_m^2} < \beta < k)$
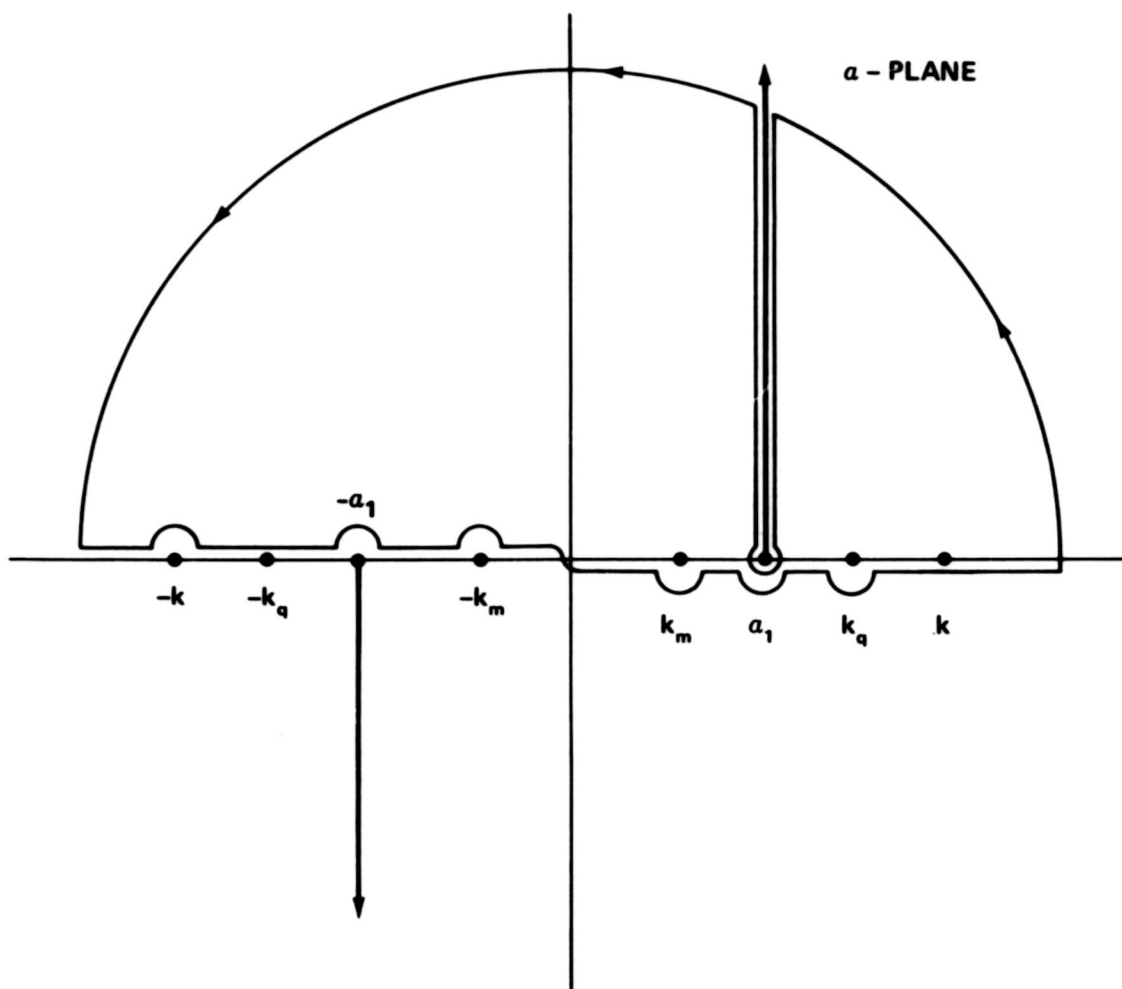
130

a – PLANE

$-a_1$

$-k$ $-k_q$ $-k_m$

k_m a_1 k_q k

(Contour of integration for two acoustically fast modes corresponding to Figure 12h)

Figure 19 – Case 2 Integration Contour for I_1^{mq} ($\beta: \sqrt{k^2 - k_q^2} < \beta < \sqrt{k^2 - k_m^2}$)
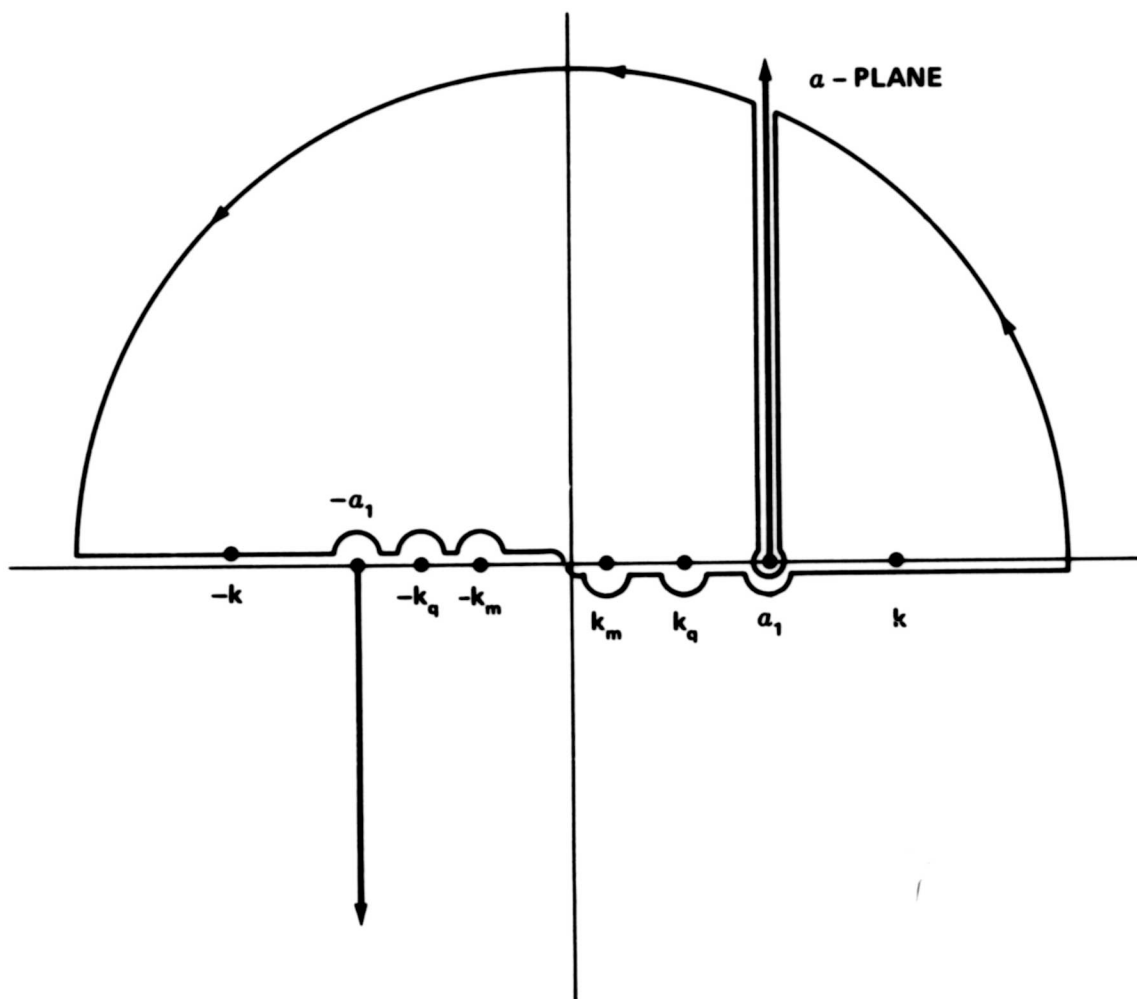
(Contour of integration for two acoustically fast modes corresponding to Figure 12h)

Figure 20 – Case 2 Integration Contour for I_1^{mq} $(\beta : \beta < \sqrt{k^2 - k_q^2})$

APPENDIX C

MATHEMATICAL REPRESENTATION OF TURBULENCE EXCITATION AND EVALUATION OF JOINT AND CROSS ACCEPTANCES

C1. CROSS-SPECTRAL DENSITY OF TURBULENCE (BLOCKED) PRESSURE

The turbulence excitation function is assumed to be described by a semiempirical model devised by Maestrello.[1,12] The model represents the *normalized* cross-correlation function for the turbulence, which is the blocked pressure, between two points (x,y) and (x',y') at times t and t', respectively, by

$$R(\eta,\mu,\tau) = \frac{e^{\frac{-|\eta|}{U_c \theta}} \sum_{a=1}^{3} \dfrac{A_j K_j}{K_j^2 + (1/FU_c)^2 \, [\eta - U_c \tau)^2 + \mu^2]}}{\sum_{j=1}^{3} \dfrac{A_j}{K_j}} \tag{108}$$

Here $\eta = x - x'$, $\mu = y - y'$, $\tau = t - t'$, $F = \dfrac{\delta^*}{U_\infty}$; δ^* is the boundary layer displacement thickness, U_∞ and U_c are respectively the free-stream and turbulence convection velocities, θ is the eddy lifetime for steady convection and A_j, K_j are nondimensional constants (see notation).

The cross-spectral density of the *unnormalized* exciting field is

$$S_{p_{b\ell}}(\bar{x}|\bar{x}';\omega) = S_{p_{b\ell}}(\eta,\mu;\omega) = R(\eta,\mu,o) \int_{-\infty}^{\infty} R(\eta,\mu,\tau) \, e^{-i\omega\tau} \, d\tau$$

$$= R(\eta,\mu,o) \frac{e^{\frac{-|\eta|}{U_c \theta}}}{\sum_{j=1}^{3} \dfrac{A_j}{K_j}} \sum_{a=1}^{3} A_j K_j \int_{-\infty}^{\infty} \frac{e^{-i\omega\tau} \, d\tau}{K_j^2 + (1/FU_c)^2 \, [(\eta - U_c\tau)^2 + \mu^2]}$$

With slight algebraic manipulation, the integral is evaluated as follows (see page 59 in Leibowitz and Wallace[1]).

$$\int_{-\infty}^{\infty} \frac{e^{-i\omega\tau} \, d\tau}{K_j^2 + (1/FU_c)^2 \, [(\eta - U_c\tau)^2 + \mu^2]} = \int_{-\infty}^{\infty} \frac{F^2 e^{-i\omega\tau} \, d\tau}{\left\{ [(K_j F)^2 + (\mu/U_c)^2]^{1/2} \right\}^2 + \left(\tau - \dfrac{\eta}{U_c} \right)^2}$$

$$= \frac{\pi F^2 \, e^{- \sqrt{(K_j F)^2 + (\mu/U_c)^2} |\omega| - \frac{i\eta\omega}{U_c}}}{\sqrt{(K_j F)^2 + (\mu/U_c)^2}}$$

Hence

$$S_{p_{b\ell}}(\bar{x}|\bar{x}';\omega) = R(\eta,\mu,o)\, e^{\dfrac{-|\eta|}{U_c\theta}} \left[\dfrac{\pi F^2}{\displaystyle\sum_{j=1}^{3}\dfrac{A_j}{K_j}}\right] \sum_{j=1}^{3} \dfrac{A_j K_j\, e^{-\sqrt{(K_j F)^2 + (\mu/U_c)^2}\,|\omega| - \dfrac{i\eta\,\omega}{U_c}}}{\sqrt{(K_j F)^2 + (\mu/U_c)^2}}$$

$$\approx \langle p_{b\ell}^2\rangle_t\, e^{\dfrac{-|\eta|}{U_c\theta}} \left[\dfrac{\pi F^2}{\displaystyle\sum_{j=1}^{3}\dfrac{A_j}{K_j}}\right] \sum_{j=1}^{3} \dfrac{A_j K_j\, e^{-\sqrt{(K_j F)^2 + (\mu/U_c)^2}\,|\omega| - \dfrac{i\eta\omega}{U_c}}}{\sqrt{(K_j F)^2 + (\mu/U_c)^2}} \qquad (109a)$$

because

$$R(\eta,\mu,o) = \left[\overline{p^2(x,y,t)\, p^2(x',y',t')}\right]^{1/2} \approx \langle p_{b\ell}^2\rangle_t = \int_0^\infty S_{p_{b\ell}}(\omega)\, d\omega$$

To evaluate $\langle p_{b\ell}^2\rangle_t$ we use the measured dimensionless power spectral density given by Equation (B7) of Reference 1, namely,[*]

$$S_{p_{b\ell}}(\omega) = \dfrac{\tau_w^2\, \delta^*}{U_\infty} \sum_{j=1}^{3} A_j\, e^{-K_j F\omega} \qquad (109b)$$

---

[*]An alternative method can be utilized to derive Equation (110). Consider the one-sided (unnormalized) power spectral density

$$S_{p_{b\ell}}(\omega) = \dfrac{\tau_w^2\,\delta^*}{U_\infty} \sum_{j=1}^{3} A_j\, e^{-K_j F\omega} \qquad ; \omega > 0$$

We now treat $S_{p_{b\ell}}(\omega)$ in the infinite range $-\infty, \infty$ as a two-sided power spectrum by taking one-half the foregoing value and letting $S_{p_{b\ell}}(\omega) \to S_{p_{b\ell}}(|\omega|)$, a nonnegative even function of ω. Thus

$$R(\tau)_{\text{unnormalized}} = \tfrac{1}{2}\int_{-\infty}^{\infty} S_{p_{b\ell}}(|\omega|)\, e^{i\omega\tau}\, d\omega = \pi\int_{-\infty}^{\infty} S_{p_{b\ell}}(|f|)\, e^{i2\pi f\tau}\, df; \qquad \begin{array}{l} -\infty < \omega < \infty \\ -\infty < f < \infty \end{array}$$

$$= \dfrac{\pi\tau_w^2\,\delta^*}{U_\infty}\sum_{j=1}^{3} A_j \int_{-\infty}^{\infty} e^{-K_j F|2\pi f|}\, e^{i2\pi f\tau}\, df = \dfrac{\pi\tau_w^2\,\delta^*}{U_\infty}\sum_{j=1}^{3}\dfrac{A_j K_j F}{\pi[\tau^2 + (K_j F)^2]} = \tau_w^2 \sum_{j=1}^{3}\dfrac{A_j K_j F^2}{\tau^2 + (K_j F)^2}$$

where we have used page 632 in Campbell and Foster[37] with $a = K_j F$.

Hence $R(0) \equiv \langle p_{b\ell}^2\rangle_t = \tau_w^2 \sum_{j=1}^{3}\dfrac{A_j}{K_j}$ which is Equation (110).

Note that $\dfrac{R(\tau)_{\text{unnormalized}}}{R(0)} = R(\tau)_{\text{normalized}}$; see Equation (B8) of Reference 1.

Therefore

$$\langle p_{b\ell}^2 \rangle_t = \frac{\tau_w^2 \delta^*}{U_\infty} \sum_{j=1}^{3} \int_0^\infty A_j e^{-K_j F \omega} \, d\omega = \frac{\tau_w^2 \delta^*}{U_\infty} \sum_{j=1}^{3} \frac{A_j}{F K_j} = \tau_w^2 \sum_{j=1}^{3} \frac{A_j}{K_j}$$

$$\approx 1.296 \times 10^{-5} \rho^2 U_\infty^4 \tag{110}$$

because

$$\sum_{j=1}^{3} \frac{A_j}{K_j} = 6.66 \tag{111a}$$

and*

$$\tau_w = \frac{C_f}{2} \rho U_\infty^2 = \frac{2.78 \times 10^{-3}}{2} \rho U_\infty^2 \tag{111b}$$

Substituting Equations (110) and (111a) and letting $F = \frac{\delta^*}{U_\infty}$ in Equation (109), we get

$$S_{p_{b\ell}}(\bar{x}|\bar{x}';\omega) = 6.11 \times 10^{-6} \rho^2 U_\infty^2 \delta^{*2} e^{\frac{-|\eta|}{U_c \theta}} \sum_{j=1}^{3} A_j K_j \frac{e^{-\sqrt{(K_j F)^2 + (\mu/U_c)^2}\,|\omega| - \frac{i\eta\omega}{U_c}}}{\sqrt{(K_j F)^2 + (\mu/U_c)^2}}$$

$$\tag{111c}$$

C2. WAVENUMBER-FREQUENCY SPECTRUM OF TURBULENCE (BLOCKED) PRESSURE

The wavenumber-frequency spectrum of the blocked pressure is

$$\Phi_{p_{b\ell}}(k_x, k_y;\omega) = \int_{-\infty}^{\infty} \int_{-\infty}^{\infty} S_{p_{b\ell}}(\bar{x}|\bar{x}';\omega) e^{-i(k_x \eta + k_y \mu)} \, d\eta \, d\mu$$

$$= 6.11 \times 10^{-6} \rho^2 U_\infty^2 \delta^{*2} \int_{-\infty}^{\infty} e^{\frac{-|\eta|}{U_c \theta}} e^{-i(\frac{\omega}{U_c} + k_x)\eta} \, d\eta$$

$$\cdot \sum_{j=1}^{3} A_j K_j \int_{-\infty}^{\infty} \frac{e^{-\sqrt{(K_j F)^2 + (\mu/U_c)^2}\,|\omega|}}{\sqrt{(K_j F)^2 + (\mu/U_c)^2}} e^{-i k_y \mu} \, d\mu \tag{112a}$$

---

* $\tau_w^2 = \left[\frac{C_f}{2}\rho U_\infty^2\right]^2 = \frac{\langle p_{b\ell}^2 \rangle_t}{\sum_{j=1}^{3} \frac{A_j}{K_j}} = \frac{\langle p_{b\ell}^2 \rangle_t}{6.66}$. Assuming that $\langle p_{b\ell}^2 \rangle_t = \left[\frac{(7.2 \times 10^{-3})}{2}\rho U_\infty^2\right]^2$ we compute

$C_f = \left[\frac{(7.2 \times 10^{-3})^2}{6.66}\right]^{1/2} \approx 2.78 \times 10^{-3}$.

135

Now

$$\int_{-\infty}^{\infty} e^{\frac{-|\eta|}{U_c\theta}} e^{-i\left(\frac{\omega}{U_c} + k_x\right)\eta} d\eta = \frac{2U_c\theta}{1 + \theta^2(\omega + k_x U_c)^2}; \quad \begin{array}{l} -\infty < \omega < \infty \\ -\infty < k_x < \infty \end{array}$$

and

$$\int_{-\infty}^{\infty} \frac{e^{-|\omega|\sqrt{(K_j F)^2 + (\mu/U_c)^2}}}{\sqrt{(K_j F)^2 + (\mu/U_c)^2}} e^{-ik_y\mu} d\mu = \int_{-\infty}^{\infty} \frac{U_c e^{\frac{-|\omega|}{U_c}\sqrt{(K_j F U_c)^2 + \mu^2}}}{\sqrt{(K_j F U_c)^2 + \mu^2}} e^{-ik_y\mu} d\mu$$

$$= \pi\left[-iH_0^{(2)}\left(\pm iK_j F U_c \sqrt{\left(\frac{|\omega|}{U_c}\right)^2 + k_y^2}\right)\right]U_c; \quad \begin{array}{l} -\infty < \omega < \infty \\ -\infty < k_y < \infty \end{array}$$

$$\rightarrow \pi\left[-iH_0^{(2)}\left(-iK_j F U_c \sqrt{k_y^2 + \left(\frac{|\omega|}{U_c}\right)^2}\right)\right]U_c; \quad \begin{array}{l} -\infty < \omega < \infty \\ -\infty < k_y < \infty \end{array}$$

$$= \pi\left[iH_0^{(1)}\left(iK_j F U_c \sqrt{k_y^2 + \left(\frac{\omega}{U_c}\right)^2}\right)\right]U_c; \quad \begin{array}{l} -\infty < \omega < \infty \\ -\infty < k_y < \infty \end{array}$$

where in evaluating the preceding integral we have used Equation (14b) with $r = K_j F U_c$, $x = \mu$, $t = -k_y$, and $a = \frac{-i|\omega|}{U_c}$. But $a^2 = -\left(\frac{|\omega|}{U_c}\right)^2 = -\left(\frac{\omega}{U_c}\right)^2$. For the argument of $H_0^{(2)}$, we have selected the (–) sign to ensure that $H_0^{(2)} \rightarrow 0$ as $k_y \rightarrow \infty$. Finally we have let the real quantity $-iH_0^{(2)}(-iK_j F U_c) \rightarrow iH_0^{(1)}(iK_j F U_c)$; (see Abramowitz and Stegun,[38] Equation (9.1.39) on page 361). Hence, substituting the evaluated integrals into Equation (112a), with $U_c = 0.8\, U_\infty$, we obtain

$$\Phi_{p_{b\ell}}(k_x, k_y, \omega) = 7.8 \times 10^{-6} \rho^2 U_\infty^4 \delta^{*2} \frac{\theta}{1 + \theta^2(\omega + k_x U_c)^2} \sum_{j=1}^{3} A_j K_j \left[i\pi H_0^{(1)}\left(iK_j F U_c \sqrt{k_y^2 + (\omega/U_c)^2}\right)\right]$$

$$\begin{array}{l} ; -\infty < \omega < \infty \\ \quad -\infty < k_x < \infty \\ \quad -\infty < k_y < \infty \end{array} \tag{112b}$$

C3. JOINT AND CROSS ACCEPTANCE FUNCTIONS

The joint and cross acceptance functions are defined by the following equations with $t = n$ and $t \neq n$ respectively

$$j_{tn}^2 = \frac{1}{A_p^2} \frac{1}{S_{p_{b\ell}}(\omega)} \int_{A_p} \int_{A_p'} S_{p_{b\ell}}(\bar{x}|\bar{x}';\omega)\, \psi^t(\bar{x})\, \psi^n(\bar{x}')\, d\bar{x} d\bar{x}' \tag{113}$$

$$= \frac{1}{A_p^2} \frac{1}{S_{p_{b\ell}}(\omega)} \int_{-\infty}^{\infty} \int_{-\infty}^{\infty} \Phi_{p_{b\ell}}(k_x, k_y;\omega) \left[\int_{A_p} \psi^t(\bar{x}) e^{ik_x\eta} d\bar{x}\right] \left[\int_{A_p'} \psi^n(\bar{x}') e^{ik_y\mu} d\bar{x}'\right] dk_x dk_y$$

136

where we have used Equation (112a) to write $S_{p_{b\ell}}(\omega)$ in terms of its Fourier transform $\Phi_{p_{b\ell}}$ and interchanged the $d\bar{x}\, d\bar{x}'$ and $dk_x\, dk_y$ integrals. From Equations (50) and (51) this equation can be written as

$$j_{tn}^2 = \frac{1}{A_p^2 S_{p_{b\ell}}(\omega)} \int_{-\infty}^{\infty} \int_{-\infty}^{\infty} \Phi_{p_{b\ell}}(k_x,k_y;\omega) \left[\int_{A_p'} \psi^n(\bar{x}') e^{-i(k_x x' + k_y y')} d\bar{x}' \right]$$

$$\cdot \left[\int_{A_p} \psi^t(\bar{x}) e^{+i(k_x x + k_y y)} d\bar{x} \right] dk_x\, dk_y$$

$$= \frac{1}{A_p^2 S_{p_{b\ell}}(\omega)} \int_{-\infty}^{\infty} \int_{-\infty}^{\infty} \Phi_{p_{b\ell}}(k_x,k_y;\omega)\, S_n(k_x,k_y)\, S_t^*(k_x,k_y)\, dk_x\, dk_y \qquad (114)$$

where $S_n(k_x,k_y)$ represents $S_{mn}(k_x,k_y)$ and $S_t(k_x,k_y)$ represents $S_{qr}(k_x,k_y)$, i.e., n→mn, t → qr, tn → mnqr in general. If t = n then tn → nn → mnmn.

JOINT ACCEPTANCES

Substituting Equations (52e) and (112b) into (114) gives the following equation for the joint acceptances; note that the joint acceptances defined by setting t = n implies that the mode numbers m = q, n = r in Equation (52e).

$$j_{tn}^2(\omega) \to j_{nn}^2(\omega) \equiv j_{mnmn}^2(\omega) = \frac{9.81 \times 10^{-5}\, \rho^2 U_\infty^4 \delta^{*2} k_m^2 k_n^2\, \theta}{A_p^2 S_{p_{b\ell}}(\omega)}$$

$$\cdot \int_{-\infty}^{\infty} \frac{[1 - (-1)^m \cos k_x a]\, dk_x}{(k_x^2 - k_m^2)^2\, [1 + \theta^2(\omega + k_x U_c)^2]} \sum_{j=1}^{3} A_j K_j$$

$$\cdot \int_{-\infty}^{\infty} \frac{[1 - (-1)^n \cos k_y b] \left[iH_0^{(1)}\left(iK_j F U_c \sqrt{k_y^2 + (\omega/U_c)^2}\right) \right]}{(k_y^2 - k_n^2)^2} dk_y \qquad (115)$$

$$; -\infty < \omega < \infty$$
$$; -\infty < k_x < \infty$$
$$; -\infty < k_y < \infty$$

Hence using the approximations (since $-\infty < k_x < \infty$, $-\infty < k_y < \infty$)

$$\frac{[1-(-1)^m \cos k_x a]}{(k_x^2 - k_m^2)} \approx \frac{\pi a}{4k_m^2} \delta(k_x \pm k_m) = \frac{\pi a}{4k_m^2}\left[\delta(k_x+k_m) + \delta(k_x-k_m)\right]$$

$$\frac{[1-(-1)^n \cos k_y b]}{(k_y^2 - k_n^2)^2} \approx \frac{\pi a}{4k_n^2} \delta(k_y \pm k_n) = \frac{\pi b}{4k_n^2}\left[\delta(k_y + k_n) + \delta(k_y-k_n)\right]$$

we have for the first integral in Equation (115)

$$\int_{-\infty}^{\infty} \frac{[1-(-1)^m \cos k_x a]\, dk_x}{(k_x^2 - k_m^2)^2\, [1 + \theta^2(\omega + k_x U_c)^2]} = \int_{-\infty}^{0} \frac{\pi a}{4k_m^2} \frac{\delta(k_x + k_m)}{[1 + \theta^2 (\omega + k_x U_c)^2]}\, dk_x + \int_{0}^{\infty} \frac{\pi a}{4k_m^2} \frac{\delta(k_x - k_m)}{[1 + \theta^2 (\omega + k_x U_c)^2]}\, dk_x$$

$$= \frac{\pi a}{4k_m^2}\left[\frac{1}{1 + \theta^2 (\omega - k_m U_c)^2} + \frac{1}{1 + \theta^2 (\omega + k_m U_c)^2}\right]$$

$$\approx \frac{\pi a}{2k_m^2} \frac{1}{1 + \theta^2 (\omega - k_m U_c)^2}$$

because in treating the wavenumber-frequency spectrum for the turbulence pressures outside of

the convection region, i.e., in the low wavenumber region, we assume $k_m \ll \frac{\omega}{U_c}$ so that

both of the foregoing integrals are nearly equal,* or

$$\frac{1}{1 + \theta^2 (\omega - k_m U_c)^2} + \frac{1}{1 + \theta^2 (\omega + k_m U_c)^2} \approx \frac{2}{1 + \theta^2 (\omega - k_m U_c)^2} \quad (116a)$$

For the second integral in Equation (115) we have

$$\int_{-\infty}^{\infty} \frac{[1 - (-1)^n \cos k_y b]}{(k_y^2 - k_n^2)^2} \left[iH_0^{(1)}\left(iK_j FU_c\sqrt{k_y^2 + (\tfrac{\omega}{U_c})^2}\right)\right] dk_y$$

$$= \frac{\pi b}{4k_n^2}\int_{-\infty}^{0} \delta(k_y + k_n)\left[iH_0^{(1)}\left(ik_j FU_c\sqrt{k_y^2 + (\tfrac{\omega}{U_c})^2}\right)\right]dk_y + \frac{\pi b}{4k_n^2}\int_{0}^{\infty} \delta(k_y - k_n)\left[iH_0^{(1)}\left(ik_j FU_c\sqrt{k_y^2 + (\tfrac{\omega}{U_c})^2}\right)\right]dk_y$$

*But within the convected region, the first integral predominates. For if $\omega > 0$, then a maximum occurs at

$k_x = \frac{-\omega}{U_c} = -k_m$ and if $\omega < 0$, a maximum occurs at $k_x = \frac{-\omega}{U_c} = k_m$; see Figure 9 of Reference 1.

$$= \frac{\pi b}{2 k_n^2} \ i H_o^{(1)} \left(i k_j F U_c \sqrt{k_n^2 + \left(\frac{\omega}{U_c}\right)^2} \right)$$

Substituting the preceding integral evaluations as well as Equations (109b) and (111b) into Equation (115), we obtain

$$j_{mnmn}^2 = 125.4 \left(\frac{U_\infty \delta^* \theta}{A_p} \right) \frac{\sum\limits_{j=1}^{3} A_j K_j \left[i H_o^{(1)} \left(i K_j F U_c \sqrt{k_n^2 + \left(\frac{\omega}{U_c}\right)^2} \right) \right]}{\left[1 + \theta^2 (\omega - k_m U_c)^2 \right] \left[\sum\limits_{j=1}^{3} A_j \ e^{\frac{-K_j \delta^* \omega}{U_c}} \right]} \tag{116b}$$

CROSS ACCEPTANCES

We now show that the cross acceptances can be neglected for slow speed flows. Substituting Equations (52e) and (112b) into (114) gives the following equation for the cross acceptances; $k_m \neq k_q$; $k_n \neq k_r$.

$$j_{tn}^2(\omega) \equiv j_{mnqr}^2(\omega) = \frac{9.81 \times 10^{-5} \ \rho^2 U_\infty^4 \ k_m k_n k_q k_r \ \theta}{A_p^2 \ S_{p_{b\ell}}(\omega)} \int\limits_{-\infty}^{\infty} \frac{\left[1 - (-1)^m \cos k_x a \right] dk_x}{(k_x^2 - k_m^2)(k_x^2 - k_q^2) \left[1 + \theta^2 (\omega + k_x U_c)^2 \right]}$$

$$\cdot \sum\limits_{j=1}^{3} A_j K_j \int\limits_{-\infty}^{\infty} \frac{\left[1 - (-1)^n \cos k_y b \right] \left[i H_o^{(1)} \left(i K_j F U_c \sqrt{k_y^2 + \left(\frac{\omega}{U_c}\right)^2} \right) \right] dk_y}{(k_y^2 - k_n^2)(k_y^2 - k_r^2)}$$

where

$$- \infty < \omega < \infty$$

$$- \infty < k_x < \infty$$

$$- \infty < k_y < \infty \tag{117a}$$

Write the first integral for $k_m < k_q$ as the sum of two integrals $\int\limits_{-\infty}^{0} + \int\limits_{0}^{\infty}$ and let $k_x \rightarrow -k_x$ in

in the $\int\limits_{-\infty}^{0}$ integral only.

139

$$\int_{-\infty}^{\infty} \frac{[1-(-1)^m \cos k_x a] \, dk_x}{(k_x^2-k_m^2)(k_x^2-k_q^2) \, [1+\theta^2(\omega+k_x U_c)^2]} = \int_{-\infty}^{0} \frac{[1-(-1)^m \cos k_x a] \, dk_x}{(k_x^2-k_m^2)(k_x^2-k_q^2) \, [1+\theta^2(\omega+k_x U_c)^2]}$$

$$+ \int_{-0}^{\infty} \frac{[1-(-1)^m \cos k_x a] \, dk_x}{(k_x^2-k_m^2)(k_x^2-k_q^2) \, [1+\theta^2(\omega+k_x U_c)^2]}$$

$$= \int_{0}^{\infty} \frac{[1-(-1)^m \cos k_x a]}{(k_x^2-k_m^2)(k_x^2-k_q^2)} \left[\frac{1}{1+\theta^2(\omega-k_x U_c)^2} + \frac{1}{1+\theta^2(\omega+k_x U_c)^2} \right] dk_x \qquad (117b)$$

$$= \int_{0}^{k'} [\;] \, dk_x + \int_{k'}^{\infty} [\;] \, dk_x$$

where [ ] is the integrand of Equation (117b). Physically we are concerned with slow-speed flows. Thus we conveniently select the common limit k' greater than k but somewhat smaller than $\frac{\omega}{U_c}$; i.e., $k_m < k_q < k' < \frac{\omega}{U_c}$.

For the first integral, the range of integration for the variable k_x is $0 < k_x < k'$. Since $k'U_c < \omega$ implies $k_x U_c < \omega$, the integral reduces as an approximation to

$$\frac{2}{1+\theta^2\omega^2} \int_{0}^{k'} \frac{[1-(-1)^m \cos k_x a] \, dk_x}{(k_x^2-k_m^2)(k_x^2-k_q^2)} \qquad : \quad k_m \neq k_q$$

which is negligible compared to the first integral in Equation (115); note that $\frac{2}{1+\theta^2\omega^2} < 2$.

For the second integral, the range of integration for the variable k_x is $k' < k_x < \infty$ where k' is chosen slightly less than $\frac{\omega}{U_c}$. For $k_m < k_q < k' < k_x < \infty$, the integral is

$$\int_{k'}^{\infty} \frac{[1-(-1)^m \cos k_x a]}{(k_x^2-k_m^2)(k_x^2-k_q^2)} \left[\frac{1}{1+\theta^2(\omega-k_x U_c)^2} + \frac{1}{1+\theta^2(\omega+k_x U_c)^2} \right] dk_x$$

Since $(k_x^2-k_m^2)(k_x^2-k_q^2) \approx k_x^4$ and $\int_{k'}^{\infty} [\;] \, dk_x$ is a maximum at $\omega=k_x U_c$, then the integral

reduces as an approximation to

140

$$\frac{2(1+2\omega^2\theta^2)}{1+4\omega^2\theta^2} \int_{k'}^{\infty} \frac{[1-(-1)^m\cos k_x a]}{k^4} dk_x$$

which is negligible compared to the first integral in Equation (115); note that $\frac{2(1+2\omega^2\theta^2)}{1+4\omega^2\theta^2} < 2$.

Similarly, the second integral in Equation (117a) is negligible for $k_n \neq k_r$.

Hence in subsequent analyses the cross acceptance functions will be assumed to be identically zero.

APPENDIX D

EQUATIONS USED IN COMPUTER PROGRAM*

D1. CROSS-SPECTRAL DENSITY OF PLATE DISPLACEMENT

Substituting Equation (113) into (37) and (116b) together with (109b) and (111b) into the resulting equation we get (note: ignoring cross acceptances, $j_{tn} \rightarrow j_{nn} \equiv j_{mnmn}$, i.e., $t \equiv n \rightarrow mn$. Also $r \rightarrow qr$, $1 \rightarrow kl$.)

$$S_w(x,y|x',y';\omega) = \sum_{q,r} \sum_{m,n} \sum_{k,l} \sum_{m,n} \bar{a}_{qrmn} \psi^{qr}(x,y) \bar{a}^*_{klmn} \psi^{kl}(x',y') \left[j^2_{mnmn} A_p^2 S_{p_{bl}}^{(\omega)} \right]$$

$$= 125.4 \, A_p^2 \left(\frac{U_\infty \delta^* \Theta}{A_p} \right) \sum_{m,n} \frac{\sum_{j=1}^{3} A_j K_j \left[iH_o^{(1)} \left(iK_j FU_c \sqrt{k_n^2 + \left(\frac{\omega}{U_c}\right)^2} \right) \right]}{\left[1 + \Theta^2 \left(\omega - k_m U_c \right)^2 \right]} \left[\frac{S_{p_{bl}}^{(\omega)}}{\sum_{j=1}^{3} A_j e^{-\frac{K_j \delta^* \omega}{U_c}}} \right]$$

$$\bullet \sum_{q,r} \bar{a}_{qrmn} \psi^{qr}(x,y) \sum_{k,l} \bar{a}^*_{klmn} \psi^{kl}(x',y')$$

$$= 2.42 \times 10^{-4} \rho^2 U_\infty^4 \delta^{*2} A_p O \sum_{m,n} \frac{\sum_{j=1}^{3} A_j K_j \left[iH_o^{(1)} \left(iK_j FU_c \sqrt{k_n^2 + \left(\frac{\omega}{U_c}\right)^2} \right) \right]}{\left[1 + \Theta^2 \left(\omega - k_m U_c \right)^2 \right]}$$

$$\bullet \sum_{q,r} \bar{a}_{qrmn} \psi^{qr}(x,y) \sum_{k,l} \bar{a}^*_{klmn} \psi^{kl}(x',y') \qquad (118)$$

D2. CROSS-SPECTRAL DENSITY OF PRESSURE IN THE CAVITY

Substituting Equations (37) and (113) into Equation (38) and then (116b) together with Equations (109b) and (111b) in the resulting equation we get (note: ignoring cross acceptances, $j_{tn} \rightarrow j_{nn} \equiv j_{mnmn}$. Also $r \rightarrow qr$, $1 \rightarrow kl$ and $\bar{\xi} \equiv x,y,z \equiv \bar{x},z$; $\bar{\xi}' \equiv x',y',z' \equiv \bar{x}',z'$)

---

*All of the working equations developed in this appendix have been programmed for digital computation except Equations (124) and (125) in Section D5.

Preceding page blank

$$S_{p_i}(x,y,z|x',y',z';\omega) = \rho_c \omega^4 \sum_{q,r} \sum_{m,n} \sum_{k,l} \sum_{m,n} \bar{a}_{qrmn} \, \bar{a}^*_{klmn}$$

$$\bullet \; j^2_{mnmn} \, A_p^2 \, S_{p_{bl}}(\omega) \int_{A_p} G_p^*(\bar{x}|\bar{\xi};\omega) \, \psi^{qr}(\bar{x}) \, d\bar{x} \int_{A'_p} G_p(\bar{x}'|\bar{\xi}';\omega) \, \psi^{kl}(\bar{x}') \, d\bar{x}'$$

$$= 125.4 \left(\frac{U_\infty \delta^* O}{A_p} \right) \left(A_p^2 \, \rho_c^2 \, \omega^4 \right) \sum_{m,n} \frac{\sum_{j=1}^{3} A_j K_j \left[i H_o^{(1)} \left(i K_j F U_c \sqrt{k_n^2 + \left(\frac{\omega}{U_c} \right)^2} \right) \right]}{\left[1 + \Theta^2 \left(\omega - k_m U_c \right)^2 \right]}$$

$$\bullet \left[\frac{S_{p_{bl}}(\omega)}{\sum_{j=1}^{3} A_j \, e^{-\frac{k_j \delta^* \omega}{U_c}}} \right]$$

$$\bullet \sum_{q,r} \sum_{k,l} \bar{a}_{qrmn} \, \bar{a}^*_{klmn} \int_{A_p} G_p^*(\bar{x}|\bar{\xi};\omega) \, \psi^{qr}(\bar{x}) \, d\bar{x} \int_{A'_p} G_p(\bar{x}'|\bar{\xi}') \, \psi^{kl}(\bar{x}') \, d\bar{x}'$$

$$= 2.42 \times 10^{-4} \, \rho^2 \rho_c^2 U_\infty^4 A_p \delta^{*2} \omega^4 O \sum_{m,n} \frac{\sum_{j=1}^{3} A_j K_j \left[i H_o^{(1)} \left(i K_j F U_c \sqrt{k_n^2 + \left(\frac{\omega}{U_c} \right)^2} \right) \right]}{\left[1 + \Theta^2 \left(\omega - k_m U_c \right)^2 \right]}$$

$$\bullet \sum_{q,r} \sum_{k,l} \bar{a}_{qrmn} \, \bar{a}^*_{klmn} \int_{A_p} G_p^*(\bar{x}|\bar{\xi};\omega) \, \psi^{qr}(\bar{x}) \, d\bar{x} \int_{A'_p} G_p(\bar{x}'|\bar{\xi}';\omega) \, \psi^{kl}(\bar{x}') \, d\bar{x}'$$

We evaluate the integrals in the preceding equation by use of Equations (52a,b) and (105b), observing that for $G_p(\bar{x}'|\bar{\xi}')$ the symbol $\bar{x}' \equiv x', y'$ represents a source point on the surface $z' = 0$, whereas $\bar{\xi}' = x', y', z'$ is a field point in the interior of the cavity.

$$\int_{A'_p} G_p(\bar{x}'|\bar{\xi}') \, \psi^{kl}(\bar{x}') \, d\bar{x}'$$

$$= \frac{1}{V} \sum_{a,\beta,\gamma=0} \frac{\epsilon_a \epsilon_\beta \epsilon_\gamma \left[\left(\lambda_n^2 - \Lambda_n^2 - k_c^2 \right) + i 2 \lambda_n \Lambda_n \right] \cos \frac{a\pi x}{a} \cos \frac{\beta\pi y}{b} \cos \frac{\gamma\pi z}{c}}{\left(\lambda_n^2 - \Lambda_n^2 - k_c^2 \right) + 4 \lambda_n^2 \Lambda_n^2}$$

$$\bullet \left[\int_o^a \sin \frac{k\pi x'}{a} \cos \frac{a\pi x'}{a} \, dx' \right] \left[\int_o^b \sin \frac{l\pi y'}{b} \cos \frac{\beta\pi y'}{b} \, dy' \right]$$

$$= \frac{A_p A_{ka} A_{l\beta}}{4\pi^2 V} \sum_{a,\beta,\gamma=0} \frac{\epsilon_a \epsilon_\beta \epsilon_\gamma \left[\left(\lambda_n^2 - \Lambda_n^2 - k_c^2 \right) + i2\lambda_n \Lambda_n \right] \cos \frac{a\pi x}{a} \cos \frac{\beta\pi y}{b} \cos \frac{\gamma\pi z}{c}}{\left(\lambda_{a,\beta,\gamma}^2 - \Lambda_{a,\beta,\gamma}^2 - k_c^2 \right) + 4 \lambda_{a,\beta,\gamma}^2 \Lambda_{a,\beta,\gamma}^2}$$

where A_{ka}, $A_{l\beta}$ are obtained from Equation (107).

$\int_{A_p} G_p^* (\bar{x}|\bar{\xi};\omega) \psi^{qr}(\bar{x}) d\bar{x}$ is evaluated from the foregoing result by letting $i \to -i$,

$k \to q$, $1 \to r$ and $x,y,z \longrightarrow x',y',z'$, respectively, and $a,\beta,\gamma \longrightarrow a',\beta',\gamma'$, respectively. Observe that for $G_p^* (\bar{x}|\bar{\xi})$, the symbol $\bar{x} \equiv x,y$ represents a source point on the surface $z = 0$ whereas $\bar{\xi} = x,y,z$ is a field point in the interior of the cavity. Substituting the evaluated integrals into the equation for $S_{p_i} (x,y,z|x',y',z';\omega)$, we get the cross-spectral density of the cavity pressures of any two field points in the cavity located at x,y,z and x',y',z', respectively.

$$S_{p_i} (x,y,z|x',y',z';\omega) = 1.55 \times 10^{-7} \left(\frac{\rho^2 \rho_c^2 U_\infty^4 A_p^3 \delta^{*2} \omega^4 \Theta}{V^2} \right)$$

$$\bullet \left\{ \sum_{q,r} \sum_{k,l} \sum_{m,n} \bar{a}_{qrmn} \bar{a}_{klmn}^* \frac{\sum_{j=1}^{3} A_j K_j \left[iH_0^{(1)} \left(iK_j FU_c \sqrt{k_n^2 + \left(\frac{\omega}{U_c} \right)^2} \right) \right]}{\left[1 + \Theta^2 \left(\omega - k_m U_c \right)^2 \right]} \right.$$

$$\bullet \sum_{a,\beta,\gamma=0}^{\infty} \sum_{a',\beta',\gamma'=0}^{\infty} \frac{\epsilon_a \epsilon_\beta \epsilon_\gamma \epsilon_{a'} \epsilon_{\beta'} \epsilon_{\gamma'} \left[\left(\lambda_{a\beta\gamma}^2 - \Lambda_{a\beta\gamma}^2 - k_c^2 \right) + i2\lambda_{a\beta\gamma} \Lambda_{a\beta\gamma} \right]}{\left[\left(\lambda_{a\beta\gamma}^2 - \Lambda_{a\beta\gamma}^2 - k_c^2 \right)^2 + 4 \lambda_{a\beta\gamma}^2 \Lambda_{a\beta\gamma}^2 \right]}$$

$$\bullet \frac{\left[\left(\lambda_{a'\beta'\gamma'}^2 - \Lambda_{a'\beta'\gamma'}^2 - k_c^2 \right)^2 - i2 \lambda_{a'\beta'\gamma'} \Lambda_{a'\beta'\gamma'} \right]}{\left[\left(\lambda_{a'\beta'\gamma'}^2 - \Lambda_{a'\beta'\gamma'}^2 - k_c^2 \right)^2 + 4 \lambda_{a'\beta'\gamma'}^2 \Lambda_{a'\beta'\gamma'}^2 \right]}$$

$$\bullet A_{ka} A_{l\beta} A_{qa'} A_{r\beta'} \cos \frac{a\pi x}{a} \cos \frac{\beta\pi y}{b} \cos \frac{\gamma\pi z}{c}$$

$$\bullet \left. \cos \frac{a\pi x'}{a} \cos \frac{\beta\pi y'}{b} \cos \frac{\gamma\pi z'}{c} \right\} \qquad (119)$$

When $x',y',z' \equiv x,y,z$, the power spectral density of the pressure in the cavity is represented by the real part of equation (119).

D3. SPECTRAL DENSITY OF POWER RADIATED INTO THE HALF-SPACE

Substituting Equations (46) and (113) into (42) and then (116b) together with Equations (109b) and (111b) into the resulting equation, we get (note: ignoring cross acceptances, $j_{tn} \rightarrow j_{mn} \equiv j_{mnmn}$, also $s \equiv l \rightarrow kl$, i.e., $\psi^s(\bar{x}) \rightarrow \psi^l(\bar{x}^l) \equiv \psi^{kl}(\bar{x}^l)$ since $\bar{x} \rightarrow \bar{x}^l$, also $r \rightarrow qr$.)

$$W_{rad}^{ext}(\omega) = i\rho\omega^3 A_p^2 S_{p_{bl}}(\omega) \sum_{m,n} \sum_{q,r} \sum_{k,l} \bar{a}_{qrmn} \bar{a}_{klmn}^* \cdot \bar{J}^{qrkl}(\omega) j_{mnmn}^2(\omega) \quad (120)$$

$$= 125.4 \left(\frac{U_\infty \delta^* \Theta}{A_p}\right) i\rho\omega^3 A_p^2 \sum_{m,n} \frac{\sum_{j=1}^{3} A_j K_j \left[iH_0^{(1)} \left(iK_j F U_c \sqrt{k_n^2 + \left(\frac{\omega}{U_c}\right)^2}\right)\right]}{\left[1 + \Theta^2 \left(\omega - k_m U_c\right)^2\right]}$$

$$\bullet \left[\frac{S_{p_{bl}}(\omega)}{\sum_{j=1}^{3} A_j e^{-\frac{K_j \delta^* \omega}{U_c}}}\right]$$

$$= 2.42 \times 10^{-4} i\rho^3 \omega^3 A_p U_\infty^4 \delta^{*2} \Theta \sum_{m,n} \frac{\sum_{j=1}^{3} A_j K_j \left[iH_0^{(1)} \left(iK_j F U_c \sqrt{k_n^2 + \left(\frac{\omega}{U_c}\right)^2}\right)\right]}{\left[1 + \Theta^2 \left(\omega - k_m U_c\right)^2\right]}$$

$$\bullet \sum_{q,r} \bar{a}_{qrmn}(\omega) \sum_{k,l} \bar{a}_{klmn}^*(\omega) \bar{J}^{qrkl}(\omega) \quad (121)$$

where $\bar{J}^{qrkl}$ has been evaluated for various interacting modes in Appendix B.

The real part* of Equation (121) represents the real power radiated into half-space. The imaginary part represents the reactive power generated in the half-space.

D4. CROSS-SPECTRAL DENSITY OF PRESSURE IN THE HALF-SPACE

Substituting Equation (37) and (113) into (43a) and then Equations (116b), (109b), and (111b) into the resulting equation, we get (note: ignoring cross acceptances, $j_{tn} \longrightarrow j_{nn} \equiv j_{mnmn}$. Also $\bar{\xi} = x,y,z$; $\bar{\xi}' = x',y',z'$ represent separate points in the half-space and $r \rightarrow qr$, $l \rightarrow kl$).

---

*Note: $Re[i(a + ib)] = Re[ia - b] = -b = \mathcal{J}m(a + ib)$.

$$S_{p_2}(\bar{\xi}|\bar{\xi}';\omega) = \frac{\rho^2\omega^4}{(2\pi)^4}A_p^2 S_{p_{bl}}^{(\omega)} \sum_{q,r}\sum_{k,l}\sum_{m,n} a_{qrmn}\,\bar{a}_{klmn}^*$$

$$\bullet\left[\int_{A_p} G_p^{o*}(\bar{x}|\bar{\xi};\omega)\,\psi^{qr}(\bar{x})\,d\bar{x}\right]\left[\int_{A_p'} G_p^o(\bar{x}'|\bar{\xi}';\omega)\,\psi^{kl}(\bar{x}')\,d\bar{x}'\right]J_{mnmn}^2$$

$$= \frac{\rho^2\omega^4}{(2\pi)^4}A_p^2 \sum_{q,r}\sum_{k,l}\sum_{m,n}\bar{a}_{qrmn}\,\bar{a}_{klmn}^*\left[\int_{A_p} G_p^{o*}(\bar{x}|\bar{\xi};\omega)\,\psi^{qr}(\bar{x})\,d\bar{x}\right]$$

$$\bullet\left[\int_{A_p'} G_p^o(\bar{x}'|\bar{\xi}';\omega)\,\psi^{kl}(\bar{x}')\,dx^{-1}\right]\left[125.4\left(\frac{U_\infty\delta^*\Theta}{A_p}\right)\right]$$

$$\bullet\frac{\sum_{j=1}^{3}A_jK_j\left[iH_o^{(1)}\left(iK_jFU_c\sqrt{k_n^2+\left(\frac{\omega}{U_c}\right)^2}\right)\right]}{\left[1+\Theta^2\left(\omega-k_mU_c\right)^2\right]}\left[\frac{S_{p_{bl}}^{(\omega)}}{\sum_{j=1}^{3}A_j\,e^{-\frac{K_j\delta^*\omega}{U_c}}}\right]$$

$$= 1.55\times10^{-7}\rho^4\omega^4A_pU_\infty^4\delta^{*2}\Theta\sum_{q,r}\sum_{k,l}\sum_{m,n}\bar{a}_{qrmn}\,\bar{a}_{klmn}^*$$

$$\bullet\left[\int_{A_p} G_p^{o*}(\bar{x}|\bar{\xi};\omega)\,\psi^{qr}(\bar{x})\,d\bar{x}\right]\left[\int_{A_p'} G_p^o(\bar{x}'|\bar{\xi}';\omega)\,\psi^{kl}(\bar{x}')\,d\bar{x}'\right]$$

$$\bullet\frac{\sum_{j=1}^{3}A_jK_j\left[iH_o^{(1)}\left(iK_jFU_c\sqrt{k_n^2+\left(\frac{\omega}{U_c}\right)^2}\right)\right]}{\left[1+\Theta^2\left(\omega-k_mU_c\right)^2\right]}\tag{122}$$

We consider the expression for $S_{p_2}(\bar{\xi}|\bar{\xi}';\omega)$ given by Equation (122) for the *far field* ($r \gg a,b$) only and use the half-space expression for $G_p^o(\bar{x},z|\bar{x}',o) \equiv G_p^o(\bar{\xi}|\bar{x}',o) \equiv G_p^o(\bar{\xi}|\bar{x}')$ given by Equation (15) with M = o, u = x - x', κ = k and* $R_{yz} = z^2 + (y - y')^2$ (note Equation (15) is *not identical* to Equation (47)). The latter is a special case of

---

*In Equation (15) let R → R_{yz} to symbolically indicate, the dependence of R on y, y' and z only. This contrasts with the definition for R introduced here (below) which is dependent on the coordinates of the field point anywhere in the half-space. Thus we will avoid ambiguity in definition and interpretation of R defined earlier and now.

Equation (15) for $M = 0$, $z = 0$). Thus, here

$$G_p^o\ (\bar{x}'|\bar{\xi}';\omega) = \frac{-2\pi i\ e^{ikr}}{r}$$

where (see Figure 21)

$$r = \sqrt{\left(x_p - x'\right)^2 + R_{yz}^2} = \sqrt{\left(x_p' - x'\right)^2 + \left(y_p - y'\right)^2 + (0 - z')^2}$$

The subscript "p" denotes values of the coordinates at any point *on the plate*. Now, as shown on page 70–71 of Leibowitz[5]

$$r \approx R - \bar{r}_0 \bullet \bar{r}_j$$

where $R^2 = x'^2 + y'^2 + z'^2$ and $\bar{r}_0$ is a unit vector along R. Thus

$$\bar{r}_0 = \bar{i}\,\frac{x'}{R} + \bar{j}\,\frac{y'}{R} + \bar{k}\,\frac{z'}{R}$$

where

$$\frac{x'}{R} = \cos\Theta_1 \quad ; \quad \frac{y'}{R} = \cos\Theta_2 \quad ; \quad \frac{z'}{R} = \cos\Theta_3$$

also

$$\bar{r}_j = \bar{i}x_p + \bar{j}y_p + 0 \cdot z$$

Thus, approximately

$$r = R - \left(\bar{i}\,\frac{x'}{R} + \bar{j}\,\frac{y'}{R} + \bar{k}\,\frac{z'}{R}\right)\left(\bar{i}x_p + \bar{j}y_p + \bar{k} \cdot 0\right)$$

$$= R - \left[x_p\left(\frac{x'}{R}\right) + y_p\left(\frac{y'}{R}\right)\right]$$

and

$$G_p^o\ (\bar{x}'|\bar{\xi}';\omega) = \frac{-2\pi i}{R}\ e^{ikR}\ e^{-ik\frac{x'}{R}x_p}\ e^{-ik\frac{y'}{R}y_p}$$
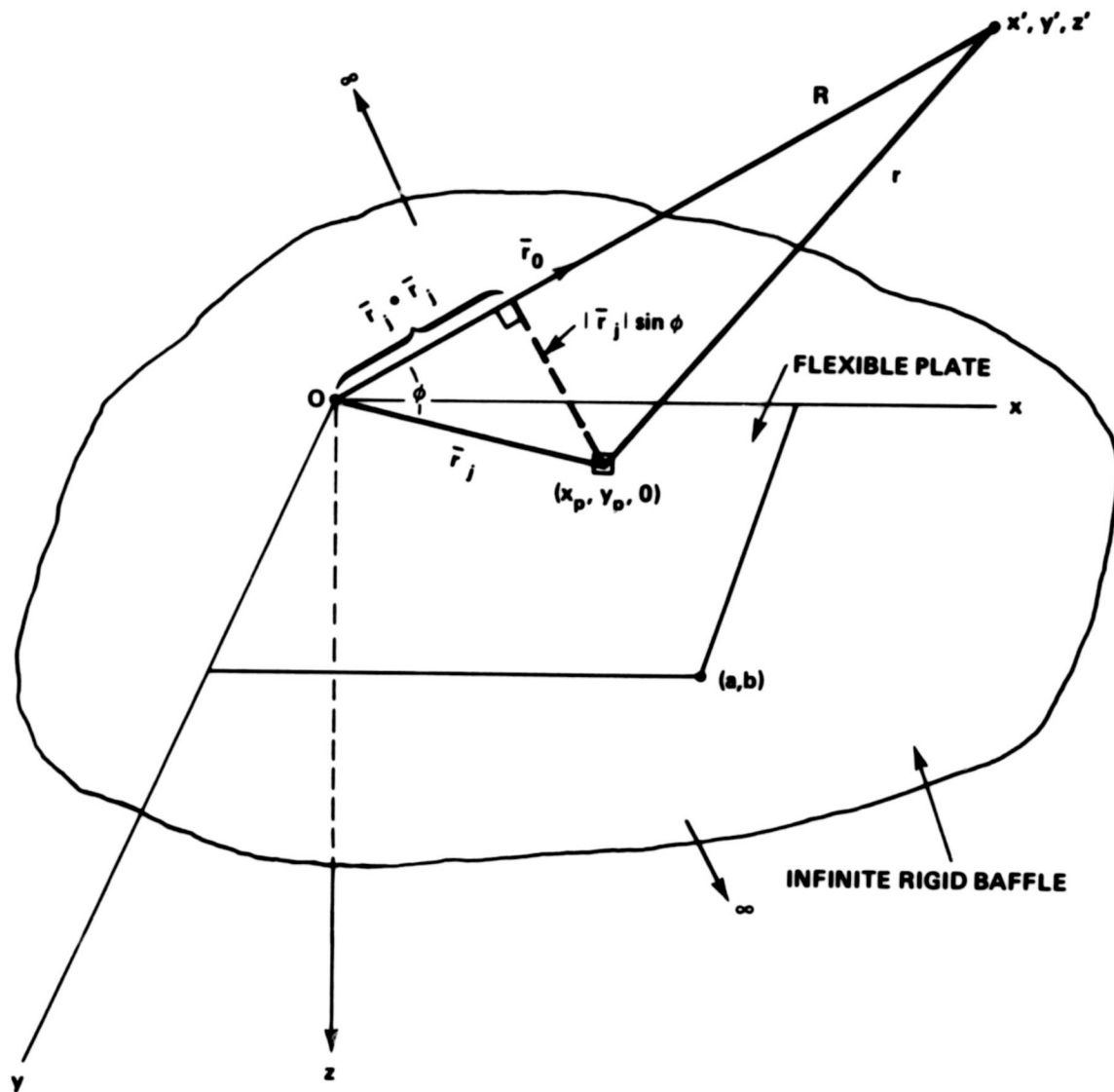
Figure 21 – Coordinate System Showing Vector Relationships

We now use the preceding material to evaluate the integrals in Equation (122).

We let the acoustic wavenumber $k \to k_o = \dfrac{\omega}{c_o}$ to differentiate between the acoustic wavenumber k and the index k. Hence*

$$\int_{A_p} G_p^o(\bar{x}'|\bar{\xi}';\omega)\,\psi^{kl}(\bar{x}')\,d\bar{x}'$$

$$= \frac{-2\pi i\ e^{ik_o R}}{R} \int_0^a \int_0^b e^{-\frac{ik_o x'}{R}x_p} \sin\frac{k\pi x_p}{a}\, e^{-\frac{ik_o y'}{R}y_p} \sin\frac{l\pi y_p}{b}\, dx_p\, dy_p$$

$$= \frac{-2\pi i\ e^{ik_o R}}{R} \int_0^a e^{-\frac{ik_o x'}{R}x_p} \sin\frac{k\pi x_p}{a}\, dx_p \int_0^b e^{-\frac{ik_o y'}{R}y_p} \sin\frac{l\pi y_p}{b}\, dy_p$$

From Korn and Korn[30] (see their Equation (461), page 967)

$$\int e^{ax_p} \sin\beta x_p\, dx_p = \frac{e^{ax_p}}{a^2+\beta^2}(a\sin\beta x_p - \beta\cos\beta x_p)$$

Let $a = \dfrac{-ik_o x'}{R}$ and $\beta = \dfrac{k\pi}{a}$, then

$$I_1 = \int_0^a e^{-\frac{ik_o x'}{R}x_p} \sin\frac{k\pi x_p}{a}\, dx_p = \left\{ \frac{e^{-\frac{ik_o x'}{R}x_p}}{-\left(\frac{k_o x'}{R}\right)^2 + \left(\frac{k\pi}{a}\right)^2} \left[\frac{-ik_o x'}{R}\sin\frac{k\pi x_p}{a} - \frac{k\pi}{a}\cos\frac{k\pi x_p}{a}\right] \right\}_0^a$$

$$= \frac{e^{-\frac{ik_o x'}{R}a}}{\left[\left(\frac{k\pi}{a}\right)^2 - \left(\frac{k_o x'}{R}\right)^2\right]}\left[o - \frac{k\pi}{a}(-1)^k\right] - \frac{\left[o - \frac{k\pi}{a}\right]}{\left[\left(\frac{k\pi}{a}\right)^2 - \left(\frac{k_o x'}{R}\right)^2\right]}$$

$$= \frac{\frac{k\pi}{a}}{\left[\left(\frac{k\pi}{a}\right)^2 - \left(\frac{k_o x'}{R}\right)^2\right]}\left[1 - (-1)^k\ e^{-\frac{ik_o x'}{R}a}\right]$$

---

*In the denominator of $G_p^o(x'|\xi';\omega)$, we let $r \to R$ with small error.

Similarly

$$I_2 = \int_o^b e^{-\frac{ik_oy'}{R}\,y_p}\,\sin\frac{l\pi y_p}{b}\,dy_p = \frac{\frac{k\pi}{b}}{\left[\left(\frac{k\pi}{b}\right)^2 - \left(\frac{k_oy'}{R}\right)^2\right]}\left[1 - (-1)^\ell\,e^{-\frac{ik_oy'}{R}\,b}\right]$$

Thus

$$\int_{A_p} G_p^o\,(\bar{x}'|\bar{\xi}';\omega)\,\psi^{kl}\,(\bar{x}')\,d\bar{x}' = \frac{-2\pi i\,e^{ik_oR}}{R}\,I_1 I_2$$

We use the preceding results to evaluate $\int_{A_p} G_p^{o*}\,(\bar{x}|\bar{\xi};\omega)\,\psi^{qr}\,(\bar{x})\,d\bar{x}$ for field points at x, y, z by letting $k \to q$, $l \to r$, $x' \to x$, $y' \to y$, $z' \to z$ and $i \to -i$. Thus, substituting the integral evaluations into Equation (122), with $k_k = \frac{k\pi}{a}$, $k_l = \frac{l\pi}{b}$, $k_q = \frac{q\pi}{a}$, $k_r = \frac{r\pi}{b}$ and $k_o = \frac{\omega}{c_o}$ we get

$$S_{p_2}\,(x,y,z|x',y',z';\omega) = 6.12 \times 10^{-6}\,\rho^4\omega^4 A_p U_\infty^4 \delta^{*2}\,\theta$$

$$\bullet\;\frac{e^{i\frac{\omega}{c_o}\sqrt{x^2 + y^2 + z^2}}}{\sqrt{x^2 + y^2 + z^2}}\cdot\frac{e^{-i\frac{\omega}{c_o}\sqrt{x'^2 + y'^2 + z'^2}}}{\sqrt{x'^2 + y'^2 + z'^2}}$$

$$\bullet\;\sum_{k,\ell}\frac{k_k k_\ell\left[1 - (-1)^k\,e^{-i\frac{\omega}{c_o}\,x'\,a/\sqrt{x'^2 + y'^2 + z'^2}}\right]\left[1 - (-1)^\ell\,e^{-i\frac{\omega}{c_o}\,y'\,b/\sqrt{x'^2 + y'^2 + z'^2}}\right]}{\left[k_k^2 - \frac{(\omega/c_o)^2\,x'^2}{x'^2 + y'^2 + z'^2}\right]\left[k_\ell^2 - \frac{(\omega/c_o)^2\,y'^2}{x'^2 + y'^2 + z'^2}\right]}$$

151

$$\bullet \sum_{q,r} \frac{k_q k_r \left[1 - (-1)^q e^{i\frac{\omega}{c_o} x a/\sqrt{x^2 + y^2 + z^2}}\right]\left[1 - (-1)^r e^{i\frac{\omega}{c_o} y b/\sqrt{x^2 + y^2 + z^2}}\right]}{\left[k_q^2 - \frac{(\omega/c_o)^2 x^2}{x^2 + y^2 + z^2}\right]\left[k_r^2 - \frac{(\omega/c_o)^2 y^2}{x^2 + y^2 + z^2}\right]}$$

$$\bullet \sum_{m,n} \bar{a}_{qrmn}(\omega)\, \bar{a}^*_{k\,mn}(\omega) \cdot \frac{\sum_{j=1}^{3} A_j k_j \left[iH_0^{(1)}\left(ik_j F U_c \sqrt{k_n^2 + (\omega/U_c)^2}\right)\right]}{\left[1 + \theta^2 \left(\omega - k_m U_c\right)^2\right]} \tag{123}$$

where x,y,z and x',y',z' are any two points in the far field of the half-space.

D5.   ADDITIONAL RESULTS OF ANALYSIS

The analytical results presented in this section have not yet been programmed for digital computation.

(a) Spectral Density of Complex Power Generated in the Cavity

Substituting Equations (28) and (113) into (43e) and (116b) together with Equations (109b) and (111b) into the resulting equation we get (note: in Equation (28) let $s \to \ell$ then $\bar{I}^{rs} \to \bar{I}^{r\ell} \equiv \bar{I}^{qrk\ell}$ and neglecting cross coupling $j_{tn} \to j_{nn} \equiv j_{mnmn}$).

$$W_{rad}^{int}(\omega) = i\rho_c \omega^3 A_p^2 S_{p_{bl}}(\omega) \sum_{m,n} \sum_{q,r} \sum_{k,\ell} \bar{a}_{qrmn}\, \bar{a}^*_{k\ell mn}\, \bar{I}^{qrk\ell}(\omega) j_{mnmn}(\omega)$$

$$= 125.4 \left(\frac{U_\infty \delta^* e}{A_p}\right)\left(i\rho_c \omega^3 A_p^2\right) \sum_{m,n} \frac{\sum_{j=1}^{3} A_j K_j \left[iH_0^{(1)}\left(iK_j F U_c \sqrt{k_n^2 + \left(\frac{\omega}{U_c}\right)^2}\right)\right]}{\left[1 + \Theta^2 \left(\omega - k_m U_c\right)^2\right]}$$

$$\bullet \left[\frac{S_{p_{bl}}(\omega)}{\sum_{j=1}^{3} A_j e^{-\frac{K_j \delta^* \omega}{U_c}}}\right]$$

$$\bullet \sum_{q,r} \bar{a}_{qrmn}(\omega) \sum_{k,\ell} \bar{a}^*_{k\ell mn}(\omega)\, \bar{I}^{qrk\ell}(\omega)$$

$$= 2.42 \times 10^{-4}\, i\rho_c\, \rho^2\, \omega^3\, A_p\, U_\infty^4\, \delta^{*2}\, \theta$$

152

$$\bullet \sum_{m,n} \frac{\sum_{j=1}^{3} A_j k_j \left[i \, H_0^{(1)} \left(i k_j \, F U_c \, \sqrt{k_n^2 + (\omega/U_c)^2} \right) \right]}{\left[1 + \theta^2 \left(\omega - k_m U_c \right)^2 \right]}$$

$$\bullet \sum_{q,r} \bar{a}_{qrmn}(\omega) \sum_{k,\ell} \bar{a}_{k\ell mn}^{*}(\omega) \, \bar{I}^{qrk\ell}(\omega) . \tag{124}$$

where $\bar{I}^{qrk\ell}$ has been evaluated for almost hard as well as hard walls. The results are given by Equation (106).

The real part of Equation (124) represents the real power radiated into the cavity. The imaginary part represents the reactive power generated in the cavity.

(b) General Expression for Cross-Spectral Density of Near and Far Field Pressures in the Half-Space

The *general expression* for the cross-spectral density of pressure anywhere in the half-space, $S_{p_2}(\bar{\xi}|\bar{\xi}';\omega)$, can be obtained from Equation (122). To obtain the near-field results,* the integrals involving the half-space Green function must be evaluated for the various types of modes. This effort is comparable in size to that involved in evaluating the half-space coupling coefficients. For instance, consider the evaluation of the second integral in Equation (122). Using Equation (13) with M=o and subsequently Equations (51) and (52d) in this integral, we get, letting $\eta = x - x'$, $\mu = y - y'$ and $\zeta = \sqrt{k^2 - k_x^2 - k_y^2}$

$$\int_{A_p} G_p^o (\bar{x}|\bar{\xi}';\omega) \, \psi^{k\ell}(\bar{x}') \, d\bar{x}'$$

$$= \int_{-\infty}^{\infty}\int_{-\infty}^{\infty} \left[\int_0^a \int_0^b \frac{e^{i[k_x\eta + k_y\mu - \zeta z']}}{\zeta} \, \psi^{k\ell}(x,y) \, dx \, dy \right] dk_x \, dk_y$$

$$= \int_{-\infty}^{\infty}\int_{-\infty}^{\infty} \frac{e^{-i[k_x x' + k_y y' + \zeta z']}}{\zeta} \left[\int_0^a \int_0^b e^{i(k_x x + k_y y)} \, \psi^{k\ell}(x,y) \, dx \, dy \right] dk_x + dk_y$$

$$= \int_{-\infty}^{\infty}\int_{-\infty}^{\infty} \frac{e^{-i[k_x x' + k_y y' + \zeta z']}}{\zeta} \, S_{k\ell}^{*}(k_x, k_y) \, dk_x \, dk_y$$

---

*The results for the far field are also included in the solution of the general expression given by Equation (122).

$$= k_k k_\ell \int_{-\infty}^{\infty} \int_{-\infty}^{\infty} \frac{e^{-i[k_x x' + k_y y' + \zeta z']} \left[1 - (-1)^k e^{ik_x a} \right] \left[1 - (-1)^\ell e^{ik_y b} \right] dk_x \, dk_y}{\left(k_x^2 - k_k^2 \right) \left(k_y^2 - k_\ell^2 \right) \sqrt{k^2 - k_x^2 - k_y^2}} \quad (125)$$

Following our earlier procedure in connection with the evaluation of Equation (54), let $k_x = a$ and $k_y = \beta$. Then the integral given by Equation (125) can be written

$$\int_{A'_p} G_p^0 \left(\bar{x}' | \bar{\xi}'; \omega \right) \psi^{k\ell} \left(\bar{x}' \right) d\bar{x}'$$

$$= k_k k_\ell \int_{-\infty}^{\infty} \frac{[1 - (-1)^\ell e^{ib\beta}]}{\left(\beta^2 - k_k^2 \right)} \left\{ \int_{-\infty}^{\infty} \frac{e^{-i\left(x'a + y'\beta + z' \sqrt{k^2 - a^2 - \beta^2} \right)} \left[1 - (-1)^k e^{iaa} \right] da}{\left(a^2 - k_k^2 \right) \left(k^2 - a^2 - \beta^2 \right)^{\frac{1}{2}}} \, d\beta \right\}$$

$$= k_k k_\ell \int_{-\infty}^{\infty} \frac{[1 - (-1)^\ell e^{ib\beta}]}{\left(\beta^2 - k_k^2 \right)} I'_k (\beta) \, d\beta$$

where

$$I'_k (\beta) = \int_{-\infty}^{\infty} \frac{e^{-i\left(x'a + y'\beta + z' \sqrt{k^2 - a^2 - \beta^2} \right)} \left[1 - (-1)^\ell e^{iaa} \right] da}{\left(a^2 - k_k^2 \right) \left(k^2 - a^2 - \beta^2 \right)^{\frac{1}{2}}}$$

evaluates to two different functions of β according to $\beta \leq k$ or $\beta > k$. The evaluation of $I'_k(\beta)$ and then $\int_{A'_p} G_p^0 \left(\bar{x}' | \bar{\xi}'; \omega \right) \psi^{k\ell} \left(\bar{x}' \right) d\bar{x}'$ as well as the analogous expression $\int_{A_p} G_p^{0*} \left(\bar{x} | \bar{\xi}; \omega \right) \psi^{qr} \left(\bar{x} \right) d\bar{x}$, by contour integration, and subsequently of Equation (125) is beyond the scope of the present report.

APPENDIX E

EXTENSIONS OF THEORY

In this appendix we discuss the extension of the previous theory to clamped-clamped plates for M (Mach No.) = 0 and to both simply supported and clamped plates for M > 0.

E1. CLAMPED PLATES, M=0

The results presented in Appendixes B, C, and D for M (Mach Number) = 0 are applicable to simply supported plate configurations. However, the theory can be adapted to yield results for clamped-clamped plate configurations. This follows because as discussed Leibowitz and Wallace,[3] it is possible to make a simplified and realistic computation for the vibroacoustic response of clamped-clamped plates. The computation accounts for certain similarities and dissimilarities between the clamped-clamped plate configuration and the simply supported plate configuration. Thus, for computing the vibroacoustic response of thin clamped-clamped rectangular plates, the natural frequencies and modes are adequately represented when the modal frequencies are calculated by considering the true (clamped-clamped) end conditions but using mode shapes which consider the end conditions as simple supports. This computation is valid as an approximation because at higher mode numbers, the mode shapes assumed by a clamped-clamped plate closely match those of a simply supported plate whose dimensions are somewhat smaller. On the other hand, there are significant differences in the resonance frequencies of these plates. Accordingly, the concepts discussed in Reference 3 can be used to adapt the computer program in Appendix G to handle the clamped plate case (with no cavity) if (a) the clamped-clamped plate *in vacuo* and fluid-loaded resonance frequencies are calculated by the methods of Reference 3 and (b) the plate dimensions used in the calculation of the half-space coupling coefficients and of the plate cross-spectral densities are assumed to be smaller by the ratios

$$a' = \frac{1.05\, a}{1 + \dfrac{0.5}{m}} \qquad\qquad b' = \frac{1.05\, b}{1 + \dfrac{0.5}{n}}$$

E2. SIMPLY SUPPORTED AND CLAMPED-CLAMPED PLATES, M > 0

Our objective here is to compute the half-space coupling coefficients for simply supported and clamped-clamped plates for M > 0 (note $I^{rs} \neq f(M)$).

In Equation (27) let $r \to mn$, $s \to qr$ and note that $G_p^0(\bar{x}'|\bar{x}) \equiv G_p^0(\bar{x}|\bar{x}')$. Then

$$J^{mnqr} = \frac{-i\, 1}{4\pi^2 k^2}$$

155

where, *in contrast to Equation (28)*

$$I = \int_0^{a'} \int_0^{b'} \psi^{mn} (x',y') \left[\int_0^a \int_0^b L' \, G_p^o (x,y|x',y') \, L \, \psi^{qr} (x,y) \, dx \, dy \right] dx' \, dy'$$

$$= \int_0^{a'} \int_0^{b'} \psi^{mn} (x',y') \left\{ \int_0^b \left[\int_0^a k \, G_p^o \, L \, \psi^{qr} (x,y) \, dx + i \, M \int_0^a \frac{\partial G_p^{o'}}{\partial x'} \, L \, \psi^{qr} (x,y) \, dx \right] dy \right\} dx' \, dy'$$

Now, inspection of Equation (13) shows that

$$\frac{\partial G_p^o}{\partial x'} = - \, \frac{\partial G_p^o}{\partial x}$$

so that

$$I = \int_0^{a'} \int_0^{b'} \psi^{mn} (x',y') \left\{ \int_0^b \left[\int_0^a k \, G_p^o \, L \, \psi^{qr} (x,y) \, dx - i \, M \int_0^a \frac{\partial G_p^o}{\partial x} \, L \, \psi^{qr} (x,y) \, dx \right] dy \right\} dx' \, dy'$$

Integrating by parts with $u = L\psi^{qr}$, $du = \frac{\partial}{\partial x} L\psi^{qr} dx$, $dv = \frac{\partial G_p^o}{\partial x} dx$ and $v = G_p^o$, the last integral is evaluated as follows

$$\int_0^a \frac{\partial G_p^o}{\partial x} \, L \, \psi^{qr} (x,y) \, dx = G_p^o \, L \, \psi^{qr} \, \Big|_0^a - \int_0^a G_p^o \, \frac{\partial}{\partial x} \, L \, \psi^{qr} \, dx$$

$$= G_p^o (a,y|x',y') \left[k \, \psi^{qr} (a,y) + i \, M \, \frac{\partial \psi^{qr} (a,y)}{\partial x} \right]$$

$$- G_p^o (o,y|x',y') \left[k \, \psi^{qr} (o,y) + i \, M \, \frac{\partial \psi^{qr} (o,y)}{\partial x} \right]$$

$$- \int_0^a G_p^o \, \frac{\partial}{\partial x} \, L \, \psi^{qr} \, dx$$

For either a simply supported or clamped plate:

$$\psi^{qr} (o,y) \equiv \psi^{qr} (a,y) \equiv o$$

Hence for either case:

$$I = \int_0^{a'} \int_0^{b'} \psi^{mn}(x',y') \left\{ \left[\int_0^b \int_0^a k\, G_p^o\, L\, \psi^{qr}(x,y)\, dx + i\, M \int_0^a G_p^o \frac{\partial}{\partial x} L\, \psi^{qr}(x,y)\, dx \right] dy \right.$$

$$\left. + M^2 \int_0^b \left[G_p^o(a,y|x',y') \frac{\partial \psi^{qr}(a,y)}{\partial x} - G_p^o(o,y|x',y') \frac{\partial \psi^{qr}(o,y)}{\partial x} \right] dy \right\} dx'\, dy'$$

$$= \int_0^{a'} \int_0^{b'} \psi^{mn}(x',y') \left\{ \int_0^b \int_0^a G_p^o(x,y|x',y')\, L^2\, \psi^{qr}(x,y)\, dx\, dy \right.$$

$$\left. + M^2 \int_0^b \left[G_p^o(a,y|x',y') \frac{\partial \psi^{qr}(a,y)}{\partial x} - G_p^o(o,y|x',y') \frac{\partial \psi^{qr}(o,y)}{\partial x} \right] dy \right\} dx'\, dy'$$

$$= \int_0^{a'} \int_0^{b'} \int_0^b \int_0^a \psi^{mn}(x',y')\, G_p^o(x,y|x',y')\, L^2\, \psi^{qr}(x,y)\, dx\, dy\, dx'\, dy'$$

$$+ M^2 \int_0^{a'} \int_0^{b'} \psi^{mn}(x',y') \int_0^b \left[G_p^o(a,y|x',y') \frac{\partial \psi^{qr}(a,y)}{\partial x} - G_p^o(o,y|x',y') \frac{\partial \psi^{qr}(o,y)}{\partial x} \right] dy\, dx'\, dy'$$

The expression $\bar{J}^{mnqr} = \dfrac{-i\, I}{4\pi^2 k^2}$ is now further evaluated; here I is given by the above equation, applicable to either supported or clamped plates.

In the foregoing equations, $G_p^o(x,y|x',y')$ is given by Equation (15) with $z = 0$ (hence $R = \sqrt{z^2 + (y-y')^2} \to \gamma = y - y'$ and $\mu = \dfrac{x - x'}{\sqrt{1 - M^2}} = \dfrac{x - x'}{\beta}$ where $\beta = \sqrt{1 - M^2}$). Hence $\mu \sqrt{1 - M^2} = \mu\beta = x - x' = \eta$. It is convenient to write G_p^o in the form

$$G_p^o(x,y|x',y') \equiv G_p^o(\bar{x}|\bar{x}') = G_p^o(\beta\mu, \beta\gamma) = \frac{-2\pi i}{\beta}\, e^{-i\kappa \frac{M}{\beta}(\beta u)}\, \frac{e^{i\frac{\kappa}{\beta}\sqrt{(\beta\mu)^2 + (\beta\gamma)^2}}}{\frac{1}{\beta}\sqrt{(\beta\mu)^2 + (\beta\gamma)^2}}$$

The Fourier transform of $G_p^o(\beta\mu, \beta\gamma)$ and its inverse are defined by Equations (48a,b); note that in those equations, $\mu \to \gamma$ here and the definition of G_p^o here is more general than that of Equation (47) because $M \geq 0$.

$$G_p^0 (k_x, k_y) = \int_{-\infty}^{\infty} \int_{-\infty}^{\infty} G_p^0 (\eta, \gamma) \, e^{-i[k_x \eta + k_y \gamma]} \, d\eta \, d\gamma$$

$$= \frac{1}{\beta} \int_{-\infty}^{\infty} \int_{-\infty}^{\infty} G_p^0 (\beta\mu, \beta\gamma) \, e^{-i\left[k_x \beta\mu + \frac{k_y}{\beta}(\beta\gamma)\right]} \, d(\beta\mu) \, d(\beta\gamma)$$

$$G_p^0 (\eta, \gamma) = \frac{1}{(2\pi)^2} \int_{-\infty}^{\infty} \int_{-\infty}^{\infty} G_p^0 (k_x, k_y) \, e^{i(k_x \eta + k_y \gamma)} \, dk_x \, dk_y$$

where $G_p^0 (\beta\mu, \beta\gamma)$ is given above and $G_p^0 (k_x, k_y)$ is evaluated at the end of this appendix. Hence, interchanging integrals

$$\bar{J}^{mnqr} = \frac{-i}{(2\pi)^4 k^2} \left\{ \int_{-\infty}^{\infty} \int_{-\infty}^{\infty} G_p^0 (k_x, k_y) \left[\int_0^a \int_0^b \psi^{mn} (x',y') \, e^{-i(k_x x' + k_y y')} \, dx' \, dy' \right] \right.$$

$$\cdot \left[\int_0^a \int_0^b L^2 \psi^{qr} (x,y) \, e^{+i(k_x x + k_y y)} \, dx \, dy \right] dk_x \, dk_y$$

$$\left. + M^2 \int_0^{a'} \int_0^{b'} \psi^{mn} (x',y') \int_0^b \left[G_p^0 (a,y|x',y') \frac{\partial \psi^{qr} (a,y)}{\partial x} - G_p^0 (o,y|x',y') \frac{\partial \psi^{qr} (o,y)}{\partial x} \right] dy \, dx' \, dy' \right\}$$

From Equation (50), with $s \rightarrow mn$, the first double integral in brackets is $S_{mn} (k_x, k_y)$. However, the second double integral in brackets is denoted by

$$\mathcal{S}_{qr}^* (k_x, k_y) = \int_0^a \int_0^b \left(k + i M \frac{\partial}{\partial x} \right)^2 \psi^{qr} (x,y) \, e^{i(k_x x + k_y y)} \, dx \, dy \, ; \, M \geq 0$$

which is not equivalent to Equation (51).

Thus, in general, for either a simply supported or clamped plate with $M \geq 0$,

$$\bar{J}^{mnqr} = \frac{-i}{(2\pi)^4 k^2} \left\{ \int_{-\infty}^{\infty} \int_{-\infty}^{\infty} G_p^0 (k_x, k_y) \, S_{mn} (k_x, k_y) \, \mathcal{S}_{qr}^* (k_x, k_y) \, dk_x \, dk_y \right.$$

$$\left. + M^2 \int_0^{a'} \int_0^{b'} \psi^{mn} (x',y') \int_0^b \left[G_p^0 (a,y|x',y') \frac{\partial \psi^{qr} (a,y)}{\partial x} - G_p^0 (o,y|x',y') \frac{\partial \psi^{qr} (o,y)}{\partial x} \right] dy \, dx' \, dy' \right\}$$

We make the following observations:

1. For M=0, the second double integral term vanishes and $\mathscr{S}_{qr}^{*} \rightarrow k^2 \mathscr{S}_{qr}^{*}$ where $\mathscr{S}_{qr}^{*}$ is given by Equation (51). In this case, the foregoing equation reduces to Equation (49) which has been previously evaluated for *simply supported* plates whose modal configurations are given by Equations (52a,b); see Equations (52) – (54).

2. For $M \geq 0$ and for a *simply supported* plate, we can use Equations (52a,b) to determine $S_{mn} \mathscr{S}_{qr}^{*}$ and therefore J^{mnqr}. An outline of the procedure follows

$$\mathscr{S}_{qr}^{*} = \int_0^a \int_0^b \left(k + i\, M\, \frac{\partial}{\partial x} \right)^2 \psi^{qr}(x,y)\, e^{i(k_x x + k_y y)}\, dx\, dy$$

$$= \int_0^a \int_0^b \left(k^2 - M^2\, \frac{\partial^2}{\partial x^2} + i\, 2k\, M\, \frac{\partial}{\partial x} \right) \sin k_q x\, \sin k_r y\, e^{i(k_x x + k_y y)}\, dx\, dy$$

$$= \left(k^2 + k_q^2\, M^2 \right) \int_0^a \int_0^b \sin k_q x\, \sin k_r y\, e^{+i(k_x x + k_y y)}\, dx\, dy$$

$$+ i\, 2k\, k_q\, M \int_0^a \int_0^b \cos k_q x\, \sin k_r y\, e^{+i(k_x x + k_y y)}\, dx\, dy$$

The first double integral is equivalent to Equation (51) which is evaluated to (52d). The second integral is evaluated in a similar manner. Thus, we find

$$\mathscr{S}_{qr}^{*} = \left(k^2 k_q k_r + k_q^3 k_r M^2 - 2ik\, k_q k_y k_x M \right) \left(\frac{\left[(-1)^q\, e^{ik_x a} - 1 \right] \left[(-1)^r\, e^{ik_y b} - 1 \right]}{\left[k_x^2 - k_q^2 \right] \left[k_y^2 - k_r^2 \right]} \right)$$

and using Equation (52c) together with the preceding equation,

$$S_{mn} \mathscr{S}_{qr}^{*} = \left[k^2 \underline{K}_1 + \underline{K}_2 - ik_y k_x \underline{K}_3 \right] \frac{\left[1 + (-1)^{q+m} - (-1)^m e^{-ik_x a} - (-1)^q e^{ik_x a} \right] \left[1 + (-1)^{n+r} - (-1)^n e^{-ik_y b} - (-1)^r e^{ik_y b} \right]}{\left(k_x^2 - k_m^2 \right) \left(k_x^2 - k_q^2 \right) \left(k_y^2 - k_n^2 \right) \left(k_y^2 - k_r^2 \right)}$$

where

$$\underline{K}_1 = k_m\, k_n\, k_q\, k_r$$

$$\underline{K}_2 = k_m\, k_n\, k_q^3\, k_r\, M^2$$

$$\underline{K}_3 = 2k\, k_m\, k_n\, k_q\, M$$

159

Substituting the foregoing expression for $S_{mn} \mathcal{S}_{qr}^*$ and $\psi^{mn}(x',y')$, $\psi^{qr}(a,y)$, $\psi^{qr}(o,y)$ respectively given by Equations (52a,b) as well as the appropriate expressions* for G_p^o into the last expression previously presented for $\bar{J}^{mnqr}$, we will obtain a general working expression (for *simply supported* plates and $M \geq 0$) which includes Equation (53) for the special case $M=0$. Detailed evaluation of $\bar{J}^{mnqr}$ is beyond the scope of this report.

3. For $M \geq 0$ and for a *clamped-clamped* plate, an additional boundary condition obtains:

$$\frac{\partial \psi^{qr}(o,y)}{\partial x} \equiv \frac{\partial \psi^{qr}(a,y)}{\partial x} \equiv 0$$

Hence, for this case,

$$\bar{J}^{mnqr} = \frac{-i}{(2\pi)^4 k^2} \int_{-\infty}^{\infty} \int_{-\infty}^{\infty} G_p^o(k_x,k_y) \, S_{mn}(k_x,k_y) \, \mathcal{S}_{qr}^*(k_x,k_y) \, dk_x \, dk_y$$

where $G_p^o(k_x,k_y)$ is determined below and S_{mn} and $\mathcal{S}_{qr}^*$ are evaluated for the mode shapes of a *clamped-clamped* plate given in Reference 3. For the special case $M=0$, $\mathcal{S}_{qr}^*(k_x,k_y) \rightarrow k^2 S_{qr}^*(k_x,k_y)$. Observe that for this case S_{mn} and S_{qr}^* are again given by Equations (50) and (51), respectively, but ψ^{mn} and ψ^{qr} are now the modes for *clamped-clamped* plates.

EVALUATION OF $G_p^o(k_x,k_y)$ FOR $M \geq 0$

From the previous analysis, the Fourier transform of the expression given for $G_p^o(\beta\mu, \beta\gamma)$ is

$$G_p^o(k_x,k_y) = \frac{-2\pi i}{\beta} \int_{-\infty}^{\infty} e^{-i\left(k_x + \kappa \frac{M}{\beta}\right)\beta\mu} \left[\int_{-\infty}^{\infty} \frac{e^{i\frac{\kappa}{\beta}\sqrt{(\beta\mu)^2 + (\beta\gamma)^2}}}{\sqrt{(\beta\mu)^2 + (\beta\gamma)^2}} e^{-i\frac{k_y}{\beta}(\beta\gamma)} d(\beta\gamma) \right] d(\beta\mu)$$

To evaluate the second integral within the brackets, we use the inverse transform of the equation given by Gradshteyn and Ryzhik[25] (see their formula 6.616, page 710), i.e.,

$$i\pi H_0^{(1)}\left(r\sqrt{a^2 - t^2}\right) = \int_{-\infty}^{\infty} \frac{e^{ia\sqrt{r^2 + x^2}}}{\sqrt{r^2 + x^2}} e^{-itx} \, dx$$

---

*The expression for $G_p^o(a,y|x',y')$ and $G_p^o(o,y|x',y')$ are obtained directly from the expression for $G_p^o(x,y|x',y')$ previously given and the expression for $G_p^o(k_x,k_y)$ is determined below by means of the Fourier transform. For the special case $M=0$ it will of course reduce to the expression given in Appendix B.

with

$$a = \frac{\kappa}{\beta} , \quad r = \beta\mu , \quad x = \beta\gamma \quad \text{and} \quad t = \frac{k_y}{\beta} .$$

Thus

$$G_p^o (k_x, k_y) = \frac{-2\pi i}{\beta} \int_{-\infty}^{\infty} e^{-i\left(k_x + \kappa \frac{M}{\beta}\right)\beta\mu} \left[i\pi H_0^{(1)} \left(\beta\mu \sqrt{\frac{\kappa^2}{\beta^2} - \frac{k_y^2}{\beta^2}} \right) \right] d(\beta\mu)$$

Let $\beta\mu = -\lambda$; then

$$G_p^o (k_x, k_y) = \frac{+2\pi i}{\beta} \int_{-\infty}^{\infty} e^{+i\left(k_x + \kappa \frac{M}{\beta}\right)\lambda} \left[i\pi H_0^{(1)} \left(\frac{-\lambda}{\beta} \sqrt{\kappa^2 - k_y^2} \right) \right] d\lambda$$

Now

$$H_0^{(1)} \left(\frac{-\lambda}{\beta}\sqrt{\kappa^2 - k_y^2} \right) = H_0^{(1)} \left(\frac{i\lambda}{\beta} \cdot i\sqrt{\kappa^2 - k_y^2} \right) = H_0^{(1)} \left(\sqrt{k_y^2 - \kappa^2} \cdot \sqrt{0^2 - \left(\frac{\lambda}{\beta}\right)^2} \right) = H_0^{(1)} \left(\frac{1}{\beta}\sqrt{k_y^2 - \kappa^2} \cdot \sqrt{0^2 - \lambda^2} \right)$$

Therefore

$$G_p^o (k_x, k_y) = \frac{-2\pi^2}{\beta} \int_{-\infty}^{\infty} e^{i\left(k_x + \frac{\kappa M}{\beta}\right)\lambda} \left[H_0^{(1)} \left(\frac{1}{\beta}\sqrt{k_y^2 - \kappa^2} \cdot \sqrt{0^2 - \lambda^2} \right) \right] d\lambda$$

To evaluate this integral, we obtain the Fourier transform of $H_0^{(1)}$ using the aforementioned equation in Reference 25, namely,

$$\int_{-\infty}^{\infty} e^{itx} H_0^{(1)} \left(r\sqrt{a^2 - t^2} \right) dt = \frac{-2i \, e^{ia\sqrt{r^2 + x^2}}}{\sqrt{r^2 + x^2}}$$

with

$$x = k_x + \frac{\kappa M}{\beta} , \quad t = \lambda , \quad r = \frac{1}{\beta}\sqrt{k_y^2 - \kappa^2} , \quad a = 0$$

Thus

$$G_p^0 (k_x, k_y) = \frac{-2\pi^2}{\beta} (-2i) \frac{e^{i0}}{\sqrt{\frac{k_y^2 - \kappa^2}{\beta^2} + \left(k_x + \frac{\kappa M}{\beta}\right)^2}}$$

$$= \frac{(2\pi)^2 i}{\sqrt{k_y^2 - \kappa^2 + \beta^2 k_x^2 + 2\kappa M\beta k_x + \kappa^2 M^2}}$$

Multiplying numerator and denominator by $i = \sqrt{-1}$,

$$G_p^0 (k_x, k_y) = \frac{-(2\pi)^2}{\sqrt{\kappa^2 (1 - M^2) - 2kMk_x - (1 - M^2) k_x^2 - k_y^2}}$$

$$= \frac{-(2\pi)^2}{\sqrt{k^2 - 2k Mk_x - (1 - M^2) k_x^2 - k_y^2}} = \frac{-(2\pi)^2}{\zeta}$$

where we have used $\beta^2 = 1 - M^2$, $\kappa = \frac{k}{\sqrt{1 - M^2}} = \frac{k}{\beta}$. For the special case M=0 only,

$$G_p^0 (k_x, k_y) \rightarrow \frac{-(2\pi)^2}{\sqrt{k_x^2 - k_x^2 - k_y^2}}$$ which agrees with the result immediately preceding

Equation (49) hitherto obtained.

APPENDIX F

COMPARISON OF PRESENT RESULTS WITH THOSE OF DAVIES

For convenience in comparing the present results with Davies original work[9], we observe that his radiation coefficients

$$R_{mnqr} = S_{mnqr} + i\, T_{mnqr}$$

are related to the intermodal coupling coefficients calculated herein through the following relations (accounting for different normalization schemes and coordinate systems)*

$$S_{mnqr} = \frac{-4\rho c_0 k}{A_p} J_R{}^{mnqr}$$

$$T_{mnqr} = \frac{4\rho c_0 k}{A_p} J_x{}^{mnqr} = -\omega m_{mnqr}$$

We now compare the present results with those of Davies for the various modal domains previously treated in computation; the comparisons indicate the extension of Davies results by the methods of analysis used in this report.

---

*Compare the intermodal coupling coefficient term in the modal equation, Equation (29), with the corresponding coefficient term in Equation (B18) of Reference 4 or 5, observing that the positive axis in the direction of plate vibration in Figure 1 of the present report is opposite to that used by Davies. Further, the normalization constant for $\psi_{mn}\,\psi_{qr}$ given by Equation (52) is equal to unity whereas Davies used a normalization constant of

$$\left(\sqrt{\frac{2}{A_p}}\right)\left(\sqrt{\frac{2}{A_p}}\right) = \frac{4}{A_p} \quad \text{for } \psi_{mn}\,\psi_{qr}. \quad \text{Hence, we get}$$

$$\omega^2 \rho J^{mnqr} = \omega^2 \rho \left(J_x{}^{mnqr} + i\, J_R{}^{mnqr}\right)\left(\frac{4}{A_p}\right) = -i\omega R_{mnqr} \equiv -i\omega \left(S_{mnqr} + i\, T_{mnqr}\right)$$

or

$$S_{mnqr} = \frac{-4\rho\omega}{A_p} J_R{}^{mnqr} = \frac{-4\rho c_0 k}{A_p} J_R{}^{mnqr}$$

$$T_{mnqr} = \frac{4\rho\omega}{A_p} J_x{}^{mnqr} = \frac{4\rho c_0 k}{A_p} J_x{}^{mnqr}$$

163

F1. TWO Y-EDGE MODES

Two Y-edge modes, k_m, $k_q > k$; $k_n = k_r < k$

Using Equation (69b),

$$S_{mnqr} = \frac{-4\rho c_o k}{A_p} \left\{ \frac{- bk_m k_q \left[1 - (-1)^m J_o \left(a\sqrt{k^2 - k_n^2} \right) \right]}{2 \left(k_{mn}^2 - k^2 \right) \left(k_{qn}^2 - k^2 \right)} \right\} \delta_{nr}$$

In the limit $k_n^2 = k_r^2 \ll k^2$; k_m, $k_q \gg k$ and $ka \gg \pi$ (for which J_o (ak) $\ll 1$); see special Case 3 following Equation (69c):

$$S_{mnqr} = \frac{2\rho c_o}{A_p} \frac{kb}{k_m k_q} \delta_{nr}$$

which is identical to Davies* original approximation given by Equation (B43) or Equation (B46) of Reference 5.

Using Equation (69c) with the limiting conditions, $k_n^2 = k_r^2 \ll k^2$; $k_q^2 \gg k_m^2 \gg k^2$; $\left(\frac{1}{a} \right)^2 \ll k^2$; see special Case 4 following Equation (69c)

$$T_{mnqr} = \frac{4\rho c_o k}{A_p} \left\{ \frac{-b}{\pi k_m k_q} \ln \left[(1 + \sqrt{2}) \frac{k_m}{k} \right] \right\} \delta_{nr}$$

$$= \frac{-4\rho c_o}{\pi A_p} \frac{kb}{k_m k_q} \ln \left[(1 + \sqrt{2}) \frac{k_m}{k} \right] \delta_{nr}$$

which is in good agreement with Davies original approximation

$$T_{mnqr} = \frac{-4\rho c_o}{\pi A_p} \frac{kb}{k_m k_q} \ln \frac{2k_{mn}}{k} \delta_{nr} \; ; \; k_{mn} = \sqrt{k_m^2 + k_n^2} \approx k_m$$

given by Equation (B32) or the first term on the right hand side of Equation (B40) of Reference 4.

---

*In comparing the present results with those in References 5 and 4 the reader should (as the author did) make the appropriate interchange of symbols in going from x-edge modes to y-edge modes and conversely; similar relabeling should be made for the other modal domains.

Two Y-edge modes, $k_m = k_q > k$; $k_n = k_r < k$

Using Equation (70c) with $ka \ll 1$, corresponding to special Case 1 following Equation (70d), the results for S_{mnmn} are seen to be a particular case of the preceding results for S_{mnqr} corresponding to $m = q$ and $n = r$

$$S_{mnqr} = \frac{2\rho c_o}{A_p} \frac{kb}{k_m^2} \delta_{mq} \delta_{nr}$$

It therefore agrees with Equation (43) or (B46) of Reference 5.

Using Equation (70d) with $k_{mn}^2 = k_m^2 + k_n^2 \gg k^2$, corresponding to special Case 2 following Equation (70d),

$$T_{mnqr} = \frac{4\rho c_o k}{A_p} \left(\frac{-A_p}{4k_{mn}} \right) = \frac{-\rho c_o k}{k_{mn}}$$

which is identical to Davies original approximation as given by Equation (B34) of Reference 4.

F2. CORNER MODES

Two corner modes, k_m, $k_q > k$; k_n, $k_r > k$

Using Equation (73b),

$$S_{mnqr} = \frac{-4\rho c_o k}{A_p} \left\{ \frac{-2k}{\pi k_m k_n k_q k_r} \left[1 - (-1)^m \frac{\sin ka}{ka} - (-1)^n \frac{\sin kb}{kb} - (-1)^{m+n} \frac{\sin k\sqrt{a^2 + b^2}}{k\sqrt{a^2 + b^2}} \right] \right\}$$

$$= \frac{8\rho c_o}{\pi A_p} \frac{k^2}{k_m k_n k_q k_r} \left[1 - (-1)^m \frac{\sin ka}{ka} - (-1)^n \frac{\sin kb}{kb} - (-1)^{m+n} \frac{\sin k\sqrt{a^2 + b^2}}{k\sqrt{a^2 + b^2}} \right]$$

which is identical to Davies original approximation as given by Equation (B27) of Reference 5.

Using Equation (74) with $k_m = k_q$, $k_n = k_r$,

$$T_{mnqr} = \frac{4\rho ck}{A_p} \left[\frac{-A_p}{4 \left(k_m^2 + k_n^2 - k^2 \right)^{1/2}} \right] \delta_{mq} \delta_{nr}$$

$$= -\rho c \frac{k}{k_{mn}} \quad \text{for} \quad k_{mn}^2 = k_m^2 + k_n^2 \gg k^2$$

which is identical to Davies original approximation as given by Equation (B39) of Reference 4.

F3. Y-EDGE — ACOUSTICALLY FAST (AF) MODES

Y-edge — acoustically fast modes, k_m, k_n, $k_r < k$; $k_q > k$

Using Equation (80),—

$$S_{mnqr} = \frac{-4\rho c_o k}{A_p} \left[\frac{(-1)^m \, k_m \, k_q \, b}{2 \, (k^2 - k_m^2 - k_n^2)(k^2 - k_q^2 - k_n^2)} \, J_o \left(a\sqrt{k^2 - k_n^2} \right) \right] \delta_{nr}$$

For the limiting condition k_m^2, $k_n^2 = k_r^2 \ll k^2$; $k_q^2 \gg k^2$ corresponding to the first special case following Equation (81),

$$S_{mnqr} = \frac{-4\rho c_o k}{A_p} \left[\frac{(-1)^m \, k_m \, k_q \, b \, J_o \, (ak)}{2 \, k^2 \left(-k_q^2 \right)} \right] \delta_{nr}$$

$$= (-1)^m \frac{4\rho c_o k_m \, b}{2 \, A_p \, k \, k_q} \, J_o \, (ak) \, \delta_{nr}$$

The Davies result is for large ka (ka≫1) so we can use the approximation

$$J_o \, (ka) \approx \sqrt{\frac{2}{\pi ka}} \, \cos \left(ka - \frac{\pi}{4} \right)$$

yielding for J_R^{mnqn} the result given by special Case 2 following Equation (81). We obtain a result

$$S_{mnqr} = (-1)^m \frac{4\rho c_o}{\pi A_p} \, \frac{km}{k \, k_q} \, \sqrt{\frac{\pi}{2 \, ka}} \, \cos \left(ka - \frac{\pi}{4} \right) \delta_{nr}$$

which is identical to Equation (B48) of Reference 5.

Using the third special case for J_x^{mnqn} following Equation (81), we get for k_m^2, k_n^2, $k_m^2 + k_n^2 \ll k^2 \ll k_q^2$; $\left(\frac{1}{a} \right)^2 \ll k^2$

$$T_{mnqr} = \frac{4\rho c_o k}{A_p} \left[\frac{k_m \, b}{\pi k_q \, k^2} \, \ln 2.4 + \frac{(-1)^m \, (k_m b) \, (ka)}{\pi k_q \, k^2} \right] \delta_{nr}$$

$$\approx (-1)^m \frac{4\rho c_o}{\pi A_p} \, kb \, \frac{k_m}{k_q \, k^2} \, ka \, \delta_{nr}$$

because the second term in brackets on the right hand side predominates* for $ka \gg 1$. Davies gets

$$T_{mnqr} = \frac{-4\rho c_o}{A_p} \, kb \, \frac{k_m}{k_q \, k^2} \, \delta_{nr}$$

which is close to the result that would be obtained considering the first term in brackets on the right hand side to predominate. It appears as if Davies did not obtain the correct dominant term for this case.

F4. Y-EDGE – CORNER MODES

Y-edge – corner modes. $k_m, k_q > k; k_n < k; k_r > k$

Using Equation (82)

$$S_{mnqr} = \frac{-4\rho c_o k}{A_p} \left[\frac{1}{\pi k_r \, k_m \, k_q} \, \ln \frac{k - k_n}{k + k_n} \right] \delta_{mq}$$

For the first special case following Equation (83), with $\ln \dfrac{k - k_n}{k + k_n} \approx -2 \dfrac{k_n}{k}$

$$S_{mnqr} = \frac{-4\rho c_o k}{A_p} \left[\frac{-2 \, k_n}{\pi k_r \, k_m \, k_q \, k} \right]$$

$$= \frac{8\rho c_o}{\pi A_p} \, \frac{k_n}{k_r \, k_m \, k_q}$$

which is identical to Equation (B34) of Reference 5.

Using Equation (83)

$$T_{mnqr} = \frac{4\rho c_o k}{A_p} \left[\frac{a}{2\pi k_r \, k_m} \, \ln \frac{k - k_n}{k + k_n} \right] \delta_{mq}$$

For the second special case following Equation (83) $\ln \dfrac{k - k_n}{k + k_n} \approx -2 \dfrac{k_n}{k}$

---

*For greater exactness, we add that for $1 \ll ka < 10$ both terms are of the same order for any given values of k_m and k_q. Moreover, the average contribution of several modes to the response (fixed q, variable m) is greater for the first term than for the second term due to the fluctuating sign, associated with $(-1)^m$, in the latter term.

$$T_{mnqr} = \frac{4\rho c_0 k}{A_p} \left[\frac{-k_n a}{\pi k_r k_m k} \right] \delta_{mq}$$

$$= \frac{-4\rho c_0}{\pi A_p} k_m a \frac{k_n k_r}{k_r^2 k_m^2} \delta_{mq}$$

The Davies result, given by Equation (B41) of Reference 4, namely,

$$T_{mnqr} = \frac{-4\rho c_0}{\pi A_p} ka \frac{k_n k_r}{k_{mn}^2 k_{qr}^2} \delta_{mq}$$

$$\approx \frac{-4\rho c_0}{\pi A_p} ka \frac{k_n k_r}{k_m^2 k_{qr}^2} \quad ; \quad k_{mn}^2 = k_m^2 + k_n^2 \approx k_m^2$$

is not in agreement with the preceding result for T_{mnqr}. If, however, $k_r^2 \gg k_q^2 = k_m^2$, then $k_{qr}^2 = k_q^2 + k_r^2 \approx k_r^2$ and

$$T_{mnqr} \approx \frac{-4\rho c_0}{\pi A_p} ka \frac{k_n k_r}{k_r^2 k_m^2} \delta_{mq}$$

Now we recall that the approximation for $\ln \frac{k - k_n}{k + k_n}$ *cancelled the "k" in the numerator* in both of the original S_{mnqr} and T_{mnqr} equations presented in this section and that the resulting (final) equation for S_{mnqr}, *which does not contain "k"*, is identical to Davies corresponding result. Hence, it seems plausible that the final equation for T_{mnqr} should not contain a "k" either. In fact, if in the preceding equation $k \rightarrow k_m$, then Davies results and those derived here are compatible. The author therefore surmises that "k" in the preceding equation may possibly be due to a typographical error and should be replaced by "k_m".

F5. ACOUSTICALLY FAST (AF) MODES

Two acoustically fast modes, k_m, k_n, k_q, $k_r < k$

Using Equation (86a), for $k_m = k_q$; $k_n = k_r$

$$S_{mnqr} = \frac{-4\rho c_0 k}{A_p} \left[\frac{-A_p}{4 \left(k^2 - k_m^2 - k_n^2 \right)^{1/2}} \right] \delta_{mq} \delta_{nr}$$

168

$$= \frac{\rho c_0 k}{\left(k^2 - k_m^2 - k_n^2\right)^{1/2}} \, \delta_{mq} \, \delta_{nr}$$

which agrees with Equation (B39) of Reference 5 if, in accordance with Equation (B36) of the reference, we include the contribution of k_m^2 in the derivation, i.e., if $k_m^2 \ll k^2$. If we do take $k_m^2 \ll k^2$, then the above result is identical to Equation (B39) of the reference. And if we take k_m^2, $k_n^2 \ll k^2$, then the result is identical to Equation (B40) or the first term of Equation (B49) of the reference.

Using Equation (87) with $k_m \neq k_q$, $k_n = k_r$

$$S_{mnqr} = \frac{-4\rho c_0 k}{A_p} \left[\frac{(-1)^m \, k_m \, k_q \, b}{2 \left(k^2 - k_m^2 - k_n^2\right)\left(k^2 - k_q^2 - k_n^2\right)} \, J_0 \left(a \sqrt{k^2 - k_n^2}\right) \right]$$

Now for k_m^2, k_n^2, k_q^2, $k_r^2 \ll k^2$ and for large ka, corresponding to special Case 1 following Equation (90)

$$S_{mnmn} = \frac{-4\rho c_0 k}{A_p} \left[\frac{(-1)^m \, k_m \, k_q \, b}{\pi k^4} \left(\frac{\pi}{2ka}\right)^{1/2} \cos\left(ka - \frac{\pi}{4}\right) \right] \delta_{nr}$$

$$= - (-1)^m \frac{4\rho c_0}{\pi A_p} \frac{k_m \, k_q}{k^4} \, k \, b \left(\frac{\pi}{2ka}\right)^{1/2} \cos\left(ka - \frac{\pi}{4}\right) \delta_{nr}$$

which is identical to the third term of Equation (B49) of reference 5, except for sign; inspection of Equations (B37) and (B45) of the reference indicates that the Davies sign appears to be in error.

Using Equation (90), we can obtain an expression for T_{mnqn} which holds for $k_n = k_r < k$; $k_m \neq k_q < k$. However, from special Case 2 following Equation (90) we observe that $T_{mnqn} \approx 0$ (since $J_x^{mnqn} \approx 0$) for k_m^2, k_n^2, $k_m^2 + k_n^2 \ll k^2$; k_q^2, k_r^2,

$k_q^2 + k_r^2 \ll k^2$; $\left(\frac{1}{a}\right)^2 \ll k^2$. This agrees with the Davies findings as given on page 66 of Reference 4.

F6.   EDGE MODES

Two edge modes; k_m, k_n, k_q, $k_r < k$; k_{mn}^2, $k_{qr}^2 > k^2$

Using Equations (91c) and (92), i.e., for the conditions $k_n = k_r$, $k_m \neq k_q$,

$$S_{mnqr} = \frac{-4\rho c_0 k}{A_p} \left\{ \frac{-b}{2\, k_m\, k_q} \left[1 - (-1)^m\, J_0\left(a\sqrt{k^2 - k_n^2}\right) \right] \right\} \delta_{nr}$$

$$\approx \frac{2\rho c_0}{A_p} \frac{k\, b}{k_m\, k_q} \left[1 - (-1)^m\, J_0\,(ka) \right] \delta_{nr}$$

Now for $ka \gg 1$

$$S_{mnqr} \approx \frac{2\rho c_0 k\, b}{A_p\, k_m\, k_q} \delta_{nr}$$

which is identical to Equation (B46) or Equation (B32) (ignoring the negligible last term) of Reference 5.

Using Equations (94) and (95), i.e., for the conditions $k_n = k_r$, $k_m \neq k_q$, with $k_m^2,\ k_n^2,\ k_q^2 \ll k^2$; $\left(\frac{1}{a}\right)^2 \ll k^2$ and considering only the first term of the summation in Equation (95),

$$T_{mnqr} = \frac{4\rho c_0 k}{A_p} \left\{ \frac{-b}{\pi k_m\, k_q} \left[\ln\left(\frac{k(1+\sqrt{2})}{k^2}\right) + \frac{\left(k_q^2 - k_m^2\right)\ln k^2}{2\left(k_q^2 - k_m^2\right)} + (-1)^m\, ka \right] \right\} \delta_{nr}$$

$$= \frac{-4\rho c_0}{\pi A_p} \frac{k\, b}{k_m\, k_q} \left[\ln\,(1 + \sqrt{2}) + (-1)^m\, ka \right] \delta_{nr}$$

$$\approx \frac{-(-1)^m\, 4\rho c_0 k^2}{\pi k_m\, k_q} \delta_{nr}$$

since the second term in brackets predominates. Davies does not appear to give a corresponding result for T_{mnqn}. Therefore no comparison can be made.

In computer calculations, the intermodal coupling coefficients evaluated here are more generally and easily used than the more limited evaluations by Davies; see Davies[9] and Leibowitz[5,6] for further discussion and application of the coefficients.

APPENDIX G

COMPUTER PROGRAM

G1. PROCEDURES

The computer program which follows mechanizes four equations:

Equation (118)	cross-spectral density of plate displacement
Equation (119)	cross-spectral density of pressure in the cavity
Equation (121)	spectral density of power radiated into the half-space
Equation (123)	cross-spectral density of pressure in the half-space

The basic hypothesis is that the response and radiation can be adequately described by the resonant modes of the plate. Since we are concerned with frequencies below the critical frequency, all resonant modes of interest are acoustically slow ($k_{mn} > k$). Although fast modes exist at these resonance frequencies, they are all mass-controlled (nonresonant). Davies[9,10] has shown that for heavy fluid loading, only a few modes (perhaps only one or two which are resonant near the excitation frequency) are responsible for the measured response and radiation. Thus, the program searches for those modes whose (fluid-loaded) resonances are close to the excitation frequency and the intermodal coupling coefficients are calculated only for those modes. It is further assumed that the excluded "nonresonant" modes are not strongly coupled to the resonant modes. In this fashion, the matrix of $\bar{a}_{qrmn}$'s is kept relatively small, essentially dependent only on the effective bandwidth of the resonant modes; thus the summations involved in the equations are quite restricted.

As stated above, the program must determine the modes to be used before beginning the calculation of the spectral quantities. The exact resonance frequencies of the modes are quite difficult to determine. Neglecting cross-coupling terms as well as all damping terms, the resonances are very near the frequencies determined by the homogeneous modal equation obtained from Equation (29).

$$- M_{mn} \text{Re} \left(\bar{Y}_{mn} \right) + \omega^2 \left(\rho_c I_x^{mnmn} - \rho J_x^{mnmn} \right) = 0 \tag{126}$$

where, by Equation (22), $\text{Re} \left(\bar{Y}_{mn} \right) = \omega_s^2 - \omega^2$. However, the fluid-loaded mode resonances can be estimated with sufficient accuracy, as (see proof below)

$$\bar{f}_{mn} = \frac{f_{mn}}{\left[1 + \dfrac{\rho + \rho_c \coth k_{mn} c}{m k_{mn}} \right]^{\frac{1}{2}}} \tag{127}$$

The value of $\bar{f}_{mn}$ must lie within a modal bandwidth of the excitation frequency for the mode to be selected. The resultant $\bar{f}_{mn}$ is never used in the calculation. Once the mode

is selected, the final answer will be based on the actual response of that mode, the exact resonance frequency of which will be close to but not necessarily equal to $\bar{f}_{mn}'$. The exact resonance frequency is never needed in the calculation.

The program is designated as an experimental program. Program development was intended to determine basic operational feasibility with only limited data input and output capabilities. The program is written in FORTRAN IV.

Proof of Equation (127)

In Equation (A33) of Reference 4 and (by an alternative procedure) in Equation (C7) of Reference 6, it was shown that the resonance frequencies of a plate in an infinite rigid baffle and subject to fluid loading on one side can be represented with sufficient accuracy by the frequency – wavenumber relation*

$$\bar{f}_{mn} = \frac{f_{mn}}{\left[1 + \dfrac{\rho}{\rho_s \left(k_m^2 + k_n^2 - k^2\right)^{\frac{1}{2}} h}\right]} = \frac{f_{mn}}{\left[1 + \dfrac{\rho/k_{mn}}{m}\right]^{\frac{1}{2}}} \text{ for } k_{mn} > k$$

where

ρ = density of the fluid

m = $\rho_s h$ is the structural mass per unit area of the plate

μ_{mn} = $\left(k_m^2 + k_n^2 - k^2\right)^{\frac{1}{2}} = \left(k_{mn}^2 - k^2\right)^{\frac{1}{2}}$ = the eigenvalue for the fluid-loaded plate which is real for acoustically slow modes

$\dfrac{\rho}{k_{mn}}$ = added mass per unit area of the fluid in the half-space; see Equation (A28) Reference 4.

The fluid-loaded mode resonances for a plate-cavity system can be estimated with sufficient accuracy by including the effects of the cavity loading in the above formulation. Following Pretlove[16], but accounting for the different coordinate systems, we now determine this effect for a blocked (rigid) cavity; note however, that the cavity is bounded by a flexible vibrating plate.**

The sound field within the cavity is governed by the nondissipative linear wave equation of acoustics for a homogeneous, loss and source-free medium at rest.

---

*This equation accounts for autocoupling only. The frequency-wavenumber relation accounting for both modal autocoupling and modal cross coupling for the plate is given by Equations (C25) or (C29) of Reference 6. Introduction of cavity effects including both types of coupling requires extension of the following analysis for the cavity.

**The approach is somewhat similar to that used by Dyer wherein all of the interior surfaces except the plate were assumed to be pressure release surfaces; see pages 22-25 of Reference 1.

$$\nabla^2 \phi - \frac{1}{c_0^2} \frac{\partial^2 \phi}{\partial t^2} = \frac{\partial^2 \phi}{\partial x^2} + \frac{\partial^2 \phi}{\partial y^2} + \frac{\partial^2 \phi}{\partial z^2} - \frac{1}{c_0^2} \frac{\partial^2 \phi}{\partial t^2} = 0$$

Assume a general solution for the wave equation in the form of normal modes m,n

$$\phi(x,y,z,t) = \sum_{m,n} \cos \frac{m\pi x}{a} \cos \frac{n\pi y}{b} \, h_{mn}(z) \, e^{-i(\omega t + \psi)}$$

Substituting the modal expression for ϕ into the wave equation, we get the second order homogeneous ordinary differential equation

$$h_{mn}''(z) - \mu_{mn}^2 \, h_{mn}(z) = 0$$

where the dashes denote differentiation with respect to z, and where

$$\mu_{mn}^2 = h_{mn}^2 - k^2 = \pi^2 \left[\left(\frac{m}{a} \right)^2 + \left(\frac{n}{b} \right)^2 \right] - \frac{\omega^2}{c_0^2}$$

is a real positive quantity for modes whose frequencies lie below the critical frequency.

Since all interior surfaces except that for the vibrating plate are treated as rigid, thus excluding the effects of absorption at the walls, the boundary conditions for the velocities are

$$\dot{u} = \frac{\partial \phi}{\partial x} = 0 \qquad \text{at } x = 0, a$$

$$\dot{v} = \frac{\partial \phi}{\partial y} = 0 \qquad \text{at } y = 0, b$$

$$\dot{w} = \frac{\partial \phi}{\partial z} = w_p(x,y,t) \text{ at } z = 0$$

$$\dot{w} = \frac{\partial \phi}{\partial z} = 0 \qquad \text{at } z = c$$

where u,v,w are the displacements of the cavity walls along x,y,z, respectively.

The solutions for the differential equations are:

$$h_{mn}(z) = A_{mn} \cosh \mu_{mn} z + B_{mn} \sinh \mu_{mn} z$$

$$h_{mn}'(z) = \mu_{mn} \left[A_{mn} \sinh \mu_{mn} z + B_{mn} \cosh \mu_{mn} z \right]$$

From the boundary condition $\frac{\partial \phi}{\partial z} = 0$ at $z = c$

$$0 = h'_{mn} = \mu_{mn} \left[A_{mn} \sinh \mu_{mn} c + B_{mn} \cosh \mu_{mn} c \right]$$

whence

$$A_{mn} = - B_{mn} \coth \mu_{mn} c$$

$$B_{mn} = - A_{mn} \tanh \mu_{mn} c$$

From the boundary condition $\frac{\partial \phi}{\partial z} = \dot{w}_p$ at $z = 0$, suppressing the temporal variation $e^{-i(\omega t + \psi)}$

$$\dot{w}_p(x,y) = \sum_{m,n} \cos \frac{m\pi x}{a} \cos \frac{n\pi y}{b} \mu_{mn} \left[A_{mn} \sinh (0) + B_{mn} \cosh (0) \right]$$

$$= \sum_{m,n} \cos \frac{m\pi x}{a} \cos \frac{n\pi y}{b} \mu_{mn} B_{mn}$$

$$= - \sum_{m,n} \cos \frac{m\pi x}{a} \cos \frac{n\pi y}{b} A_{mn} \mu_{mn} \tanh \mu_{mn} c$$

Alternatively,

$$h_{mn}(z) = A_{mn} \left[\cosh \mu_{mn} z - \tanh \mu_{mn} c \sinh \mu_{mn} z \right]$$

Therefore,

$$\phi_{mn} = \sum_{m,n} \cos \frac{m\pi x}{a} \cos \frac{n\pi y}{b} A_{mn} \left[\cosh \mu_{mn} z - \tanh \mu_{mn} c \sinh \mu_{mn} z \right]$$

and

$$\left. \frac{\partial \phi}{\partial z} \right|_{z=0} = \dot{w}_p(x,y) = \sum_{m,n} \cos \frac{m\pi x}{a} \cos \frac{n\pi y}{b} A_{mn} \mu_{mn} \left[\sinh (0) - \tanh \mu_{mn} c \cosh (0) \right]$$

$$= - \sum_{m,n} A_{mn} \mu_{mn} \cos \frac{m\pi x}{a} \cos \frac{n\pi y}{b} \tanh \mu_{mn} c$$

which verifies our preceding result for $\dot{w}_p(x,y)$.

Since the plate pressure $p^i\big|_{z=0} = \rho_c \dfrac{\partial \phi}{\partial t}\big|_{z=0}$, then the modal pressure (pressure for a given mode) at the plate is (after suppressing $e^{-i(\omega t + \psi)}$)*

$$P^i_{mn} = -i\omega\rho_c \, \phi_{mn}(x,y,z)\big|_{z=0} = -i\omega\rho_c \, A_{mn} \cos\frac{m\pi x}{a} \cos\frac{n\pi y}{b}$$

and the modal impedance

$$Z_{mn}(x,y,z)\big|_{z=0} = \frac{\dot{P}^i_{mn}(x,y)}{\left[\dot{w}_p(x,y)\right]_{mn}} = \frac{-i\omega \, \rho_c \, A_{mn}}{-A_{mn} \, \mu_{mn} \tanh \mu_{mn}c}$$

$$= \frac{-i\omega \, \rho_c \, \coth \mu_{mn}c}{\mu_{mn}} = -i\omega \, m_c$$

Hence the added mass per unit area due to the fluid enclosed by the cavity is

$$m_c = \frac{\rho_c \, \coth \mu_{mn}c}{\mu_{mn}}$$

$$\approx \frac{\rho_c \, \coth k_{mn}c}{k_{mn}} \quad \text{for} \quad k_{mn} > k$$

The total added mass per unit area accounting for fluid loading on both sides of the plate, i.e., considering half-space and cavity fluid loading, is therefore $m_{\text{total added mass}} = \dfrac{\rho}{k_{mn}}$

$+ \dfrac{\rho_c \, \coth k_{mn}c}{k_{mn}}$. Hence, incorporating the total added mass into the formulation for $\bar{f}_{mn}$

$$\bar{f}_{mn} = \frac{f_{mn}}{\left[1 + \dfrac{\rho + \rho_c \coth k_{mn}c}{m \, k_{mn}}\right]^{1/2}} = \frac{f_{mn}}{\left[1 + \dfrac{m_{\text{total added mass}}}{m}\right]^{1/2}} \; ; \; k_{mn} > k$$

which represents the completion of the proof.

---

*For the impedance $Z_{mn} = \dfrac{P^i_{mn}}{(\dot{w}_p)_{mn}}$, the temporal factors for P_{mn} and $\dot{w}_{mn}$ would cancel if included.

G2. INPUT DATA FORMAT

There are 29 input data cards. Cards 1–4 require certain physical parameters to define the plate cavity system and its excitation. Card 5 is the control card used to specify the spectral quantity (or quantities) to be calculated. Cards 6 and 7 are used to specify the frequencies at which the calculations are to be made. Cards 8–17 can be used to specify up to 10 points on the plate for which cross and power spectral densities are to be calculated. All combinations of point pairs will be calculated.

Cards 18–20 are used to input from one to three coordinate points in the cavity and Cards 21–23 up to three other points in the cavity for which the cross-spectral densities, paired with the locations given on Cards 18–20, are to be calculated. That is, each point or location in the cavity specified on Cards 18–20 will be paired with each point on Cards 21–23. Thus to get the PSD, a point appearing on one of Cards 18–20 must also appear on one of Cards 21–23. Cards 24–26 and 27–29 perform the identical functions in the distant far field in the half-space. The data cards are specified as follows:

Card 1 (6F10.0)

Variable	Columns	Description
A	1–10	Plate dimension in x-direction (ft)
B	11–20	Plate dimension in y-direction (ft)
C	21–30	Cavity depth (ft)
ALFA	31–40	Cavity wall absorption coefficient (n.d.)
RHϕC	41–50	Fluid density in cavity (lb/ft^3)
CSC	51–60	Sound speed in cavity fluid (ft/sec)

Card 2 (4F10.0)

Variable	Columns	Description
AH	1–10	Plate thickness (ft)
RHϕP	11–20	Plate density (lb/ft^3)
CL	21–30	Dilatational wave speed in plate (ft/sec)
ETA	31–40	Plate structural damping loss factor (n.d.)

Card 3 (2F10.0, E10.3, F10.0, E10.3, F10.0)

Variable	Columns	Description
RHϕ	1–10	Half-space fluid density (lb/ft^3)
U	11–20	Free-stream velocity (ft/sec)
ANU	21–30	Kinematic viscosity, half-space fluid (ft^2/sec)
A$\dot{X}$	31–40	Distance from plate center to turbulence-inducing leading edge (ft)
THETA	41–50	Turbulence eddy decay period (sec)
CS	51–60	Sound speed in half-space (ft/sec)

Card 4 (6F10.0)

Variable	Columns	Description
A1	1–10	
A2	11–20	Maestrello TBL constants (n.d.) [References 1,12]
A3	21–30	
K1	31–40	(See Glossary of Symbols)
K2	41–50	
K3	51–60	

Card 5 (4I2)

Variable	Columns	Description
ID1	1,2	Flag: 1=compute S_w , 0 = do not compute
ID2	3,4	Flag: 2=compute Sp_i , 0 = do not compute
ID3	5,6	Flag: 3=compute W_{rad}^{ext} , 0 = do not compute
ID4	7,8	Flag: 4=compute Sp_2 , 0 = do not compute

Cards 6 and 7 (8F10.0/8F10.0)

Variable	Columns	Description
FREQ(1)	1−10	First frequency to be calculated
FREQ(2)	11−21	Second frequency to be calculated
.	.	
.	.	
.	.	
FREQ(8)	71−80	Eighth frequency to be calculated
FREQ(9)	1−10	Ninth frequency to be calculated
.	.	
.	.	
.	.	
FREQ(16)	71−80	Sixteenth frequency to be calculated

Note: If only FREQ(1) through FREQ(n) are to be calculated, set FREQ(n+1) through FREQ(16) = 0.0

Cards 8−17 (2F8.0, 9 (/2F8.0)

Variable	Columns	Description
XP(1)	1−8	X-coordinate on plate, point 1 (in)
YP(1)	9−16	Y-coordinate on plate, point 1 (in)
XP(2)	1−8	X-coordinate on plate, point 2 (in)
YP(2)	9−16	Y-coordinate on plate, point 2 (in)
.	.	
.	.	
.	.	
XP(10)	1−8	X-coordinate on plate, point 10 (in)
YP(10)	9−16	Y-coordinate on plate, point 10 (in)

Note: If only coordinate pairs [XP(1), YP(1)] through [XP(n), YP(n)] are to be calculated, set coordinate pairs [XP(n+1), YP(n+1)] through [XP(10), YP(10)] = 0.0

Cards 18–20 (3F3.0/3F8.0/3F8.0)

Variable	Columns	Description
XC(1)	1–8	X-coordinate in cavity, point 1 (in)
YC(1)	9–16	Y-coordinate in cavity, point 1 (in)
ZC(1)	17–24	Z-coordinate in cavity, point 1 (in)
XC(2)	1–8	X-coordinate in cavity, point 2 (in)
YC(2)	9–16	Y-coordinate in cavity, point 2 (in)
ZC(2)	17–24	Z-coordinate in cavity, point 2 (in)
XC(3)	1–8	X-coordinate in cavity, point 3 (in)
YC(3)	9–16	Y-coordinate in cavity, point 3 (in)
ZC(3)	17–24	Z-coordinate in cavity, point 3 (in)

Note: If only one point (or two points) to be used to calculate cross-spectral densities with those cavity locations to be specified on Cards 21–24, set the remaining points to 0.0. If XC(2) = 0.0, only coordinate position [XC(1), YC(1), ZC(1)] will be calculated. Similarly if XC(3) = 0.0, only the coordinate locations on Cards 18 and 19 will be calculated.

Cards 21–23 (3F8.0 /3F8.0/3F8.0)

Variable	Columns	Description
X1C(1)	1–8	X'-coordinate in cavity, point 1 (in)
Y1C(1)	9–16	Y'-coordinate in cavity, point 1 (in)
Z1C(1)	17–24	Z'-coordinate in cavity, point 1 (in)
X1C(2)	1–8	X'-coordinate in cavity, point 2 (in)
Y1C(2)	9–16	Y'-coordinate in cavity, point 2 (in)
Z1C(2)	17–24	Z'-coordinate in cavity, point 2 (in)
X1C(3)	1–8	X'-coordinate in cavity, point 3 (in)
Y1C(3)	9–16	Y'-coordinate in cavity, point 3 (in)
Z1C(3)	17–24	Z'-coordinate in cavity, point 3 (in)

Note: If X1C(2) = 0.0, only location [X1C(1), Y1C(1), Z1C(1)] will be calculated. If X1C(3) = 0.0, locations on cards 21 and 22 will be calculated.

Cards 24–26 (3F8.0/3F8.0/3F8.0)

Variable	Columns	Description
X1(1)	1–8	X-coordinate in half-space, point 1 (in)
Y1(1)	9–16	Y-coordinate in half-space, point 1 (in)
Z1(1)	17–24	Z-coordinate in half-space, point 1 (in)
X1(2)	1–8	X-coordinate in half-space, point 2 (in)
Y1(2)	9–16	Y-coordinate in half-space, point 2 (in)
Z1(2)	17–24	Z-coordinate in half-space, point 2 (in)
X1(3)	1–8	X-coordinate in half-space, point 3 (in)
Y1(3)	9–16	Y-coordinate in half-space, point 3 (in)
Z1(3)	17–24	Z-coordinate in half-space, point 3 (in)

Note: Comments on Cards 18–20 are applicable.

Cards 27–29 (3F8.0/3F8.0/3F8.0)

Variable	Columns	Description
X2(1)	1–8	X'-coordinate in half-space, point 1 (in)
Y2(1)	9–16	Y'-coordinate in half-space, point 1 (in)
Z2(1)	17–24	Z'-coordinate in half-space, point 1 (in)
X2(2)	1–8	X'-coordinate in half-space, point 2 (in)
Y2(2)	9–16	Y'-coordinate in half-space, point 2 (in)
Z2(2)	17–24	Z'-coordinate in half-space, point 2 (in)
X2(3)	1–8	X'-coordinate in half-space, point 3 (in)
Y2(3)	9–16	Y'-coordinate in half-space, point 3 (in)
Z2(3)	17–24	Z'-coordinate in half-space, point 3 (in)

Note: Comments on Cards 21–23 are applicable.

G3. OUTPUT VARIABLES

Output variable names are as follows (for variables refer to the Glossary of Symbols):

Variable	Name	Units
f_{mn}	FMN	Hz
$\bar{f}_{mn}$	FMNB	Hz
k_{mn}	KMN	in^{-1}
$S_w(\bar{x}\|\bar{x}';\omega)$	SW	$in^{-2}/(rad/sec)$
$S_{p_i}(\bar{\xi}\|\bar{\xi}';\omega)$	SPI	$(lb/in^2)^2/(rad/sec)$
$W_{rad}^{ext}(\omega)$	SPOWER	$(lb\text{-}in/sec)/(rad/sec)$
$S_{p_2}(\bar{\xi}\|\bar{\xi}';\omega)$	SP2	$(lb/in^2)^2/(rad/sec)$

G4. PROGRAM OUTPUT

Given below is the program output format:

1

RESPONSE AND RADIATION OF WATER-LOADED PLATE CAVITY SYSTEM SUBJECT TO BOUNDARY LAYER TURBULENCE

CAVITY SIZE A = _____ B = _____ C = _____ WALL ABSORPTION = _____

PLATE THICKNESS = _____ LOSS FACTOR = _____

FREE-STREAM VELOCITY = _____ BOUNDARY LAYER
DISPLACEMENT THICKNESS = _____

Cavity size, plate thickness, and boundary layer displacement thickness are in in., free-stream velocity in ft/sec.

2

FREQUENCY = _____

J	M	N	FMN	FMNB	KMN
1	-	-	-	-	-
2	-	-	-	-	-
.	.	.	.	.	.
.	.	.	.	.	.
.	.	.	.	.	.
JMAX	-	-	-	-	-

FREQUENCY = _____

REAL PART OF ALPHA MATRIX

A(1,1) = _____   A(1,2) = _____ · · ·

    ·   ·

    ·   ·

    ·   ·

FREQUENCY = _____

IMAGINARY PART OF ALPHA MATRIX

A(1,1) = _____   A(1,2) = _____ · · ·

    ·   ·

    ·   ·

    ·   ·

Dimensionally, the real and imaginary parts of the ALPHA matrix ($\bar{a}_{qrmn}$) have units of in/lb$_f$.

The desired spectral densities will be written in the following formats.

FREQUENCY = _____

CROSS SPECTRAL DENSITY OF PLATE DISPLACEMENT

SW = CW – SQRT (-1)* QW (IN**2)/(RAD/SEC)

(X1,Y1)	(X2,Y2)	CW	QW
– –	– –	–	–
– –	– –	–	–
· ·	· ·	·	·
· ·	· ·	·	·
· ·	· ·	·	·
– –	– –	–	–

The cross-spectral density functions are given in terms of the coincident spectral density functions and the quadrature spectral density functions.

FREQUENCY = _____

CROSS SPECTRAL DENSITY OF INTERNAL PRESSURE

SPI = CIP − SQRT(-1)*QPI   ((LB/IN**2)**2)/(RAD/SEC)

(X1,Y1,Z1)	(X2,Y2,Z2)	CPI	QPI
-	-	-	-
-	-	-	-
.	.	.	,
.	.	.	,
.	.	.	.
-	-	-	-

SPECTRAL DENSITIES OF RADIATED POWER

SPOWER = CPOWER − SQRT(-1)*QPOWER   ((LB-IN)/SEC)/(RAD/SEC)

FREQUENCY (HZ)	CPOWER	QPOWER
-	-	-

FREQUENCY = _____

CROSS-SPECTRAL DENSITY OF FAR-FIELD PRESSURE

SP2 = CP2 − SQRT(-1)*QP2   ((LB/IN**2)**2)/RAD/SEC)

(X1, Y1, Z1)	(X2, Y2, Z2)	CP2	QP2
-	-	-	-
-	-	-	-
.	.	.	.
.	.	.	.
.	.	.	.
-	-	-	-

Following completion of the spectral densities calculation, the frequency is incremented.

G5.   PROGRAM LISTING

The experimental program listing follows. The main program requires Subroutines CPMINV, MATINS, BESJ, and Function Subprogram HANK. These are also listed.

```
      PROGRAM POPE (TAPE5=INPUT,TAPE6=OUTPUT)
C   EXPERIMENTAL PROGRAM - JOB 117891
C     PROGRAM COMPUTES THE RESPONSE AND RADIATION OF A FLUID LOADED
C     PLATE CAVITY SYSTEM OWING TO BOUNDARY LAYER TURBULENCE EXCITATION
C     TBL IS DESCRIBED BY THE MAESTRELLO  CORRELATION FUNCTION
C     CALCULATION IS BASED ON RESPONSE AND RADIATION OF RESONANT
C     ACOUSTICALLY SLOW MODES (FREQUENCIES BELOW THE CRITICAL FREQUENCY)
C     COUPLING OF RESONANT A/S MODES IS INCLUDED
C     THE FOLLOWING QUANTITIES ARE COMPUTED:
C         (A) THE NARROW BAND POWER SPECTRAL DENSITY OR CROSS SPECTRAL
C             DENSITY OF PLATE DISPLACEMENT
C         (B) THE NARROW BAND POWER SPECTRAL DENSITY OR CROSS SPECTRAL
C             DENSITY OF CAVITY ACOUSTIC PRESSURES FOR HARD OR ALMOST
C             HARD WALLS
C         (C) THE NARROW BAND SPECTRAL DENSITY OF POWER RADIATED INTO
C             THE HALF-SPACE ABOVE THE PLATE
C         (D) THE NARROW BAND POWER SPECTRAL DENSITY OR CROSS SPECTRAL
C             DENSITY OF PRESSURE IN THE DISTANT FAR FIELD
C     REQUIRES SUBROUTINES CPMINV, MATINS,BESJ AND FUNCTION SUBPROGRAM
C     HANK / CALCULATIONS PERFORMED IN UNITS OF LB, IN, SEC
C     CAVITY WALL ABSORPTION COEFFICIENT TAKEN AS A CONSTANT
C     PLATE MODES STRUCTURAL DAMPING TAKEN IDENTICAL FOR ALL MODES -
C     CONSTANT INDEPENDENT OF FREQUENCY
      COMPLEX    ALPHA, ALPHC, Y, AJ, AI , SW  , PSIKL , PSIQR
      COMPLEX    S, SPI, CSUM3, CSUM4, CSUM5, CSUM6, CSUM7, CSUM8
      COMPLEX    CSUM9, CSUM10, SPOWER, CSUM11, CSUM12, CSUM13, CR1, CR2
      COMPLEX    CSUM61,CSUM71, CSUM81, CSUM91, SP2
      EQUIVALENCE  (IAMAX, JAMAX), (IBMAX, JBMAX), (ICMAX, JCMAX)
      EQUIVALENCE  (JMAX, MNMAX), (JMAX, KLMAX), (JMAX, IQRMAX)
      DIMENSION X2(10), Y2(10), Z2(10), R1(3),SP2(3,3),CP2(3,3),QP2(3,3)
      DIMENSION ALPHA(50,50), ALPHC(50,50), Y(50), YR(50), YX(50)
      DIMENSION AI(50,50), AIR(50,50), AIX(50,50)
      DIMENSION AJ(50,50), AJR(50,50), AJX(50,50)
      DIMENSION XY(50)
      DIMENSION E(100,100), INDEX(100,3), FREQ(16)
      DIMENSION AM(50), AN(50), FMN(50), FMNB(50), AKMN(50), AKM(50)
      DIMENSION AKN(50), DELTE(50), WFMN(50), JX(50), CAPA(50,20)
      DIMENSION CAPB(50,20), EPABC(20,20,20),ALAMDA(20,20,20)
      DIMENSION BLAMDA(20,20,20), X1(10), Y1(10),Z1(10)
      DIMENSION SIKL(10), SIQR(10), SW(10,10), S(10,10)
      DIMENSION PSIKL(10), PSIQR(10), CW(10,10), QW(10,10), SPI(3,3)
      DIMENSION CPI(3,3), QPI(3,3), SPOWER(16), CPOWER(16), QPOWER(16)
      DIMENSION CP1(3), P2(3), CR2(3),XP(10),YP(10),XC(10),X1C(10)
      DIMENSION YC(10),Y1C(10),ZC(10),Z1C(10),IY(50),JY(50)
C   INPUT CAVITY DIMENSIONS,ABSORPTION COEFFICIENT,CAVITY FLUID DENSITY,
C      SOUND SPEED IN CAVITY
      READ (5,1000) A,B,C,ALFA,RHOC,CSC
 1000 FORMAT (6F10.0)
      A=A*12.0
      B=B*12.0
      C=C*12.0
```

```
      RHOC= RHOC/(1728.0*386.4)
      CSC=CSC*12.0
C INPUT PLATE THICKNESS,DENSITY,COMPRESSION WAVESPEED,STRUCTURAL DAMPING
      READ (5,1001) AH,RHOP,CL,ETA
 1001 FORMAT(4F10.0)
      AH=AH*12.0
      RHOP=RHOP/(1728.0*386.4)
      CL=CL*12.0
      AP=A*H
C  INPUT HALF-SPACE FLUID DENSITY,FREESTREAM VELOCITY,KINEMATIC
C  VISCOSITY,DISTANCE FROM LEADING EDGE,EDDY DECAY PERIOD,SOUND SPEED
      READ (5,1002) RHO,U,ANU,AX,THETA,CS
 1002 FORMAT (2F10.0,F10.3,F10.0,E10.3,F10.0)
C  INPUT TBL CONSTANTS
      READ (5,1003) A1,A2,A3,AK1,AK2,AK3
 1003 FORMAT (6F10.0)
C  INPUT DESIRED CALCULATION INDEX (NO CALCULATION IF ZERO)
C    1 = CROSS SPECTRAL DENSITY OF PLATE DISPLACEMENT
C    2 = CROSS SPECTRAL DENSITY OF CAVITY PRESSURE
C    3 = SPECTRAL DENSITY OF POWER RADIATED TO HALF SPACE
C    4 = CROSS SPECTRAL DENSITY OF FAR FIELD PRESSURE
      READ (5,1004) ID1,ID2,ID3,ID4
 1004 FORMAT(4I2)
C     INPUT FREQUENCIES TO BE CALCULATED (16 MAX)
      READ (5,1005) (FREQ(II),II=1,16)
 1005 FORMAT(8F10.0 / 8F10.0)
      RHO=RHO/(1728.0*386.4)
      AMASS=RHOP*AH*AP/4.0
      READ (5,700) ((XP(J),YP(J),J=1,10)
  700 FORMAT (2F8.0, 9(/ 2F8.0))
      READ (5,800) ((XC(J),YC(J),ZC(J),J=1,3)
      READ (5,800) ((X1C(J),Y1C(J),Z1C(J),J=1,3)
  800 FORMAT (3F8.0 / 3F8.0 / 3F8.0)
      READ (5,800) ((X1(J),Y1(J),Z1(J),J=1,3)
      READ (5,800) ((X2(J),Y2(J),Z2(J),J=1,3)
      WRITE (6,500)
      WRITE (6,621)
  621 FORMAT (4X,33HEXPERIMENTAL PROGRAM - JOB 117891)
      WRITE (6,622)
  622 FORMAT (//,8X,95HRESPONSE AND RADIATION OF WATER LOADED PLATE CAVI
     1TY SYSTEM SUBJECT TO BOUNDARY LAYER TURBULENCE)
      WRITE (6,623) A,B,C,ALFA
  623 FORMAT (//,8X,15HCAVITY SIZE   A=,F6.2,4H   B=,F6.2,4H   C=,F6.2,18H
     1 WALL ABSORPTION=,F4.2)
      WRITE (6,624) AH,ETA
  624 FORMAT (//,8X,16HPLATE THICKNESS=,F5.3,14H   LOSS FACTOR=,F4.2)
      AX=AX*12.0
      THETA2=THETA**2
      U=U*12.0
      UU=U/12.0
      ANU=ANU*144.0
```

```
      DSTAR=(0.37*AX/8.0)*((U*AX/ANU)**-0.2)
      AF  =  DSTAR / U
      UC=0.8*U
      CS=CS*12.0
      WRITE (6,625) UU ,DSTAR
  625 FORMAT (//,8X,21HFREE STREAM VELOCITY=,F4.1,40H   BOUNDARY LAYER DI
     1SPLACEMENT THICKNESS=,F5.3)
      PI=3.14159
      C2= PI*AH*CL/(4.0* 1.732)
      II=0
 1101 II=II+1
      IF (II.EQ.17) GO TO 1100
      IF (FREQ(II).EQ.0.0)   GO TO  1100
      CALL  SECOND(W)
      WRITE(6,6000) W,II
 6000 FORMAT(////   5H USED, F8.3, 34H SECONDS CPU AT START OF FREQUENCY
     2    I4)
      CALL PSECOND(W)
      WRITE(6,6001) W
 6001 FORMAT(1H+, 51X, F8.3,   7H PP SEC///1H )
      W= 2.0*PI* FREQ(II)
      WNO1= U/CS
      WNO2= W/CSC
      WNO12 = WNO1**2
      WNO22=WNO2*WNO2
      C3= RHO*(W**2)
      C4= RHOC*(W**2)
C DETERMINE  RESONANT ACOUSTICALLY  SLOW  MODES
      C1=0.0
    9 C1=C1+1
      J=0
      M=1
      N=1
    1 HKMN=(((FLOAT(M)*PI /A)**2)+ ((FLOAT(N)*PI/B)**2))** 0.5
      IF (WNO1-HKMN) 2,2,4
    2 FRMN= C2*(((FLOAT(M)/A)**2)+((FLOAT (N)/B) **2 ))
      FRMNH=FRMN/ (( 1.0 +( RHO / (RHOP*AH*HKMN))+((RHOC/TANH(HKMN*C))/
     1    (RHOP*AH*HKMN )))** 0.5)
      DELTAE = PI*FRMNH*ETA/ 2.0
      DELTAE = C1*DELTAE
      FMNHL=FRMNH - (DELTAE/2.0)
      FMNHH=FRMNH + (DELTAE/2.0)
      IF ( FMNHH - FREQ(II)) 4,5,6
    6 N=N+1
      GO TO 1
    4 IF ( FMNHH -FREQ(II))    5,5,7
    7 IF (N.EQ.1) GO TO 8
      N=1
      M=M+1
      GO TO 1
    5 J= J+1
```

```
      AM(J)= M
      AN(J)= N
      FMN(J) = FRMN
      FMNB(J) = FRMNB
      AKMN(J) = BKMN
      AKM(J)= AM(J)* (PI/A)
      AKN(J)= AN(J)* (PI/B)
      DFLTE(J)=DELTAE
      JX(J)=J
      V=V+1
      GO TO 1
    8 CONTINUE
      JMAX=J
      IF(JMAX.EO.0) GO TO 9
      WRITE (6,500)
  500 FORMAT (1H1)
      WRITE (6,711) FREQ(II)
      WRITE (6,501)
  501 FORMAT (4X,37HJ    M    N       FMN       FMNB      KMN,//)
      WRITE (6,503)((JX(J),AM(J),AN(J),FMN(J),FMNB(J),AKMN(J)),J=1,JMAX)
  503 FORMAT(/3X,I2,2X,F3.0,1X,F3.0,3X, F7.0, 2X,F7.0,2X,F7.3)
C  CALCULATE MATRIX OF ALPHAS
C     INDEX J=(M,N)    INDEX I=(Q,R)
      DO 45  J=1,JMAX
      WFMN(J)= 2.0*PI*FMN(J)
   45 CONTINUE
      DO 46 J=1,JMAX
      YX(J)=(WFMN(J)**2)*(1.-((W/WFMN(J))**2))*(-1.0*AMASS)
      YR(J)= ((WFMN(J)**2)*ETA)*AMASS
      Y(J)= CMPLX (YX(J),YR(J))
   46 CONTINUE
      IMAX=JMAX
      DO 310  J=1, JMAX
      IMIN=J
      DO 310 I=IMIN,IMAX
      AJR(J,I)=0.0
      AJX(J,I)=0.0
      IQM=(-1)**IFIX(AM(J) + AM(I))
      INR=(-1)**IFIX(AN(J) + AN(I))
      IF(IQM.NE.1) GO TO 209
      IF(INR.NE.1) GO TO 209
      IF (AKM(J)-WNO1) 10,20,20
   10 IF (AKN(J)-WNO1) 30,40,40
   20 IF (AKN(J)-WNO1) 50,50,60
   30 IF (AKM(I)-WNO1) 70,80,80
   40 IF (AKM(I)-WNO1) 90,100,100
   50 IF (AKM(I)-WNO1) 110,120,120
   60 IF (AKM(I)-WNO1) 130,140,140
   70 IF (AKN(I)-WNO1) 150,160,160
   80 IF (AKN(I)-WNO1) 170,180,180
   90 IF (AKN(I)-WNO1) 190,200,200
```

187

```
100 IF (AKN(I)-WNO1) 210,220,220
110 IF (AKN(I)-WNO1) 230,240,240
120 IF (AKN(I)-WNO1) 250,260,260
130 IF (AKN(I)-WNO1) 270,280,280
140 IF (AKN(I)-WNO1) 290,300,300
150 GO TO 209
160 GO TO 209
170 GO TO 209
180 GO TO 209
190 GO TO 209
200 CONTINUE
    X=((WNO12-(AKM(J)**2))**0.5)*B
    IF (AM(J).NE.AM(I)) GO TO 201
    D=0.01
    CALL BESJ(X,0.BJ,D,IER)
    AJR(J,I)=((-A*AKN(J)*AKN(I)*(1.0-(((-1.0)**IFIX(AN(J)))*BJ)))*C3)/
   1 (2.0*((AKMN(J)**2)-WNO12)*((AKMN(I)**2)-WNO12))
    GO TO 202
201 AJR(J,I)=0.0
202 CONTINUE
    IF (AM(J).NE.AM(I)) GO TO 203
    X3= -A/(PI*AKN(J)*AKN(I))
    X4=  WNO1*((2.0*WNO12 -(AKM(J)**2))**0.5)
    X5=  WNO1*((WNO12  - (AKM(J)**2))**0.5)
    IF (AKN(I).EQ.AKN(J)) GO TO 204
    X6=  0.5/((AKN(I)**2)-(AKN(J)**2))
    X7= (AKN(I)**2)* ALOG((AKN(J)**2) + WNO12)
    X8= (AKN(J)**2)* ALOG((AKN(I)**2) + WNO12)
    X9= X6*(X7-X8)
    GO TO 205
204 X9=ALOG(AKN(J))-0.5-(AP/(4.0*(((AKMN(J)**2)-WNO12)**0.5)*X3))
205 CONTINUE
    X10= ALOG(X4/X5)+X9
    X11= (-1.0)**IFIX(AN(I))
    X12= ((WNO12-(AKM(I)**2)+((1.0/B)**2))**0.5)+(1.0/B)
    X13= ((-1.0)*X11)*(ALOG(X12*WNO1/X5)-(B*((X12-(1.0/B))-X5/WNO1)))
    SUM=0.0
    JIMAX=3
    DO 206 JI=1,JIMAX
    IJI=JI-1
    ISUM1=(-1)**(IJI+IFIX(AN(I)))
    ISUM2=1
    IC=  (2*IJI)+1
    DO 207 JJ=1,IC
    ISUM2= ISUM2*IJ
207 CONTINUE
    ISUM2=ISUM2**2
    SUM3= (B*X5/WNO1)**((2*IJI)+1)
    SUM=SUM + (((FLOAT(ISUM1))*SUM3)/(FLOAT(ISUM2)))
206 CONTINUE
    X14=((AKN(J)**2)*(AKN(I)**2))/((AKMN(J)**2)-WNO12)
```

188

```
    1   *((AKMN(I)**2)-WNO12))
        X15 =X14*SUM
        AJX(J.I)=C3*X3*(X10+X13+X15)
        GO TO 208
203 AJX(J.I)=0.0
208 CONTINUE
209 AJ(J.I)=CMPLX(AJX(J.I).AJR(J.I))
        AJ(I.J)=AJ(J.I)
        GO TO 310
210 GO TO 209
220 CONTINUE
        IF(AKM(J).GT.AKM(I)) GO TO 221
        X18 = C3*ALOG((WNO1-AKM(J))/(WNO1+AKM(J)))
        AJR(J.I)= X18/(PI*AKM(I)*AKN(J)* AKN(I))
        IF (AN(J).EQ.AN(I)) DNR=1.0
        IF (AN(J).NE.AN(I)) DNR=0.0
        AJX(J.I)=(X18**3*DNR)/(2.0*PI*AKM(I)*AKN(J))
        GO TO 209
221 X18=C3*ALOG((WNO1-AKM(I))/(WNO1+AKM(I)))
        AJR(J.I)=X18/ (PI*AKM(J)*AKN(J)*AKN(I))
        IF (AN(J).EQ.AN(I)) DNR=1.0
        IF (AN(J).NE.AN(I)) DNR=0.0
        AJX(J.I)=(X18**3*DNR)/(2.0*PI*AKM(J)*AKN(J))
        GO TO 209
230 GO TO 209
240 GO TO 209
250 CONTINUE
        X=((WNO12-AKN(J)**2 )**0.5)*A
        IF (AN(J).NE.AN(I)) GO TO 251
        D=0.01
        CALL BESJ (X.0.BJ.D.IER)
        AJR(J.I)=((-B*AKM(J)*AKM(I)*(1.0-(((-1.0)**IFIX(AM(J)))*BJ)))*C3)/
    1   (2.0*((AKMN(J)**2)-WNO12)*((AKMN(I)**2)-WNO12))
        GO TO 252
251 AJR(J.I)=0.0
252 CONTINUE
        IF(AN(J).NE.AN(I)) GO TO 253
        X3= -B/(PI*AKM(J)*AKM(I))
        X4= WNO1 + ((2.0 * WNO12 - (AKN(J)**2))**0.5)
        X5= WNO1 + ((WNO12 - (AKN(J)**2)) ** 0.5)
        IF (AKM(I).EQ.AKM(J)) GO TO 254
        X6 = 0.5/((AKM(I)**2)-(AKM(J)**2))
        X7 = (AKM(I)**2)*ALOG((AKM(J)**2)+WNO12)
        X8 = (AKM(J)**2)*ALOG((AKM(I)**2) + WNO12)
        X9 = X6*(X7-X8)
        GO TO 255
254 X9 =ALOG(AKM(I))-0.5-(AP/(4.0*(((AKMN(J)**2)-WNO12)**0.5)*X3))
255 CONTINUE
        X10 = ALOG(X4/X5)+X9
        X11 = (-1.)**IFIX(AM(J))
        X12 = ((WNO12-(AKN(I)**2)+((1./A)**2))**0.5)+(1./A)
```

```
      X13 =((-1.0)*X11)*(ALOG(X12*WN01/X5)-(A*((X12-(1./A))-X5/WN01)))
      SUM = 0.0
      JIMAX= 3
      DO 256 JT=1, JIMAX
      IJI=J1-1
      ISUM1=(-1)**(IJI+IFIX(AM(J)))
      ISUM2=1
      IC=(2*IJT)+1
      DO 257 JJ=1,IC
      ISUM2 =ISUM2*JJ
  257 CONTINUE
      ISUM2 = ISUM2 ** 2
      SUM3=(A*X5/WN01)**((2*IJT)+1)
      SUM=SUM+(((FLOAT(ISUM1))*SUM3)/(FLOAT(ISUM2)))
  256 CONTINUE
      X14=((AKM(J)**2)*(AKM(I)**2))/(((AKMN(J)**2)-WN012)
     1 *((AKMN(I)**2)-WN012))
      X15=X14*SUM
      AJX(J,I)=C3*X3*(X10+X13+X15)
      GO TO 259
  253 AJX(J,I)=0.0
  259 CONTINUE
      GO TO 209
  260 CONTINUE
      IF(AKN(J).GT.AKN(I)) GO TO 261
      X18 =C3* ALOG((WN01-AKN(J))/(WN01+AKN(J)))
      AJR(J,I)=X18/(PI*AKN(I)*AKM(J)*AKN(I))
      IF(AM(J).EQ.AM(I)) DNR=1.0
      IF(AM(J).NE.AM(I)) DNR=0.0
      AJX(J,I) = (X18*A*DNR)/(2.0*PI*AKN(I)*AKM(J))
      GO TO 209
  261 X18= C3*ALOG((WN01-AKN(I))/(WN01+AKN(I)))
      AJR(J,I)=X18/(PI*AKN(I)*AKM(J)*AKM(I))
      IF(AM(J).EQ.AM(I)) DNR=1.0
      IF(AM(J).NE.AM(I)) DNR=0.0
      AJX(J,I)=(X18*A*DNR)/(2.0*PI*AKN(J)*AKM(J))
      GO TO 209
  270 GO TO 209
  280  GO TO 220
  290 GO TO 260
  300 CONTINUE
      X18= (-1.0)**IFIX(AM(J))
      X22= (-1.0)**IFIX(AN(J))
      AKA= WN01*A
      BKB= WN01*B
      CKC= WN01*(((A**2)+(B**2))**0.5)
      X3= (-1.0)** IFIX(AM(I)+AN(J))
      AJR(J,I) =((-2.0*WN01)/(PI*AKM(J)*AKN(J)
     1       *AKM(I)*AKN(I)))* (1.0-(X18*SIN(AKA)/AKA)
     2       -(X22*SIN(BKB)/BKB)-(X3*SIN(CKC)/CKC)).
      IF(AN(J).EQ.AN(I)) DNR = 1.0
```

```
      IF(AN(J).NE.AN(I)) DNR = 0.0
      IF(AM(J).EQ.AM(I)) DMQ = 1.0
      IF(AM(J).NE.AM(I)) DMQ = 0.0
      X1B=((-B*C3*DNR)/(PI*AKM(J)*AKM(I)))
      X23=((-A*C3*DMQ)/(PI*AKN(J)*AKN(I)))
      IF (AKN(I) .EQ. AKM(J))  GO TO  4005
      X3 = -ALOG(WNO1)+((((AKM(I)**2)*ALOG((AKM(J)**2)
     1       +WNO12))-((AKM(J)**2)*ALOG((AKM(I)**2)
     2       +WNO12)))/(2.0*((AKM(I)**2)-(AKM(J)**2))))
      GO TO 4006
 4005 X3= -ALOG(WNO1) + ALOG (AKM(J)) - 0.5
 4006 IF (AKN(I) .EQ. AKN(J))  GO TO 4007
      X4 = -ALOG(WNO1)+((((AKN(I)**2)*ALOG((AKN(J)**2)
     1       +WNO12))-((AKN(J)**2)*ALOG((AKN(I)**2)
     2       +WNO12)))/(2.0*((AKN(I)**2)-(AKN(J)**2))))
      GO TO 4008
 4007 X4 = -ALOG(WNO1) + ALOG(AKN(J)) - 0.5
 4008 X5 = ((C3*AP/4.0)/((((AKMN(J)**2)-WNO12)**0.5))*DNR*DMQ
      AJX(J,I)=(X1B*X3)+(X23*X4)-X5
      GO TO 209
  310 CONTINUE
C   CALCULATE MAXIMUM VALUES OF ALPHA, BETA, GAMMA
      IAMAX=((2.0*FREQ(II)*A)/CSC)+ 1
      IBMAX=((2.0*FREQ(II)*B)/CSC)+ 1
      ICMAX=((2.0*FREQ(II)*C)/CSC)+ 1
      C10=C4*(AP**2)/((PI**4)*16.0*A*B*C)
      DO 410 J=1,JMAX
      IMIN= J
      DO 410 I=IMIN,JMAX
      ATX(J,I)=0.0
      AIB(J,I)=0.0
      IOM=(-1)** IFIX(AM(J)+AM(I))
      INR=(-1)** IFIX(AN(I)+AN(I))
      IF(IOM.NE.1) GO TO 420
      IF(INR.NE.1) GO TO 420
      DO 410 IA=1,IAMAX
      AA=IA-1
      JA=AA
      IF(JA.EQ.0) FPA=1.0
      IF(JA.GT.0) FPA=2.0
      IF(IFIX(AM(I)).EQ.JA) GO TO 411
      X11=(AM(I)+AA)*PI
      X22=(AM(I)-AA)*PI
      CAPA(I,IA)=(((1.0-COS(X11))/X11)+((1.0-COS(X22))/X22))*PI
      GO TO 412
  411 CAPA(I,IA)=0.0
  412 CONTINUE
      DO 410 IB=1,IBMAX
      BB=IB-1
      JB=BB
      IF(JB.EQ.0) FPB=1.0
```

191

```
      IF (J3.GT.0) EP4=2.0
      IF(IFIX(AN(I)).EQ.JH) GO TO 415
      X11=(AN(I)+HH)*PI
      X22=(AN(I)-HR)*PI
      CAPB(I,IH)=(((1.0-COS(X11))/X11)+((1.0-COS(X22))/X22))*PI
      GO TO 416
  415 CAPB(I,IR)=0.0
  416 CONTINUF
      PROD=CAPA(I,IA)*CAPA(J,IA)*CAPB(I,IR)*CAPB(J,IB)
      DO 410 IC=1,ICMAX
      CC=IC-1
      JC=CC
      IF (JC.EQ.0) EPC=1.0
      IF (JC .GT. 0)  EPC=2.0
      FPABC(IA,IB,IC)=FPA*FPB*EPC
      IF(FPABC(IA,IB,IC) .EQ. 1.0)   GO TO 5555
      SLAMDA= PI*((((AA/A)**2)+((BB/B)**2)+((CC/C)**2))**0.5)
      CLAMDA=((WNO2*ALFA)/(8.0*SLAMDA))*((EPA/A)+(FPB/B)+(EPC/C))
      D2= 2.0*SLAMDA*CLAMDA
      D1= (SLAMDA**2)-(CLAMDA**2)-WNO22
      D= (D1**2)+(D2**2)
      ALAMDA(IA,IB,IC)=D1/D
      BLAMDA(IA,IB,IC)=D2/D
      GO TO 5556
 5555 ALAMDA(IA,IB,IC)=1.0/(-WNO22)
      BLAMDA(IA,IB,IC)=0.0
 5556 AI1=C10*ALAMDA(IA,IB,IC)*FPABC(IA,IB,IC)*PROD
      AI2=C10*BLAMDA(IA,IB,IC)*FPABC(IA,IB,IC)*PROD
      AIX(J,I)=AIX(J,I)+AI1
      AIR(J,I)=AIR(J,I)+AI2
  420 CONTINUE
  410 CONTINUE
      DO 430 J=1,JMAX
      IMIN=J
      DO 430 I=IMIN,IMAX
      AI(J,I)= CMPLX(AIX(J,I),AIR(J,I))
      AI(I,J)=AI(J,I)
  430 CONTINUE
      DO 600 J=1,JMAX
      DO 600 I=1,IMAX
      ALPHA(J,I)=AI(J,I)-AJ(J,I)
  600 CONTINUE
      DO 610 J=1,JMAX
      ALPHA(J,J)=ALPHA(J,J)+Y(J)
  610 CONTINUE
      NN=50
      N2=2*JMAX
      CALL CMPINV(ALPHA,NN,JMAX,ALPHA,ID,F,N2,INDEX)
C   SUBROUTINE CMPINV REQUIRES SUBROUTINE MATINS
      DO 620 J=1,JMAX
      DO 620 I=1,IMAX
```

```
      ALPHC(J,I)= CONJG(ALPHA(J,I))
  620 CONTINUE
      WRITE (6,500)
      WRITE (6,711) FREQ(II)
  711 FORMAT(//,11X,10HFREQUENCY=,F8.0,//)
      WRITE (6,611)
  611 FORMAT(11X,25HREAL PART OF ALPHA MATRIX,//)
      DO 612 I=1,IMAX
      DO 613 J=1,JMAX
      XYZ(J)=REAL(ALPHA(I,J))
      IY(J)=I
  613 JY(J)=J
      WRITE(6,614)  (IY(J),JY(J),XYZ(J),J=1,JMAX)
  614 FORMAT((5(2X,2HA(,I2,1H,,I2,2H)=,E13.6)))
  612 CONTINUE
      WRITE (6,500)
      WRITE (6,711) FREQ(II)
      WRITE (6,615)
  615 FORMAT (11X,30HIMAGINARY PART OF ALPHA MATRIX,//)
      DO 616 I=1,IMAX
      DO 617 J=1,JMAX
      XYZ(J)=AIMAG(ALPHA(I,J))
      IY(J)=I
  617 JY(J)=J
      WRITE(6,614)  (IY(J),JY(J),XYZ(J),J=1,JMAX)
  616 CONTINUE
      WRITE (6,500)
      IF(II).NE.1) GO TO 2000
      J=1
  702 IF(XP(J).EQ.0.0) GO TO 701
      IF(J.EQ.10) GO TO 703
      J=J+1
      GO TO 702
  701 JJMAX = J-1
      GO TO 704
  703 JJMAX =10
  704 IIMAX=JJMAX
      C100= (0.000121)*(RHO**2)*(U**4)*(DSTAR**2)*AP*THETA*2.0
      DO 710 J=1,JJMAX
      IMIN=J
      DO 710 I=IMIN,IIMAX
      SW(J,I)= CMPLX(0.0,0.0)
      DO 709 MN= 1,MNMAX
      C50= 1.0 +(THETA2*((W-(AKM(MN)*UC))**2))
      Z =AK1*AF*UC*SQRT((AKN(MN)**2)+((W/UC)**2))
      ZZ=AK2*Z/AK1
      ZZZ=AK3*Z/AK1
      SUM1=((A1*AK1*HANK(Z)+A2*AK2*HANK(ZZ)+A3*AK3*HANK(ZZZ))*C100)/C50
      DO 709 KL=1,KLMAX
      SIKL(J)=SIN(AKM(KL)*XP(J))*SIN(AKN(KL)*YP(J))*SUM1
      PSIKL(J)=CMPLX(SIKL(J),0.0)
```

193

```
      DO 709 IOR=1,IORMAX
      SIQR(I)=SIN(AKM(IOR)*XP(I))*SIN(AKN(IOR)*YP(I))
      PSIOR(I)= CMPLX(SIQR(I),0.0)
      S(J,I)=ALPHA(IOR,MN)*ALPHC(KL,MN)*PSIKL(J)*PSIOR(I)
      SW(J,I)= S(J,I)+SW(J,I)
  709 CONTINUE
      SW(I,J)=CONJG(SW(J,I))
  710 CONTINUE
      DO 718 J=1,JJMAX
      DO 718 I=1,IIMAX
      CW(J,I)= REAL(SW(J,I))
      QW(J,I)= -AIMAG(SW(J,I))
  718 CONTINUE
      WRITE (6,711) FREQ(II)
      WRITE (6,712)
  712 FORMAT(4X,8HHCROSS SPECTRAL DENSITY OF PLATE DISPLACEMENT    SW = C
     1W - SQRT(-1)*QW    (IN**2)/(RAD/SEC),//)
      WRITE (6,713)
  713 FORMAT (4X,32H( X1  ,  Y1  )  (  X2  ,  Y2  ),10X,2HCW,16X,2HQW,/
     1/)
      WRITE (6,715)(( XP(J),YP(J),XP(I),YP(I),CW(J,I),QW(J,I) ,J=1,
     1JJMAX),I=1,IIMAX)
  715 FORMAT((5X,F6.2,1X,F6.2,4X,F6.2,1X,F6.2,6X,E13.6,5X,E13.6)/)
 2000 IF(IOP.NE.2) GO TO 3000
      J=1
  802 IF(XC(J).EQ.0.0) GO TO 801
      IF(J.EQ.3) GO TO 803
      J=J+1
      GO TO 802
  801 JJMAX=J-1
      GO TO 804
  803 JJMAX=3
  804 CONTINUE
      I=1
  822 IF(X1C(I).EQ.0.0) GO TO 821
      IF(I.EQ.3) GO TO 823
      I=I+1
      GO TO 822
  821 IIMAX=I-1
      GO TO 824
  823 IIMAX=3
  824 CONTINUE
      C101=0.0000000776*(RHO**2)*(RHOC**2)*(U**4)*(A2**3)*(DSTAR**2)*2.0
     1 *(W**4)*THETA/((A*B*C)**2)
      DO 810 J=1,JJMAX
      DO 810 I=1,IIMAX
      SPI(J,I)= CMPLX(0.0,0.0)
      DO 829 MN=1,MNMAX
      C51=1.0 + (THETA2*((W-AKM(MN)*UC) **2))
      Z=AK1*AF*UC*SQRT((AKN(MN)**2)+((W/UC)**2))
      ZZ= AK2*Z/AK1
```

194

```
      ZZZ=AK3*Z/AK1
      SUM1 = ((A1*AK1*HANK(Z)+A2*AK2*HANK(ZZ)+A3*AK3*HANK(ZZZ))*C101)/C51
      CSUM3= CMPLX(SUM1,0.0)
      DO 809 KL=1,KLMAX
      CSUM4 = CSUM3 * ALPHC(KL,MN)
      DO 809 IQR=1,IQRMAX
      CSUM5 = CSUM4* ALPHA (IQR,MN)
      DO 809 IA=1,IAMAX
      AA=IA-1
      CSUM6 = CSUM5*CAPB(KL,IA)*COS((AA*PI/A)*XC(J))
      DO 809 IB=1,IBMAX
      BB=IB-1
      CSUM7 = CSUM6* CAPH(KL,IA)*COS((BB*PI/B)*YC(J))
      DO 809 IC=1,ICMAX
      CC=IC-1
      CSUM8 = CSUM7 * EPARC(IA,IB,IC)* CMPLX(ALAMDA(IA,IB,IC),BLAMDA(IA,
     1IB,IC))*COS((CC*PI/C)*ZC(J))
      DO 809 JA=1,JAMAX
      AAA=JA-1
      CSUM9=CSUM8*CAPB(IQR,JA)*COS((AAA*PI/A)*X1C(I))
      DO 809 JB=1,JBMAX
      BBB=JB-1
      CSUM10=CSUM9*CAPH(IQR,JB)*COS((BBB*PI/B)*Y1C(I))
      DO 809 JC=1,JCMAX
      CCC=JC-1
      BLMDA=BLAMDA(JA,JB,JC)*(-1.0)
      S(J,I) = CSUM10*EPARC(JA,JB,JC)*CMPLX(ALAMDA(JA,JB,JC),BLMDA)
     1     * COS((CCC*PI/C)*Z1C(I))
      SPI(J,I)= S(J,I) + SPI(J,I)
  809 CONTINUE
  810 CONTINUE
      DO 819 J=1,JJMAX
      DO 819 I=1,IIMAX
      CPI(J,I) = REAL(SPI(J,I))
  819 QPI(J,I) = -AIMAG(SPI(J,I))
      WRITE(6,500)
      WRITE(6,711) FREQ(II)
      WRITE(6,812)
  812 FORMAT(4X,98HCROSS SPECTRAL DENSITY OF INTERNAL PRESSURE    SPI = C
     1PI - SQRT(-1)*QPI    ((LB/IN**2)**2)/(RAD/SEC),//)
      WRITE (6,813)
  813 FORMAT (4X,46H(   X1   ,   Y1   ,   Z1   ) (   X2   ,   Y2   ,   Z2   ),10X,
     13HCPI,16X,3HQPI,//)
      WRITE(6,815)    ((XC(J),YC(J),ZC(J),X1C(I),Y1C(I),Z1C(I),CPI(J,I),
     1QPI(J,I) ,J=1,JJMAX),I=1,IIMAX)
  815 FORMAT(5X,F6.2,1X,F6.2,1X,F6.2,4X,F6.2,1X,F6.2,1X,F6.2,6X,E13.6,5X
     1,E13.6)
 3000 IF(IJJ.NE.3) GO TO 4000
      C102=0.000121*(RHO**3)*(W**3)*AP*(U**4)*(DSTAR**2)*THETA*2
      SPOWER(II)=CMPLX(0.0,0.0)
      DO 909 MN=1,MNMAX
```

195

```
      C52 = 1.0 + (THETA2*((W-(AKM(MN)*UC))**2))
      Z=AK1*AF*UC*SQRT((AKN(MN)**2)+((W/UC)**2))
      ZZ=AK2*Z/AK1
      ZZZ=AK3*Z/AK1
      SUM1=((A1*AK1*HANK(Z)+A2*AK2*HANK(ZZ)+A3*AK3*HANK(ZZZ))*C102)/C52
      CSUM11=CMPLX(0.0,SUM1)
      DO 909 KL=1,KLMAX
      CSUM12 =CSUM11*ALPHC(KL,MN)
      DO 909 IQR=1,IQRMAX
      CSUM13 =CSUM12 *ALPHA(IQR,MN)*AJ(IQR,KL)/C3
      SPOWER(II) = CSUM13 + SPOWER(II)
  909 CONTINUE
      CPOWER(II) = REAL(SPOWER(II))
      QPOWER(II) = -AIMAG(SPOWER(II))
      WRITE (6,500)
      WRITE (6,995)
  995 FORMAT (4X,97HSPECTRAL DENSITIES OF RADIATED POWER     SPOWER = CPOW
     1ER - SQRT(-1)*QPOWER   ((LB-IN)/SEC)/(RAD/SEC),//)
      WRITE (6,996)
  996 FORMAT (4X,14HFREQUENCY (HZ),12X,6HCPOWER,12X,6HQPOWER,//)
      WRITE(6,997)  FREQ(II),CPOWER(II),QPOWER(II)
  997 FORMAT (7X,F8.0,12X,F13.6,5X,E13.6)
 4000 IF(ID4.NE.4) GO TO 5000
      J=1
  952 IF(X1(J).EQ.0.0) GO TO 951
      IF(J.EQ.3) GO TO 953
      J=J+1
      GO TO 952
  951 JJMAX=J-1
      GO TO 954
  953 JJMAX=3
  954 CONTINUE
      I=1
  962 IF(X2(I).EQ.0.0) GO TO 961
      IF(I.EQ.3) GO TO 963
      I=I+1
      GO TO 962
  961 IIMAX=I-1
      GO TO 964
  963 IIMAX=3
  964 CONTINUE
      C103=0.00000306*(RHO**4)*(W**4)*AP*(U**4)*(DSTAR**2)*THETA*2.0
      DO 970 J=1,JJMAX
      X=X1(J)
      Y=Y1(J)
      Z=Z1(J)
      R1(J)=SQRT(X**2 + Y**2 + Z**2)
      AKR1= WNO1*R1(J)
      CR1(J)=CMPLX(0.0,AKR1)
      CSUM3 =C103* CEXP(CR1(J))/R1(J)
      DO 970 I=1,IIMAX
```

196

```
      SP2(J,I)=CMPLX(0.0,0.0)
      XPRIME=X2(I)
      YPRIME=Y2(I)
      ZPRIME=Z2(I)
      R2(I)= SQRT(XPRIME**2 + YPRIME**2 + ZPRIME**2)
      AKR2= -WNO1*R2(I)
      CR2(I)=CMPLX(0.0,AKR2)
      CSUM4 = CSUM3* CEXP(CR2(I))/R2(I)
      DO 970 KL=1,KLMAX
      SUM5 = AKM(KL)* AKN(KL)
      SM6 = (-1.0)* WNO1* XPRIME* A / R2(I)
      CSUM6 = CMPLX(0.0,SM6)
      SM7 = (-1.0)* WNO1* YPRIME* B / R2(I)
      CSUM7 = CMPLX(0.0,SM7)
      CSUM8 = CSUM4*(1.0-(((-1.0)**IFIX(AM(KL)))*CEXP(CSUM6)))*(1.0-(((-
     11.0)**IFIX(AN(KL)))*CEXP(CSUM7)))*SUM5
      SM9 =(AKM(KL)**2)-((WNO12*(XPRIME**2))/(R2(I)**2))
      SM10=(AKN(KL)**2)-((WNO12*(YPRIME**2))/(R2(I)**2))
      CSUM9=CSUM8/(SM9 * SM10)
      DO 970 IQR= 1,IQRMAX
      SUM51= AKM(IQR) * AKN(IQR)
      SM61 = WNO1*X*A/R1(J)
      CSUM61= CMPLX(0.0,SM61)
      SM71= WNO1*Y * B / R1(J)
      CSUM71= CMPLX(0.0,SM71)
      CSUM81= CSUM9 * SUM51 * (1.0-(((-1.0)**IFIX(AM(IQR)))*CEXP(CSUM61)
     1))*(1.0-(((-1.0)**IFIX(AN(IQR)))*CEXP(CSUM71)))
      SM91=(AKM(IQR)**2)- ((WNO12 * (X**2))/(R1(J)**2))
      SM101 =(AKN(IQR)**2)-((WNO12 * (Y**2))/(R1(J)**2))
      CSUM91 = CSUM81/(SM91 * SM101)
      DO 970 MN = 1, MNMAX
      V= AK1*AF*UC * SQRT ((AKN(MN)**2) + ((W/UC) **2))
      VV=AK2*V/AK1
      VVV= AK3*V/AK1
      SUM1 =   A1*AK1*HANK(V)+A2*AK2*HANK(VV)+A3*AK3*HANK(VVV)
      C54= 1.0+(THETA2 * ((W - (AKM(MN)*UC))**2))
      SUM1 = SUM1/C54
      S(J,I) = CSUM91 * ALPHA(IQR,MN)*ALPHC(KL,MN) * SUM1
      SP2(J,I) = S(J,I) + SP2(J,I)
  970 CONTINUE
      DO 978 J=1,JJMAX
      DO 978 I=1,IIMAX
      CP2(J,I)=REAL(SP2(J,I))
      QP2(J,I)=-AIMAG(SP2(J,I))
  978 CONTINUE
      WRITE (6,500)
      WRITE (6,711) FREQ(II)
      WRITE (6,992)
  992 FORMAT (4X,97HCROSS SPECTRAL DENSITY OF FARFIELD PRESSURE   SP2 =
     1CP2 - SQRT(-1)*QP2   ((LB/IN**2)**2)/(RAD/SEC),//)
      WRITE (6,980)
```

```
  980 FORMAT (4X,46H(  X1   .  Y1   .  Z1  )  (  X2   .  Y2   .  Z2  ),10X,3
     1HCP2,16X,3HQP2,//)
        WRITE (6,993) (((X1(J),Y1(J),Z1(J),X2(I),Y2(I),Z2(I),CP2(J,I),QP2(
     1J,I)),J=1,JJMAX),I=1,IIMAX)
  993 FORMAT(5X,F6.2,1X,F6.2,1X,F7.2,3X,F6.2,1X,F6.2,1X,F7.2,5X,E13.6,5X
     1,F13.6)
 5000 GO TO 1101
 1100 CONTINUE
      END
      FUNCTION HANK(X)
      IF (X-3.0) 1,2,2
    1 IF (X-0.3) 3,4,4
    3 HANK  = (0.636)* ALOG(1.123/X)
      RETURN
    2 HANK  = (0.022)*EXP(-1.07*(X-3.0))
      RETURN
    4 HANK  = (0.84)*EXP(-1.35*(X-0.3))
      RETURN
      END
       SUBROUTINE CMPINV(A,N,N1,C,ID   ,E,N2,INDEX)
COMPLEX MATRIX INVERSION    S GOOD   6/10/71
C         METHOD BY LANCZOS, APPLIED ANALYSIS, PAGE 137
C
C WHERE A IS COMPLEX INPUT MATRIX (NOT DESTROYED BY ROUTINE)
C         N      DIMENSION OF A AND C
C         N1     NUMBER OF ROWS IN A AND C CURRENTLY FULL
C         C      INVERSE RESULT MATRIX (MAY BE SAME AS A)
C         ID     WILL BE SET BY ROUTINE TO 1 IF SUCCESSFUL INVERSION
C                                          2    MATRIX SINGULAR
C         E      TEMPORARY ARRAY SOLVING N2 X N2 SYSTEM
C         N2     N1 + N1
C         INDEX    TEMPORARY ARRAY USED IN INVERSION   (N2,3)
C
C      REQUIRES ALSO  AM MAT4  (MATINS)
C
       DIMENSION A(N,N),C(N,N),E(N2,N2),INDEX(N2,3)
       COMPLEX A,C
      NM = N1
C       EXPAND SYSTEM TO N2 X N2
       DO 2 I=1,NM
       IN = I+NM
       DO 2 J=1,NM
       JN = J+NM
       E(I,J) = REAL (A(I,J))
       E(IN,JN) = E(I,J)
       E(IN,J) = AIMAG(A(I,J))
       E(I,JN) = -E(IN,J)
    2  CONTINUE
       CALL MATINS(E,N2,N2,DUM,0,0,DET,ID,INDEX)
       DO 4 I = 1,NM
       IN = I+NM
```

198

```
      DO 4 J = 1,NM
      C(I,J) = CMPLX(F(I,J),F(IN,J))
  4    CONTINUE
      RETURN
      END
      SUBROUTINE MATINS(A,NR,N1,B,NC,M1,DETERM,ID,INDEX)
C        MATRIX INVERSION WITH ACCOMPANYING SOLUTION OF SIMUL. EQ.
C     PIVOT METHOD
C     FORTRAN IV SINGLE PRECISION WITH ADJUSTABLE DIMENSION
C     NOVEMBER 1971    S GOOD  NAVAL SHIP R + D CENTER
C          WHERE CALLING PROGRAM MUST INCLUDE
C                  DIMENSION  A(NR,NR),  B(NR,NC),  INDEX(NR,3)
C          WHERE NR,NC ARE DIMENSIONS OF A,B,INDEX
C          N1    IS THE ORDER OF A
C          M1    IS THE NUMBER OF COLUMN VECTORS IN B(MAY BE 0)
C       DETERM WILL CONTAIN DETERMINANT ON EXIT
C          ID    WILL BE SET BY ROUTINE TO 2 IF MATRIX A IS SINGULAR
C                1 IF INVERSION WAS SUCCESSFUL
C          A     THE INPUT MATRIX WILL BE REPLACED BY A INVERSE
C          B     THE COLUMN VECTORS WILL BE REPLACED BY CORRESPONDING
C                SOLUTION VECTORS
C          INDEX WORKING STORAGE ARRAY
C          IF IT IS DESIRED TO SCALE THE DETERMINANT CARD 29  MAY BE
C          DELETED AND DETERM PRESET BEFORE ENTERING THE ROUTINE
C
C                  DIMENSION  A(NR,NR),  B(NR,NC),  INDEX(NR,3)
      EQUIVALENCE (IROW,JROW), (ICOLUM,JCOLUM), (AMAX, T, SWAP)
C
C     INITIALIZATION
C
      N=N1
      M=M1
      DETERM = 1.0
      DO 20 J=1,N
  20  INDEX(J,3) = 0
      DO 550 I=1,N
C
C     SEARCH FOR PIVOT ELEMENT
C
      AMAX = 0.0
      DO 105 J=1,N
      IF (INDEX(J,3)-1) 60, 105, 60
  60  DO 100 K=1,N
      IF (INDEX(K,3)-1) 80, 100, 715
  80  IF (   AMAX -ABS (A(J,K))) 85, 100, 100
  85  IROW=J
      ICOLUM =K
      AMAX = ABS (A(J,K))
 100  CONTINUE
 105  CONTINUE
      INDEX(ICOLUM,3) = INDEX(ICOLUM,3) +1
```

```
      INDEX(I,1)=IROW
      INDEX(I,2)=ICOLUM
C
C     INTERCHANGE ROWS TO PUT PIVOT ELEMENT ON DIAGONAL
C
      IF (IROW-ICOLUM) 140, 310, 140
  140 DETERM=-DETERM
      DO 200 L=1,N
      SWAP=A(IROW,L)
      A(IROW,L)=A(ICOLUM,L)
  200 A(ICOLUM,L)=SWAP
      IF(M) 310, 310, 210
  210 DO 250 L=1, M
      SWAP=B(IROW,L)
      B(IROW,L)=B(ICOLUM,L)
  250 B(ICOLUM,L)=SWAP
C
C     DIVIDE PIVOT ROW BY PIVOT ELEMENT
C
  310 PIVOT   =A(ICOLUM,ICOLUM)
      DETERM=DETERM*PIVOT
  330 A(ICOLUM,ICOLUM)=1.0
      DO 350 L=1,N
  350 A(ICOLUM,L)=A(ICOLUM,L)/PIVOT
      IF(M) 380, 340, 360
  360 DO 370 L=1,M
  370 B(ICOLUM,L)=B(ICOLUM,L)/PIVOT
C
C     REDUCE NON-PIVOT ROWS
C
  380 DO 550 L1=1,N
      IF(L1-ICOLUM) 400, 550, 400
  400 T=A(L1,ICOLUM)
      A(L1,ICOLUM)=0.0
      DO 450 L=1,N
  450 A(L1,L)=A(L1,L)-A(ICOLUM,L)*T
      IF(M) 550, 550, 460
  460 DO 500 L=1,M
  500 B(L1,L)=B(L1,L)-B(ICOLUM,L)*T
  550 CONTINUE
C
C     INTERCHANGE COLUMNS
C
      DO 710 I=1,N
      L=N+1-I
      IF (INDEX(L,1)-INDEX(L,2)) 630, 710, 630
  630 JROW=INDEX(L,1)
      JCOLUM=INDEX(L,2)
      DO 705 K=1,N
      SWAP=A(K,JROW)
      A(K,JROW)=A(K,JCOLUM)
```

200

```
      A(K,JCOLUM)=SWAP
  705 CONTINUE
  710 CONTINUE
      DO 730 K = 1,N
      IF(INDEX(K,3) -1) 715,720,715
  720   CONTINUE
  730   CONTINUE
      ID = 1
  810 RETURN
  715 ID = 2
      GO TO 810
      END
      SUBROUTINE BESJ(X,N,BJ,D,IER)
C
C
C
C     ..................................................................
C
C        SUBROUTINE BESJ
C
C        PURPOSE
C           COMPUTE THE J BESSEL FUNCTION FOR A GIVEN ARGUMENT AND ORDER
C
C        USAGE
C           CALL BESJ(X,N,BJ,D,IER)
C
C        DESCRIPTION OF PARAMETERS
C           X   -THE ARGUMENT OF THE J BESSEL FUNCTION DESIRED
C           N   -THE ORDER OF THE J BESSEL FUNCTION DESIRED
C           BJ  -THE RESULTANT J BESSEL FUNCTION
C           D   -REQUIRED ACCURACY
C           IER-RESULTANT ERROR CODE WHERE
C               IER=0   NO ERROR
C               IER=1   N IS NEGATIVE
C               IER=2   X IS NEGATIVE OR ZERO
C               IER=3   REQUIRED ACCURACY NOT OBTAINED
C               IER=4   RANGE OF N COMPARED TO X NOT CORRECT (SEE REMARKS)
C
C        REMARKS
C           N MUST BE GREATER THAN OR EQUAL TO ZERO, BUT IT MUST BE
C           LESS THAN
C              20+10*X-X** 2/3    FOR X LESS THAN OR EQUAL TO 15
C              90+X/2             FOR X GREATER THAN 15
C
C        SUBROUTINES AND FUNCTION SUBPROGRAMS REQUIRED
C           NONE
C
C        METHOD
C           RECURRENCE RELATION TECHNIQUE DESCRIBED BY H. GOLDSTEIN AND
C           R.M. THALER,*RECURRENCE TECHNIQUES FOR THE CALCULATION OF
C           BESSEL FUNCTIONS*,M.T.A.C.,V.13,PP.102-108 AND I.A. STEGUN
C           AND M. ABRAMOWITZ,*GENERATION OF BESSEL FUNCTIONS ON HIGH
C           SPEED COMPUTERS*,M.T.A.C.,V.11,1957,PP.255-257
```

```
C
C
C         ...........................................................
C
C
          BJ=.0
          IF(N)10,20,20
   10     IER=1
          RETURN
   20     IF(X)30,30,31
   30     IER=2
          RETURN
   31     IF(X-15.)32,32,34
   32     NTEST=20.+10.*X-X** 2/3
          GO TO 36
   34     NTEST=90.+X/2.
   36     IF(N-NTEST)40,38,38
   38     IER=4
          RETURN
   40     IER=0
          N1=N+1
          BPREV=.0
C
C         COMPUTE STARTING VALUE OF M
C
          IF(X-5.)50,60,60
   50     MA=X+6.
          GO TO 70
   60     MA=1.4*X+60./X
   70     MB=N+IFIX(X)/4+2
          MZERO=MAX0(MA,MB)
C
C         SET UPPER LIMIT OF M
C
          MMAX=NTEST
  100     DO 190 M=MZERO,MMAX,3
C
C         SET F(M),F(M-1)
C
          FM1=1.0E-28
          FM=.0
          ALPHA=.0
          IF(M-(M/2)*2)120,110,120
  110     JT=-1
          GO TO 130
  120     JT=1
  130     M2=M-2
          DO 150 K=1,M2
          MK=M-K
          BMK=2.*FLOAT(MK)*FM1/X-FM
          FM=FM1
          FM1=BMK
```

```
      IF (MK-N-1)150,140,150
140   BJ=BMK
150   JT=-JT
      S=1+JT
160   ALPHA=ALPHA+BMK*S
      BMK=2.*FMJ/X-FM
      IF (N)180,170,180
170   BJ=BMK
180   ALPHA=ALPHA+BMK
      BJ=BJ/ALPHA
      IF (ABS(BJ-BPREV)-ABS(D*BJ))200,200,190
190   BPREV=BJ
      IER=3
200   RETURN
      END
```

203

REFERENCES

1. Leibowitz, R.C. and D.R. Wallace, *Engineering Guide and Computer Programs for Determining Turbulence-Induced Vibration and Radiation of Plates,* NSRDC Report 2976 (Jan 1970).

2. Leibowitz, R.C. and D.R. Wallace, *Computer Program for Correction of Boundary Layer Pressure Fluctuations for Hydrophone Size and Boundary Layer Thickness Effects-Option 1,* NSRDC Report 2976A (Sep 1970).

3. Leibowitz, R.C. and D.R. Wallace, *Computer Program for Plate Vibration Including the Effects of Clamped and Rotational Boundaries and Cylindrical Curvature-Option 2,* NSRDC Report 2976B (Jan 1971).

4. Leibowitz, R.C., *Methods for Computing Fluid Loading and the Vibratory Response of Fluid-Loaded Finite Rectangular Plates Subject to Turbulence Excitation-Option 3,* NSRDC Report 2976C (Sep 1971).

5. Leibowitz, R.C., *Methods for Computing Radiation Damping and the Vibratory Response of Fluid-Loaded and Acoustically Radiating Finite Rectangular Plates Subject to Turbulence Excitation-Option 4,* NSRDC Report 2976D (Mar 1972).

6. Leibowitz, R.C., *Theoretical and Experimental Methods for Determining the Far-Field Acoustic Pressure Radiated by Arbitrarily Excited Finite Rectangular Plates in a Dense Fluid with Application to Turbulence Excitation-Option 5,* NSRDC Report 2976E (Nov 1974).

7. Pope, L.D., *On the Transmission of Sound through Finite Closed Shells: Statistical Energy Analysis, Modal Coupling and Nonresonant Transmission,* Univ Houston, Dept Mech Eng Tech Report 21 (Aug 1970); also J. Acous. Soc. Am. Vol 50, p. 1004 (1971).

8. Pope, L.D., *Response and Radiation of a Fluid Loaded Plate-Cavity System Excited by Boundary Layer Turbulence,* Bolt Beranek and Newman, Inc. Report 2594 (Dec 1973).

9. Davies, H.G., *Acoustic Radiation from Fluid Loaded Rectangular Plates,* MIT Acoust. and Vib. Lab. Report 71476-1 (1969).

10. Davies, H.G., *Low Frequency Random Excitation of Water-Loaded Rectangular Plates,* J. Sound Vib. Vol. 15, No. 1, p. 107 (1971).

11. Pope, L.D. and R.C. Leibowitz, *Intermodal Coupling Coefficients for a Fluid-Loaded Rectangular Plate,* J. Acous. Soc. Am. (Aug 1974).

12. Maestrello, L., *Use of Turbulent Model to Calculate the Vibration and Radiation Responses of a Panel with Practical Suggestions for Reducing Sound Level*, J. Sound Vib., Vol. 15, No. 3, pp. 407–448 (1967).

13. Lyon, R.H. and G. Maidanik, *Power Flow between Linear Coupled Oscillators*, J. Acoust. Soc. Am., Vol. 34, No. 5 (May 1962).

14. Ungar, E.E., *Fundamentals of Statistical Energy Analysis of Vibrating Systems*, Tech Report AFFDL-TR-66-52 (May 1966).

15. Lyon, R.H., *Noise Reduction of Rectangular Enclosures with One Flexible Wall*, J. Acoust. Soc. Am., Vol. 35, No. 11 (Nov 1963).

16. Pretlove, A.J., *Free Vibrations of a Rectangular Panel Backed by a Closed Rectangular Cavity*, J. Sound Vib., Vol. 2, No. 3, pp. 197-209 (1965).

17. Pretlove, A.J., *Forced Vibrations of a Rectangular Panel Backed by a Closed Rectangular Cavity*, J. Sound Vib., Vol. 3, No. 3, pp. 252-261 (May 1966).

18. Eichler, E., *Thermal Circuit Approach to Vibrations in Coupled Systems and the Noise Reduction of a Rectangular Box*, J. Acoust. Soc. Am., Vol. 37, No. 6 (Jun 1965).

19. Kihlman, T., *Sound Radiation into a Rectangular Room. Applications to Airborne Sound Transmission in Buildings*, Acustica, Vol. 18 (1967).

20. Fahy, F.J., *Vibration of Containing Structures by Sound in the Contained Fluid*, J. Sound Vib., Vol. 10, No. 3, pp. 490-512, (1969) and ISVR Report 11 (Nov 1968).

21. Cockburn, J.A. and A.C. Jolly, *Structural-Acoustic Response, Noise Transmission Losses and Interior Noise Levels of an Aircraft Fuselage Excited by Random Pressure Fields*, Technical Report AFFDL-TR-68-2 (Aug 1968).

22. Bhattacharya, M.C. and M.J. Crocker, *Forced Vibration of a Panel and Radiation of Sound into a Room*, Acustica, Vol. 22 (1969-70).

23. Guy, R.W. and M.C. Bhattacharya, *The Transmission of Sound through a Cavity-Backed Finite Plate*, J. Sound Vib., Vol. 27, No. 2, pp. 207-223 (1973).

24. Morse, P.M. and K.U. Ingard, *Theoretical Acoustics*, McGraw-Hill, New York (196.

25. Gradshteyn, I.S. and I.M. Ryzhik, *Table of Integrals, Series, and Products*, Academic Press, New York (1965).

26. Maestrello, L. and T.L.J. Linden, *Response of an Acoustically Loaded Panel Excited by Supersonically Convected Turbulence*, J. Sound Vib., Vol. 16, No. 3, pp. 365-384 (1971).

27. Meirovitch, L., *Analytical Methods in Vibration*, MacMillan Company, New York (1967).

28. Hurty, W.C. and M.F. Rubinstein, *Dynamics of Structures*, Prentice-Hall, Inc. (1964).

29. Gardner, M.F. and J.L. Barnes, *Transients in Linear Systems*, John Wiley and Sons, New York (1942).

30. Korn, G.A. and T.M. Korn, *Mathematical Handbook for Scientists and Engineers*, McGraw-Hill Book Company, (1961).

31. Maidanik, G., *Response of Ribbed Panels to Reverberant Acoustic Fields*, J. Acous. Soc. Am., Vol. 34, p. 809 (1962).

32. Kraichnan, R.H., *Noise Transmission from Boundary Layer Pressure Fluctuations*, J. Acous. Soc. Am., Vol. 29, p. 65 (195).

33. Dwight, H.B., *Tables of Integrals and Other Mathematical Data*, MacMillan Company, (1947) pp. 45-46.

34. Peirce, B.O., *A Short Table of Integrals*, Third Edition, Ginn and Company, Boston, Mass. (1929).

35. Kinsler, L.E. and A.R. Frey, *Fundamentals of Acoustics*, Second Edition, John Wiley and Sons, New York (1950).

36. Morse, P. and H. Feshbach, *Methods of Theoretical Physics*, McGraw-Hill, New York (1953).

37. Campbell, G.A. and R.M. Foster, *Fourier Integrals for Practical Application*, D. Van Nostrand Company, Inc., Princeton, N.J. (1951).

38. Abramowitz, M. and I.A. Stegun, *Handbook of Mathematical Functions*, U.S. Dept. Comm., Nat. Bur. Stand., Appl. Math. Series 55 (Jun 1964).

39. Leibowitz, R.C., *Vibroacoustic Response of Turbulence Excited Thin Rectangular Finite Plates in Heavy and Light Fluid Media*, J. Sound Vib., Vol. 40, No. 4, pp. 441-495 (Jun 1975).

BIBLIOGRAPHY

Arnold, R.R., *Vibration of a Cavity Backed Panel*, MIT Acoustics and Vibration Laboratory Report 70208-7 (Dec 1971).

Corcos, G.M. and H.W. Liepmann, *On the Transmission Through a Fuselage Wall of Boundary Layer Noise*, McDonnel Douglas Corporation, Santa Monica Division, Report SM-19570 (1955).

Corcos, G.M. and H.W. Liepmann, *On the Contribution of Turbulent Boundary Layers to the Noise Inside a Fuselage*, NACA Tech. Memo 1420 (Dec 1956).

Crocker, M.J. and A.J. Price, *Sound Transmission Using Statistical Energy Analysis*, J. Sound Vib., Vol. 9, No. 3, pp. 469-486 (1969).

Dowell, E.H., *Transmission of Noise from a Turbulent Boundary Layer Through a Flexible Plate into a Closed Cavity*, J. Acous. Soc. Am., Vol. 46, No. 1, Part 2 (1969).

Dowell, E.H. and H.M. Voss, *The Effect of a Cavity on Panel Vibration*, AIAA J. (Feb 1963).

Fahy, F.J., *On Simulating the Transmission Through Structures of Noise from Turbulent Boundary Layer Pressure Fluctuations*, J. Sound Vib., Vol. 3, No. 1, pp. 57-81 (1966).

Guy, P.W. and A.J. Pretlove, *Cavity-Backed Panel Resonance*, J. Sound Vib., 27, 128-129 (1973).

Obermeier, F., *On the Response of Elastic Plates Backed by Enclosed Cavities to Turbulent Flow Excitation*, MIT Dept. Naval Arch. and Mar. Eng. Technical Report 70208-6 (Apr 1971).

Pretlove, A.J. and A. Craggs, *A Simple Approach to Coupled Panel-Cavity Vibrations*, J. Sound Vib., Vol. 11, No. 2, pp. 207-215 (1970).

Price, A.J. and M.J. Crocker, *Sound Transmission Through Double Panels Using Statistical Energy Analysis*, J. Acous. Soc. Am., Vol. 47, No. 3, Part 1 (1970).

Ribner, H.S., *Boundary-Layer-Induced Noise in the Interior of Aircraft*, UTIA Report 37 (Apr 1956).

Vaicaitis, R. et al, *Nonlinear Panel Response from a Turbulent Boundary Layer*, Am. Inst. Aeron. and Astron. J., Vol. 10, No. 7 (Jul 1972).

Yaneske, P.P., *A Restatement of the Principles of Coincidence and Resonance*, J. Sound Vib., Vol. 25, No. 1, pp. 51-73 (1972).